Effects of the Physical Microenvironment on Endometrial Cancer Cells (Ishikawa)

Tan Li Hui

A thesis submitted for the degree of
Doctor of Philosophy,
At the University of Otago, Christchurch,
New Zealand

February 2016

Abstract

With the realization that mechanical signals are important in controlling cancer cell behaviours, a new *in vitro* model has been developed to incorporate physical signals in laboratory studies. Here, we developed a system to fabricate hard polymers with imprinted cell topography, which we called a Bioimprint, and then we used the Bioimprint as the platform to culture endometrial cancer cells on. With Bioimprint high resolution of cell replicas were produced with cell-like features that retain all the micro- and nanoscale details of the cells. This enabled us, importantly, to study the effect of surface physical topography on endometrial cancer cell behaviours. The physical topography we used here was the cell-like topography that the cells encounter in real cell microenvironments.

We fabricated the Bioimprint of cells onto polymethacrylate (pMA) and compared the cells cultured on it to the cells on flat pMA. pMA is not a common cell culture material, therefore, we compared cell culture on pMA with the conventional cell culture materials: glass and polystyrene (pST). We then fabricated the Bioimprint onto pST, and compared the response of cells cultured on the replica with that cultured on the flat pST. Moreover, on pST, the Bioimprint was made in two forms: pit-like (negative) versus hump-like (positive) topographies, which enabled us to further investigate the effect of distinct topographies on cell behaviours. We also extended our study on flat and pST Bioimprints to study the effect of culture serum, fetal bovine serum (FBS), on cell responses to surface physical topography.

In this report, we characterized the behaviours of endometrial cancer cells and studied the biological changes in response to culture substrate materials and culture substrate with cell-like topography. We examined cell adhesion, morphology, spreading, expression of adhesion molecules and growth. The studies of pST Bioimprints were extended to examine the cell protein profile, and cell responses to anticancer agents, in serum-supplemented or serum-free culture media.

The comparison between glass, tissue culture grade pST and pMA showed that substrate material modulated cell behaviours. Additionally, imprinting with cell-like topography also

altered cell behaviours. Here, we showed that Ishikawa endometrial cancer cells spread wider and grew faster on glass and pST compared to pMA. Further, on the pMA surface that was imprinted with cell-like topography, the cells spread and grew better compared to cells on flat pMA. On the other hand, when pST, which is a favourable cell culture surface, was imprinted with the cell-like topography, the topographical effect was to restrict cell spreading and growth.

Most importantly, the change in cell growth behaviour was modulated through different proliferation biomolecules on each of these pMA and pST Bioimprints, indicating again the interaction of chemical and physical topography in regulating cell behaviours. In addition, the comparison between pST hump-like versus the pit-like topographies showed that the cells on the hump-like topography showed a greater response of an alteration of cell growth, expression of adhesion molecules when compared to cells on flat substrate. Furthermore, relative to cells on (f)pST proteomics analysis similarly showed that cells on hump-like topography had more alteration in protein expression than cells on pit-like topography. Most of these identified proteins were involved in cell energy homeostasis, growth and structural modulation.

Additionally, the extended studies with culture serum without FBS again showed that endometrial cancer cells responded to physical topography. The cell responses were different from those in culture medium supplemented with FBS. This again indicated that the topographical influences on cells were in turn affected by chemical factors (the biological source of serum chemical factors). Notably, cell culture in serum free medium similarly showed a greater tropographical response to the hump-like topography compared to cells on a flat substrate.

Here, we reveal the potential of targeting cell mechano-signalling as cancer treatment, and also this project describes a culture platform that inherently incorporates physical signals in laboratory cell culture studies. This is the first report that showed that Ishikawa endometrial cancer cells respond to the culture substrate material and cell-like physical topography.

Acknowledgement

First, with greatest gratitude I acknowledge all my supervisors: Professor John Evans (Department of Obstetrics and Gynaecology, University of Otago, Christchurch), Professor Maan Alkaisi (Electrical and Computer Engineering Department, University of Canterbury, Christchurch) and Associate Professor Peter Sykes (Department of Obstetrics and Gynaecology, University of Otago, Christchurch). Thank you for your trust, patience and understanding all the way through to completion of this thesis. Not only this, I am really inspired by their knowledge and their passion for science and research. My PhD life would definitely not have been completed without the encouragement from them.

Also, I am indebted to my many colleagues who were so helpful in guiding me. A very special thanks to Dr Kenny Chitcholtan, he was so obliging in teaching me all the laboratory skills and his cheerfulness and kindness turned the laboratory to an enjoyable place to work in. Most importantly, without his help in getting permission for me to do certain experiments in Dr Jacqui Keenan's and Dr Ashley Garrill's laboratories, my project would not have been able to start due to the closure of laboratories in University of Otago, Christchurch after the earthquake. Also thanks to Dr Volker Nock and Dr Lynn Murray who taught me the fabrication techniques. Moreover, I greatly appreciate their effort in setting up Biological Applications Laboratory at Canterbury University; this allowed me to do cell culture in Canterbury University. Also, I wish to thank Dr Jonathan Williman who shared his statistical expertise with me, my data analysis would not have been that smooth without assistance from him. Further, I would like to thank Dr Gloria Evans who helped in proofreading my thesis.

It is my great pleasure to acknowledge the support and help from Obstetrics and Gynaecology Department for being so supportive financially and so helpful in dealing with my student admission. Also appreciation to Electrical and Computer Engineering department for giving me an office space after the earthquake, and of course thanks to Dr Jacqui Keenan and Dr Ashley Garrill for letting me work in their labs after the earthquake.

I would like to also thank the MacDiarmid Institute of Advanced Materials and Nanotechnology for funding this project and supporting me with a scholarship. Also thank to the University of Otago for supporting my earthquake extension's scholarship.

Last but not least, I would like to dedicate this thesis to my parents, my sister and my brothers. To my dad, you are my exemplar, I am deeply inspired by your thoughtfulness, your wisdom and your optimism in facing what you are going through as a stroke survivor. To my superwoman mum, thank you for being so patient, caring and supportive. Your strength and your love keep me moving on all the time. Also thanks to my siblings, for your supports and love all the time, without you taking care of our parents, I would not have had the chance of travelling far from home to pursue a PhD here.

Presentations and Publication Arising from this Thesis

Publication:

Li Hui Tan, Peter H Sykes, Maan M Alkaisi, John J Evans.
The characteristics of Ishikawa endometrial cancer cells are modified by substrate topography with cell-like features and the polymer surface.
International Journal of Nanomedicine. Accepted 29 May 2015.

Commissioned Report for External Body:

J J Evans, L H Tan and K Chitcholtan
Anticancer Effects of Seaweed Extracts on Endometrial Cancer Cells; A report of preliminary studies
Prepared for Leanne Bramley of Sustainable Seafood NZ Ltd by, December 2011.

New Zealand and International Conference Presentations

T Tan, PH Sykes, MM Alkaisi, JJ Evans
Cancer Cell Response to Culture Substrate Topography [Paper chosen for double Poster and Oral presentations]
5th Annual Symposium "Physics of Cancer"
University of Leipzig, Stauffenbergallee 2, 01099 Dresden, Germany. 2-5 October 2014.

John J Evans, Li Hui Tan, Peter H Sykes, and Maan M Alkaisi,
Topography of the Microenvironment Determines Cancer Cell Behaviour
16th International Congress of Endocrinology & The Endocrine Society's 96th Annual Meeting & Expo (ICE/ENDO). Abstract #13518 MON-0315. Chicago, IL, USA. 21-24 June 2014.

T Tan, PH Sykes, MM Alkaisi, JJ Evans
Behaviour of Cancer Cells on a Surface Imprinted with their Own Features
Queenstown, New Zealand: Medical Sciences Congress (MedSciNZ), 26-28 Aug 2013.

JJ Evans LM Murray, L H Tan, K Chitcholtan, J Muys, V Nock, PH Sykes, MM Alkaisi
The Forces of Biology: Mechanotransduction as the Cure for Cancer
Christchurch School of Medicine, University of Otago, Christchurch. 12 August 2013.

JJ Evans, LM Murray, L H Tan, K Chitcholtan, J Muys, V Nock, PH Sykes, MM Alkaisi
The Forces of Biology: Mechanotransduction in the Uterus.
Centre for Neuroendocrinology, Dunedin, 12 July 2013.

Evans, J.J., Murray, L.M., Tan, L.H., Chitcholtan, K., Alkaisi, M.M. (2013)
Endometrial cells – Effects of the neighbourhood.
NZ Network Symposium for Reproductive Science. Wellington 15 March 2013.

Murray, L M, Tan, LH, Alkaisi, MM, Evans, JJ
Living conditions of cancer cells and the neighbourhood.
New Zealand Society for Oncology James Cook Hotel, Wellington May 2-4, 2012.

Evans, J J, Murray, L M, Tan, L H, Chitcholtan, K, Alkaisi, MM
Functioning of cancer cells is altered by changes in the surroundings
3rd Australia & New Zealand Micro/Nanofluidics and Bionano Symposium,
Rutherford House, Victoria University of Wellington, 12-13 April 2012.

T Tan, PH Sykes, MM Alkaisi, JJ Evans
Controllable Endometrial Cancer by Physical and Chemical Environment
The MacDiarmid Institute for Advanced Materials and Nanotechnology Student and Post-Doc Symposium, Christchurch, New Zealand, 22-23 November 2012.

T Tan, PH Sykes, MM Alkaisi, JJ Evans
Living Conditions of Cancer Cells and the Neighbourhood. . (Recycled poster presentation).
Health Research Society of Canterbury annual Poster Expo, Christchurch, New Zealand, 24 July 2012.

University of Otago, Christchurch Research Seminar Presentation

Topographical Control of Cancer Cell Behaviour (April 2014)

3 Minutes Thesis Competition 2013, University of Otago, Christchurch

FORCE-able CANCER CELLS

Laboratory for Cell and Protein Regulation Group Oral Presentations

- Interaction between Cancer Cells and Their Physical Environment (August 2011)
- A Gift from the Sea – Seaweed. (September 2011).
- Cell and Extracellular Mechanical Force: A Trip from Integrins to DNA. (November 2011).
- Effects of Substrates on Endometrial Cancer Cells (February 2012)
- Proliferation of Endometrial Cancer Cells on Glass, Polystyrene, Flat Biopolymer and Bioimprint. (March 2012).
- Effects of the Microenvironment on the Behaviours of Cells. (July 2012).
- Cell Behavioural and Functional Responses on Different Cell Culture Substrates. (September 2012).
- Cell Behaviours on Different Flat Surfaces and Surfaces with Micro-scale Features. (January 2013).

- Cell Responses on Different Cell Culture Substrates. (February 2013).
- Journal club: Functional Replication of The Tendon Tissue Microenvironment by A Bioimprinted Substrate and the Support of Tenocytic Differentiation of Mesenchymal Stem Cells. (April 2013).
- Local Tissue Environment Effets on Cell Behaviours. (June 2013).
- Endometrial Cancer Cells and Their Physical Environment. (August 2013).
- Characteristics of Cancer Cells on Surfaces with Their Own Features. (August 2013).
- Nitric Oxide: Physiology and Pathology. (October 2013).
- Mechanical Constraints and Cancer. (November 2013).
- Cancer Cells on Surfaces with Their Own Features. (December 2013).
- Bioimprints-A New Platform for Biomechanical Study. (January 2014).
- Journal club: Probing the Chemo-Mechanical Effects of an Anti-Cancer Drug Emodin on Breast Cancer Cells. (February 2014).
- iTRAQ Results Analysis. (May 2014).
- Interaction of Physics and Biology in the Study of Endometrial Cancer. (July 2014)
- Ishikawa Cell Growth and Response to Cisplatin and Paclitaxel on Different Surface Topography. (March 2015).

Nanofabrication Lab Group Meeting's Presentation

Cancer Cell Responses to Different Surfaces (November 2012)

Table of Contents

Abstract i

Acknowledgement iii

Presentations and Publication Arising from this Thesis v

Table of Contents viii

List of Figures xx

List of Tables xxv

List of Abbrevations xxvi

Chapter 1 Introduction 1

1.1 An Overview of Cancer Occurrence 1

1.2 Role of Mechanical Signals in Normal Tissue Development 4

1.3 In Vitro Culture Substrate and Its Influence on Cultured Cells 7

1.4 Mechanical Signals in Tumorigenesis 12

1.5 Tumour Mechanotransduction Studies 17

1.6 In Vitro Culture Substrate in Cancer Studies 19

1.7 Bioimprint 21

1.8 Project Outline 23

1.9 Thesis Outline 25

1.10 Implications 27

Chapter 2 Methods and Materials 29

2.1 Materials and Solution Recipe 29

2.2 Cell Culture Protocols and Reagents Preparation 39

2.2.1 Cell Culture Medium Preparation 39

2.2.2 Cell Culture 39

2.2.3 Cell Counting 40

2.2.4 Cell Freezing 41

2.2.5 Cell Thawing 42
2.3 PDMS gel and Bioimprint 42
2.4 Cell Fixation 43
2.4.1 Cell Fixation for Bioimprint or Immunofluorescent or Chemical Staining 43
2.4.2 Cell Fixation for Scanning Electron Microscope Examination 43
2.5 Proliferation Assay 43
2.5.1 Coomassie Blue Cell Number Standard curve 44
2.5.2 Adherent Cell Quantitation 45
2.5.3 Non-adherent Cell Quantitation 46
2.6 ImageJ Measurement of Cell Area 47
2.7 Cell Preferential Attachment 48
2.8 RGDS and RGES Treatments 50
2.9 Total Protein Measurement 50
2.10 Western Blot 51
2.10.1 Cell Lysing for Western Blot 51
2.10.2 Gel Preparation and Electrophoresis 51
2.10.3 Electroblotting 52
2.10.4 Antibodies Binding and Protein Bands Visualization 52
2.10.5 Western blot densitometry normalisation 53
2.10.6 ImageJ analysis of Western blot images 55
2.10.7 Coomassie gel staining 56
2.11 Immunofluorescent Staining 57
2.12 Cell Morphology, Area and Circularity Measurements 58
2.13 iTRAQ analysis (cell lysing and data analysis) 58
2.14 VEGF ELISA Assay 60
2.15 Nitric Oxide Assay 61
2.16 Cell Treatments 61

2.16.1 Cell EGCG and $CoCl_2$ Treatments 61
2.16.2 Aldosterone Treatment 62
2.16.3 Cisplatin and Paclitaxel Treatments 62
2.17 Statistical Analysis 63
Chapter 3 The Making of Bioimprint 64
3.1 Introduction 64
3.2 Protocol of Making Bioimprint 65
3.2.1 PDMS Circular Chambers 65
3.2.1.1 PDMS Circular Chambers for Cell Culture for Making of Bioimprint 65
3.2.1.2 PDMS Circular Chambers for Cell Culture on Glass and Tissue Culture Grade Polystyrene 66
3.2.2 Polymethylacrylate (pMA) Culture Substrates 67
3.2.2.1 The Making of Polymethacrylate (pMA) Flat and Bioimprint Culture Substrates 67
3.2.2.2 Cell Culture on Polymethacrylate (pMA) Flat and Bioimprint Culture Substrates 68
3.2.3 Polystyrene (pST) Bioimprints 69
3.2.3.1 Positive pST Bioimprint 70
3.2.3.2 Negative pST Bioimprint 70
3.2.3.3 Flat pST 71
3.2.3.4 Cell Culture on pST Microscope Slide Bioimprints 72
3.3 Discussion 72
3.4 Conclusion 74
Chapter 4 Influences of Substrate Material and Topography on Cancer Cell Morphology and Spreading 75
4.1 Introduction 75
4.2 Hypotheses 79
4.3 Aims 79

4.4 Experimental Approach 80
4.5 Results 81
4.5.1 Ishikawa Endometrial Cancer Cell Morphology 81
4.5.1.1 Ishikawa Endometrial Cancer Cell Morphology on Glass and Tissue Culture Grade Polystyrene, Polymethacrylate Flat and Bioimprint Culture Substrates 81
4.5.1.2 Ishikawa Endometrial Cancer Cell Morphology on Flat, Negative and Positive Bioimprint Polystyrene Slides 86
4.5.2 Ishikawa Endometrial Cancer Cell Cytoskeleton 90
4.5.2.1 Ishikawa Endometrial Cancer Cell Cytoskeleton on Glass and Tissue Culture Grade Polystyrene, Polymethacrylate Flat and Bioimprint Culture Substrates 90
4.5.2.2 Ishikawa Endometrial Cancer Cell Cytoskeleton on Flat, Negative and Positive Bioimprint Polystyrene Slides 92
4.5.3 Ishikawa Endometrial Cancer Cell Spreading Area and Circularity 93
4.5.3.1 Ishikawa Endometrial Cancer Cell Spreading Area and Circularity on Glass, Tissue Culture Grade Polystyrene, Polymethacrylate Flat and Bioimprint Culture Substrates 93
4.5.3.2 Ishikawa Endometrial Cancer Cell Spreading Area and Circularity on Flat, Negative and Positive Bioimprint Polystyrene Slides 95
4.5.4 Specificity of Ishikawa Endometrial Cancer Cell Alignment on Surface Topography 97
4.5.4.1 Ishikawa Endometrial Cancer Cells on Ishikawa Polystyrene Microscope Slide Bioimprints 97
4.5.4.2 Ishikawa Endometrial Cancer Cells on C2C12 Murine Myoblast Polystyrene Microscope Slide Bioimprints 98
4.6 Discussion 99
4.6.1 Ishikawa Endometrial Cancer Cell on Glass, Tissue Culture Grade Polystyrene and Polymethacrylate Flat and Bioimprint Culture Substrates 99

4.6.2 Ishikawa Endometrial Cancer Cell on Flat, Negative and Positive Bioimprint Polystyrene Slides....101
4.7 Conclusion....102
Chapter 5 Influences of Substrate Material and Topography on Ishikawa Endometrial Cancer Cell Adhesion Molecules and Cell Cytoskeleton....103
5.1 Introduction....103
5.5.1 Integrins....103
5.1.2 Focal Adhesion (FA)....105
5.1.3 Cell Cytoskeleton....105
5.1.4 Nitric Oxide Secretion....107
5.2 Hypotheses....109
5.3 Aims....109
5.4 Experimental Approach....110
5.5 Results....111
5.5.1 Ishikawa Endometrial Cancer Cell β1 integrin Expression....111
5.5.1.1 Cell β1 Integrin Expression on Glass, Tissue Culture Polystyrene and Polymethacrylate Polymer Flat and Bioimprint Culture Substrates....111
5.5.1.2 Cell β1 Integrin Expression on Flat, Negative and Positive Bioimprint Polystyrene Slides....112
5.5.2 Ishikawa Endometrial Cancer Cell FAK Expression and Activation (pFAK/FAK Ratio) and pFAK Distribution....113
5.5.2.1 Cell FAK Expression and Activation (pFAK/FAK Ratio) on Glass, Tissue Culture Polystyrene and Polymethacrylate Polymer Flat and Bioimprint Culture Substrates....113
114
5.5.2.2 Cell FAK Expression and Activation (pFAK/FAK Ratio) on Flat, Negative and Positive Bioimprint Polystyrene Slides....115
5.5.3 Ishikawa Endometrial Cancer Cell β1 integrin Co-exists with pFAK in cell cytoplasm....117

5.5.3.1 β1 Integrin co-exists with pFAK in same cell cytoplasm on Glass, Tissue Culture Polystyrene and Polymethacrylate Polymer Flat and Bioimprint Culture Substrates 117

5.5.3.2 Cell β1 integrin co-exists with pFAK in the cell cytoplasm on Flat, negative and positive bioimprint polystyrene slides 119

5.5.4 Ishikawa Endometrial Cancer Cell Actin Expression 120

5.5.4.1 Cell Actin Expression on Glass, Tissue Culture Polystyrene and Polymethacrylate Polymer Flat and Bioimprint Culture Substrates 120

5.5.4.2 Cell Actin Expression on Flat, Negative and Positive Bioimprint Polystyrene Slides 121

5.5.5 Ishikawa Endometrial Cancer Cell Cytokeratin-18 Expression 122

5.5.5.1 Cell Cytokeratin-18 Expression on Glass, Tissue Culture Polystyrene and Polyethacrylate Polymer 122

5.5.5.2 Cell Cytokeratin-18 Expression on Flat, Negative and Positive Bioimprint Polystyrene Slides 123

5.5.6 Ishikawa Endometrial Cancer Cell β1 Integrin Blocking 124

5.5.7 Ishikawa Endometrial Cancer Cell Nitric Oxide Secretion 125

5.5.7.1 Aldosterone Effects on Cell Cortical Actin at Different Concentrations 125

5.5.7.2 Cell Cortical Actin Filaments on Flat, Negative and Positive Bioimprint Polystyrene Slide with or without Aldosterone Treatment 127

5.5.7.3 Cell Nitric Oxide Secretion on Flat, Negative and Positive Bioimprint Polystyrene Slide with or without Aldosterone Treatment 129

5.6 Discussion 130

5.6.1 Cell Culture on Glass, Tissue Culture Grade Polystyrene and Polymethacrylate Flat and Bioimprint Culture Substrates 130

5.6.2 Cell Culture on Flat, Negative and Positive Bioimprint Polystyrene Slides 131

5.6.3 Summary 134

5.7 Conclusion 134

Chapter 6 Influences of Substrate Material and Topography on Ishikawa Endometrial Cancer Cell Adhesion, Growth and Activation of MAPK/ERK and PI3K /AKT Pathways 136

6.1 Introduction 136

6.2 Hypotheses 138

6.3 Aims 138

6.4 Experimental Approach 139

6.5 Results 140

6.5.1 Ishikawa Endometrial Cancer Cell Adhesion and Growth 140

6.5.1.1 Ishikawa Endometrial Cancer Cell Adhesion and Growth on Glass, Tissue Culture Grade Polystyrene and Polymethacrylate Flat and Bioimprint Culture Substrates 140

6.5.1.2 Ishikawa Endometrial Cancer Cell Adhesion and Growth on Flat, Negative and Positive Bioimprint Polystyrene Slides 142

6.5.1.3 Time Point of Analyses 143

6.5.1.4 Ishikawa Endometrial Cancer Cell Growth on Flat, Negative and Positive Human Dermal Microvascular Endothelial Cell Bioimprint Polystyrene Slides 143

6.5.2 Ishikawa Endometrial Cancer Cell Cycle Biomolecules and Proliferation Marker Expression 144

6.5.2.1 Cell Cyclin D2 Expression on Glass, Tissue Culture Polystyrene and Polymethacrylate Polymer Flat and Bioimprint Culture Substrates 145

6.5.2.2 Cell PCNA, Cyclin D2, B1 and B2 Expression on Flat, Negative and Positive Bioimprint Polystyrene Slides 146

6.5.3 Ishikawa Endometrial Cancer Cell ERK Signalling 148

6.5.3.1 Cell ERK/pERK Ratio on Glass, Tissue Culture Polystyrene and Polymethacrylate Polymer Flat and Bioimprint Culture Substrates 148

6.5.3.2 Cell pERK/ERK ratio on Flat, Negative and Positive Bioimprint Polystyrene Slides 149

6.5.4 Ishikawa Endometrial Cancer Cell PI3K/AKT Signalling 150
6.5.4.1 Cell AKT/pAKT Ratio on Flat, Negative and Positive Bioimprint Polystyrene Slides 150
6.6 Discussion 151
6.7 Conclusion 153
Chapter 7 Proteomic Analysis of Ishikawa Endometrial Cancer Cell on Flat, Negative and Positive Bioimprint Polystyrene Slides 155
7.1 Introduction 155
7.2 Aim 156
7.3 Experimental Approach 156
7.4 Results 157
7.4.1 Identification of Changed Proteins 157
7.5 Discussion 160
7.5.1 DNA Condensation 160
7.5.2 Extracellular Matrix Proteins, Cell Structural and Cell Migration 162
7.5.3 Signalling Pathways 164
7.5.4 Energy Modulation 166
7.5.5 Cell growth and viability 169
7.5.6 Proteins involved in intermediary functions 170
7.6 Conclusion 172
Chapter 8 Influences of Substrate Material and Topography on Endometrial Cancer Cell VEGF Secretion and Responses to Cancer Therapeutic Drugs 174
8.1 Introduction 174
8.2 Hypotheses 177
8.3 Aims 178
8.4 Experimental Approach 178
8.5 Results 179
8.5.1 Cell VEGF Secretion 179

8.5.1.1 Cell VEGF Secretion on Glass, Tissue Culture Polystyrene and Polymethacrylate Flat and Bioimprint Culture Substrates 179
8.5.1.2 Cell VEGF Secretion on Flat, Negative and Positive Bioimprint Polystyrene Slides 180
8.5.2 Cisplatin and Paclitaxel Treatments for Cells on Flat, Negative and Positive Bioimprint Polystyrene Slides 181
8.5.2.1 Cell Proliferation 181
8.5.2.2 Expression of Cell PCNA 182
8.5.2.3 Expression of Cell Cyclin B1, B2 and D2 183
8.6 Discussion 185
8.6.1 VEGF Secretion in Cells Growing on Glass, Tissue Culture Polystyrene and Polymethacrylate Flat and Bioimprint Culture Substrates 185
8.6.2 VEGF Secretion in Cells Growing on Flat, Negative and Positive Bioimprint Polystyrene Slides 186
8.6.3 Cisplatin and Paclitaxel Influence on Cell Growth on Flat, Negative and Positive Bioimprint Polystyrene Slides 188
8.7 Conclusion 190
Chapter 9 Influences of Substrate Topography on Ishikawa Endometrial Cancer Cell in Culture Medium without FBS Factors 191
9.1 Introduction 191
9.2 Hypothesis 193
9.3 Aims 193
9.4 Experimental Approach 193
9.5 Results 194
9.5.1 Ishikawa Endometrial Cancer Cell Morphology in Serum-Free Culture Medium 194
9.5.2 Ishikawa Endometrial Cancer Cell Cytoskeleton in Serum-Free Culture Medium 195

9.5.3 Ishikawa Endometrial Cancer Cell Spreading Area and Circularity on Flat, Negative and Positive Bioimprint Polystyrene Slides in Serum-Free Culture Medium.....196

9.5.4 Ishikawa Endometrial Cancer Cell β1 Integrin Expression on Flat, Negative and Positive Bioimprint Polystyrene Slides in Serum-Free Culture Medium.....197

9.5.5 Ishikawa Endometrial Cancer Cell FAK Expression and Activation (pFAK/FAK) on Flat, Negative and Positive Bioimprint Polystyrene Slides in Serum-Free Culture Medium.....198

9.5.6 Ishikawa Endometrial Cancer Cell Cytoskeleton Expression and Nitric Oxide Secretion on Flat, Negative and Positive Bioimprint Polystyrene Slides in Serum-Free Culture Medium.....202

9.5.6.1 Ishikawa Endometrial Cancer Cell Actin and Cytokeratin-18 Expression on Flat, Negative and Positive Bioimprint Polystyrene Slides in Serum-Free Culture Medium.....202

9.5.6.2 Ishikawa Endometrial Cancer Cell Cortical Actin Filaments on Flat, Negative and Positive Bioimprint Polystyrene Slides in Serum-Free Culture Medium with or without Aldosterone Treatment.....204

9.5.6.3 Ishikawa Endometrial Cancer Cell Nitric Oxide Secretion on Flat, Negative and Positive Bioimprint Polystyrene Slides in Serum-Free Culture Medium.....206

9.5.7 Ishikawa Endometrial Cancer Cell Growth and Expression of Proliferation Marker and Cell Cycle Molecules on Flat, Negative and Positive Bioimprint Polystyrene Slides in Serum-Free Culture Medium.....207

9.5.7.1 Ishikawa Endometrial Cancer Cell Numbers on Flat, Negative and Positive Bioimprint Polystyrene Slides in Serum-Free Culture Medium.....208

9.5.7.2 Ishikawa Endometrial Cancer Cell Cyclin PCNA and B2, D2 Expression on Flat, Negative and Positive Bioimprint Polystyrene Slides in Serum-Free Culture Medium.....208

9.5.8 Ishikawa Endometrial Cancer Cell Proteomic Analysis on Flat, Negative and Positive Bioimprint Polystyrene Slides in Serum-Free Culture Medium.....210

9.5.8.1 Identification of Changed Proteins.....210

9.5.9 Cisplatin and Paclitaxel Treatments on Ishikawa Endometrial Cancer Cells on Flat, Negative and Positive Bioimprint Polystyrene Slides in Serum-Free Culture Medium....213
9.5.9.1 Cisplatin and Paclitaxel Effects on Ishikawa Endometrial Cancer Cell VEGF Secretion on Flat, Negative and Positive Bioimprint Polystyrene Slides in Serum-Free Culture Medium....213
9.5.9.2 Cisplatin and Paclitaxel Effects on Ishikawa Endometrial Cancer Cell Growth on Flat, Negative and Positive Bioimprint Polystyrene Slides in Serum-Free Culture Medium....214
9.5.9.3 Cisplatin and Paclitaxel Effects on Ishikawa Endometrial Cancer Cell PCNA and Cycle Regulators Expression on Flat, Negative and Positive Bioimprint Polystyrene Slides in Serum-Free Culture Medium....215
9.6 Discussion....218
9.6.1 Ishikawa Endometrial Cancer Cell Initial Attachment and Morphology in Culture Medium without FBS....218
9.6.2 Ishikawa Endometrial Cancer Cell Expression of Cell Cytoskeleton and Adhesion Molecules in Culture Medium without FBS....218
9.6.3 Ishikawa Endometrial Cancer Cell Growth in Culture Medium without FBS....219
9.6.3.1 Summary....220
9.6.4 Ishikawa Endometrial Cancer Cell Protein Profile in Culture Medium without FBS....221
9.6.4.1 Cell Stress Responses....221
9.6.4.2 Cell Epigenetic Regulation....223
9.6.4.3 Cell Growth....225
9.6.4.4 Cell Cytoskeleton....226
9.6.4.5 Cell Signalling Biomolecules....227
9.6.4.6 Proteins involved in intermediatery functions....228
9.6.4.7 Venn diagram of all significant proteins in culture medium with and without FBS conditions....231

9.6.4.8 Summary....235
9.6.5 Ishikawa Endometrial Cancer Cell Responses to Cisplatin and Paclitaxel in Culture Medium without FBS....236
9.6.5.1 Cisplatin and Paclitaxel Treatments Effects on Cell VEGF Secretion in Culture Medium without FBS....236
9.6.5.2 Cisplatin and Paclitaxel Effects on Cell Growth in Culture Medium without FBS....237
9.6.5.3 Cisplatin and Paclitaxel Effects on Cell Growth on Negative Polystyrene Microscope Slide Bioimprint....238
9.7 Conclusion....239
Chapter 10 Conclusion....242
References 248

List of Figures

Figure 1 Ishikawa endometrial cancer cells grew preferentially on the Bioimprint surface. Adopted from (Murray, 2011,unpublished work). 23
Figure 2 Dimension of a haemocytometer 41
Figure 3 ImageJ measurement of cell spreading area. (a) An image of ImageJ toolbox. 47
Figure 4 Representative images of alignment of 'before' and 'after' cell culture on the substrate. 49
Figure 5 GAPDH expression in cells cultured on glass, tissue culture grade pST, (f)pMA and (-ve)pMA. 54
Figure 6 ImageJ measurement of densitometry 55
Figure 7 PDMS block with circular chambers on glass microscope slide. 66
Figure 8 The making of pMA UV curable polymer. 67
Figure 9 Schematic outline of the making of (f)pST, (-ve)pST and (+ve)pST. 69
Figure 10 Representative scanning electron microscope images of the Bioimprints. 71
Figure 11 Representative images of Ishikawa endometrial cancer cells on glass culture substrate at 6, 24, 48 and 60 hours. 82
Figure 12 Representative images of Ishikawa endometrial cancer cells on tissue culture grade pST at 6, 24, 48 and 60 hours. 83
Figure 13 Representative images of Ishikawa endometrial cancer cells on (f)pMA at 6, 24, 48 and 60 hours. 84
Figure 14 Representative images of Ishikawa endometrial cancer cells on (-ve)pMA at 6, 24, 48 and 60 hours. 85
Figure 15 Representative images of Ishikawa endometrial cancer cells on (f)pST at 6, 24, 48 and 60 hours. 87
Figure 16 Representative images of Ishikawa endometrial cancer cells on (-ve)pST at 6, 24, 48 and 60 hours. 88
Figure 17 Representative images of Ishikawa endometrial cancer cells on (+ve)pST at 6, 24, 48 and 60 hours. 89
Figure 18 Representative images of Ishikawa endometrial cancer cell actin filaments and Cytokeratin-18 staining on glass, pST, (f)pMA and (-ve)pMA. 91

Figure 19 Representative images of Ishikawa endometrial cancer cell actin filaments and Cytokeratin-18 staining on (f), (-ve) and (+ve)pST.....92
Figure 20 Ishikawa endometrial cancer cell spreading area on glass, tissue culture grade pST, (f)pMA and (-ve)pMA.....94
Figure 21 Ishikawa endometrial cancer cell circularity on glass, tissue culture grade pST, (f)pMA and (-ve)pMA.....94
Figure 22 Ishikawa endometrial cancer cell spreading area on (f)pST, (-ve)pST and (+ve)pST imprint. 96
Figure 23 Ishikawa endometrial cancer cell circularity on (f)pST, (-ve)pST and (+ve)pST imprint.....96
Figure 24 Ratio of the measured Ishikawa cell area to the proposed cell area on respective surfaces. 97
Figure 25 Ratio of the measured Ishikawa cell area to the proposed cell area on respective surfaces. 98
Figure 26 Cell adhesion at different contact angle. Fibroblasts (open squares); L cells (open circles) and endothelial cells (open triangles and filled circles).....100
Figure 27 Diagram of hetero-dimer integrin.....104
Figure 28 Ishikawa endometrial cancer cell β1 integrin expression on glass, tissue culture grade pST, (f)pMA and (-ve)pMA. 111
Figure 29 Ishikawa endometrial cancer cell β1 integrin expression on (f), (-ve) and (+ve)pST. 112
Figure 30 Ishikawa endometrial cancer cell expression levels of FAK and pFAK on glass, tissue culture grade pST, (f)pMA and (-ve)pMA. 114
Figure 31 Ishikawa endometrial cancer cell FAK activation on glass, tissue culture grade pST, (f)pMA and (-ve)pMA. 114
Figure 32 Ishikawa endometrial cancer cell FAK and pFAK expression on (f), (-ve) and (+ve)pST. 115
Figure 33 Ishikawa endometrial cancer cell pFAK/FAK on (f), (-ve) and (+ve)pST. 115
Figure 34 Ishikawa endometrial cancer cell FAK and pFAK expression on (f), (-ve) and (+ve)pST at 3 hours. 116
Figure 35 Ishikawa endometrial cancer cell pFAK/FAK on (f), (-ve) and (+ve)pST at 3 hours. 117
Figure 36 Representative images of double-staining of β1 integrin and pFAK in cells cultured on (A) glass (B) tissue culture grade pST (C) (f)pMA (D) (-ve)pMA. 118

Figure 37 Representative images of double-staining of β1integrin and pFAK in cells cultured on (A)(f)pST (B)(-ve)pST (C) (+ve)pST. 119
Figure 38 Ishikawa endometrial cancer cell actin expression on glass, tissue culture grade pST and (f)pMA and (-ve)pMA. 120
Figure 39 Ishikawa endometrial cancer cell actin expression on (f), (-ve) and (+ve)pST. 121
Figure 40 Ishikawa endometrial cancer cell Cytokeratin-18 expression on glass, tissue culture grade pST and (f)pMA versus (-ve)pMA. 122
Figure 41 Ishikawa endometrial cancer cell Cytokeratin-18 expression on (f), (-ve) and (+ve)pST. 123
Figure 42 Effects of β1 blockage on cell initial adhesion. 124
Figure 43 Representative images of Ishikawa endometrial cancer cell actin filaments staining. 126
Figure 44 Representative images of Ishikawa endometrial cancer cell actin filaments staining. 128
Figure 45 Ishikawa endometrial cancer cell NO secretion at 7mins and 24 hours with or without aldosterone on (f), (-ve) and (+ve)pST. 129
Figure 46 Boxplots of (A) pFAK and (B) Actin expression levels. 132
Figure 47 Percentage of adherent Ishikawa cells on glass, tissue culture grade pST, flat and (-ve)pMA at 6 and 60 hours. 140
Figure 48 Number of Ishikawa cells on glass, tissue culture grade pST, flat and (-ve)pMA at 60 hours. 141
Figure 49 Ishikawa cell numbers on (f)pST, (-ve)pST and (+ve)pST at 6 and 60 hours. 142
Figure 50 Ishikawa cell numbers on (f)pST, (-ve)pST and (+ve)pST of human dermal microvascular endothelial cell 60 hours. 144
Figure 51 Ishikawa endometrial cancer cell cyclin D2 expression on glass, tissue culture grade pST, (f)pMA and (-ve)pMA. 145
Figure 52 Ishikawa endometrial cancer cell PCNA expression on (f), (-ve) and (+ve)pST. 146
Figure 53 Ishikawa endometrial cancer cell (A) cyclin B1, (B) B2 and (C) D2 expression on (f), (-ve) and (+ve)pST. 147
Figure 54 Ishikawa endometrial cancer cell pERK/ERK on glass, tissue culture grade pST, (f)pMA and (-ve)pMA. 148
Figure 55 Ishikawa endometrial cancer cell ERK/pERK on (f), (-ve) and (+ve)pST. 149
Figure 56 Ishikawa endometrial cancer cell AKT/pAKT on (f), (-ve) and (+ve)pST. 150

Figure 57 Ishikawa endometrial cancer cell VEGF secretion with or without $CoCl_2$ and EGCG Treatments on glass, tissue culture grade pST, (f)pMA and (-ve)pMA. 179
Figure 58 Ishikawa endometrial cancer cell VEGF secretion with or without (A) cisplatin, paclitaxel and (B) $CoCl_2$, EGCG Treatments on (f), (-ve) and (+ve)pST. 180
Figure 59 Ishikawa endometrial cancer cell number with or without cisplatin and paclitaxel treatments on (f), (-ve) and (+ve)pST. 181
Figure 60 Ishikawa endometrial cancer cell PCNA expression with or without cisplatin and paclitaxel treatments on (f), (-ve) and (+ve)pST. 182
Figure 61 Ishikawa endometrial cancer cell (A) cyclin B1, (B) B2 and (C) D2 expression on (f), (-ve) and (+ve)pST with or without cisplatin and paclitaxel treatments. 184
Figure 62 Representative images of Ishikawa endometrial cancer cell morphology in culture medium without FBS. 194
Figure 63 Representative images of Ishikawa endometrial cancer cell actin filaments and Cytokeratin-18 staining. 195
Figure 64 Ishikawa endometrial cancer cells (A) spreading area and (B) circularity on (f)pST, (-ve)pST and (+ve)pST in medium without FBS. 196
Figure 65 Ishikawa endometrial cancer cell β1 integrin expression on (f), (-ve) and (+ve)pST, in medium without FBS. 197
Figure 66 Effects of β1 blockage on cell initial adhesion in serum-free culture medium. 197
Figure 67 Ishikawa endometrial cancer cell (B) FAK and pFAK expression and (C) pFAK/FAK on (f)pST, (-ve)pST and (+ve)pST in serum-free culture medium. 199
Figure 68 Ishikawa endometrial cancer cell pFAK/FAK on (f), (-ve) and (+ve)pST. 200
Figure 69 Ishikawa endometrial cancer cell FAK and pFAK expression and on (f)pST, (-ve)pST and (+ve)pST in serum-free culture medium at 3 hours. 201
Figure 70 Ishikawa endometrial cancer cell pFAK/FAK on (f), (-ve) and (+ve)pST at 3 hours. 201
Figure 71 Ishikawa endometrial cancer cell actin expression on (f)pST, (-ve)pST and (+ve)pST in serum-free culture medium. 203
Figure 72 Ishikawa endometrial cancer cell Cytokeratin-18 expression on (f)pST, (-ve)pST and (+ve)pST in serum-free culture medium. 203
Figure 73 Representative images of Ishikawa endometrial cancer cell actin filaments staining. 205
Figure 74 Ishikawa endometrial cancer cell NO secretion in serum-free medium with or without aldosterone at 7min and 24 hours. 206

Figure 75 Ishikawa cell numbers on (f)pST, (-ve)pST and (+ve)pST in serum-free medium at 6 and 60 hours. 208
Figure 76 Ishikawa endometrial cancer cell PCNA expression on (f)pST, (-ve)pST and (+ve)pST in serum-free culture medium. 208
Figure 77 Ishikawa endometrial cancer cell (A) cyclin B2 and (B) D2 expression on (f), (-ve) and (+ve)pST in serum-free culture medium. 209
Figure 78 Ishikawa endometrial cancer cell VEGF secretion with or without cisplatin and paclitaxel treatment on (f)pST, (-ve)pST and (+ve)pST in serum-free culture medium. 213
Figure 79 Ishikawa endometrial cancer cell number with or without cisplatin and paclitaxel treatments on (f)pST, (-ve)pST and (+ve)pST in serum-free culture medium. 214
Figure 80 Ishikawa endometrial cancer cell PCNA expression with or without cisplatin and paclitaxel treatments on (f)pST, (-ve)pST and (+ve)pST in serum-free culture medium. 216
Figure 81 Ishikawa endometrial cancer cell (A) cyclin B1, (B) B2 and (C) D2 expression on (f), (-ve) and (+ve)pST with or without cisplatin and paclitaxel treatments. 217
Figure 82 Venn diagrams of proteins identified from iTRAQ analysis of samples of culture with FBS and without FBS and the intersect protein between these samples. 233

List of Tables

Table 1 Materials and equipment used in this project including the suppliers and locations of distributors in New Zealand. 29
Table 2 Reagents and recipes used in this project.. 36
Table 3 A table showing average of total cell protein (mg/mL) of samples (f), (-ve) and (+ve)pST, in medium with or without FBS.. 50
Table 4 Summary of Results from Section 6.5.1.1, 6.5.2.1, 6.5.3.1 151
Table 5 Summary of Results from Section 6.5.1.2, 6.5.2.2, 6.5.3.2, 6.5.4.1 151
Table 6 List of proteins that were up-regulated or down-regulated in comparisons between (+ve) / (f)pST, (-ve) / (f)pST and (+ve) / (-ve)pST. 158
Table 7 The proteins under the functional group of DNA condensation. 160
Table 8 The proteins under the functional group of extracellular matrix proteins, cell structural and cell migration. 162
Table 9 The proteins under the functional group of signaling pathway. 164
Table 10 The up-regulated proteins under the functional group of cell energy modulation. 166
Table 11 The proteins under the functional group of cell growth and viability. 169
Table 12 The proteins with intermediary functions. 170
Table 13 Summary of results of section 8.5.2. 188
Table 14 List of proteins that were up-regulated or down-regulated in comparisons between (+ve) / (f)pST, (-ve) / (f)pST and (+ve) / (-ve)pST. 211
Table 15 Summary of Results from Section 9.5.7. 219
Table 16 The proteins under the functional group of cell stress response. 221
Table 17 The protein under the functional group of cell epigenetic regulation. 223
Table 18 The proteins under the functional group of cell growth. 225
Table The proteins under the functional group of cell cytoskeleton structure. 226
Table 20 The proteins under the functional group of cell signaling biomolecules. 227
Table 21 The proteins with intermediary functions. 228
Table 22 Summary of Results from Section 9.5.9. 236

List of Abbrevations

IGF-1	Insulin growth factor-1
NoRC	Nucleolar remodelling complex
(+ve)pST	Positive (hump-like) polystyrene Bioimprint
(f)pMA	flat polymethacrylate
(f)pST	flat polystyrene
(-ve)pMA	Negative (pit-like) polymethacrylate Bioimprint
(-ve)pST	Negative (pit-like) polystyrene Bioimprint
2D	Two-dimensional
2-DE	2-dimensional electrophoresis
3D	Three-dimensional
5-FU	5-fluorouracil
AFM	Atomic force microscope
AMP	Adenosine monophosphate
APC	Adenomatous polyposis coli
ATAC	Ada2a-containing
ATP	Adenosine triphosphate
BRCA1	Breast cancer 1
BRCA2	Breast cancer 2
BSA	Bovine serum albumin
Cdc 42	Cell division control protein 42
CDKN1A	Cyclin-dependent kinase inhibitor 1A
CHO	Chinese hamster ovary
CO_2	Carbon dioxide
CoA	Coenzyme A
$COCl_2$	Cobalt chloride
Cox-2	Cyclooxygenase-2
CSN5	COP9 signalosome complex subunit 5
DC	Detergent compatible
DMEMF12	Dulbecco's Modified Eagle Medium:Nutrient Mixture F-12
DMSO	Dimethyl sulfoxide
DNA	Deoxyribonucleic acid

DT	Dunning prostatic adenocarcinoma
DTT	Dithiothreitol
EC	(−)-epicatechin
ECG	(−)-epicatechin-3-gallate
ECL	Enhanced chemiluminescence
ECM	Extracellular matrix
EDTA	Ethylenediaminetetraacetic acid
EGC	(−)-epigallocatechin
EGCG	(−)-epigallocatechin-3-gallate
EGDMA	Ethylene glycol dimethylacrylate
EGF	Epidermal growth factor
EGFR	Epidermal growth factor receptor
EGTA	Ethylene glycol tetraacetic acid
ELISA	Enzyme-linked immuno assay
EMT	Epithelial-to-mesenchymal
eNOS	Endothelial nitric oxide synthases
ER	Endoplasmic reticulum
ERBB2	Receptor tyrosine-protein kinase erbB-2
ERK	Extracellular signal-regulated kinases
FA	Focal adhesion
F-actin	Filamentous actin
FAK	Focal adhesion kinase
FBS	Fetal bovine serum
FITC	Fluorescein isothiocyanate
FX	Focal complexes
G-actin	Globular actin
GAPDH	Glyceraldehyde 3-phosphate dehydrogenase
H_2SO_4	Sulfuric acid
HCC	Hepatocellular carcinoma
HCl	Hydrogen chloride
HDAC	Histone deacetylase
hENT1	human equilibrative nucleoside transporter-1

HMEC-1	Human dernal microvascular endothelial cells
HPMC	Hydroxypropyl methycellulose
HRP	Horseradish peroxidase
HSP	Heat shock protein
IC fixation buffer	Intracellular fixation buffer
IF	Intermediate filament
iNOS	inducible nitric oxide synthases
IRF8	Interferon regulatory factor 8
ITIH2	Inter-alpha-trypsin inhibitor heavy chain H2 precursor
ITPK1	Inositol-tetrakisphosphate 1-kinase
iTRAQ	Isobaric tags for relative and absolute quantitation
LH	Linker histone
LOX	Lysyl oxidase
MAPK/ERK	Mitogen-activated protein kinase/extracellular signal-regulated kinases
Me^{2+}	$Methyl^{2+}$
MIF	Macrophage migration inhibitory factor
MMP	Matrix metalloproteinase
mRNA	messenger RNA
MSCs	Mesenchymal cells
SV40	Simian virus 40
NaCl	Sodium chloride
NaOH	Sodium hydroxide
nNOS	Neuronal nitric oxide synthases
NO	Nitric oxide
NP-40	Nonidet P-40
NSCLC	Non-small cell lung carcinoma
polyHEMA	Poly-2-hydroxyethyl methacrylate
OxPhos	Oxidative phosphorylation
p53/TP53	Tumor protein p53
pAKT	Phosphorylated protein kinase B
PAM	Polyacrylamide

PBS	Phosphate-buffered saline
PBST	Phosphate-buffered saline-Tween®-20
PCNA	Proliferating cell nuclear antigen
PDMS	Polydimethylsiloxane
Pen/Strep	Penicillin/Streptomycin
pERK	Phosphorylated-extracellular signal-regulated kinases
pFAK	phosphorylated FAK
PI3K/AKT	Phosphoinositide 3-kinase/Protein kinase B
PLCγ-PKC	Phosphorylation of phospholipase-Cγ-protein kinase C
PLGA	Poly(lactic-co-glycolic) acid
pMA	Polymethacrylate
PMMA	Polymethylmethacrylate
POLD3	Polymerase(DNA-directed) delta 3
pST	Polystyrene
PTEN	Phosphatase and tensin homolog
PVDF	Polyvinylidene difluoride
Rac-1	Ras-related C3 botulinum toxin substrate 1
RGDS	L-arginylglycyl-L-α-aspartyl-L-serine
RGES	Arginyl-glycyl-glutamyl-serine
Rho	Ras homolog gene family
RIPA	Radio-immunoprecipitation assay
RMS	Root mean square
RNA	Ribonucleic acid
ROCK	Rho-associated protein kinase
ROS	Reactive Oxygen Species
RSV	Rous sarcoma virus
Scx	Scleraxis
SDS	Sodium dodecyl sulfate
SDS PAGE	Sodium dodecyl sulfate-polyacrylamide gel electrophoresis
SEM	Standard error of the mean
SHROOM2	Shroom family member 2
Skp-2	S-phase-associated protein

SLIRP	SRA stem-loop-interacting RNA-binding protein
SMARCA5	SWI/SNF-related matrix-associated actin-dependent regulator of chromatin subfamily A member 5
Src	Proto-oncogene tyrosine-protein kinase
S-S	Disulfide bond
STAT3	Signal transducer and activator of transcription 3 isoform 3
SVM	Seminal vesicle mesenchyma
TBS	Tris-buffered saline
TBST	Tris-buffered saline-Tween®-20
TCEP	Tris(2-carboxyethyl)phosphine
TEMED	Tetramethylethylenediamine
TMB	Tetramethylbenzidine
TPZ	Tirapazamine
TRIP6	Thyroid receptor-interacting protein 6
TRIS	Tris(hydroxymethyl)aminomethane
VEGF	Vascular endothelial growth factor
WICH	WSTF-ISWI chromatin remodeling

Chapter 1 Introduction

1.1 An Overview of Cancer Occurrence

Cancer is a disease in which cells can grow infinitely and immortally forming a tumour, and in malignant cases, cancer cells can spread to different parts of a body. Cancer remains the main cause of death for both males and females in New Zealand and accounted for one-third of deaths in 2011. In 2011, 21,050 cases of cancer were registered in New Zealand, and 8891 deaths were reported. Maori cancer registration rate is 391.8 per 100,000 and mortality rate of 206.4 per 100,000 population, which are higher than non-Maori population (registration rate 360.8 per 100,000 and mortality rate 137.7 per 100,000 non-Maori) according to the Ministry of Health (Ministry of Health, 2014). Besides, gynaecological cancer in New Zealand constitutes 10% of all cancer cases. Endometrial cancer is the most common gynaecological cancer, with about 315 new cases and 80 deaths reported every year (The New Zealand Gynaecological Cancer Foundation, no date). Also, endometrial cancer rates are higher in Maori women compared to European women in New Zealand, with the rate of 19.8 and 13.6 per 100,000, respectively (Ministry of Health, 2014). Among the identified risk factors for endometrial cancer are obesity, nulliparity, late menopause, consumption of Tamoxifen and family history. In this project, the Ishikawa endometrial cancer cell line was used as the model for endometrial cancer study.

Due to the complexity of cancer, finding a complete effective cure is a challenge for scientists. Surgical removal of a tumour was traditionally the only treatment for cancer yet it is limited to the localized tumour. Later in the mid-20th century, the first chemotherapy drug, chlormethine, was used to treat lymphoma (Gilman, 1963). Then, with the introduction of radiation therapy, surgery or chemotherapy was often used in combination with radiation therapy to treat cancer. Although these treatments could kill cancer cells successfully, they also killed normal cells and patients often experienced side effects such as hair loss, appetite loss, diarrhoea, nausea and vomiting or even an increased risk of developing a second

cancer. For this reason, treatments that cause less adverse side effects have been developed such as gene therapy, hormone therapy, immunotherapy or a combination of each with any other form of treatments. Though the side effects are less harmful, patients would still experience problems like depression, weight gain, hair loss and memory problems, to name a few. Also, these therapies are limited to certain types of cancers. Despite the limitations of these discussed cancer therapies, they still modestly lengthen the lives of patients, but clearly, more cancer research is needed in order to develop new therapies or improve the available therapies to optimize the treatment effects with minimized risk to patients.

The field of cancer research has been changing along with the expansion of knowledge in biochemistry, proteomics and biomolecular research. Cancer research has been focusing on finding the self-sustaining growth signals and anti-apoptotic characteristic of cancer cells and targeting relevant pathways aiming to eradicate them. Then, with an advance in molecular study technologies, scientists have started to hypothesize that these failing biochemistry functions of cancer cells are due to genetic defects. For instance, the risk of colorectal cancer increases with the presence of common gene variation near Cyclin-Dependent Kinase Inhibitor 1A (CDKN1A), polymerase (DNA-directed), delta 3(POLD3) and shroom family member 2(SHROOM2) genes (Dunlop et al., 2012). In addition to that, mutation of inheritable cancer susceptibility genes, like breast cancer 1 (BRCA1) or breast cancer 2 (BRCA2), has been known to increase risk of breast cancer and ovarian cancer (Welcsh & King, 2001).

Moreover, recent advancement in cancer genome sequencing enables further characterization of different types of tumour tissues, both primary and secondary tumours, and also the normal tissues adjacent to the tumours. With the whole genome analysis, tumours' genome sequence data, copy number and sequence variants, chromosomal translocations and fusion genes, gene expression, miRNA expression, and alternative splicing events can be profiled. Indeed, there is now a more defined characterization for different types of tumours with this technique, for instance, the use of whole genome sequencing has identified subtypes in 100 patients with pancreatic ductal adenocarcinomas (Waddell et al., 2015) and whole genome sequencing has been used to differentiate between

chemotherapy sensitive and resistant genotypes among 92 advanced ovarian cancer patients (Patch et al., 2015).

Many studies have identified the genes that can put a person at high risk of cancer, and this helps in cancer prevention, diagnosis and developing personalised medicine or helping in developing new treatments targeting the biological pathways that are affected by these genes. Yet recently it was realized that genetic and biochemical pathway defects are not the only explanations. To support this idea, a person can have multi-mutated cells without developing a tumour. For instance, a person with inherited mutated BRCA oncogene will have the gene in all cells but it will only increase risk of developing a tumour in breast tissue or ovary (Bissell & Hines, 2011). Moreover, another study that investigated chromosomal rearrangement of the normal lobules adjacent to breast tumours reported that the normal lobules with normal structure adjacent to tumour cells had an abnormal chromosomal rearrangement (Deng et al., 1996). This study shows that tissue cells with abnormal chromosomal arrangement can still have normal phenotype. It may be suggested that, according to the interpretation (Bissell & Hines, 2011) underlying this thesis, these pre-malignant cells may develop into cancerous cells when the microenvironment permits. For example, in addition to having normally functioning mutated cells, the human body could also have high percentage of tumours that are termed 'occult tumours', which exist as part of the tissue and will not develop into malignant tumour (Bissell & Hines, 2011). It has been suggested that a mutated cell will only turn into a cancerous cell or an occult tumour will only become a malignant tumour when their microenvironments are permissive (Bissell & Hines, 2011). Moreover, a series of hallmarks as steps in cancer progression has been postulated (Hanahan and Weinberg, 2000; 2011) and these have been used to underpin many studies. However this approach has resulted in only incremental improvements in treatments, which suggests other factors may be involved. Pickup et al. (Pick up et al., 2014) used the hallmark categories to present a discussion in favour of a pivotal role for the physical environment. For example, adhesion of cells to the ECM activated Ras, Rac GTPases and ERK and PI3K pathways (Schwartz & Assoian, 2001; Pylayeva et al., 2009) which enabled cancer cells to acquire self-sustained growth. Further, interaction of cells with the ECM and stiffening of tumour ECM inhibited growth suppressors (Kim et al., 2008; O'Connell et al., 2000; Mouw et al., 2014) and apoptosis (Lim et al., 2008; Lewis et al., 2002), increased the expression of telomerase (Kunimura et al., 1998), which is essential

for immortal growth and metastasis (Yu et al., 2009). Further, stiffened ECM enhanced angiogenesis (Montesano et al., 1983; Mammoto et al., 2009; Liu & Agarwal, 2010) and restructuring of the ECM promoted metastasis (Pathak & Kumar, 2012; Pickup et al., 2013). In addition, stiffening of the ECM may play a role in preventing immune destruction on cancer cells (O'Connor et al. 2012) by regulating cancer cell metabolism through PI3K signalling (Grassian et al., 2011; Zhang & Hochwald, 2014). Also, dysregulation of the ECM may promote genetic instability and mutations that ultimately contribute to cancer development (Radisky et al., 2005; Zhou et al., 1993).

The lack of attention in looking at cancer biomechanical features may explain why current cancer research is having a relatively low success rate. There appears to be a few gaps that need more attention when undertaking cancer research in order to improve or speed up the process of developing new cancer treatments. One of the issues would be to realize the importance of biomechanical modulation in cancer initiation and development and to incorporate this concept into the existing biochemical knowledge. Secondly, an *in vitro* model with incorporation of the concept of biomechanical signals should be developed.

Before emphasizing the need of studying the cancer cell microenvironment in tumour development and progression, the role of mechanical signals in normal tissue development and homeostasis is discussed first, followed by discussion of how a change in mechanical signals leads to tumorigenesis. And then some studies that investigated this area both in normal tissue and cancerous tissue are presented. And lastly, the outline of this thesis is included.

1.2 Role of Mechanical Signals in Normal Tissue Development

Mechanobiology is the study of mechanical signalling in the biological system whereas mechanotransduction is the cellular process of detecting mechanical stimuli and conveying them into intracellular biochemical signals. Biological tissues and cells are surrounded by extracellular matrix (ECM), neighbouring cells, basement membrane, fluids or

biomolecules. The interactions and contacts with surroundings expose the tissues and cells to mechanical stimuli. The ECM, which is the main mechanical mediator between cells and the surroundings, is a collection of structural biomolecules secreted by cells. Cells receive mechanical loads from the surrounding ECM or neighbouring cells and respond by changes in cell behaviours and structures, which subsequently affects the cytoskeletal generated force that acts on ECM, or affects the secretion of ECM proteins. Remodelling of ECM on the other hand further alters the force that acts on cells. This feedback-loop continues until a force balance between the cell and the ECM compartment is reached. The reciprocal force interaction between cell and ECM components is named mechanoreciprocity. Mechanoreciprocity remodelling of ECM was demonstrated in a study done by Lee et al. in which mechanical force but not growth factors triggered ECM restructuring (Lee et al., 2003). The reciprocal relationship is crucial for ensuring optimal cell and tissue growth and function and can be seen in many circumstances, e.g., changing the structure and the components of ECM during wound healing, tissue homeostasis maintenance (Bell et al., 1979; Ehrlich et al., 1991; Schiro et al., 1991) and during tissue formation as cells migrate through ECM (Grinnell & Lamke, 1984; Harris et al., 1981; Klein et al., 1991). The mechanical forces that act on tissues and cells exist in different forms; these include compression and tensional force, hydrostatic load and shear force. Compression and tensional forces are forces that are applied perpendicular to the surface, such as the force acting on or from neighbouring cells or ECM; whereas shear forces are forces that are parallel to the surface such as the force of blood flow that acts on endothelial cells of blood vessels.

Though biochemistry, molecular biology and genetics explain a lot about the development of biological systems, mechanical signalling is also an important mechanism to manipulate tissue development and homeostasis, maintain cell uniform growth and regulate cell migration or differentiation. Physical forces have been actually appreciated to be important in organ or tissue development and tissue shape regulation since early in 1945 (Thompson, 1945). The ECM structure that determines its mechanical properties must be spatially and temporally well-controlled because optimum tissue function and morphology development requires different stiffness and arrangement of ECM fibres. One of the examples of mechanical signal regulation of biological structure formation can be seen in the growth of *Drosophila melanogaster* wing imaginal disc; slower growing cells in the vicinity of faster-

growing cells would undergo apoptosis to maintain uniform growth. The mechanism behind this distance regulation was proposed to be through mechanical feedback (Shraiman, 2005). More examples of mechanical cues in the regulation of tissue development can be seen in lung development in which mechanical forces resulting from lung expansion determines fetal lung structure development (Hooper & Wallace, 2006), and the types of mechanical force (distension or contraction) determines the phenotypic expression of alveolar cells (Dobbs & Gutierrez, 2001). Another example is the formation of vessels such as blood vessels and lymph vessels; it has been observed that under high unidirectional fluid shear force, the cytoskeleton of the vascular endothelial cells (ECs) formed a uniform structure aligned with the flow direction, which resulted in ECs elongation, and formed tube-like structures. Oppositely, ECs arranged themselves randomly under low shearing force (Dai et al., 2004; Tzima et al., 2002; Tzima et al., 2001).

Not only initial tissue development and formation are influenced by environmental forces. Throughout the lifetime of an organism, tissue homeostasis is also manipulated by forces. For example, through frequent exercises, bone tissues would experience compression stress constantly which subsequently resulted in high hyaluronan in articular cartilage that gave a stronger bone structure; on the contrary, less motility could cause loss of hyaluronan and aggrecan, which was the main cause of arthritis-associated joint degeneration (Haapala et al., 1996). Also, the muscle built up resulting from frequent exercise, was the result of mechanical tension stimulation of the formation of myofibrils of skeletal muscle (Weitkunat et al., 2014). The need of mechanical signals in tissue homeostasis also can be seen in an acute tendon injury mouse model. In a normal physiological situation, mechanical forces regulated the expression of Scleraxis (Scx) which was required for the formation of tendon tissue, whereas when injury occurred, in which the mechanical signals were disrupted, force-regulated secretion of TGF-β led to tenocyte death (Maeda et al., 2011). Also, in cases of acute injury such as bone fracturing, biomechanical signals were needed for bone repairing (Chao et al, 2003).

In addition to tissue development and homeostasis, physical signals are also important in cellular development and maintenance, in which cells interact dynamically and bi-directionally with the surrounding biomechanical signals. Cell responses to external

biomechanical signals depend on the nature of the mechanical signal such as the type, magnitude, direction or duration of the experienced force signal. Different influences of different biomechanical signals can be seen in a study which showed that cyclic force stimulated higher protein tyrosine phosphorylation than continuous force in an osteoblastic cell line (Schmidt et al., 1997). Besides, cell features that are regulated by mechanical forces are cell shape, motility, growth and differentiation. An example in mechanical signal regulation of cell shape and cell motility is in the regulation of PC-12 neurite morphology and motility, which involved compression force alignment of neurite microtubules (Dennerll et al., 1988). On the other hand, it has been shown that the early phase of axon growing required an exertion of forces to the surroundings from the growing cones at axon tips (Betz et al., 2011; Lamoureux et al., 1989); then in the late phase, it required a pulling force from target tissue, a process that has been termed stretch growth (Weiss, 1941). Furthermore, by using a stretchable substrate, Chang and his colleague showed that the extension of neural stem cell's neurite and axon was enhanced with increased substrate stretching and neurite outgrowth was oriented along with substrate stretching, moreover, neural stem cell differentiation depended on the direction of stretching, i.e. parallel or perpendicular stretching (Chang et al., 2013). Other examples of biomechanical signal regulation of cell fate were the force-stimulated differentiation of keratinocytes (Gormar et al., 1990), and also differentiation of breast epithelial cells into tubules, which were found to be modulated by the collagen density and rigidity in ECM (Wozniak et al., 2003).

Clearly, mechanical signals are important in regulating tissue and cell development and homeostasis. In fact, in the past decades, collaborations between engineers and biologists have enabled an incorporation of mechanical studies in laboratory cell studies. Different culture substrates and culture models have been developed and cells are observed to behave differently in the presence of different mechanical signals.

1.3 In Vitro Culture Substrate and Its Influence on Cultured Cells

In vitro cell culture was first done in 1907 by Ross Harrison (Harrison, 1907). Thereafter cultures were grown as an explant culture, as hanging drop or at the bottom of glass flasks

and petri dishes. In the mid-1900s, due to the disadvantages of using glass as culture substrates because of low cell attachment for primary cell lines and the need of careful cleaning, disposable polystyrene (pST) started to be used as cell culture substrate. In addition to the ease of handling, pST is easy to mould and can be surface treated by either corona discharge or by gas plasma treatment to enhance cell attachment. However, both glass and pST culture substrates are unnatural flat and hard surfaces for cells to attach and grow on; and following the appreciation that mechanical signals from the cell microenvironment is one of the factors that controls cell behaviours, the making of biomimetic substrates that have the same or similar physical features to the cell microenvironment is especially important in tissue engineering, tissue implantation and in understanding the role of these forces in cell development.

The most studied aspects of physical microenvironments that change cell behaviours are stiffness and surface topography. The stiffness of the cell microenvironment determines the compression force that acts on cells. In the laboratory setting it has been observed that motility of cells is dependent on the microenvironment stiffness in which fibroblasts and smooth muscle cells move and migrate towards a stiffer culture environment (Wang et al., 2001; Wong et al., 2003). Furthermore, in an absence of cell-cell adhesion, fibroblasts and endothelial cells can only spread on stiff but not on soft surfaces (Yeung et al., 2005). Culture substrates with tailor-made stiffness can be produced by using biocompatible materials such as polydimethylsiloxane (PDMS), polyacrylamide (PAM) gel, hydrogel and so on. Alternatively, cells are grown as a cluster or as a 3D Matrigel model in which the cells are in a 3D microenvironment with stiffness similar to the real tissue environment. Evidence has shown that cells cultured in the 3D model behaved differently to cells cultured on a flat surface. Cells growing in 3D culture showed different adhesion patterns (Cukierman et al., 2001), shape, proliferation and gene expression (Gruber & Hanley, 2000). Though 3D culture is the most physiologically relevant *in vitro* cell culture model, it has relatively high cost, and complex handling compared to conventional 2D cell culture making it not an ideal model to be used for investigating elementary biochemical questions such as preliminary investigation of cell responses to drugs, secretion level of cytokines and high throughput screening assays. Hence, a model that is simpler than the 3D model but an improved 2D culture that incorporates the physical factors would be ideal for ‘preliminary’ drug studies before moving on to the 3D culture.

On the other hand, the surface topography is another physical feature that gives cells mechanical signals, and the cell responses to surface geometry are termed topographic cell responses. Topographic influence on cells will be discussed in more detail below because this is the main focus of this project. The ECM surrounding cells consists of curvature, grooves, ridges, holes or lattice structures. These different geometries would influence the cell adhesion, spreading, orientation, polarity, migration, growth and functions. In fact, topographic cell responses were described early in cell culture history as contact guidance of cell growth (Weiss, 1941).

New advances of nanofabrication techniques such as soft lithography (Liliensiek, et al., 2006), micro-photopatterning (Gilchrist et al., 2014), capillary force lithography (Kwon et al., 2011), microscope projection photolithography (Kwon et al., 2011), electron beam lithography (Teixeira et al., 2003; Tsimbouri et al.,2013; Wood, 1988), photo lithography (Hamilton et al., 2007; Murugan et al. 2010), and self-assembly monolayers (Murugan et al., 2010; Mrksich et al.,1996) enable the making of substrates with controlled topography. Substrates with controlled and designed topography; such as grooves (Hamilton et al., 2007; Nikkhah et al., 2012; Rovensky, 2011; Wood, 1998), columns (Rovensky, 2011), pitch (Hamilton et al., 2007; Nikkhah et al., 2012), pillars (Nomura et al., 2006), pores (Zinger et al.,2004) and surface roughness (Dalby et al., 2007; Kawahara et al., 2004) have started to be used in guiding cell position and differentiation.

However due to the diversity of scales, materials and the cell types studied, the precise mechanism of how cells sense and respond to surface topography remains unclear. The current idea is that cell spreading is constrained by the topography which then changes the distribution of adhesion molecules and the alignment of actin filaments that are connected to signalling molecules, thence triggering signalling pathways according to the spatial and temporal distribution and activation of the adhesion molecules (Anselme et al, 2010; Chen et al., 1997; Frey et al., 2006; Maheshwari et al., 2000; Provenzano& Keely, 2011; Yim et al., 2010).

A well-designed study done by Chen and his co-workers showed how adhesion area affected cell behaviours. They created substrate surfaces designed with adhesive islands of different sizes, which allowed control over the cell adhesion surface areas. They elegantly showed that spreading on a larger area was required for cells to survive and grow, and cells could not survive when their spreading and shape formation were restricted on substrate surfaces (Chen et al., 1997). Further, because cells adhere to their microenvironment through transmembrane receptors and integrins, a study that modulated the cell integrin-mediated adhesion showed that cell adhesion was linked to one of the three components of the cell cytoskeleton, actin filaments. In this study, integrin ligand spatial density and distribution were controlled and fabricated on culture substrate, and cells with different integrin clustering were seen to have different organization and motility of actin filaments (Maheshwari et al., 2000). The idea that cell response to topography is actin filament-dependent is supported by the observations that different cell lines with various actin arrangements have different topographical responses. Fibroblasts, for example, are cells that have bundles of straight actin filaments; Dunn showed that fibroblasts failed to bend at an angle $>16^{o}$ degree because the actin bundles made them resistant to bending (Dunn & Heath, 1976). This restriction in bending was not observed in endothelial cells because endothelial cells have less straight actin bundles and so they were shown to be more flexible in curving on surfaces (Rovensky, 2011). Hence, surface topography affects cell spreading and movement through modulating the cell's actin structure.

An alteration in actin filaments stretching or bending will activate the formation of focal adhesion (FA), which is an assembly of biomolecules that regulates transmission of mechanical signals between cells and their extracellular matrix. By culturing cells on nano-scaled pattern substrates, cell actin microfilaments and FA were observed to align along with nano-scaled features; also, the width of ridge defined the width of FA formed (Teixeira et al., 2003). Another study that quantified the force applied from cells on patterned elastomer substrates reported that the force had linear dependency on the area and intensity of focal adhesions formed between the cells and the substrate surface (Balaban et al., 2001).

Eventually, the cell FA formation, distribution and activation (through phosphorylation of focal adhesion kinase (FAK)) determine the downstream signallings that are linked to FA and change the cell behaviours including cell proliferation, differentiation and cell secretion. For instance, cells adhered on surfaces with groove topography activated the mitogen-activated protein kinase/extracellular signal-regulated kinases (MAPK/ERK) pathway through phosphorylation of FAK-Proto-oncogene tyrosine-protein kinase (Src) complex, yet on flat substrates, MAPK/ERK activation was FAK-Src independent (Hamilton & Brunette, 2007). Also, fibroblasts reduced growth on a rough surface (Pennisi et al., 2011) and epithelial cells decreased growth on grooved surfaces (Liliensiek et al., 2006). Furthermore, bone cell differentiation can be modulated by surface roughness (Dalby et al., 2007; Kawahara et al., 2004; Lim et al., 2005). For example, Dalby and his colleagues showed that mesenchymal stem cells can be stimulated to differentiate and produce bone mineral with osteoblastic morphology on nanotopography polymethylmethacrylate (PMMA), without any chemical stimulant. Also, the effect was regulated by the shape and distribution of the nano-pattern (Dalby et al., 2007). On the other hand, cell functional behaviours such as fibroblast secretion of tenascin decreased on grooved titanium surfaces (Goto & Brunette, 1998) and the half-life of the secreted matrix metalloproteinase (MMP)-2 messenger RNA (mRNA) was altered on grooved surfaces (Chou et al., 1998). A recent detailed study showed that nanotopography changed the mesenchymal stem cell adhesion and the cell nuclear architecture. Changes were observed at the chromosomal level in which the packing of chromosomal territories within the nucleus were altered, and this influenced the transcription activity and functional signalling of cells. They further showed that the alteration at the cellular and nuclear levels was depended on the arrangement of the nano-scaled pits (Tsimbouri et al., 2014).

In summary, cell behaviours can be modulated through modification of cell culture substrate stiffness or substrate surface physical topography.

1.4 Mechanical Signals in Tumorigenesis

Under normal circumstances, cells are in a balanced mechanical feedback loop with their surroundings. During different development stages or when cells are encountering pathological changes, there will be a change in the biomechanical signals acting from the microenvironment on cells or vice versa. When the mechanical feedback loop fails to reach a balance, cancer may develop.

Normal cells can only grow and function normally in a microenvironment with appropriate stiffness and structure; transformed cells, on the other hand, lose the ability to probe their microenvironment stiffness and can spread and grow indefinitely regardless of abnormal environment stiffness. For example, Wang et al. showed that normal fibroblasts were able to sense alterations of stiffness of their environment and then exerted traction force and generated a force feedback loop with their environment. On the contrary, transformed fibroblasts lost the ability to probe the surrounding stiffness. The loss of this ability led to maintained growth, anti-apoptotic, enhancing spreading and continuous traction force generation of fibroblasts regardless of the stiffness of the environment (Wang et al., 2000). All these characteristics lead to the adhesion-independent growth of cancer cells. Cancer studies in the past decades have focused on biochemistry, proteomics and especially biomolecular properties. In fact, there is a need to include mechanobiology in tumorigenesis as there is increasing evidence showing that an alteration in mechanical properties of tissue and cell is part of tumorigenesis.

There is evidence in laboratory studies that showed the role of microenvironment in tumour formation. Rous sarcoma virus (RSV), which is an oncovirus, has been shown to transform fibroblast culture derived from chick embryo and caused the formation of sarcomatous tumour in newly hatched chicks. Nevertheless, RSV was not tumorigenic when it was injected into chick embryos *in ovo* (Dolberg & Bissell, 1984; Stoker et al., 1990). Interestingly, the extracted cells from the *in ovo* chicken embryo injected with RSV showed transformed phenotypes when cultured in a 2D laboratory setting (Dolberg & Bissell, 1984). These studies may imply that the microenvironment of the embryos, which is lost in

culture conditions, is required to attenuate the oncovirus transformation. Also, the role of microenvironment in regulating cancer cell phenotype can be illustrated using HMT-3522 human breast cancer cell series; these cells originated from breast luminal epithelial cells. The cells of < 200 passages are non-malignant, do not form tumours in nude mice and are called S1 cells; whereas T4-2, are cells derived from S1, are premalignant and form tumours in nude mice. Both of these cells, however, did not have a distinguishable phenotype when cultured on 2D tissue culture plastic, but only if they were cultured on 3D basement membrane, S1 cells formed functionally normal acinar structure whereas T4-2 cells formed irregular colonies (Howlett et al., 1995). Furthermore, Wang's group observed coupled and bidirectional modulation of β1-integrin and epidermal growth factor receptor (EGFR) signalling in T4-2 cells; the expression level and activation of each β1-integrin and EGFR were observed to be correlated with each other. Most importantly, this was observed only in 3D basement membrane models and not on 2D culture models, which implies that the structure or the chemical cues from the microenvironment of cells regulate the coordination of receptors (Wang et al., 1998). In agreement with this was the finding that senescent fibroblasts, the number of which increased with aging, stimulated preneoplastic and malignant fibroblasts growth, largely due to topography of ECM secreted from senescent fibroblasts, and only partly due to soluble secreted factors (Krtolica et al., 2001). In short, tumorigenesis is associated with defects in cell mechanical homeostasis.

Mechanical defects found in tumorigenesis are stiffening of tumour microenvironment (Akiri et al., 2003; Levental et al., 2009; Paszek et al., 2005; Provenzano et al., 2006; Zhao et al., 2010), restructuring of ECM (Carey et al., 2013; Kraning-Rush et al., 2012), alteration of mechanical features of cancer cells themselves (Cross, et al., 2007; Lekka et al., 1999) and also malfunction of oncogenes that are responsible for cell mechanical signalling (Martin et al., 2012; Nelson et al., 2012; Rathje et al., 2014).

Tumours are always more rigid than normal tissues, and so the mechanical signals acting from and on cancerous cells must be different from that of normal cells. For example, development of normal mammary gland to invasive cancer was associated with stiffening of the tissue and the stromal tissue surrounding it (Levental et al., 2009; Paszek et al., 2005; Provenzano et al., 2006). Tumour tissue was found to be stiff due to excessive fibrosis

(Akiri et al., 2003) and cross-linking between collagen and elastin (Decitre et al., 1998; Levental et al., 2009; Provenzano et al., 2006). Another illustration for stiffer tumour stroma can be seen in hepatic cirrhosis disease. Hepatic cirrhosis is a major cause of hepatocellular carcinoma (HCC). It was found that hepatic cirrhosis was always associated with higher fibre deposition in ECM before developing into HCC (Zhao et al., 2010). Furthermore, the observation of stiff tumorous microenvironments may explain why aging is one of the factors that increases the risk of cancer; in addition to accumulation of genetic defects, the loss of collagen resulted in increased stromal stiffness and promoted tumour development (Boyd et al., 2007; Wolfe, 1976). In addition, smoking-related lung cancer can also be linked to an alteration in tumour microenvironment. Nicotine, the main component of tobacco in cigarettes, was found to promote non-small cell lung carcinoma (NSCLC) cells proliferation, and one of the mechanisms of nicotine-stimulated NSCLC proliferation was through increasing expression of an ECM glycoprotein fibronectin that altered the ECM mechanical properties (Zheng et al., 2007).

An alteration in the stiffness of the tumour microenvironment is a process that assists tumour development. Cells in a stiff environment could adhere better and spread wider than cells on soft tissue by forming greater number of FAs and increasing Rho-associated protein kinase (ROCK) and Ras homolog gene family (Rho)-generated actin cytoskeleton contraction (Paszek & Weaver, 2004; Paszek et al., 2005). Furthermore, overexpression of the proteases MMP such as MMP1, MMP2 and MMP26, all of which are markers of metastasis, has been observed in the stiff tumour stroma (Kajita et al., 2001; Marchenko et al., 2001; Milkiewicz et al., 2007; Park et al., 2000; Sato et al., 1994; Uria & Lopez-Otin, 2000). Moreover, fluid shear stress, which is always elevated in a lump of tumour, has been shown to increase the cell secretion of insulin growth factor-1 (IGF-1) and vascular endothelial growth factor (VEGF) B and D that in turn induced cancer cell invasion (Wang et al., 2014). The secretion of growth factor promotes tumour growth whereas VEGF promotes abnormal angiogenesis in tumours. Further, an increase in compression force from ECM disrupted blood flow of existing vasculature around the tumour, which then caused a hypoxic condition in tumours that subsequently elevated cell VEGF secretion (Harris, 2002). Additionally, the elevated compression force shrunk intercellular interstitial space and caused an increment in the local concentration of growth factor and cytokines. This facilitated and enhanced auto-and paracrine signalling pathways that promoted tumour

growth (Tschumperlin et al., 2004). Nevertheless, the requirement of a stiffer microenvironment on cancer invasion is not always the case and is varied for different cancer types. Ovarian cancer, for example, showed epithelial-to-mesenchymal (EMT) morphology, increased polarization, migration, proliferation and chemoresistance on a soft substrate (McGrail et al., 2014). Though ovarian cancer growth and invasion requires a softer microenvironment, the role of physical features in cancer development is undeniable.

An alteration in the topography or the ECM physical structure is also an important factor that regulates cancer cell invasion. Cancer cells restructure their microenvironment to assist them to migrate through. For example, cancer cell remodelling of ECM increased the metastatic potential of cells (Kraning-Rush et al., 2012). Local invasion along the collagen fibres was observed when the collagen aligned perpendicularly to a tumour explant whereas invasion was suppressed when collagen alignment resembled the alignment in a non-invasive region (Provenzano et al., 2008). A tumour explant cultured on a randomly organized collagen matrix realigned the collagen fibres in a contractility-dependent manner that involved the Rho/Rho kinase pathway, which then promoted local cell invasion along the aligned collagen fibres (Provenzano et al., 2006; Provenzano et al., 2008). The need for an 'invasive' ECM structure for metastasis cancer can also be shown by Carey's lab study which showed that cell invasion was preceded by restructuring of ECM through cell-contractility realignment of ECM and proteolytic track making (Carey et al., 2013).

At the cellular level, cancerous cells are softer than non-cancerous cells. For example, the scanning force microscopic measurement of Young's modulus (a measurement of elasticity of a material, which is defined as the ratio of stress to deformation along an axis) showed that cancerous cells had lower Young's modulus than the normal cells (Lekka et al., 1999) and the softness of cells correlates to the metastatic state of cells in which metastatic cells are softer than benign cells. Cross found that metastatic cancer cells were 70% softer than the benign cells from a single patient's body fluid sample (Cross et al., 2007). There are a few factors that may explain the observation of cancer cells softening; firstly, cells soften prior to proliferation (Fritsch et al., 2010) and this was reported to be partly because filamentous actin depolymerizes and globular actin diffuses throughout the cell body as cells are entering the mitotic phase from interphase (Sanger, 1975). The soft phenotype is maybe

just part of the cancerous transformation since cancer cells are cells that proliferate continuously. Secondly, metastatic cells are cells that invade different parts of the body by moving through small openings of the basement membrane, cell-cell gaps and so on; hence, soft cells can move and squeeze through easier than hard cells.

Cancer has been related to mutations or enhanced oncogene expression; and one of the linkages between biomechanics and tumorigenesis is through activation of oncogenes that are responsible for the regulation of mechanobiology on the cytoskeleton of the cells. For instance, oncogenes such as simian virus 40 (SV40) large T antigen, c-Myc, and cyclin E were found to increase cell stiffness through up-regulating tubulin deacetylase histone deacetylase 6 (HDAC6) that increased the width of vimentin fibers and disrupted the structure of the vimentin network to a more entangled assemblage (Rathje et al., 2014). Moreover, these oncogenes also changed the spatial distribution of acetylated microtubules (Rathje et al., 2014). Oncogenes can also change the cell mechanical properties through regulating the cell actin cytoskeleton. An example of a mutated gene in cancer is the adenomatous polyposis coli (APC) tumour suppressor protein gene mutation that causes sporadic and hereditary colorectal cancer. Mutated APC was found to depolymerize actin filaments at the cell migration tip (Nelson et al., 2012). Hence, the presence of mutated APC disturbs directional cell migration as in normal gut maintenance and eventually puts cells in pre-cancerous state and increases the risk of colorectal cancer. Oncogene activation can also alter the cell sensitivity to mechanical stimuli from the surroundings, hence promoting cancer development. A specific example is the expression of receptor tyrosine-protein kinase erbB-2 (ERBB2), which is associated with a bad prognosis in breast cancer. The induction of ERBB2 increased the cell sensitivity to biomechanical stimuli and resulted in temporal up-regulation of 46 cytoskeletal genes; a further analyses of 766 breast cancer patients showed that 12 of these 46 cytoskeletal genes were associated with metastatic breast cancer (Martin et al., 2012).

Tumour initiation and development is closely related to dysfunction in mechanical signalling. Hence, there is a need to incorporate mechanical studies in cancer research.

1.5 Tumour Mechanotransduction Studies

The concept of mechanical effects on cancer initiation and development is relatively new and so fewer studies have investigated mechanotransduction in cancer cells compared to stem cells, fibroblasts and so on. But studies have now started aiming to alter the mechanical signals acting on cells by changing the tumour microenvironment or by actively exerting force on tumours. These studies show that tumour characteristics can be reversed back to normal just by altering the tumour microenvironment mechanical signals. The first example is a study that examined the influence of normal mesenchymal cells on neoplastic Dunning prostatic adenocarcinoma (DT) development. In this study, DT alone and recombinant of DT + seminal vesicle mesenchyma (SVM) were grafted in mice, and the tumorigenicity and growth of grafted cells were examined after 3 months. The presence of normal SVM cells was shown to reduce tumorigenicity and growth of DT (Hayashi & Cunha, 1991). Furthermore, another study showed that the compression force stopped the growth of malignant breast cancer tissue and changed the unorganized growth back to normal acini structure (Yang, 2012). Moreover, 3D culture which is less stiff than tumour microenvironment could revert cancer cells back to near normal phenotype (Howlett, Petersen, Steeg, & Bissell, 1994) and turned endometrial cancer cells to a less malignant appearance with slower growth behaviour (Chitcholtan et al., 2013). Also, by preventing ECM remodelling and stiffening such as through inhibiting lysyl oxidase (LOX)-dependent cross-linking of collagen, the chances of tumour formation and growth of an existing tumour were lowered (Wang et al., 1998; Weaver et al., 1997) and focal adhesion activation, PI3K activity and breast malignancy were also reduced (Levental et al., 2009).

In addition to targeting the tumour vicinity or changing the tumour mechanical properties directly, scientists also started to target cell-ECM receptor, cell cytoskeleton or biomolecules that are known to be mechano-sensitive, for example, integrin, focal adhesion molecules and actin cytoskeleton. Integrin is the cell's main adhesion molecule that anchors cells to the ECM. The total and surface expression of β1 integrin of cancerous cells has been found to be different from those of non-cancerous cells as cancer cells showed higher expression of β1 integrin (Weaver et al., 1997). In a study that blocked β1 integrin using antibody, T4-2 cells normalized their morphology and formed functional acini with normal

basement membrane structure, cell-cell contact, cell polarity and actin cytoskeleton arrangement. Moreover, these normalised cells reduced growth and became less tumorigenic when injected into nude mice (Weaver et al., 1997). Not only targeting integrin (Rucci et al., 2015; Taga et al., 2002) but targeting other adhesion molecules such as FAK, which is the downstream molecule of β1 integrin (Shanthi et al., 2014) also showed promising results in reducing tumorigenesis of cancer cells. Also, Chondramide that acts to prevent cell actin contractility may potentially inhibit tumour cell invasion (Menhofer et al., 2014).

The realization that cancerous cells have different mechanical features than normal cells led to studies that investigated cancer diagnosis and treatment monitoring based on measurement of cancer cell mechanical properties. For example, oral squamous cell compliance was quantified using microfluidic optical stretchers as a diagnosis of malignant change (Remmerbach et al., 2009). Moreover, examination of cell or tumour stiffness can be useful to predict drug responsiveness in patients. For instance, the drug transporter, human equilibrative nucleoside transporter-1 (hENT1), is correlated with patients' response to chemotheraphy; meanwhile hENT1 is also related to the stiffness, morphology and EMT state of cancer cells. Hence quantification of cancer cell stiffness can be useful in predicting drug response (Lee et al., 2014).

All these examples show that the tumour is an abnormal tissue structure, and the formation of it involves the defect of many components, hence cancer cells should be studied 'in a context' with their microenvironment. In other words, the microenvironment is important in the formation of a tumour. Though mechanical studies of cancer are at its early development stage, this field of study surely has many implications for finding new cancer therapies and improving cancer diagnosis.

1.6 In Vitro Culture Substrate in Cancer Studies

As illustrated above, where the non-malignant S1 and the malignant T4-2 cells do not show any morphological differences when cultured on 2D culture substrate, clearly the conventional cell culture on flat 2D surfaces is not a model similar enough to represent the real physiology of cells. Moreover, cells growing on fibronectin or collagen were less affected by doxorubicin compared to cells growing on flat plastic (Fourre et al., 2008; Millerot-Serrurot et al., 2010). Work from our laboratory showed that endometrial cancer cells in 3D culture were more resistant to drugs compared to cells grown on flat surfaces (Chitcholtan et al., 2012). This implies that the cell microenvironment can affect drug efficiency, which may explain why drugs that show promising results in 2D laboratory study fail in clinical studies. Furthermore, this also highlights that the physical features of the microenvironment should be considered in drug studies for a more accurate result.

The mechanical factors that influence cancer have been mostly focused on stiffness since one of the abnormalities of tumours is their altered stiffness, and cells cultured in a 3D model are becoming more common in cancer studies. Relatively few studies have investigated the topographical effect on cancer. In fact, topography is also important in regulating cancer cell morphology, adhesion and motility. For instance, on poly(lactic-co-glycolic) acid (PLGA) surfaces with nano-scaled spherical surface topographies, the lung cancer epithelial cancer cells reduced adherence at the low Root Mean Square (RMS) roughness surface compared to the surface with higher RMS surface roughness (Zhang et al., 2010a). Another study that was not intended to examine the effect of topography on cancer cells, but instead to study PDMS surface topography and wettability effects on cancer and non-cancerous cells in general, found that HeLa and 3T3 fibroblast attachment and growth were modulated by surface topography, independently from surface wettability (Kidambi et al., 2007). This behaviour of HeLa cells agreed with an earlier study, that found that HeLa cells adhered differently with different actin cytoskeleton arrangement on a surface of patterned nanopillars compared to a flat counterpart (Nomura et al., 2005). Moreover, human colon cancer cells showed preferential adherence and migrated towards the nanostructured area on a hierarchically patterned micro-and nano-structure (Kwon et al., 2011). Also, prostate cancer cells had been shown to migrate along grooved substrates

(Sarna et al., 2009). All these studies pointed out that cancer cells do sense substrate topography and are responsive to it.

A few studies that investigated the spreading of normal versus transformed cells on topographies such as cylindrical and grooved patterned surfaces showed that the responses of cells are cell type dependent and different on different topographies, and most importantly, transformed cell responses to topographic mechanical signals are different from normal cell responses. For example, a study that compared the effects of stiffness and topography on normal fibroblast (3T3) and transformed fibroblast (SaI/N) observed that the stimuli of substrate stiffness on normal fibroblast spreading and motility was more than the influences of substrate topography; yet transformed cells were nevertheless more sensitive and responsive to topography than stiffness (Tzvetkova-Chevolleau et al., 2008). Furthermore, on cylindrical topography, transformed fibroblasts were less elongated and lost the orientation along the cylinder compared to normal fibroblasts. On the other hand, opposite behaviours were observed for epithelial cells, where normal epithelial cells could bend and spread along the curvature of the cylinder, transformed epithelial cells showed increased elongation and guided alignment on the cylinder with the longitudinal arrangement of actin filaments (Rovensky, 2011). Besides, on surfaces with 15, 25 and 40 µm depth groove and 80, 155 and 200 µm space between grooves, respectively, normal fibroblasts migrated directionally from the bottom of the grooves to the area between grooves, whereas transformed fibroblasts remained in the grooves with some showing random movement from the bottom of the grooves to the area between grooves (Rovensky et al., 1971; Veselý et al., 1981).

The observation of distinct responses from normal and transformed fibroblasts and epithelial cells to substrate topography may be because fibroblasts and epithelial cells have different actin filaments alignment, and that transformed fibroblasts and epithelial cells similarly have altered their actin filaments differently from each other. Transformed fibroblasts were deprived of stress fibres compared to normal fibroblasts, hence they were less resistant to bending and spreading around the cylinder but transformed epithelial cells acquired more bundles of actin filaments, hence they were more reluctant to bend over cylinders (Rovensky, 2011). On the other hand, the groove side slope of 90^{o} degree prevented

fibroblasts from bending in the bottom of the grooves and so normal fibroblasts preferentially migrated and stayed in the area between grooves, yet transformed fibroblasts with fewer actin bundles either stayed in the bottom or moved up to area between grooves (Rovensky, 2011). These observations suggest that transformed cells can alter the cell mechano-sensitive structures that change the cell responses to topography and that cancer cell topographic responses are different from normal cells. This indicates that topographical influences on cancer cells should also be considered to be as important as the influence of stiffness on cancer development.

1.7 Bioimprint

Though the above illustrations have shown that the use of patterns gives cells the mechanical signals that change the cell behaviours, yet these regular patterns are still not the topography that the cells would encounter in a real cell microenvironment. It has been observed that there is dynamic force interaction between cells and the structured microenvironment (Albert & Schwarz, 2014; Gilchrist et al., 2014), which *in vivo*, consists of neighbouring cells. Here a substrate imprinted with cell-like topography is used to examine topographic responses of Ishikawa endometrial cancer cells. This newly developed culture substrate is named a Bioimprint. A Bioimprint is made by a technique that combines biological cell culture with soft lithography imprint technology to produce a substrate that duplicates a biological cell surface and hence creates a hard copy of the cell surface (Muys et al., 2006; Muys et al., 2006; Samsuri et al., 2010). The Bioimprint contains the topography of cells, making it a culture substrate encoded with the real cell topography and more closely resembles the physical micro-and nano-environment of cells.

The Bioimprint was first developed to make a substrate for the atomic force microscope (AFM) to examine exocytosis processes in cancer pathology (Muys et al., 2006). Exocytosis is a cellular process of secreting cytokines or hormones from intracellular to extracellular compartments; it involves the fusion of intracellular vesicular membrane with the cellular membrane, thence releasing the biomolecules contained in the vesicles. The examination of the membrane surface features regarding the rate and spatial distribution of exocytosis

process is thus useful to check on the cell physiological status. AFM is an extremely valuable tool in this regard due to the high resolution surface scanning ability to probe any invaginations across the membrane. However, AFM is not suitable for examining soft biological specimens as the scanning process of the probe will damage the soft biological structure. Hence, the Bioimprint was developed to make a hard substrate with captured cell surface topography down to the nano-scale so that it is stable enough for probing with an AFM scanning tip. The Bioimprint has been shown to have copied the fine structure on cell membrane down to 5nm (Samsuri et al., 2011).

Bioimprint is a substrate with cell-like topography, and the imprinted topography contains features of the right scale, it therefore may carry more relevant and correct biophysical signals in cell culturing. Ishikawa endometrial cells were cultured on the Bioimprint in order to study the effect of the cell-like topography on cells. A previous study that cultured Ishikawa endometrial cancer cells on the polymethacrylate (pMA) Bioimprint showed preferential adherence of cells to areas where there was captured cell topography rather than to the flat areas (Figure 1) (Murray et al., 2014). This growing preference of cells on pMA substrate may be because pMA is not an optimised cell culture material (detailed discussion in chapter 4, section 4.1 and 4.6). The cell-like topography on a non-optimised cell culture substrate may have assisted cells to adhere better than on the surrounding flat surface. Furthermore, this result showed that endometrial cancer cells sensed the cell-like topography and responded to it.

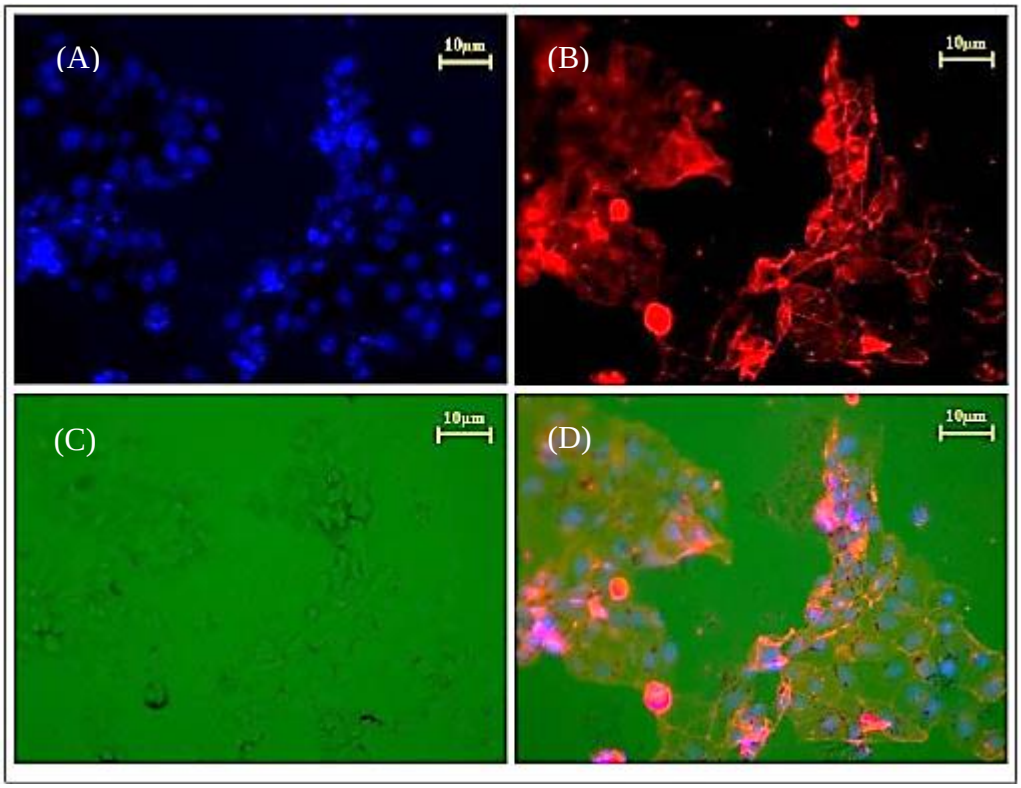


Figure 1 Ishikawa endometrial cancer cells grew preferentially on the Bioimprint surface. Adopted from (Murray, 2011,unpublished work). (A) Hoechst 33342 stained Ishikawa cell nuclei (B) Atto 594 phalloidin stained Ishikawa cell actin filaments (C) Fluorescein incorporated pMA Bioimprint (D) Overlay of fluorescently stained cells and pMA Bioimprint.

Fluorescein (green) was added in the liquid pMA biopolymer mixture before curing. The adding of fluorescein made the Bioimprint topography visible. This fluorescein incorporated pMA was used as the cell culture platform. After certain culture time, the cells were fixed and stained for their actin filaments (red) and nuclei (blue). The cell alignment relative to the Bioimprint can be examined by studying the staining.

1.8 Project Outline

The Bioimprint is a culture substrate that enables us to study the influence of topography on endometrial cancer cells. First, we compared a Bioimprint made on pMA polymer to the flat pMA substrate (abbreviation (f)pMA). This pMA surface contained a negative/pit-like Bioimprint, hence the abbreviation (-ve)pMA is used for pMA Bioimprint (Refer to Chapter

3 Section 3.2.2 for details of making and definition of (f)pMA and (-ve)pMA). We also compared these pMA substrates to the conventional cell culture substrates: glass and tissue culture grade pST.

Since pMA is not a commonly used cell culture substrate, we next developed the Bioimprint on a pST microscope slide. Besides making the Bioimprint on a more common cell culture material, the benefit of using pST to make the Bioimprint also allows us to make the topography as humps above the horizontal plane, which we call 'positive' Bioimprint, (+ve)pST, versus hollows below the horizontal, which is named 'negative' Bioimprint, (-ve)pST (Figure 9 illustrates the making of (+ve) and (-ve)pST). We then compared these two topographies to the non-imprinted flat polystyrene, (f)pST. Further, we extended our study on flat and Bioimprint pST to investigate the effect of FBS on cell responses to surface physical topography. In addition to the innovative use of the Bioimprint in this cancer cell study, this is also the first study that investigated endometrial cancer cell topographic responses.

Here we hypothesized that endometrial cancer cell behaviours will be influenced by both chemical and surface topography factors. We postulated that the cell-like topography we used here provoked endometrial cancer cells with physical signals that altered cell behaviours compared to cell culture on a flat surface. We further hypothesised that culture surface materials (with different surface chemistry) and the serum in culture medium (biological source of chemical factors) also influenced cell behaviours, and that those factors were influential in modulating cell responses to the physical environment. In short, here we studied the influence of surface physical topography both independently and incorporated with influences of substrate material and culture medium serum.

The topography alters the physical environment and the details of the mechanical forces that mediate its effects will be specific to that topography. In this project the mechanical forces have not been identified but this is the topic of another planned project in the laboratory. Nevertheless, it is reasonable to believe that the tensile and compressive forces and others that will be part of the interaction between cells and their nano- and micro-environments will be components of the integrin-mediated signalling.

1.9 Thesis Outline

In this thesis, Chapter One addresses the background of mechanical stimuli studies in biology and the recent studies that investigated mechanical signal alteration in cancer initiation and development, followed by an introduction of the development of Bioimprint for cell culture.

Next in Chapter Two, the experiment methodologies and materials used in this project are presented. Chapter Three gives a detailed discussion of the protocols for making of pMA and pST Bioimprints.

Then we examined cell morphological changes in response to substrate topography; we examined cell morphology, spreading area and cell circularity on glass, tissue culture grade pST, pMA and pST Bioimprints and the cell preferential attachment on either flat or pST Bioimprints surface. These observations are presented in Chapter Four.

Next, by using glass, tissue culture grade pST, pMA and pST Bioimprints, we investigated the changes in the expression and distribution of cell adhesion molecule, β1 integrin, the major mediator of the adhesion between a cell and the microenvironment (Bouvard et al., 2013; Gehler et al., 2013). We also studied the expression and distribution of β1 integrin downstream effector molecules: cell cytoskeleton and FAK. Further, for pST Bioimprints, we examined cell nitric oxide (NO) secretion. Cell NO secretion levels were measured because their secretion is modulated by arrangement of actin filaments. All these results (β1 integrin, cell cytoskeleton and FAK and NO secretion) are discussed in Chapter Five.

We also examined cell adhesion, growth and expression of cell growth-related biomolecules in cells on glass, tissue culture grade pST, pMA and pST Bioimprints and we present these in Chapter Six.

For Ishikawa endometrial cancer cells on pST Bioimprints, we further our studies by looking at the protein profile of cells on different substrates which we measured using isobaric tags for relative and absolute quantitation (iTRAQ) and the results are presented in Chapter Seven.

Then, as cancer cell vascular endothelial growth factor (VEGF) secretion and cell responses to cancer drugs in 3D model have been reported to be different from secretion of cells on 2D flat culture substrate (Chitcholtan et al., 2012) and VEGF is a key mediator of angiogenesis in cancer, we then examined if Ishikawa cell VEGF secretion was affected by culture substrate material and physical topography. For this, we quantified cell VEGF secretion on glass, tissue culture grade pST, pMA and pST Bioimprints, and the effect of EGCG and $CoCl_2$ on the cell VEGF secretion. Moreover, for cells on pST Bioimprints, we examined the effect of the Bioimprint on cell responses to cancer drugs (cisplatin and paclitaxel) with regard to cell VEGF secretion and cell growth. We present these observations of VEGF secretion and cell response to chemotherapy drugs in Chapter Eight.

Lastly, for cells that were grown on pST Bioimprints, we investigated the influences of the Bioimprint on cells in the absence of FBS in the culture medium. All the results including cell morphology, spreading, cell expression of adhesion biomolecules, cell growth, cell protein profile and cell responses to chemotherapy drugs, were examined and are discussed in Chapter Nine.

1.10 Implications

Chemotherapy has lengthened the lives of many patients. Yet quite often the effect is moderate and also always associated with deleterious side effects (Ouhtit et al., 2013). Though improvements have been seen with the use of combination therapy or personalised therapy that combats the dynamics and diversity of cancer progress, cancer still remains as one of the major causes of death globally. Also, reports have pointed out that drug treatments of cancer have only increased survival rates moderately yet often result in lower life quality (Fojo & Grady, 2009).

One of the recent suggestions is that the physical environment of cancer cells should be given attention in finding more efficient treatment (Lee et al., 2013). It is already known that tumours have altered mechanical properties, and cancerous cells receive and give different mechanical signals compared to normal cells; hence mechanical factors should automatically be included in cancer research. The limited number of efficient treatments of cancer and the modest effects of treatments may be partly due to poor understanding of the physical environment. To illustrate this, a reduced response to drugs by cells in a 3D environment has been observed (Chitcholtan et al., 2012). Furthermore, the interaction of cancer with the microenvironment is a dynamic process, and chemotherapy and radiotherapy resistance have been linked to the interaction between cells and their microenvironments through integrin and FA (Storch & Cordes, 2012). In addition to that, one of the reasons for adverse side effects from chemotherapy is because the drug agents do not differentiate between cancerous cells and normal cells. Hence, the understanding of mechanical signals in tumours may help in structuring chemotherapy drugs or improving drug delivery systems that can specifically target the tumours with abnormal tissue and ECM structures. In short, cancer development and progression should be understood as a tissue system and the tissue microenvironment should be targeted in treatment too.

Mechanical influences on cell development have been studied extensively on stem cells, fibroblasts and endothelial cells, with relatively few studies on cancerous cells. In addition to that, most mechanical effects on cancer initiation and development have been focused on the stiffness of the tissue microenvironment with few studies looking at the topographical effect on cancer cells (Kwon et al., 2011; Zhang et al., 2010b). Not only is this work the first study that investigates the topographical effects on endometrial cancer, our study is also unique in that features similar to cells themselves are used as substrate topography. Furthermore, the Bioimprint enables the separation of topographic effects from cell-cell adhesion and secretion as would happen in a 3D cluster. The outcome of this project will identify the influence of physical topography on endometrial cancer cells. If any effect is observed such activities should be considered when describing tumour development and developing tumour therapy. Treatment can be designed to target directly or indirectly the tumour microenvironment, or the signalling molecules that are responsive to the mechanical signals.

Chapter 2 Methods and Materials

This chapter will describe the materials, equipment (Table 1) and the recipe of the buffers used (Table 2) in this project followed by a discussion of the experiment protocols carried out in this project.

2.1 Materials and Solution Recipe

Materials and equipments are listed in Table 1 and the recipes of reagents used in this project are listed in Table 2.

Table 1 Materials and equipment used in this project including the suppliers and locations of distributors in New Zealand.

The list is grouped under separate experiments and is ordered alphabetically in each subgroup.

Cell Lines		
Human dermal microvascular endothelial cells: HMEC-1	A kind gift from the Gene Structure and Function Laboratory, Christchurch School of Medicine, New Zealand (NZ)	
Ishikawa endometrial cancer cells	A gift from Dr Mishato Nishida, Ibraki-ken, Japan	
Murine myoblast cells: C2C12	A gift from collaborative partners at Plant and Food Research in Hamilton, NZ	
Materials and Equipment	**Suppliers**	**Locations**
Cell Culture		
0.5% trypsin ethylenediaminetetraacetic acid (EDTA) (10x)	Gibco^{R} (via Invitrogen)	Auckland, NZ
Bright-Line^{TM} Haemocytometer	Sigma Aldrich	Auckland, NZ
Cell culture biological laminar flow cabinet	Thermo Fisher Scientific	Auckland, NZ
Centrifuge 5702	Eppendorf	Hamburg, Germany

Coomassie brilliant blue	Sigma Aldrich	Auckland,NZ
Cryotube	Raylab	Auckland, NZ
Dimethyl sulfoxide (DMSO)	Sigma Aldrich	Auckland, NZ
Dulbecco's modified eagle medium: nutrient mixture-F12 (DMEM-F12) medium powder	Gibco, Invitrogen	Auckland, NZ
DMEM-F12 no phenol red	Invitrogen	Auckland, NZ
Epidermal growth factor	Gibco, Invitrogen	Auckland, NZ
Falcon® 25cm ²rectangular canted neck cell culture flask	Becton, Dickinson and Company	Auckland, NZ
Falcon® 75cm ²rectangular canted neck cell culture flask	Becton, Dickinson and Company	Auckland, NZ
Fetal bovine serum (FBS)	Gibco^{R} (via Invitrogen)	Auckland, NZ
Forma steri-cycle incubator	Thermo Fisher Scientific	Auckland, NZ
Fungizone	Gibco^{R} (via Invitrogen)	Auckland, NZ
GlutaMAX (10x)	Gibco^{R} (via Invitrogen)	Auckland, NZ
Hydrocortisone	Sigma Aldrich	Auckland, NZ
Intracellular (IC) fixation buffer	Invitrogen	Auckland, NZ
MCDB 131	Gibco, Invitrogen	Auckland, NZ
Mr. Frosty™ Freezing Container	Thermo Scientific	Auckland, NZ
Penicillin/streptomycin (PenStrep) (100x)	Gibco^{R} (via Invitrogen)	Auckland, NZ
Phosphate-buffered saline (PBS) tablet	Gibco^{R} (via Invitrogen)	Auckland, NZ
Sodium bicarbonate	Sigma Aldrich	Auckland, NZ
Steritop™ filter units	MERCK Millipore	North Shore City, NZ
Trypan blue solution, 0.4%	Life Technologies, Inc., Invitrogen	Auckland, NZ

Bioimprint		
Ethylene glycol dimethacrylate (EGDMA)	Sigma Aldrich	Auckland, NZ
Heating oven	BINDER	Tuttlingen Germany
Hydroxypropyl methycellulose (HPMC)	Sigma Aldrich	Auckland, NZ
IRGAcure 2022	CIBA Specialty Chemicals	Basel, Switzerland
Methacrylic acid	Acros Organics Fisher Scientific	Auckland, NZ
Omnicure S2000	Excelitas Technologies Corp.	Waltham, MA, USA
Sylgard® 184 silicone elastomer kit	Dow Corning Australia Pty Ltd	Auckland, NZ
Ted pella plastic microscope slide	ProSciTech	CA, USA
Western Blot		
40% Acrylamide/Bis solution	Bio-Rad Laboratories	Hercules, CA, USA
Alliance 4.7 imaging system	Unitec	Cambridge, UK
Ammonium persulfate	Sigma Aldrich	Auckland, NZ
BenchMark™ protein ladder	Invitrogen	Auckland, NZ
Blotting paper	Bio-Rad Laboratories	Hercules, CA, USA
Bovine anti-mouse-horseradish peroxidase (HRP)	Life Technologies, Inc., Invitrogen	Auckland, NZ
Bovine anti-rabbit-HRP	Sigma Aldrich	Auckland, NZ
Bromophenol blue	Sigma Aldrich	Auckland, NZ
Donkey-anti-mouse-HRP	Life Technologies, Inc., Invitrogen	Auckland, NZ
Dri-block heater	Techne	Staffordshire, UK
Electrophoresis gel cast plate	Bio-Rad Laboratories	Hercules, CA, USA

Enhanced chemiluminescence (ECL) prime western blotting detection reagent plus mix	GE Healthcare	Amersham, UK
EDTA	Sigma Aldrich	Auckland, NZ
Glycerol	Sigma Aldrich	Auckland, NZ
Glycine	Sigma Aldrich	Auckland, NZ
MagicMark^{TM} XP western protein standard	Invitrogen	Auckland, NZ
Nonidet P-40 (NP-40)	Sigma Aldrich	Auckland, NZ
Orthovanadate	Sigma Aldrich	Auckland, NZ
Pierce protein-free blocking buffer	Thermo Fisher	Auckland, NZ
Polyvinylidene difluoride (PVDF) membrane	Bio-Rad Laboratories	Hercules, CA, USA
Power box	Bio-Rad Laboratories	Hercules, CA, USA
Precision plus protein^{TM} standards	Bio-Rad Laboratories	Hercules, CA, USA
Protease inhibitor tablet (complete mini)	Roche Diagnostics	Mannheim, Germany
Sodium deoxycholate	Sigma Aldrich	Auckland, NZ
Sodium dodecyl sulphate (SDS)	Sigma Aldrich	Auckland, NZ
Tetramethylethylenediamine (TEMED)	Amresco	Solon, Ohio
Tris(hydroxymethyl)aminomethane (Tris)	Sigma Aldrich	Auckland, NZ
Tween-20	Sigma Aldrich	Auckland, NZ
Immunofluorescent Staining		
Anti mouse fluorescein isothiocyanate (FITC)-488	Invitrogen	Auckland, NZ
Anti-rabbit Atto 594	Sigma Aldrich	Auckland, NZ
Bovine serum albumin (BSA) powder	Gibco^{R} (via Invitrogen)	Auckland, NZ
Hoechst 33342	Life Technologies, Inc., Invitrogen	Auckland, NZ

p-Phenylene-diamine	Sigma Aldrich	Auckland, NZ
Texas Red-X phalloidin	Life Technologies, Inc., Invitrogen	Auckland, NZ
Triton-x	Sigma Aldrich	Auckland, NZ
Primary Antibodies		
Cyclin B1,B2, D2, (proliferating cell nuclear antigen) PCNA, Cytokeratin-18, actin (C-2), focal adhesion kinase (FAK), phosphorylated-FAK (pFAK), (protein kinase B) Akt, phosphorylated-Akt (pAkt), extracellular-signal-regulated kinases 1/2 (Erk1/2), phosphorylated-ERK 1/2 (pERK1/2), β1-integrin, glyceraldehyde-3-phosphate dehydrogenase (GAPDH)	Santa Cruz Biotechnology	CA, USA
Commercial Kits		
Detergent compatible (DC) protein assay kit	Bio-Rad Laboratories	Hercules, CA,USA
DuoSet human VEGF enzyme-linked immuno assay (ELISA) development kit	R&D System (via Pharmaco)	Minneapolis, USA
Nitric oxide kit	Cayman Chemical Company (via Sapphire Bioscience)	Ann Arbor, MI, USA
VEGF ELISA		
1-step ultra 3,3',5,5'-Tetramethylbenzidine (TMB) ELISA	Thermo Fisher Scientific	Auckland, NZ
Nunc-immuno^{TM} 96-well solid plate	Sigma Aldrich	Auckland, NZ
Scanning Electron Microscope Specimen Fixation		
Glutaraldehyde	Sigma Aldrich	Auckland, NZ
Hexamethyldisilazane	Sigma Aldrich	Auckland, NZ
Osmium tetroxide	Sigma Aldrich	Auckland, NZ

iTRAQ specimen preparation		
Dithiothreitol (DTT)	Sigma Aldrich	Auckland, NZ
Ethylene glycol tetraacetic acid (EGTA)	Sigma Aldrich	Auckland, NZ
Hepes buffer	Sigma Aldrich	Auckland, NZ
Sodium fluoride	Sigma Aldrich	Auckland, NZ
Tris(2-carboxyethyl)phosphine (TCEP)	Sigma Aldrich	Auckland, NZ
Microsope		
Inverted light microscope	ACCU-SCOPE	Commack, New York
Scanning electron microscope	Jeol 7000 Field Emission scanning electron microscope	Massachusetts, USA
Zeiss Axio Imager epifluorescence microscope	Carl Zeiss AG	Oberkochen, Germany
Micellaneous		
1.7mL Eppendorf tube	Axygen (via Global Science)	Auckland, NZ
15mL centrifuge tubes	Becton, Dickinson and Company	Auckland, NZ
Aldosterone	Sigma Aldrich	Auckland, NZ
BD Falcon 10mL serological pipette	Becton, Dickinson and Company	Auckland, NZ
Cobalt chloride ($CoCl_2$)	Sigma Aldrich	Auckland, NZ
(−)-epigallocatechin-3-gallate (EGCG)	Sigma Aldrich	Auckland, NZ
ImageJ (Public domain image processing program)	Available from http://www.imagej.nih.gov/ij	National Institutes of Health (NIH), Maryland, U.S.
Microscope slide precleaned plain 75x25mm 100pcs ground edges	Fronine (via Thermo Fisher Scientific)	Auckland, NZ
Nunc® OmniTray	Sigma Aldrich	Auckland, NZ

SoftMax Pro spectrophotometric plate reader	Molecular Devices Sunnyvale	CA, USA
Sulfuric acid (H_2SO_4)	MERCK & BDH	Manawatu-Wanganui, NZ

Table 2 Reagents and recipes used in this project. The list is ordered alphabetically.

Reagents	Recipe
Cell Culture	
Cell freezing medium	90% v/v FBS 10% v/v DMSO
1x trypsin EDTA	10% v/v 10x trypsin EDTA 90% v/v sterilized PBS pH7.4
Bioimprint	
0.1% HPMC	0.1% w/v HPMC in double distilled water
Polymethacrylate (pMA) polymer mixture	6:3:1 mixture of ethylene glycol dimethacrylate (EGDMA): methacrylic acid: IRGAcure 2022
10% SDS	10% w/v SDS in double distilled water
5x trypsin EDTA	50% v/v 10x trypsin EDTA 50% v/v double distilled water
Western Blot	
10% Ammonium persulfate	10% w/v ammonium persulfate in double distilled water
Coomassie blue destaining solution	50% v/v methanol 10% v/v acetic acid 40% v/v double distilled water
Electrophoresis buffer pH8.3	25mM Tris 192mM glycine 0.1% w/v SDS
5x Laemmli loading buffer	60mM 1M Tris-HCl pH6.8 25% v/v glycerol 2% w/v SDS 0.2% w/v bromophenol blue
Radio-immunoprecipitation assay (RIPA) buffer	50mM Tris-HCl pH7.4 100mM Sodium chloride (NaCl) 5mM EDTA 1 mM Sodium orthovanadate 10% v/v glycerol

	1% w/v NP-40 0.5% w/v sodium deoxycholate 0.1% w/v SDS 1 tablet of phosphatase inhibitor cocktail
12% Separating gel	3.5 mL water 4 mL 40% acrylamide/bis solution 2.5 mL solution B 50 µL 10% ammonium persulfate 5 µL TEMED
Solution B (for western blot separating gel)	1.5 M Tris-HCl (pH8.8) 0.4% w/v SDS
Solution C (for western blot stacking gel)	0.5M Tris-HCl 0.4% w/v SDS
5% Stacking gel	2.3 mL water 0.67 mL 40% acrylamide/bis solution 1.0 mL solution C 30 µL 10% ammonium persulfate 5 µL TEMED
Transfer buffer	15.6 mM Tris base 120 mM glycine
Tris-buffered saline (TBS)	20 mM Tris-HCl pH7.5 140 mM NaCl
Tris-buffered saline –Tween®-20 (TBST)	0.1% v/v Tween®-20 in autoclaved TBS
Western blot blocking solutions (the suitable antibodies for respective blocking solutions are in parenthesis)	- 5% w/v non-fat dried milk in 0.1% v/v TBST (PCNA, Cytokeratin-18, Akt, pAkt,Erk1/2,pERK1/2,GAPDH) - 1% BSA w/v in 0.1% v/v Tween®-20 in autoclaved TBS (Cyclin B1, actin (C-2), FAK, pFAK) - Thermo Fisher Pierce Protein-free blocking solution (Cyclin D2, B2, β1-integrin)

Immunofluorescent Staining	
Anti-fading solution	90% v/v glycerol in PBS pH7.4 1 g/L p-phenylene-diamine Adjusted pH to 8.5 and stored in -20 ℃
Coomassie blue solvent	10% w/v SDS in 0.01 M hydrogen chloride (HCl)
Coomassie blue staining solution	0.2% w/v CBB stain 10% v/v acetic acid 40% v/v methanol 49.8% v/v double distilled water.
Phosphate-buffered saline-Tween®-20 (PBST)	0.05% v/v Tween®-20 in autoclaved PBS pH7.4
Texas Red-X phalloidin	200 units/mL Texas Red-X phalloidin In PBS pH7.4
VEGF ELISA	
VEGF reagent diluent	1% w/v BSA in PBS pH7.4
Scanning electron microscope	
Glutaraldehyde	2.5% v/v glutaraldehyde in double distilled water
Osmium tetroxide	1% v/v osmium tetroxide in double distilled water
Absolute ethanol	25%,50%,75% and 90% v/v absolute ethanol in double distilled water
iTRAQ Specimen Lysing	
iTRAQ lysis buffer	Phosphatase inhibitor (10 mM sodium fluoride and 1 mM orthovanadate) 1 mM EDTA/EGTA 0.1% w/v SDS 50 mM DTT 1 tablet of protease inhibitor 5 mM TCEP In hepes buffer

2.2 Cell Culture Protocols and Reagents Preparation

Cell cultures were done in sterilized conditions in a cell culture biological laminar flow cabinet and all the solutions, as well as equipment, used in cell culture were autoclaved and stored at an appropriate temperature.

2.2.1 Cell Culture Medium Preparation

The base media powder and sodium bicarbonate were dissolved in sterilized double distilled water with the aid of magnetic stirrer. Then the pH was adjusted with sodium hydroxide (NaOH) or HCl to pH 7.2. The solution was then filtered into a sterilized bottle and stored in a cold room at 4 ℃. The filtration step will bring the solution pH up to pH 7.4. This base medium was used within a month, or within a week if opened.

2.2.2 Cell Culture

Cells were cultured at 37 ℃ in a 5/95 CO_2/air incubator. For Ishikawa endometrial cancer cells and C2C12 murine myoblast cells, the cells were maintained in DMEM-F12 supplemented with 10% v/v fetal bovine serum, penicillin (100 units/ml), streptomycin (100ug/ml), Fungizone (1 μg/mL) and GlutaMAX ™ (2mM). On the other hand, HMEC-1 cells were maintained in MCDB 131 supplemented with 10ng/mL Epidermal Growth Factor and 1ng/mL hydrocortisone in addition to FBS, penicillin, streptomycin, and GlutaMAX, all with concentrations stated above.

Cells were maintained in 25cm^2 or 75cm^2 tissue culture flasks. The cell culture medium was changed every second day. Once the cells reached 70-80% confluence, the cells were harvested and used for experimental culture or for sub-culturing into a new flask. The cells used in all the experiments were all within passage 13-30. Further, the end point analysis of

all experimental cell culture was 60 hours (more discussion of the reason of this choice is in section 6.5.1.3).

To harvest the cells from a culture flask, after discarding the culture medium, the cells were washed with room temperature PBS pH7.4 to wash off any remaining medium since the FBS in the culture medium may inhibit trypsin activity. Next, sufficient 0.5% trypsin-EDTA was added to cover the cell monolayer and the flask was left in the incubator for 15-20mins until the cell-flask adhesion bonds were broken by trypsin. The cell suspension was then collected in 15 mL BD Falcon tube and spun down at a speed of 15000 rpm to get a cell pellet. This was followed by discarding of supernatant. The cells remained as a pellet at the bottom of the tube and were dispersed in an appropriate volume of culture medium. Cell counting was then performed on the re-suspension of this cell pellet.

2.2.3 Cell Counting

100 µL of cell suspension was moved into Eppendorf tubes and the cells were spun down, then the medium was removed, and the cells were resuspended with 100 µL PBS pH7.4 and 100 µL of 0.4% Trypan Blue. The reason for re-suspending cells in PBS pH7.4 was because the protein rich cell culture medium may be stained by trypan blue. The mixture was left for 3 minutes and then 10 µL of this 2x diluted cell suspension was pipetted into a Neubauer haemocytometer. The cell number was counted after 1 minute in order to allow cells to settle in the chambers.

The cell number was counted fromf the four corner squares of the Neubauer haemocytometer. The volume of one large corner square was $1mm^2$ x 0.1mm = 0.1cm x 0.1cm x 0.01cm =$10^{-4}cm^3$ or 10^{-4} ml (Figure 2). Therefore, the cell number/mL was calculated as average cell number per corner x dilution factor x 10^4/mL Only the live cells that were unstained with 0.4% Trypan Blue solution were included in the counting.

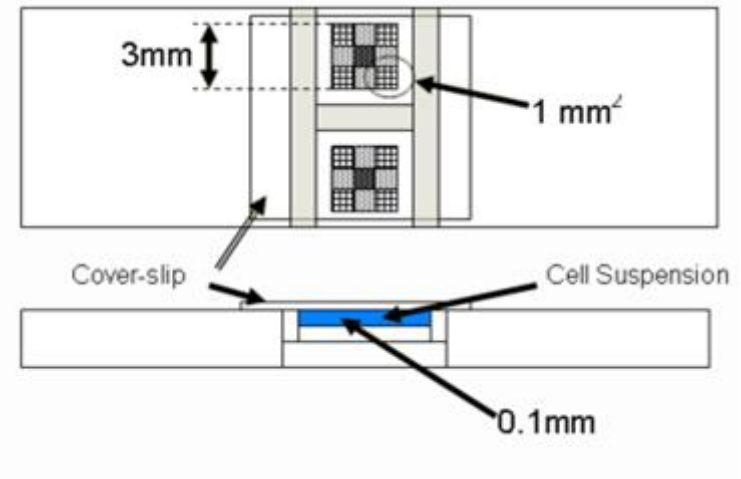


Figure 2 Dimension of a haemocytometer

Figure showing the dimension of a haemocytometer gridlines and the depth of space of the counting area.

From the known cell concentration per mL, the volume of cell suspension that contains the desired cell number was calculated followed by cell seeding with an appropriate volume of cell suspension.

2.2.4 Cell Freezing

Cell freezing was done to keep cells as cell stock. For cell freezing, the cells in culture flask were trypsinized and collected in 15mL BD Falcon tube and spun down. Then cells were re-suspended with cell freezing medium and counted. At least $1x10^6$ cells must be allocated to one cryotube to ensure maximum survival of cells upon thawing. The cryotube was then transferred to Thermo Scientific™ Mr. Frosty™ Freezing Container and stored at -20 ℃ freezer for an hour, and then Mr. Frosty™ Freezing Container was transferred to a -80 ℃ freezer overnight. Mr Frosty was used to freeze the cells in cryotubes to achieve a rate of cooling closed to -1°C/minute. Lastly, the cryotubes were transferred into liquid nitrogen tank for storage.

2.2.5 Cell Thawing

Cell thawing was done to obtain cells for cell culture. For cell thawing, a cryotube was taken out from the liquid nitrogen tank and was warmed in an incubator for 1-3 minutes; the tube should be moved to the cell culture fume hood once the outer layer of the frozen cell suspension started to thaw. There must be some unthawed frozen cell suspension to ensure that the temperature of the cell suspension did not drop suddenly. The cell suspension was then pipetted out very carefully, not to disturb the cells too much and transferred into a 15mL BD Falcon tube that had been filled with room temperature cell culture medium. The cells were then spun down followed by discarding of supernatant, and again the cells were re-suspended in new cell culture medium and were ready for re-seeding.

The medium of the cell culture of freshly thawed cells was changed one day after re-seedling to remove any dead cells and cell debris. The cells were passaged for at least 2 times before being used for the experiment.

2.3 PDMS gel and Bioimprint

The process of curing PDMS from liquid elastomer and crosslinker is described in Chapter 3 section 3.2.1.1.

The making of pMA Bioimprint and pST Bioimprints and respective control culture substrates are described in Chapter 3 section 3.2.2.1 and 3.2.3, respectively.

2.4 Cell Fixation

2.4.1 Cell Fixation for Bioimprint or Immunofluorescent or Chemical Staining

Cells ready for fixing were washed with warm PBS pH 7.4 for at least 2 times. Then IC fixation solution was added, the volume of which depended on the culture substrate surface area, but the cells must be fully covered by the fixative. Then the cells with the fixative were left at room temperature for 20 minutes. After the fixation step, the IC fixation solution was aspirated out and cells were washed with PBS pH7.4 for 3 times. The cells were now ready for experimental use.

2.4.2 Cell Fixation for Scanning Electron Microscope Examination

The cells were first rinsed twice with room temperature PBS pH7.5. Then the samples were incubated in 2.5% glutaraldehyde for 30 minutes, followed by rinsing twice with PBS pH7.4. The cells were then stained with 1% osmium tetroxide for 10 minutes, followed by rinsing with double distilled water three times. Then the samples were dehydrated using a series of absolute ethanol concentrations: 25%, 50%, 75% and 90%. Each dehydration step was for 10 minutes. Then the samples were chemically dried in hexamethyldisilizane overnight. All these procedures were carried out in a fume hood.

2.5 Proliferation Assay

In this project, two different methods were used to quantify the number of cells growing on glass, tissue culture grade pST and pMA substrates and also cells growing on (f)pST, (-ve)pST and (+ve)pST. Trypan blue counting of trypsinized cells (as described in section 2.2.3) was done on glass, tissue culture pST and pMA substrates, whereas the coomassie blue assay was done on (f), (-ve) and (+ve)pST.

For cells cultured on glass, tissue culture grade pST and pMA, cells were easily detached by trypsin since the glass and pST were both flat surfaces, and for cells on pMA substrates, the ease of trysinization was because of the weaker bonds formed between cells and pMA surface. Moreover, coomassie blue made a high background staining on a pMA material; hence trypan blue direct cell count was used for cells growing on the glass, tissue culture grade pST and pMA. On the other hand, for cells on flat and pST Bioimprints, trypan blue cell count was first used but it was then observed that some cells were trapped in the physical topography on the surface, and since coomassie blue does not leave a background staining on pST surface, coomassie blue staining was later chosen for that part of the project.

2.5.1 Coomassie Blue Cell Number Standard curve

After cell harvesting and cell counting, a cell suspension with the desired number of cells was transferred to triplicate Eppendorf tubes for standard curve cell counting. The number of cells depended on the experiment to be carried out, and the cell standard curve was constructed to cover 2x the expected cell number range of the relevant experiment.

For standard curve cell counting, a serial dilution of cell suspension in 9 Eppendorf tubes, each in triplicate was prepared with PBS pH7.4. The cells were spun down and washed once with PBS pH7.4, then the cells were spun down again and the wash liquid was pipetted out from the cell pellet carefully so that the cell pellet remained in the tube bottom. The cells were fixed and washed as described above. Coomassie stain was then added and left for 15 mins. After that, the stained cells were spun down and the stain was pipetted out, and then the stained cells were washed 3 times with double distilled water. Each washing involved adding of washing water, spinning down and pipetting out the washing solution. Lastly, the stained cells were left to dry overnight.

To quantify coomassie blue staining, 150 µL coomassie blue solvent was used to dissolve coomassie blue staining, for 10 mins on a shaker, and then 100 µL of the solution was transferred into a 96 well plate and absorbance at 595nm was determined.

The number of cells was estimated using a standard curve that relates coomassie blue staining to cell number. A standard curve was constructed for every single proliferation assay.

The use of standard curve method for relating coomassie blue staining to cell count was based on the assumption that the amount of protein in cells was similar in each cell and hence the cell number was linearly related to the total protein.

There was an uncertainty in this cell number measurement. The protein content may be varied between the spreading cells and the cells that were spun down in the Eppendorf tube (cells for standard curve's cell number measurement). Nonetheless, this method suited the cell number measurement for the non-adhered cells in suspension as they were collected from the culture medium by spinning the cells down in the Eppendorf tube.

2.5.2 Adherent Cell Quantitation

For adherent cell staining, the cell culture medium was aspirated, and the cells were washed 3 times with PBS pH7.4. This PBS wash solution must be transferred into respective labelled Eppendorf tubes for non-adherent cell counting as described in section 2.5.3. After washing, the cell monolayer was fixed. These fixed cells were washed three times with double distilled water and stained with coomassie blue for 15 mins at room temperature. The stained solution was then discarded, and the stained cells were washed by pipetting with double distilled water three times. Last, the stained samples were left to dry.

2.5.3 Non-adherent Cell Quantitation

For non-adherent cell staining, first, the cell culture medium was transferred into an Eppendorf tube and mixed with the PBS pH7.4 wash solution of corresponding adherent cells. The suspending cells were spun down. Then the cells were washed three times with PBS pH7.4 and fixed. Last, the cells in the tube were stained with coomassie blue as described above in section 2.5.1.

2.6 ImageJ Measurement of Cell Area

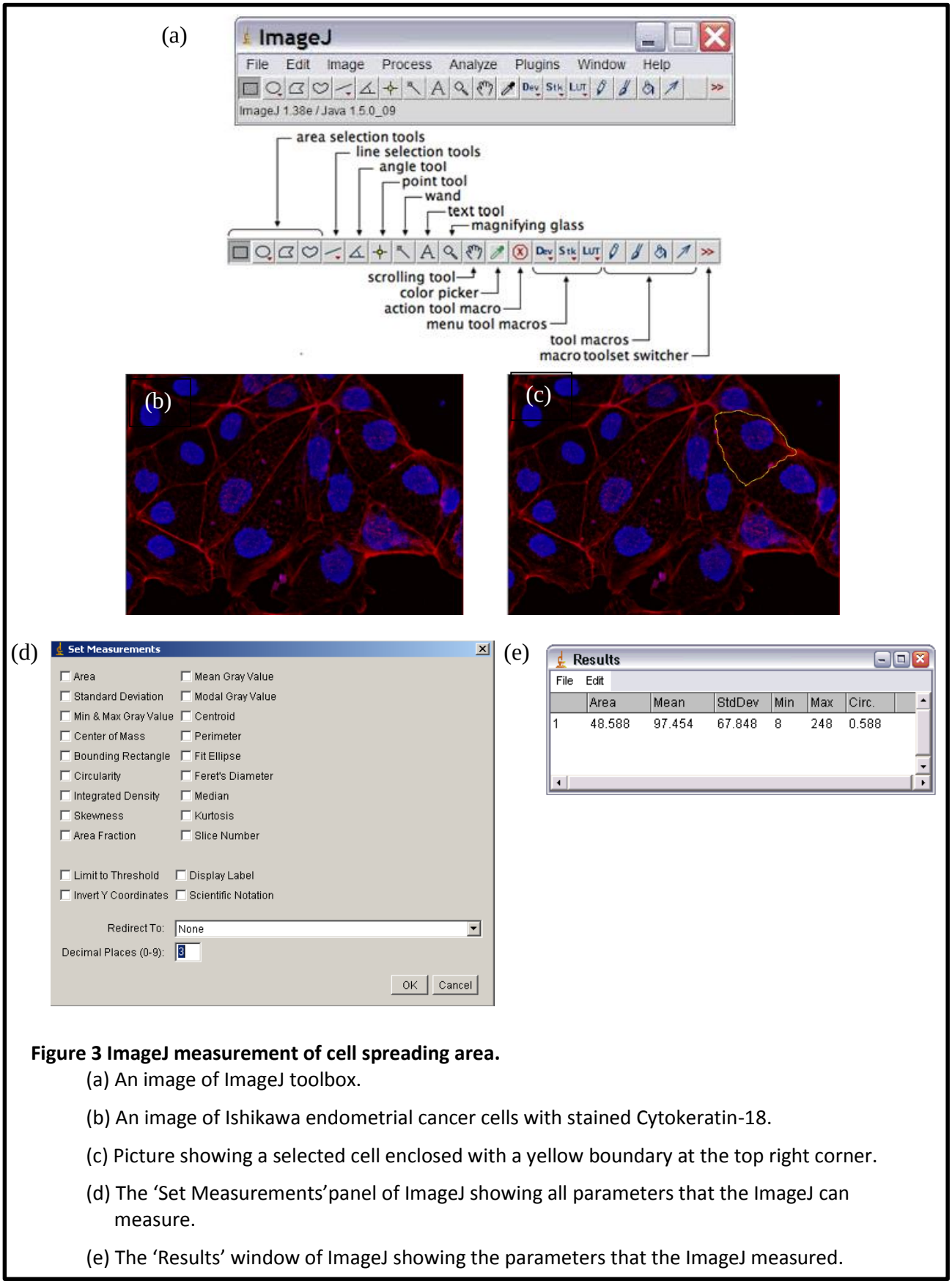


Figure 3 ImageJ measurement of cell spreading area.

(a) An image of ImageJ toolbox.

(b) An image of Ishikawa endometrial cancer cells with stained Cytokeratin-18.

(c) Picture showing a selected cell enclosed with a yellow boundary at the top right corner.

(d) The 'Set Measurements'panel of ImageJ showing all parameters that the ImageJ can measure.

(e) The 'Results' window of ImageJ showing the parameters that the ImageJ measured.

To measure cell spreading area, first, the 'pixel to distance' scale (from a measurement of a known distance) was set through Analyze>Set scale.

To measure the cell size from an image, a freehand selection tool () (Figure 3a) was used to enclose an area of a cell (Figure 3b: original cell image Figure 3c: a single cell area was selected and enclosed). And then from Analyze>Set Measurement, select the measurements of interest (Figure 3d). Then performed Analyze>Measure. The measurements were displayed in a new window (Figure 3e).

2.7 Cell Preferential Attachment

To examine cell preferential adhesion on flat or imprinted area on a culture surface, cells were seeded on a low-density Bioimprint. A low density Bioimprint was a Bioimprint culture substrate with both the flat area and the Bioimprint area. To seed the cells, the cells were suspended in culture medium and then was pipetted into the chamber The 'before' and 'after' cell seeding pictures of pST Bioimprints were taken. In order to align the 'before' and the 'after' images, the back part of each Bioimprint chamber was drawn with a grid so that the points where images were taken were known (Figure 4). When the cells in the suspension deposited and adhered on the substrate surface, the cells were exposed to the flat area and the Bioimprint area. An assumption that cells had equal chance in their allocation between flat versus imprinted areas was made. A proposed cell area on each surface was calculated as cell confluence multiplied by density of respective area. The measured cell area on each flat and Bioimprint area was then compared to the proposed cell area.

In this experiment, cells were seeded at low confluence to avoid cells from covering the Bioimprint and flat area altogether. Also, images were taken at 100x magnification so that a large area was covered per image (except for Figure 4(A) which was taken at 200x magnification for illustration purposes). Notably, coomassie blue staining was not an ideal stain to observe individual cells as an individual cell boundary was hardly visualized. Hence, if there was any difference observed, either differential deposition or difference in

cell number may be the reason of the observed differences. To minimise this, the after image was taken a short duration (24 hours) after cell seeding.

ImageJ was used to draw the outline of the Bioimprint, cell area on the Bioimprint and cell area on the flat surface. Then the respective areas were measured and a paired t-test was used to test the hypothesis.

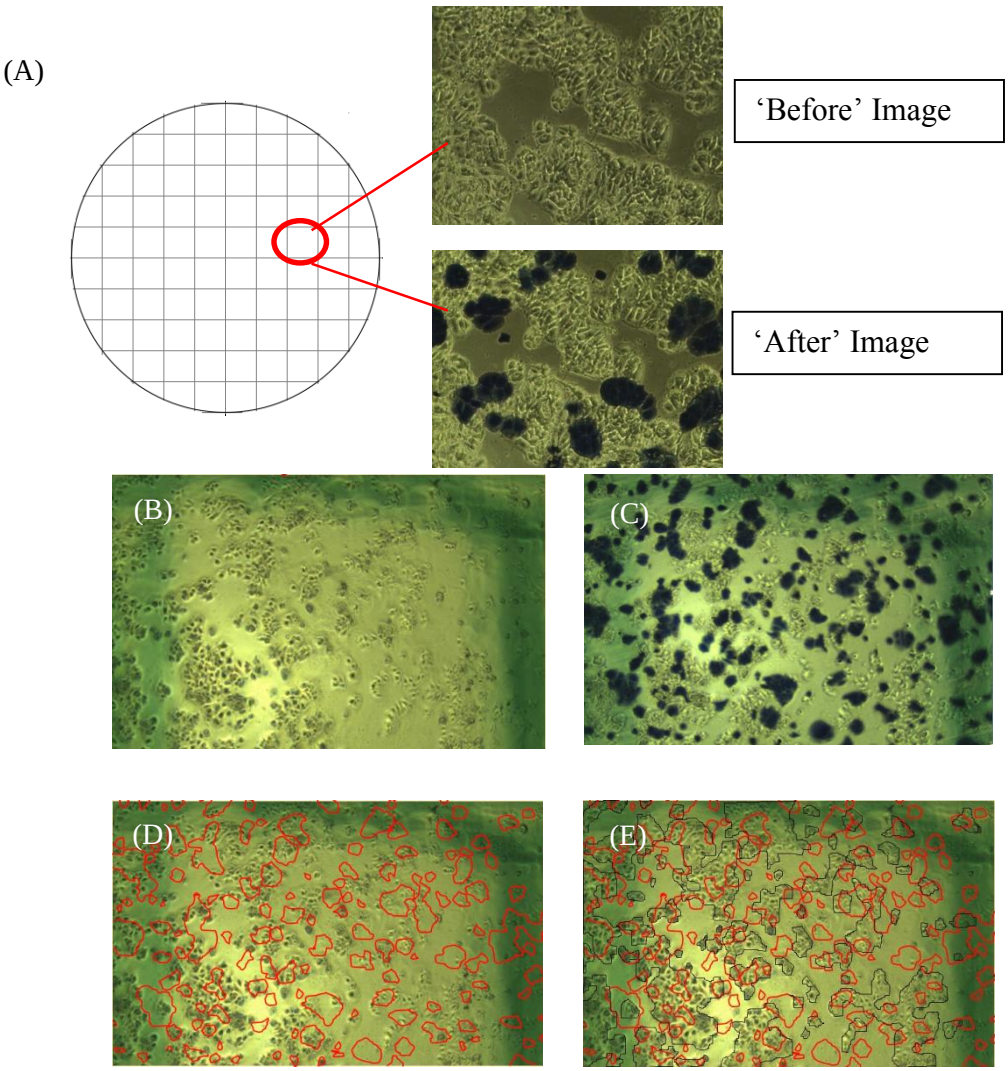


Figure 4 Representative images of alignment of 'before' and 'after' cell culture on the substrate.

(A) Grid was drawn at the back of culture substrate for aligning purposes.

(B) A pST Bioimprint before cell seeding.

(C) Coomassie blue stained cells on a pST Bioimprint.

(D) Outline of cells (in red) drawn from (C) and aligned on (B).

(E) Outlines of a pST Bioimprint area (black line) overlaid with the red cell outline. Area of cells grown on the pST Bioimprint and cells grown on the flat area were measured using ImageJ software (cell area measurement with ImageJ was detailed in section 2.6).

2.8 RGDS and RGES Treatments

Ishikawa endometrial cancer cells were pre-mixed with 100 µM L-arginylglycyl-L-α-aspartyl-L-serine (RGDS) or arginyl-glycyl-glutamyl-serine (RGES) or both before seeding on pST flat and Bioimprint substrates. After 3 hours seeding time, adherent cells and non-adherent cells were counted with haemocytometer (section 2.2.3) and percentage of adherent cells was calculated.

2.9 Total Protein Measurement

For experiments that required quantitation of total protein, the protein content was measured using Bio-Rad DC protein assay kit. Protein concentration of each sample was determined from a standard curve of BSA. To perform this assay, 5 µL of each sample was added into a well of a 96-well plate. Each sample was done in triplicate. Then, 25 µL of solution A' (mixture of 1:0.02 solution A to solution C, both provided by the kit) was added into each well, followed by 200 µL of solution B (provided by kit). The mixture was left at room temperature for 15 minutes, and the absorbance at 750nm was read.

Total Protein was used as a normalisation in western blot protein loading, VEGF ELISA and NO assays. An analysis of average protein amount of all samples showed higher total protein on (f)pST than on pST Bioimprints, and lowest total protein on (+ve)pST, both in culture with or without FBS (Table 3). This was same as cell number analysis of cultures on (f), (-ve) and (+ve)pST (Figure 49), indicating a direct relation between cell number and total cell protein.

Table 3 A table showing average of total cell protein (mg/mL) of samples (f), (-ve) and (+ve)pST, in medium with or without FBS. Data are presented as mean (SEM) of measurements of 3 independent experiments in quadruplicate.

	(f)pST	(-ve)pST	(+ve)pST
In Medium with FBS	2.00 (0.60)	1.80 (0.57)	1.67 (0.48)
In Medium without FBS	1.15 (0.57)	1.06 (0.50)	0.83 (0.39)

2.10 Western Blot

2.10.1 Cell Lysing for Western Blot

Cell culture media were aspirated, and the cells growing on respective substrates were washed with PBS pH7.4 three times. Cells were lysed with RIPA buffer containing protease inhibitor cocktail tablets for 20 minutes at 4 ℃ and were then scraped off surfaces using blue tips. The collected cell lysate was then centrifuged at 12,000 rpm for 7 minutes to spin down cell DNA or cell debris. The supernatant was transferred to a new Eppendorf tube. The cell lysates collected were used immediately or stored at -20 ℃. All samples were analysed for total protein concentration using BioRad DC protein assay kit (assay protocol was described in section 2.9). Following protein concentration determination, the loading volume of samples for each lane in sodium dodecyl sulfate-polyacrylamide gel electrophoresis (SDS-PAGE) gel was adjusted to contain 10ug of protein, and the total loading volume was made up to 15 µL with 5x Laemmli loading buffer. Then, the mixtures were boiled in a 99 ℃ heat block for 5 minutes to denature the proteins. All denatured samples were quickly cooled on ice for about 1 minute followed by brief centrifugation. The samples were adjusted to room temperature just prior to loading.

The only exception was β1 integrin cell lysate, which was not boiled at 99 ℃, but instead it was left at 37 ℃ for 15 minutes. The reason behind this was that β1 integrin is a transmembrane receptor, and the cell lipid bilayer can easily unfold upon heating which may have an impact on β1 integrin protein structure. Hence to sufficiently harvest β1 integrin protein without destroying it, the sample was left at 37 ℃.

2.10.2 Gel Preparation and Electrophoresis

An electrophoresis SDS-PAGE gel cast plate was set up and 12% separating gel was cast within the cast plate for one hour at 37 ℃. Next, 5% stacking gel with 10 wells was made on top of this separating gel at room temperature for 30 minutes.

After the SDS-PAGE gel was set up, and samples were loaded into each well. Gel electrophoresis was then run for 2 hours at 120 V constant.

2.10.3 Electroblotting

Before protein was transferred from SDS-PAGE gel onto PVDF membrane, the PVDF membrane was pre-incubated in methanol for at least 10 minutes. Next, together with clean sponge and blotting paper, the membrane was soaked in transfer buffer for at least 30 minutes before transferring.

After 30 minutes, a sandwich of SDS-PAGE gel, blotting paper and sponge was assembled, and the proteins on the gel were transferred onto PVDF membrane by the wet electroblot technique for 1 hour at 100 V constant. After immunoblotting, the membrane was incubated in blocking solution: Pierce protein-free blocking buffer, 1% or 4% BSA w/v in 0.1% TBST or 5% w/v skim milk in 0.1% TBST was used as blocking solution; the choice of blocking solution depended on the protein of interest to be detected. The blocking step was at least 1 hour at room temperature on a plate shaker.

2.10.4 Antibodies Binding and Protein Bands Visualization

Following blocking, the membrane was incubated in diluted primary antibody solution overnight at 4 ℃ followed by washing four times, each of 10 minutes duration, and with approximately 25 mL of 0.1% TBST. Meanwhile, diluted anti-rabbit or anti-mouse HRP-conjugated secondary antibody was prepared. The primary and secondary antibody dilution solution was 50% blocking solution mixed with 50% TBS-T. The membrane was then incubated with the secondary antibody for 90 minutes at room temperature with slow shaking on a plate shaker. Next, the membrane was washed four times, each for 10 minutes long, and each with roughly 25 mL 0.1% TBST. The last wash was with double distilled water for 5 minutes.

ECL Plus reagent was prepared just prior to the signal development step to avoid reaction between signal development reagents. The signal development solution was made by mixing 1 part of reagent A and reagent B provided in the ECL Plus kit. Then, the membrane was covered with this solution for 7 minutes and the chemiluminescent image was then developed with Alliance 4.7 imaging system. The densities of bands were determined using ImageJ. The densitometry measurement is not quantitatively linearly related to protein amount. It is a semi-quantitation measurement of protein amount (the protein amount is more or it is less than a control sample). The background intensity was not included in the densitometry measurement using ImageJ (discussed in section 2.10.6).

2.10.5 Western blot densitometry normalisation

In western blot analysis of protein expression, different samples are loaded into different lanes and the protein of interest is detected with HRP-conjugated antibody. First the loading needs to be normalised to ensure that a same amount of total protein is loaded into each lane. From the same amount of total proteins, the relative amount of protein of our interest can then be identified.

Also, conventionally western blot experiment would further normalise the densitometry of protein of interest with a densitometry of a housekeeping protein.

For western blot of experiments involving comparison between cells cultured on glass, tissue culture grade pST and pMA substrates, some commonly-used reference proteins such as actin, Cytokeratin-18 and glyceraldehyde 3-phosphate dehydrogenase (GAPDH) were sensitive to the substrate materials (differences in actin and Cytokeratin-18 expression levels are discussed in Chapter 5, and for GAPDH is shown in Figure 5). Therefore, western blot data for cells on experiments involving material comparison were presented using the same sample loading, ensured by total protein measurement, and also with coomassie blue gel staining on an additional gel running with the same loading for each sample (methods described in next section). An average of coomassie stain densitometry (arbitrary unit) of

glass, tissue culture grade pST, (f)pMA and (-ve)pMA were 24203, 22482, 22458 and 24193, respectively (coomassie blue stained gels are not shown). This similar densitometry reading confirmed similar loading amounts for each sample.

For western blot involving the (f), (-ve) and (+ve)pST culture substrates, the analysis used both total protein and housekeeping protein's densitometry normalisation methods.

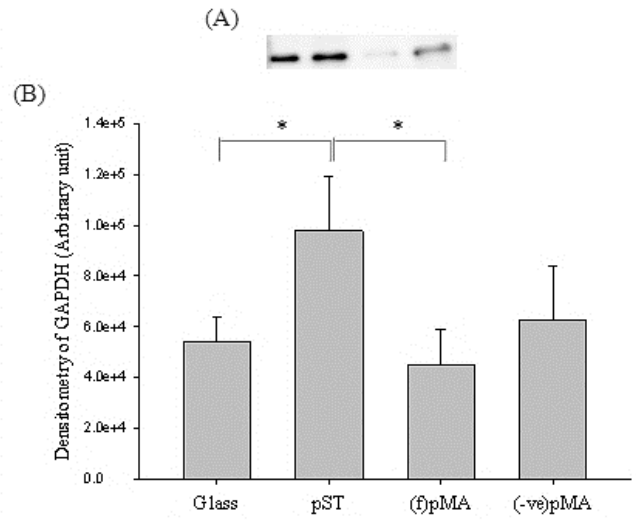


Figure 5 GAPDH expression in cells cultured on glass, tissue culture grade pST, (f)pMA and (-ve)pMA.

(A) (From left to right: glass, tissue culture grade pST, (f)pMA, (-ve)pMA) an example of GAPDH western blot protein band.

(B) Densitometry of GAPDH of cells cultured on glass, tissue culture grade pST, (f)pMA, (-ve)pMA.

Data are presented as densitometry mean ± standard error of the mean (SEM) of 4 independent experiments in triplicate. *,$p<0.05$.

2.10.6 ImageJ analysis of Western blot images

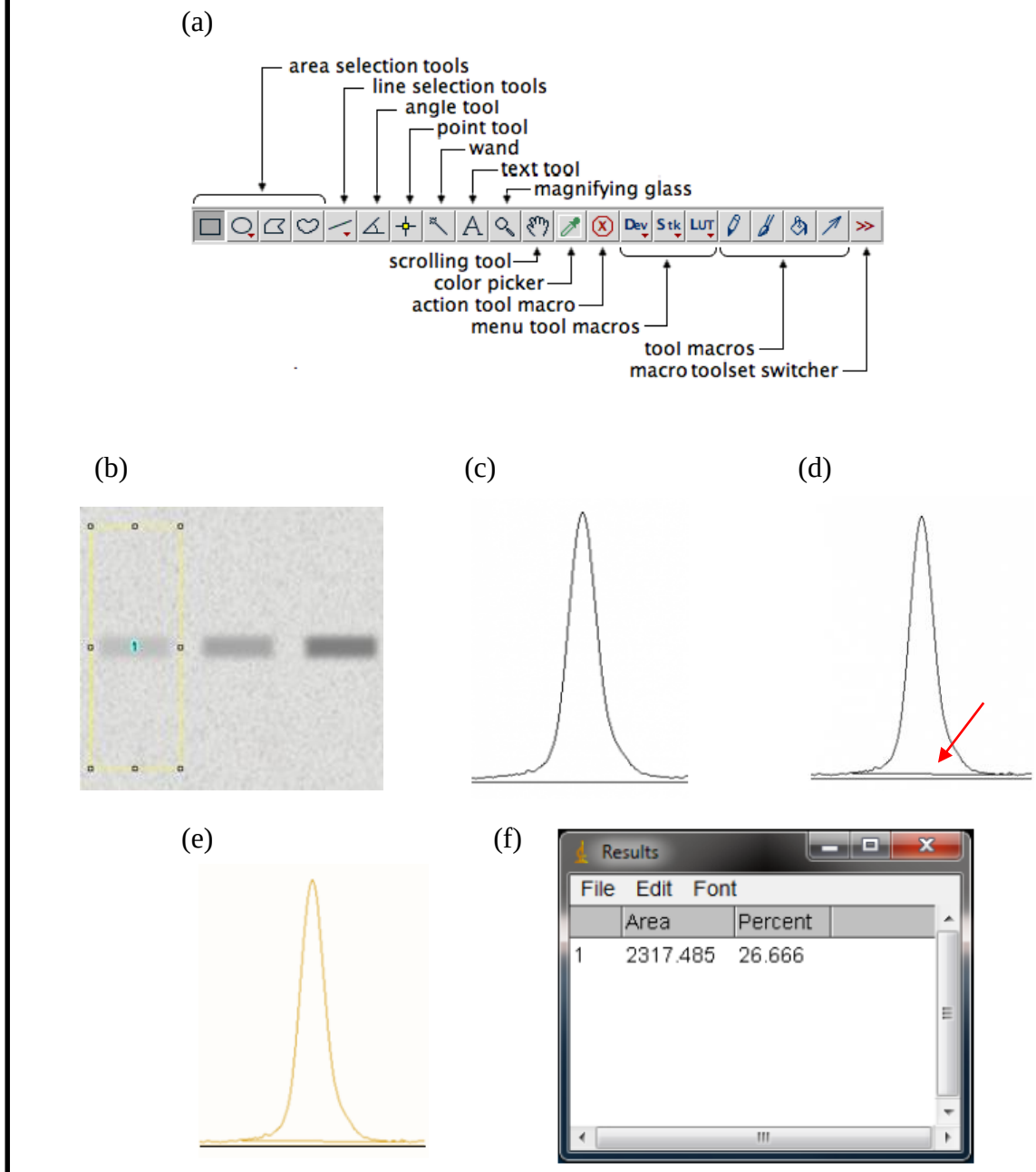


Figure 6 ImageJ measurement of densitometry

(a) An image of ImageJ toolbox.

(b) Picture showing western blot gel bands with the selected band on the left enclosed with a yellow rectangle.

(c) An image of a band's profile plot.

(d) Picture showing the profile plot in (c) is enclosed with a straight line at the base of the peak.

(e) The enclosed plot in (d) is selected and highlighted.

(f) The 'Results' window of ImageJ showing the measured area and the percent (intensity) of the western blot band.

To measure western blot gel band's densitometry. First a gel image was opened with ImageJ software. Then a rectangle selection tool () (Figure 6a) was used to select a band followed by the selection Analyze>Gels>Select First Lane. The rectangle was now set in place with a 1 in the middle of it (Figure 6b). And then, the rectangle was clicked and hold and dragged over to the second band. Then performed Analyze>Gels>Select Next Lane. The step was repeated for all the subsequent bands. After all bands were selected, performed Analyze>Gels>Plot Lanes and a profile plot of each lane was presented in a new window (Figure 6c).

The profile plot contained the relative density of the bands in the rectangle. A higher peak represented a darker band while a wider peak indicated a band with a bigger size. The peak did not reach down the baseline of the profile plot (perfect white) because of the background signal in the western blot gel images.

To analyse the profile plot, a straight line was drawn across the base of the peak () to enclose the peak hence to exclude the background signal from the measurement [(Figure 6d), red arrow points out the enclosing of the peak]. Then, the Wand tool () was used to select and highlight the peak (Figure 6e). The step was repeated for all peaks. While highlighting the peaks, densitometry measurements were shown in a new Results window (Figure 6f). The measurements in the Results window were then copied into Excel spreadsheet.

2.10.7 Coomassie gel staining

After the electrophoresis step, instead of proceeding to the electro-blotting step, the gel was transferred to a small container and then the gel was stained for 20 minutes with coomassie staining solution on a plate shaker. After that, the stain solution was discarded and a destaining solution was added. The gel was left in destaining solution on a plate shaker for an hour, and the image was then developed with the Alliance 4.7 imaging system.

2.11 Immunofluorescent Staining

Cells were grown on respective substrates until 70-80% confluent and were fixed as described above. The fixed cells were washed with cold PBS pH 7.4 for 3 times. For Cytokeratin-18 staining, cells were permeabilized with cold methanol for 10 minutes at -20 ℃ and for actin, β1 integrin and pFAK staining cells were permeabilized with 0.5% v/v Triton X-100 in PBS pH7.4 for 5 minutes at room temperature. After permeabilization, cells were washed four times with cold PBS pH7.4, each of 5 minutes duration. Then samples were blocked with 5 % w/v BSA in PBS pH7.4 for 60 min at room temperature followed by washing with cold PBS pH 7.4 for 4 times, each with 5 mins. For actin filament staining, the cells were incubated with 1/40 diluted Texas Red-X phalloidin in 2.5% BSA in PBS pH7.4. For β1 integrin and pFAK staining, the cells were incubated with the first antibody (1/100 dilution with 2.5% BSA in PBS pH7.4). Both incubations were done at 4 ℃ overnight.

For Texas Red-X phalloidin staining, following the overnight incubation, the cells were washed with cold PBS pH7.4 for 3 times, each for 10min, and the last wash with cold 0.1% v/v PBST for 10 minutes, followed by adding of anti-fading solution. The cells cultured on glass and tissue culture grade pST surfaces were then covered by glass cover slips and the samples were examined with epifluorescent microscope.

For β1 integrin and pFAK staining, after the primary antibody incubation, the cells were washed 4 times, each for 5 mins, with cold PBS pH7.4 prior to secondary antibody incubation. The samples were left with secondary antibody solution (1/500 dilution with 2.5% BSA in PBS pH7.4) for an hour at 37 ℃ in the dark. After that, 10ug/mL Hoechst 33342 solution replaced the secondary antibody solution and incubated at 37 ℃ for 20 minutes in the dark. Lastly, the samples were washed with cold PBS pH7.4 for 3 times, each for 10min, and the last wash with cold 0.1% v/v PBST for 10 minutes, followed by adding of anti-fading solution. The cells cultured on glass and tissue culture grade pST surfaces were then covered by glass cover slips, whereas the cells on pMA substrates were examined straight after staining since putting on a glass coverslip was technically difficult on the

curved surface. The samples were visualized with a Zeiss Axio Imager epifluorescence microscope. The stained samples can be stored at -20 ℃ for later microscopy examination.

2.12 Cell Morphology, Area and Circularity Measurements

Ishikawa cell morphology was examined with an inverted light microscope. The cells examined with the inverted light microscope were live cells without any fixation involved. Further, the cell morphology was also examined by studying the cell actin filaments and Cytokeratin-18 structures with an epifluorescent microscope (the staining of the cell actin filaments and Cytokeratin-18 was detailed in section 2.11).

Some of the figures presented in this thesis include arrows that point out certain cell features, the arrows are pointing out the representative examples in the images and there are many instances in the relevant figures.

For cell area and circularity measurements, cells were immunofluorescently stained for cytoskeleton-18 and were examined under an epifluorescent microscope. Pictures from 4 corners of the culture chambers were taken, and the sizes and circularities were measured using ImageJ from at least 20 cells in each of the 4 corners.

2.13 iTRAQ analysis (cell lysing and data analysis)

Cells were cultured for 60 hours, then the cell culture medium was aspirated out and the cells were washed 3 times with PBS pH7.4. Next iTRAQ lysis buffer was added into each well (100 μL each well) and left in a 4 ℃ room for 20 minutes. The cells were then scraped off the surface, and the lysate was collected in an Eppendorf tube. The lysate was spun down at 12,000 rpm for 7 min to get rid of cell debris. The remaining cell lysate supernatant was transferred to a new Eppendorf tube, and the total protein was quantified using a protein

assay kit. Sixteen wells of cultures were pooled to become one sample so that the total protein reached at least 30 ug/mL for iTRAQ analysis. The need of at least 30ug/mL protein was to ensure that there was sufficient amount of protein for total protein measurement and for protein processing. The final protein amount loaded for iTRAQ analysis was the same for all samples of protein. The samples were transported to Dunedin at room temperature.

iTRAQ involved digestion of different protein samples to peptides. Peptides in each sample of cells from the same topography were tagged with a specific isotope. The tagging will identify from which sample each peptide was derived. Thence the ratio of levels of a tagged peptide from a pair of original paired samples was calculated as *r*. iTRAQ analysis was repeated twice. Two results were pooled and the proteins were selected as significantly changed on either (+ve)pST or (-ve)pST compared to (f)pST based on the cut off *r* values of $\geqslant$1.2 as up-regulation and $\leqslant$ 0.8 as down-regulation. Further, peptide variation was the variation between the ratios of peptides from a particular protein, as a percentage. Here, proteins that had mean peptide variation of > 17 % were excluded. (more description of the iTRAQ principle and selection criteria is presented in Chapter 7 section 7.3).

2.14 VEGF ELISA Assay

Cells were cultured for 60 hours and the medium was collected in an Eppendorf tube for VEGF level analysis. The medium was aspirated from culture substrate very carefully so that no cell debris was collected which can interfere with the ELISA assay reading. Also, the collected medium was spun down at 12,000 rpm for 7 min, and the supernatant was transferred to a new tube and immediately stored at -20 ℃ until VEGF ELISA.

VEGF ELISA was performed using DuoSet Human VEGF ELISA Kit according to the manufacturer's instructions. Briefly, the immune-plate was first coated with capture antibody (anti-VEGF) and was blocked to reduce non-specific binding. Then, cell culture media of each sample was added into a corresponding well, and any secreted VEGF was captured by the capture antibody. The secondary antibody (anti-VEGF) coupled to biotin then recognized the bound VEGF. The biotin was then bound by streptavidin HRP. Then tetramethylbenzidine was added as substrate for HRP and the absorbance of the colour product was read at 570nm.

These secreted VEGF concentrations were normalized with cell number (8.5.1.1) or the total protein measured by Bio-Rad DC protein assay kit (8.5.1.2 and 9.5.9.1). The normalisation is to counteract the effect of variation in cell number among samples and to look at the VEGF secretion per cells. The common way of normalisation is by cell number. However, in sections 8.5.1.2 and 9.5.9.1, the VEGF secretion level was normalised by total protein. This was because from the same sample, the cells were lysed for western blot and the medium was collected for VEGF analysis. The cell lysates collected were unable to be used for cell counting, but the total protein of the cell lysates was measured for both VEGF and western blot normalisations. Further, as discussed in section 2.9 and the data in Table 3, a direct relation between cell number and total cell protein was observed.

2.15 Nitric Oxide Assay

Nitric oxide secretion was measured using a Cayman nitric oxide calorimetry assay kit, following the instructions from the manufacturer. This assay measured the total level of nitrate and nitrite, which are the final products of secreted nitric oxide. The total level was obtained against a standard curve of nitrate.

First, 80 µL of the sample or standard was added into a well of a 96-well plate, then 10 µL of Enzyme Cofactor Mixture was added into each sample and standard wells. This was followed by adding of 10 µL of Nitrate Reductase Mixture into samples and standards. Nitrate reductase functions to convert nitrate to nitrite. The plate was covered with aluminium foil and incubated at room temperature for two hours. After the incubation time, 50 µL of Griess Reagent R1 was added and immediately followed by adding of 50 µL of Griess Reagent R2. The mixtures were incubated for 10 minutes at room temperature (covering was optional at this step). The absorbance of the assay was read at 550nm.

2.16 Cell Treatments

2.16.1 Cell EGCG and $CoCl_2$ Treatments

Cells were cultured on respective culture substrates for 36 hours, and then the cell culture medium was replaced with medium without FBS for another 24 hours to synchronize the cells before treatments. Cells were then treated with 10 µM EGCG and 100 µM $CoCl_2$ for 24 hours. The treatment doses were determined from previous work in our lab. 10µM of EGCG was used in this project. Previously work in our lab showed that 5µM of EGCG caused significant effect on cell cluster but not on cell monolayer (Hogg et al. 2015). Here, the dose of EGCG was doubled since Ishikawa cells were grown as cell monolayer on the Bioimprint and 10µM has been reported in literature to have caused effects on cells (Wu et al., 2012). Similarly, 100µM dose of $CoCl_2$ was chosen based on the previous work in our lab (Dann, 2008).

Then the medium was collected for VEGF analysis and the cells were lysed for total protein and western blot analysis.

2.16.2 Aldosterone Treatment

We used aldosterone to soften and reduce stiffness of Ishikawa endometrial cancer cells (visualised as depolymerisation of cortical actin). First immunofluorescent staining was used to choose the aldosterone optimal concentration since the direct measurement of cell stiffness is currently unavailable. For this, we added 1nM, 10 nM and 100 nM of aldosterone to Ishikawa endometrial cells and examined the actin structure after 7mins by phalloidin staining of the actin filaments. A detection of fragmented cortical actin filaments indicated aldosterone depolymerisation of cell cortical actin. The final concentration chosen was 10 nM.

Cell culture for NO measurement was done with DMEM-F12 without phenol red as the presence of phenol red may interfere with the assay absorbance reading. Cell cultures at 60 hours were subjected to treatments. After an appropriate time, the cell culture medium was collected for nitrite level measurement. After collection into well-labelled Eppendorf tubes, the culture medium was immediately stored at -20 ℃. The cells were lysed and were quantified for the total protein. The cell lysate was stored at -20 ℃. Nitrite level was measured with Cayman nitrate/nitrite calorimetric assay. The brief method was described in section 2.15. The nitrite level was normalised with total protein.

2.16.3 Cisplatin and Paclitaxel Treatments

Ishikawa endometrial culture at 36 hours was subjected to cisplatin (20 μM) or paclitaxel (0.1 μM) for 24 hours. The treatment doses were determined from previous work in our lab (Hogg et al., 2015; Chitcholtan et al., 2012). Then the cell culture medium was collected for

VEGF level analysis, and the cells were lysed for western blot analysis. Since both of these clinical drugs were dissolved in DMSO, an equal amount of DMSO was added to another set of cell culture as the control for this study.

2.17 Statistical Analysis

The quantitative measuremets in this thesis are presented as the mean of data, plotted as bar chart, and SEM indicated by the error bar. The mean and the SEM were calculated from measurements from x independent experiments (x = the number of experiment repeat) with y replicates (the number of culture well in each experiment repeat) for each culture substrates.

The measurements in this thesis were continuous variables and were normally distributed. Further, the design of the experiments enabled paired t-test, which controlled for run-to-run variation. Hence, the student paired t-test was used to check if there is any statistical difference between compared groups in this thesis. Statistic test comparisons were carried out between 1) combinations of different culture materials 2) (f)pMA and (-ve)pMA 3) (f)pST to each (-ve) and (+ve)pST and 4) between the non-treated sample to treated sample on each culture topography.

A difference was described as ‘significant’ when $p < 0.05$ whereas a ‘trend’ was claimed when the $p > 0.05$ but a pattern of increasing or decreasing was observed between the compared samples.

The next chapter will describe in detail the making of pMA and pST Bioimprints, and the use of each in cell culture.

Chapter 3 The Making of Bioimprint

3.1 Introduction

A Bioimprint is a platform of replication of biological cell impression made by a technique based on soft lithography. It was first developed by applying a liquid PDMS polymer composite on cultured cells and allowing it to cure to capture the cell topography. The imprint captured the cell nano-and micron-features such as cell membrane vacuoles, but the high temperature and the long curing time resulted in dehydration effects on cells (Muys et al., 2006). Thereafter instead of PDMS, a photo-curable siloxane copolymer was used to make the Bioimprint, though the curing time has been greatly reduced (5 minutes) compared to PDMS moulding, the captured cell impression was still the 'average impression' of that few minutes instead of a snapshot of cells (Muys et al., 2006). Then, another UV curable polymer, ethylene glycol dimethacrylate (EGDMA)/ methacrylic acid copolymer, was used to make the Bioimprint of cells. An advantage of using this EGDMA polymer was the even shorter curing time of this co-polymer, hence reducing artefacts and offering high replication resolution (Murray, 2012; Samsuri et al., 2010). However EGDMA polymer is not fully biocompatible as a cell culture substrate, and subsequently a Bioimprint was made on treated pST microscope slides combining soft lithography and hot embossing methods (Goral et al., 2011). The utilization of pST to make the Bioimprint has two advantages; first, it is a common cell culture substrate hence the results would be relatively easy to compare to other studies. Second, the use of pST enables the making of different presentations of the Bioimprint, namely the positive and the negative Bioimprints (Figure 9).

Two polymers were used in this project, pMA and pST. The protocol for making pMA Bioimprint was based on the optimised methods developed by Murray (Murray et al., 2014) with some minor modifications. In this study, the Bioimprint was made of Ishikawa endometrial cancer cells, except for a few proof-of-concept experiments in which the Bioimprint was made of C2C12 murine myoblast cells and HMEC-1 cells. To examine the role of surface topography on cancer cell behaviours and responses, Ishikawa cells were cultured on the Bioimprint of Ishikawa cells to explore how cells respond to physical

features that resemble themselves. Biological responses and changes were analysed and will be discussed in following chapters.

3.2 Protocol of Making Bioimprint

3.2.1 PDMS Circular Chambers

3.2.1.1 PDMS Circular Chambers for Cell Culture for Making of Bioimprint

For both pMA and pST Bioimprints, the imprint was taken from cells cultured on glass microscope slides in chambers made of PDMS (Figure 7). First of all, PDMS chambers were made using the following protocol; 10 parts of Sylgard 184 Silicone Elastomer base with 1 part of Sylgard 184 Silicone Elastomer curing agent were well-mixed and poured on to a single well Omni tray to mould it as a flat sheet in a dust-free environment. This was followed by 20 minutes desiccation to remove any entrapped air bubbles introduced during mixing. This mixture was cured on a hot plate at 80 ℃ for 2 hours. The cured PDMS sheet was then cut into rectangular blocks. Each block had an area similar or smaller to a microscope glass slide. Then a cork borer with a diameter of 15 mm was used to make 3 chambers within one PDMS block and these blocks of PDMS were attached firmly to a microscope slide.

For the PDMS wells, the wells were made circular instead of any regular shape to distribute curing stress more evenly across the surface of the pMA, when used for Bioimprint process (protocol described in 3.2.2.1), though the stress was still found to be most intense at the middle of the circle which resulted in a concave pMA Bioimprint. In order to distribute the stress more evenly, the well diameter had been changed from 14mm (Murray et al., 2014) to 15 mm; this minor modification reduced the concavity of the Bioimprint platform. 15 mm PDMS chambers were used throughout the project.

The microscope glass slides with PDMS chambers were autoclaved prior to cell culture. After these PDMS chambers were sterilized, the glass slides with the PDMS chambers were ready for cell culture for the making of pMA Bioimprint (protocol described in section 3.2.2.1) and PDMS Bioimprint (protocols described in section 3.2.3).

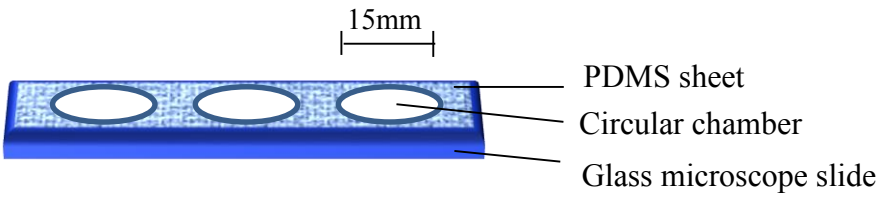


Figure 7 PDMS block with circular chambers on glass microscope slide.

Figure showing a PDMS block sticking on a glass microscope slide. Three 15mm diameter circular chambers were made on the PDMS block with a cork borer.

To culture the cells, first, the PDMS chamber was half filled with the cell culture medium, and then cells in suspension were added to the wells, followed by fully filling the well with cell culture medium. This was to maximize an equal dispersion of cells across the circular surface. The number of cells added depended on the experiment requirement for the density of the Bioimprint. After 48 hours, the cells were all fixed (protocol described in section 2.4.1), and were used for pMA Bioimprint or PDMS Bioimprint. 48 hours was chosen as this is the time point where Ishikawa endometrial cancer cells were well-spread as a monolayer. These Bioimprints were done on fixed cells which reduced the dehydration and 'average' impression capture issues as discussed in section 3.1.

3.2.1.2 PDMS Circular Chambers for Cell Culture on Glass and Tissue Culture Grade Polystyrene

For cell culture on glass and tissue culture grade pST (both as the controls for cell culture on pMA substrate), PDMS circular chambers prepared with methods described above were used to make culture chambers on glass microscope slides and tissue culture grade pST (Nunc® OmniTray). The PDMS rectangular block with circular chambers was attached

firmly onto the respective surfaces and the chamber was sterilized with absolute alcohol, followed by washing with sterile PBS pH7.4 before cell culture.

3.2.2 Polymethylacrylate (pMA) Culture Substrates

3.2.2.1 The Making of Polymethacrylate (pMA) Flat and Bioimprint Culture Substrates

Polymethacrylate (pMA) polymer was prepared from a 6:3:1 mixture of ethylene glycol dimethacrylate (EGDMA): methacrylic acid: IRGAcure 2022. A fresh mixture was made each time to minimize reaction occurrence once the solutions mixed. The mixture was then vortexed for at least 30 seconds to ensure mixing. Approximately 300 µL of the mixture was then loaded slowly into each PDMS sheet chamber and cured with 40% intense UV light for 240 seconds. Next the pMA disks were left to dry in the chamber. The PDMS blocks were peeled off and the pMA disks were collected. The surface of the pMA disk in contact with the glass microscope slide captured the impression of the cells (Figure 8 left). This surface contained a negative/pit-like Bioimprint and is named (-ve)pMA. On the other hand, the control flat polymethacrylate (f)pMA) was made by curing the same mixture on cell-free glass slides (Figure 8 right).

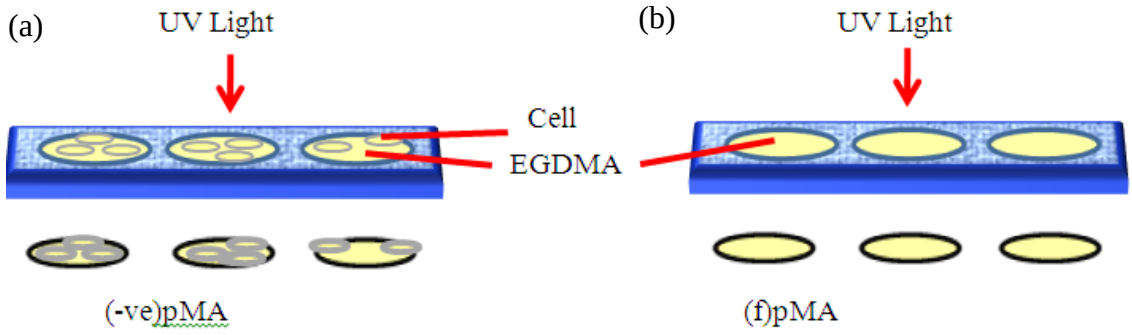


Figure 8 The making of pMA UV curable polymer.

A mixture of 6:3:1 of ethylene glycol dimethacrylate:methacrylic acid:IRGAcure2022 was loaded into a PDMS chamber with (a) fixed cells or (b) without cells. The mixture was then cured with UV light and the resulted cured polymers were (a) (-ve)pMA with captured cell topography and (b) (f)pMA with flat pMA topography.

To ensure that there was no biological residue on the pMA disk, the disks of pMA Bioimprint and flat disks were cleaned by sonication in 10% SDS followed by shaking with 5x trypsin for at least 40 minutes. All disks were then washed with double distilled water with agitation in a 24 well plate. After discarding the washing water solution, fresh double distilled water was added into each well and the disks were soaked in water overnight to dissolve any unreacted polymer. The clean biopolymer disks were next sterilized by dipping in absolute alcohol followed by rinsing with PBS to remove left over absolute alcohol. The disks were then soaked in cell culture medium DMEM-F12 without FBS for at least overnight to buffer the pMA disks to further remove any unreacted methacrylic acid.

3.2.2.2 Cell Culture on Polymethacrylate (pMA) Flat and Bioimprint Culture Substrates

In order to use pMA disks as a cell culture substrate they must be placed in a chamber that can accommodate the cell culture medium. The pMA disks were first put in a PDMS sheet chamber cut with the same diameter cork borer. Yet this often resulted in culture medium leakage due to distortion of the bond between the PDMS sheet and the glass slide while attempting to fit the pMA disk into the well. In addition to that, the volume of the medium that could be put into the PDMS well was limited.

After changing the pMA disks from 14mm to 15mm, the disks were fitted into 24 well plates that had a well diameter of 15.6mm. However there was still a 0.6 mm gap between the disk and the well, which meant that cells may have had a chance of accidently depositing onto the well plate bottom and growing on the pST surface. The use of 24 well plates to accommodate pMA disks was still a preferred method compared to fitting the pMA disks into PDMS chambers. First, it avoided the risk of culture medium leaking, and second, it allowed more culture medium to be filled in the wells. In fact, microscopic examination after removing of the pMA disks showed few or no cells had grown on the 24 wells chamber.

3.2.3 Polystyrene (pST) Bioimprints

For pST Bioimprints, the imprint was made of two forms. One was 'positive'. In this case, the features were of humps above the horizontal plane. This Bioimprint is named (+ve)pST. The second was 'negative' and the features were hollows below the horizontal and is named (-ve)pST (Figure 9).

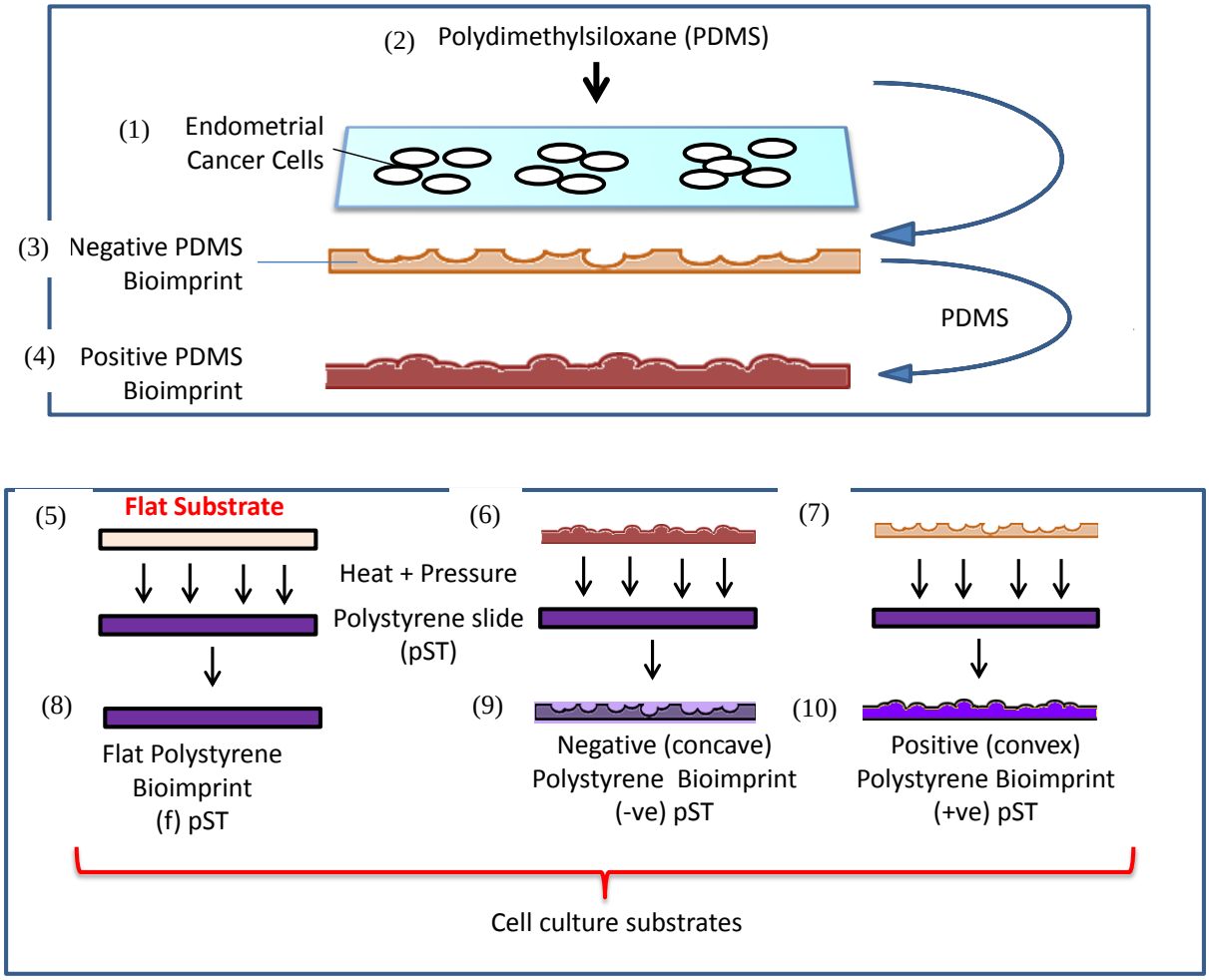


Figure 9 Schematic outline of the making of (f)pST, (-ve)pST and (+ve)pST.

Endometrial cancer cells were cultured and fixed on a glass slide (1). Liquid PDMS was poured on top of the cells and cured (2). The cured PDMS was peeled off as the negative PDMS Bioimprint (3). Liquid PDMS was poured on the negative PDMS Bioimprint obtained at (3) and cured, and then peeled off as the positive PDMS Bioimprint (4). A flat PDMS (5), the positive PDMS Bioimprint (6) and the negative PDMS (7) were pressed against a polystyrene slide. A flat polystyrene (8), negative polystyrene Bioimprint (9) and positive polystyrene Bioimprint (10) was obtained with application of heat and pressure on the moulds of (5), (6) and (7), respectively.

3.2.3.1 Positive pST Bioimprint

pST Bioimprints were made from PDMS master moulds of the cell impression. First, cells were cultured and fixed in a PDMS circular chamber made as described in section 3.2.1 followed by washing with PBS and distilled water. Then a pre-cured PDMS (34 ℃ for 2 mins) was poured on top, followed by 2 hours curing at 80 ℃. This PDMS with negative cell impressions was peeled off the glass slide and cleaned with 10% SDS and 5% trypsin (the cleaning steps as described in section 3.2.2.1 for pMA substrates), and was ready as the mould for positive pST Bioimprint.

3.2.3.2 Negative pST Bioimprint

To make positive PDMS moulds for the negative pST Bioimprint, (-ve)pST, a second layer of PDMS needed to be cured on top of the negative PDMS Bioimprint made as described in section 3.2.3.1. Two methods were used to prevent the formation of crosslinking between the two layers of PDMS during the double casting. The first method used HPMC to treat the negative PDMS Bioimprint before curing the second layer of PDMS. The negative Bioimprint was treated in 0.1% HPMC for 10 minutes on a shaker followed by washing thoroughly with distilled water on a shaker for at least one hour. A positive PDMS Bioimprint was then made by pouring another layer of PDMS onto this HPMC-treated PDMS and cured at 80 ℃ for 2 hours. This was the positive PDMS mould for negative pST Bioimprint.

The second method is named thermal aging (Ziółkowska et al., 2011). This method was used to replace the HPMC treatment method because this method did not require any chemical treatment, hence preventing the risk of chemical residue contamination of the first PDMS negative Bioimprint. In this method, the positive PDMS Bioimprint was made by pouring another layer of PDMS onto the first PDMS Bioimprint and curing at 80 ℃ for 48 hours. This long curing time enabled crosslinking of low molecular species in the master PDMS Bioimprint, hence preventing it from forming bonds with the casting PDMS layer.

To make a pST Bioimprint, a pST microscope slide was pressed against a PDMS mould, and both were sandwiched with glass microscope slides. Then, this sandwich was clamped with 6 3/4" wide binder clips to give the pressure needed for transferring the pattern, and the imprint was transferred onto the pST slides at 180 ℃ for 15 min.

Scanning electron microscope imaging (Figure 10) was done to examine the structure and resolution of the negative and positive Bioimprints. As can be seen from the images, the cell fine structure such as the filopodia (the thin membrane rod-like extensions) could be replicated faithfully down to the nanometer scale onto the pST with this method.

3.2.3.3 Flat pST

The control for pST Bioimprints was flat pST ((f)pST). (f)pST was made from flat PDMS following exactly the same procedures as the making of pST Bioimprints as described above.

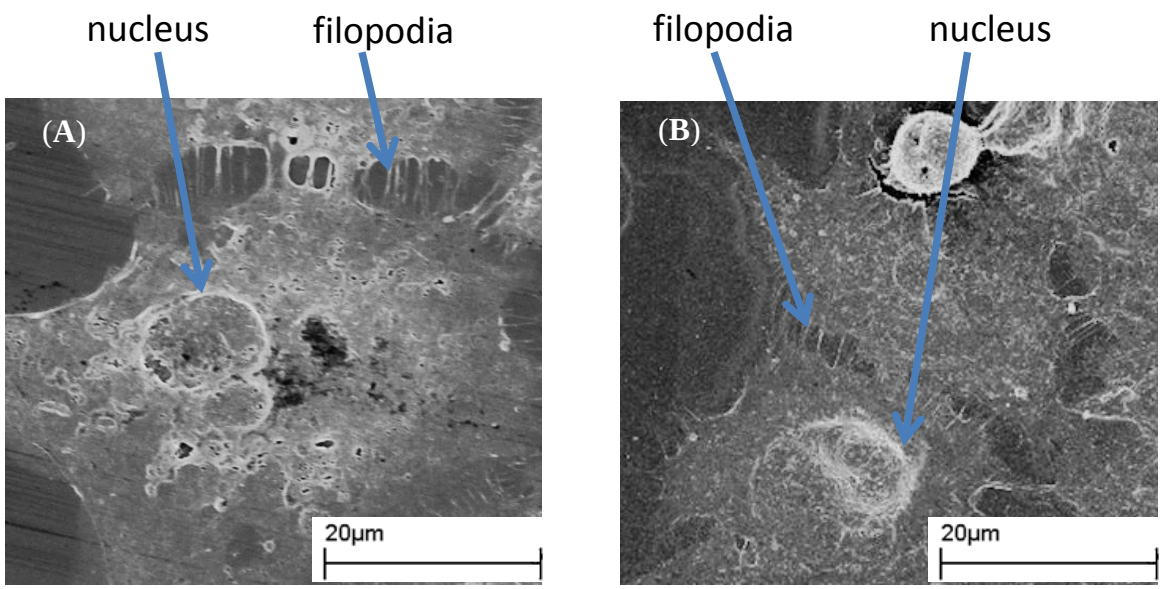


Figure 10 Representative scanning electron microscope images of the Bioimprints.

(A) A (-ve)pST imprint and (B) a (+ve)pST imprint. The images illustrate the retained fidelity of the fine features of cells during manufacture of the imprints.

3.2.3.4 Cell Culture on pST Microscope Slide Bioimprints

As described in section 3.2.1, the cell culture for making the PDMS Bioimprint was done in circular PDMS chambers, and hence, the PDMS Bioimprint that peeled off the glass slide had defined circular Bioimprint areas. This circular Bioimprint area was cut out from the non-imprinted area using a 15mm cork borer, and was pressed against a pST microscope slide during the hot embossing transfer of the Bioimprint from PDMS to pST. Because the pressure was applied only between the circular PDMS Bioimprint and the pST microscope slide, this created a circular pit on pST microscope slide only at the imprinted area, which served as a chamber for retaining cell culture medium.

To use either the negative or positive pST Bioimprints for cell culture, the pST Bioimprint was first sterilized with absolute ethanol, then rinsed with sterilized PBS pH7.4 followed by rinsing with sterilized cell culture medium without FBS. The pST Bioimprint was then ready for cell culture. Similar to cell culture on all other substrates, the Bioimprint chamber was first half-filled with cell culture medium, and then the cells were seeded into the chamber followed by filling the culture chamber with cell culture medium.

3.3 Discussion

The Bioimprint was first developed to replicate cell surface and membrane features to facilitate examination under high-resolution AFM. It was then realised that the cell-like topography of the Bioimprint may potentially be a useful substrate/platform for cell culture as it provides a physical environment with cell-like physiological features that are absent in conventional flat culture surfaces.

In this work, the Bioimprints made on pMA and pST were used, for the first time, as the culture substrate for endometrial cancer cells, and the responses of endometrial cancer cells to surface topography were studied.

There are a few technical limitations in Bioimprint making. Some improvements have been made, and will be discussed below together with suggestions that can further refine the platform. First, to ensure that the Bioimprint surface was clean enough for cell culture, after the replication process, a few cleaning steps were performed to make sure that there was no cell debris left on the Bioimprint. However, the assumption that these cleaning steps were enough to remove all biological materials has not been validated yet. Future experiments that use various staining methods for extracellular matrix or cells will be needed.

On the other hand, it was technically difficult to produce a fully confluent Bioimprint. This is because cancer cells would start to grow as a clump once they neared confluence, and if the Bioimprint was taken at that stage the imprint would lose the topography of individual cells. Hence, the densest Bioimprint would be only 80-90% confluent, which meant that the cells would still be encountering flat topography on the Bioimprint platforms. This may explain the large error bar in some experiments and the need for many repetitions for statistical robustness in most of the experiments (these experiments are presented in chapter 4 to 9 in this thesis).

In addition, each Bioimprint was sourced from a different cell culture; hence each Bioimprint was different from each other in their exact cell-like topography. Although, for the pST microscope slide Bioimprint, the PDMS Bioimprint master mould can be repeatedly used for a few times, the prolonged use of it was not recommended due to possible polymer defects resulting from repeated peeling. Hence, a methodology to turn the topography information into a computer program that enables the making of the Bioimprint from defined and constant topography information is proposed.

For pMA substrate, concavity of the pMA disk made it hard to be examined under the optical microscope. A few steps have been taken to minimise this problem, such as increasing the disk diameter from 14mm to 15mm, and the disk was made as thin as possible. Also, any unreacted methacrylic acid residue would lower the pH of the cell culture medium which is unfavourable for cells, and this was minimised by many washing

steps and overnight soaking in sterile double distilled water and cell culture medium without FBS.

On the other hand, for pST Bioimprints, the making of pST Bioimprints required the replication of cell topography onto PDMS polymer. The need for a long curing process in the PDMS Bioimprint making may cause a major issue because adding the polymer liquid on the cell layer may change the cell structure over the curing time. This concern was minimized by fixing the cells prior to making the Bioimprint. Furthermore, the making of a positive PDMS Bioimprint involved casting a second layer of PDMS on the negative PDMS Bioimprint. This required a number of peeling steps; hence often a good replication of cell features was not uniform across the Bioimprint disks due to lost information upon peeling. This was avoided only by careful peeling at this stage, and chosing only the good Bioimprints for use in cell culture.

3.4 Conclusion

Bioimprint, which is made by utilising soft lithography and hot embossing techniques, is an advanced 2D culture substrate with cell-like topography that enables biologists to study the influence of cell-like surface topography on cell growth, attachment and biological changes in response to physical environment. This could lead to the development of cell culture platforms to guide cell growth and spread. The more physiologically relevant topography of the Bioimprint compared to other regular patterns makes it a valuable tool for cell culture.

In the next few chapters, the responses of Ishikawa endometrial cancer cells to the Bioimprint were reported. First, the morphology and spreading behaviour of Ishikawa cell on pMA and pST Bioimprints were studied and were compared the response to cells on flat substrates. These results are presented in the next chapter.

Chapter 4 Influences of Substrate Material and Topography on Cancer Cell Morphology and Spreading

4.1 Introduction

Chapter three describes in detail the protocols of the making of both pMA and pST Bioimprints. Ishikawa endometrial cancer cells were cultured on the Bioimprints and then the cell morphology and spreading were examined on the Bioimprints. The results are presented in this chapter.

Cell spreading is a process where cells attach and expand their surface area across a surface. A well spread cell is a cell that extends across a large surface area and apprears flatten on the culture substrate whereas a non-adhered cell is a cell that attaches loosely on the surface appears circular. Cell spreading also reflects the cell adhesion on a surface because in order to spread on a surface, a cell will attach on the surface through adhesion molecules and then re-arrange the cell cytoskeleton to support and expand the cell body across the surface. Cell spreading is influenced by substrate material and surface topography.

Different surface properties such as wettability (hydrophilicity or hydrophobicity) (Horbett et al., 1988) and surface charge (Curtis et al., 1983), influence cell adhesion and spreading. Cell interaction with surfaces occurs indirectly, it involves cell binding to the adsorbed proteins on the substrate surfaces. The type, amount, rate and secondary conformation of protein adsorption on surfaces are in turn influenced by surface wettability and charges (Arima & Iwata, 2007; Clarke et al., 2005; Lampin et al., 1997). For example, it has been shown that proteins from culture medium serum, especially fibronectin, deposited onto surfaces assisted cells to adhere and spread, and fibronectin has been shown to be adsorbed

better on hydrophilic surfaces than on hydrophobic surfaces (Lampin et al., 1997). In a longer term culture, secreted proteins from cells such as fibronectin, laminin, collagen or other ECM fibrous proteins will replace the adsorbed proteins. These adsorption and desorption processes occur constantly and are optimum on a surface with moderate wettability (Grinnell & Feld, 1982; Lampin et al., 1997). The optimal wettability depends on the surface material and are also different among different cell types. It has been shown that endothelial cells adhered and grew better on methacrylate surface with a contact angle 40^{o} degrees (van Wachem et al., 1987). On the other hand, fibroblasts grew best on polymer surface with a contact angle 70^{o} degress (Tamada & Ikada, 1994) and L cells grew best on polymer surface with a contact angle $60\text{-}70^{o}$ (Ikada et al., 1994) (Summarized in Figure 26, adapted from Saltzman & Kyriakides, 2007).

Wettability is not the only factor that determines protein adsorption. Surface charge that is largely determined by surface functional groups also affects the deposition of proteins onto surfaces (Arima & Iwata, 2007; Evans-Nguyen et al., 2005; Thevenot et al., 2008). For example, surface charge affected the cleavage of fibrinogen to fibrin (Evans-Nguyen et al., 2005), FA assembling and integrin $\alpha5\beta1$ activation (Keselowsky et al., 2004). Moreover, surface charge determines cell morphology directly through electrostatic repulsion or attraction forces. A cell membrane is negatively charged; when cells were encountering a negatively charged surface, the extent of electrostatic repulsion was reported to be proportional to the radius of cell curvature (Parent, 1992). At a small radius (< 8Å), attractive van der Waals forces will be dominant instead of repulsive forces. For instance, on a negatively charged surface, macrophages formed small radii of pseudopodia to minimize the repulsion force (Parent, 1992). Different cell types, which have a different distribution of negative charge on the cell membrane, will have different spreading behaviour on differently charged surfaces to minimize repulsive forces.

In short, the complex combination effects of substrate surface wettability and charge determines cell adhesion and spreading behaviours, partly through adsorption of proteins onto surfaces; moreover, the outcomes are dependent on the cell type. Due to the complexity of the combined effects of various surface characteristics, and cell adhesion and spreading can be further affected by topography and mechanical factors, in which the combined effect

is different among different cell lines, there is no defined rule to predict cell spreading on a particular surface.

In this study, the three different materials used for cell culturing were glass, pST and pMA. All these three materials have contact angles, which are measurements of surface wettability, which permit cell adhesion Glass and pST are commonly used for cell culture as they allow good cell adhesion; they were included in this project to be compared to the less common cell culture substrate, pMA.

Not only substrate material but surface topography is also an important factor in influencing cell adhesion and spreading. A lot of work has been done in this regard with different cell lines: mesechyma cell, fibroblast, osteoblast, epithelial cell (Dalby et al., 2007; Karuri et al., 2004; Kidambi et al., 2007; Webb et al., 1995; Wood, 1988; Yim et al., 2010; Zinger et al., 2004) and so on. Some of these studies cultured cells on regular patterns such as pillars, pits, grooves or ridges; some in more biological mimetic 3D scaffolds made of collagen, elastin or synthetic polymers like polyamides, polylactides and so on. An even more biomimetic substrate topography was the use of bioimprinted tendon tissue microenvironment in guiding differentiation of mesenchymal cells (Tong et al., 2012).

The surface topography influence on cancer cells is nevertheless less explored, and only a few studies have examined the effect of topography on cancer cell lines, mainly in cell adhesion, growth and migration. All these studies showed that cancer cells respond to surface topography and change their behaviours (refer to the detailed discussion in Chapter 1, section 1.6).

In addition to comparing the influence of different cell culture materials, the effect of topography on endometrial cancer cells' behaviours was investigated by making the Bioimprint on pMA (Figure 8) (comparing to the flat pMA) and on pST (Figure 9) (comparing to the flat pST). Additionally, Bioimprints on pST were made as negative versus

positive topographies (Figure 9) to further investigate the effect of topography on cell behaviours.

Cell adhesion and spreading regulate cell survival and cell growth (Chen et al., 1997; Folkman & Moscona, 1978). Optimum adhesion ensures survival and growth of cells. Cell shape regulation of cell survival and growth may be partly through regulating intracellular biochemical reaction rates. This is because shape changing resulted in cell volume alteration, which then influenced local concentration of substrate and product, and ultimately affected intracellular reaction direction (Lizana et al., 2008). It has also been recently reported that NFκB localization in cells was modulated by cell morphology (Sero et al., 2015). Seeing that cell morphology can determine cell behaviours, the morphology of Ishikawa endometrial cancer cells was first checked, qualitatively and quantitatively, on different substrates.

To check the cell spreading, the cell morphology at 6, 24, 48 and 60 hours was examined with a light microscope. Then, the cell spreading area and cell circularity (the measurement of the cell roundness) were quantified. Furthermore, the spreading of actin filaments and Cytokeratin-18 of cells cultured on different substrates at 60 hours were also studied. Actin filaments were studied because they are sensitive to mechanical signals, and polymerise upon sensing exogenous forces to elevate intracellular tensional force, allowing cells to adhere and pull on an adherent surface. Cytokeratin-18 on the other hand, gives cells structural support and defines cell shape. Cytokeratin-18 restructuring can result in activation of certain intracellular biomolecules such as Rho GTPase protein, Myosin II, FAK etc (Chrzanowska-Wodnicka & Burridge, 1996; Cichowski, Brugge, & Brass, 1996; Han et al., 1997; Zheng et al.,1996) which are all biomechanically sensitive biomolecules that trigger downstream signalling pathways.

In addition, a previous study showed that cells preferentially attached on imprinted pMA surfaces (Murray et al., 2014); in this study, this idea was further tested on pST Bioimprints; by making a ‘low-confluent-Bioimprint’, cells were deposited onto a substrate with both the

flat and Bioimprint. Cell preferential attachment was then measured by comparing the spreading area between these two topographies.

4.2 Hypotheses

1. Ishikawa endometrial cancer cells have different spreading area, cell morphology and cell cytoskeleton arrangement on glass, tissue culture grade pST and pMA substrates; and between (f)pMA and (-ve)pMA as well as among (f)pST, (-ve)pST and (+ve)pST.
2. Ishikawa endometrial cancer cells have different preferential attachment between flat area and each of the (-ve) and (+ve)pST Bioimprints.

4.3 Aims

The purposes of the experiments in this chapter were to examine whether Ishikawa endometrial cells were responsive to culture substrates made of different materials or to substrates of same material but different surface topographies, by changing their forms and structures, and deposition preferences between flat and imprinted surface. Here, we aimed to:

1. Examine cell morphology at 6, 24, 48 and 60 hours on different culture substrates.
2. Examine cell actin filaments and Cytokeratin-18 spreading at 60 hours on different culture substrates.
3. Measure cell Cytokeratin-18 spreading and cell circularity on different culture substrates.
4. To determine if Ishikawa cells also show preference for binding on pST Bioimprints.

4.4 Experimental Approach

To examine cell morphology, Ishikawa cells were examined under an inverted microscope and were photographed at 6, 24, 48 and 60 hours. For cell cytoskeleton spreading, Texas Red-X phalloidin and immunofluorescent staining were used to examine actin and Cytokeratin-18, respectively. Also, cell Cytokeratin-18 spreading area and cell circularity were measured using ImageJ. For cell deposition, the cell spreading area on flat surface was measured and compared with the spreading area on imprinted surface on a same culture substrate.

4.5 Results

4.5.1 Ishikawa Endometrial Cancer Cell Morphology

4.5.1.1 Ishikawa Endometrial Cancer Cell Morphology on Glass and Tissue Culture Grade Polystyrene, Polymethacrylate Flat and Bioimprint Culture Substrates

To investigate cell adhesion and spreading, Ishikawa endometrial cancer cell images were taken after 6, 24, 48 and 60 hours so that the rate of cell adhesion and spreading on different surfaces could be compared. Cells growing on glass and tissue culture grade pST both had similar adhesion behaviour and morphology (Figure 11 and 12). Cells were first rounded and aggregated in small clusters in the medium after 6 hours of seeding; nonetheless, there were a few cells (red arrow) which had started showing attachment on the surface. From 24 hours onward, cells were all well spread on the surface and were grown to confluency (confluence is an estimation of cell density on a culture substrate) at 60 hours.

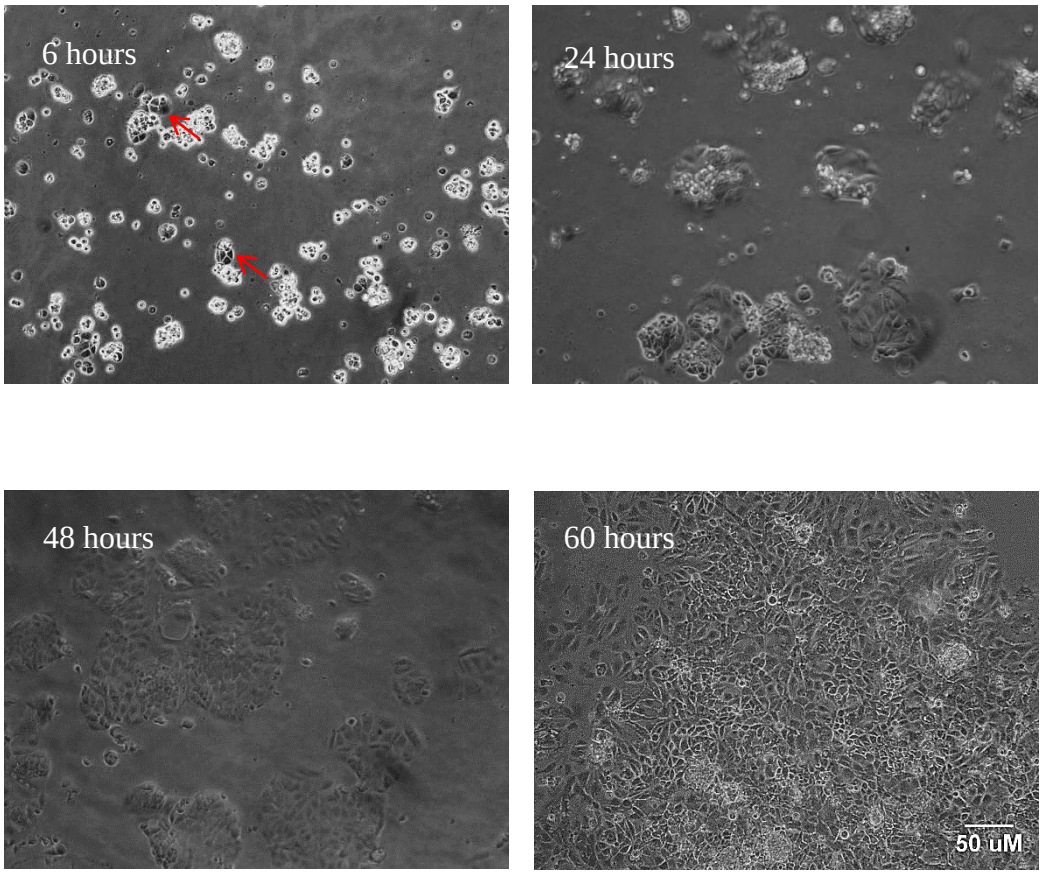


Figure 11 Representative images of Ishikawa endometrial cancer cells on glass culture substrate at 6, 24, 48 and 60 hours.

Red arrows indicate two examples of cells that showed early spreading on glass.

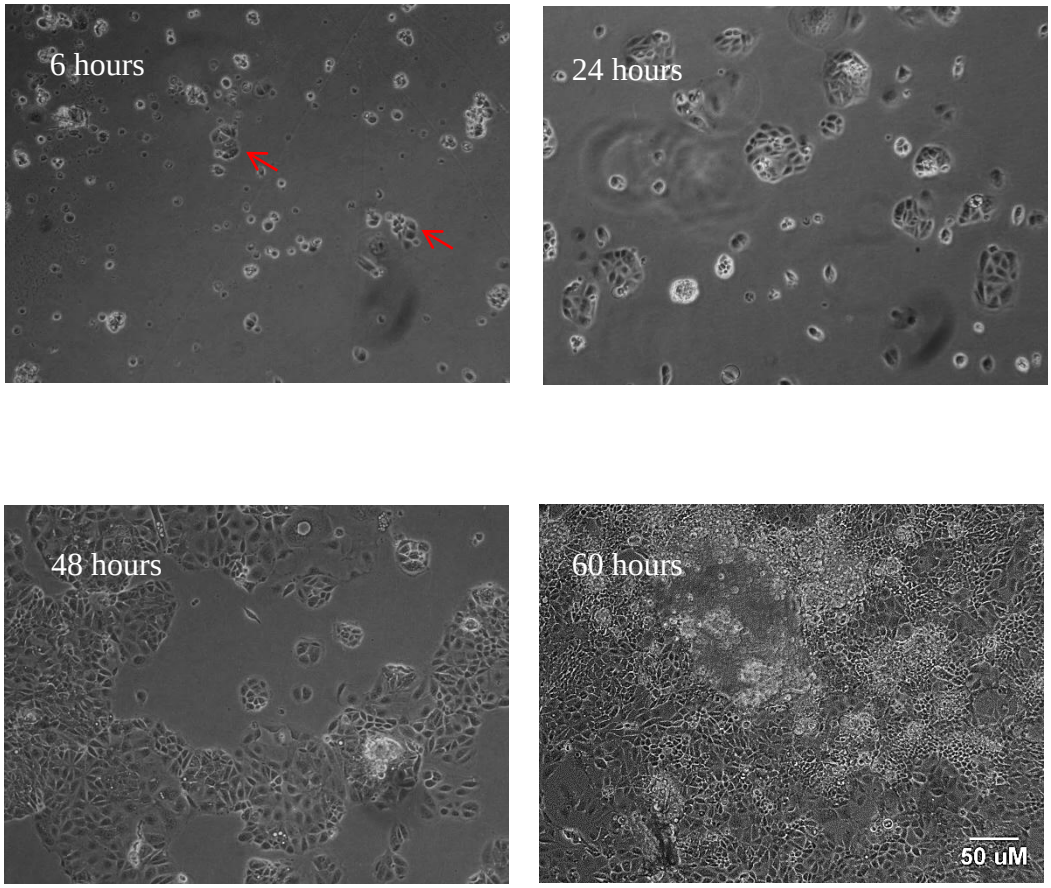


Figure 12 Representative images of Ishikawa endometrial cancer cells on tissue culture grade pST at 6, 24, 48 and 60 hours.

Red arrows indicate two examples of cells that showed early spreading on tissue culture grade pST.

In addition to glass and tissue culture grade pST, pMA was also used as our cell culture substrate. Ishikawa on (f) and (-ve)pMA both had similar adhesion behaviour and morphology to each other but distinct from Ishikawa on flat glass and tissue culture grade pST surfaces; cells looked rounded and clustered rather than flattened and spread at all times when images were taken (Figure 13 and 14). Further, at 6 and 24 hours, the cells were captured at a focal plane different from the culture substrate surface, indicating that the cells were still in the cell suspension. The culture substrate surface was identified by the visible pattern which is the texture of pMA polymer (Figure 13 and 14).

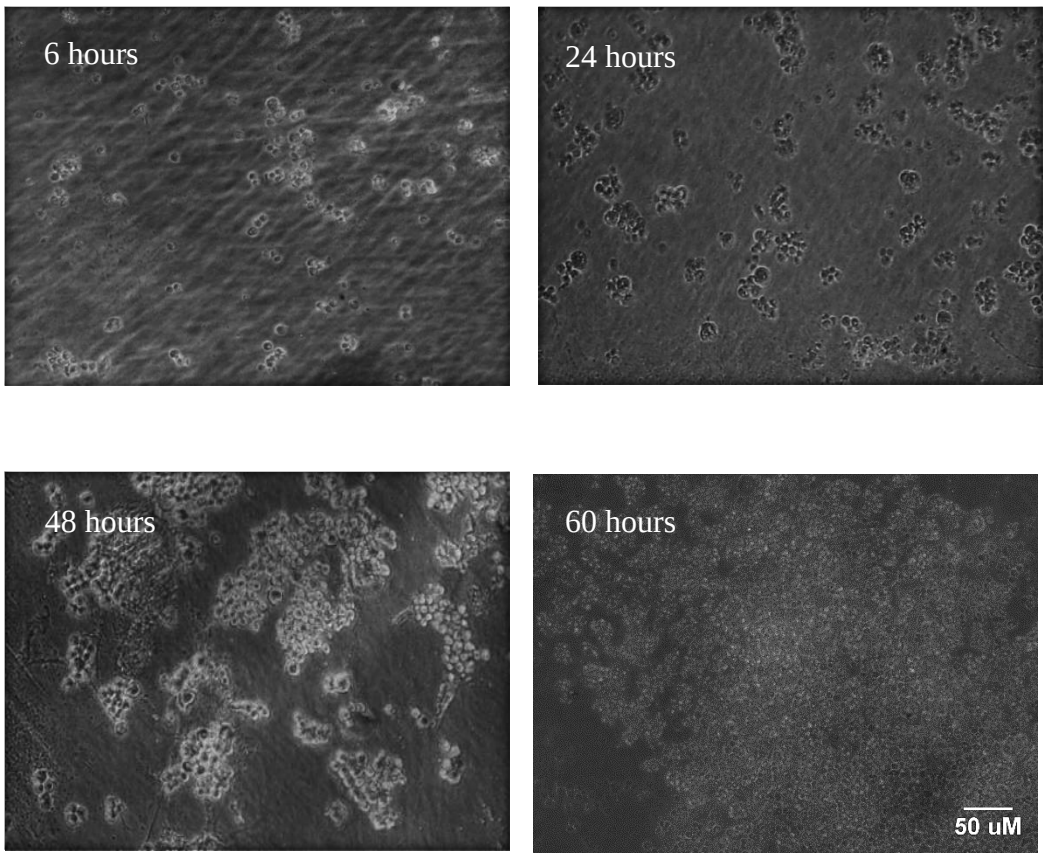


Figure 13 Representative images of Ishikawa endometrial cancer cells on (f)pMA at 6, 24, 48 and 60 hours.

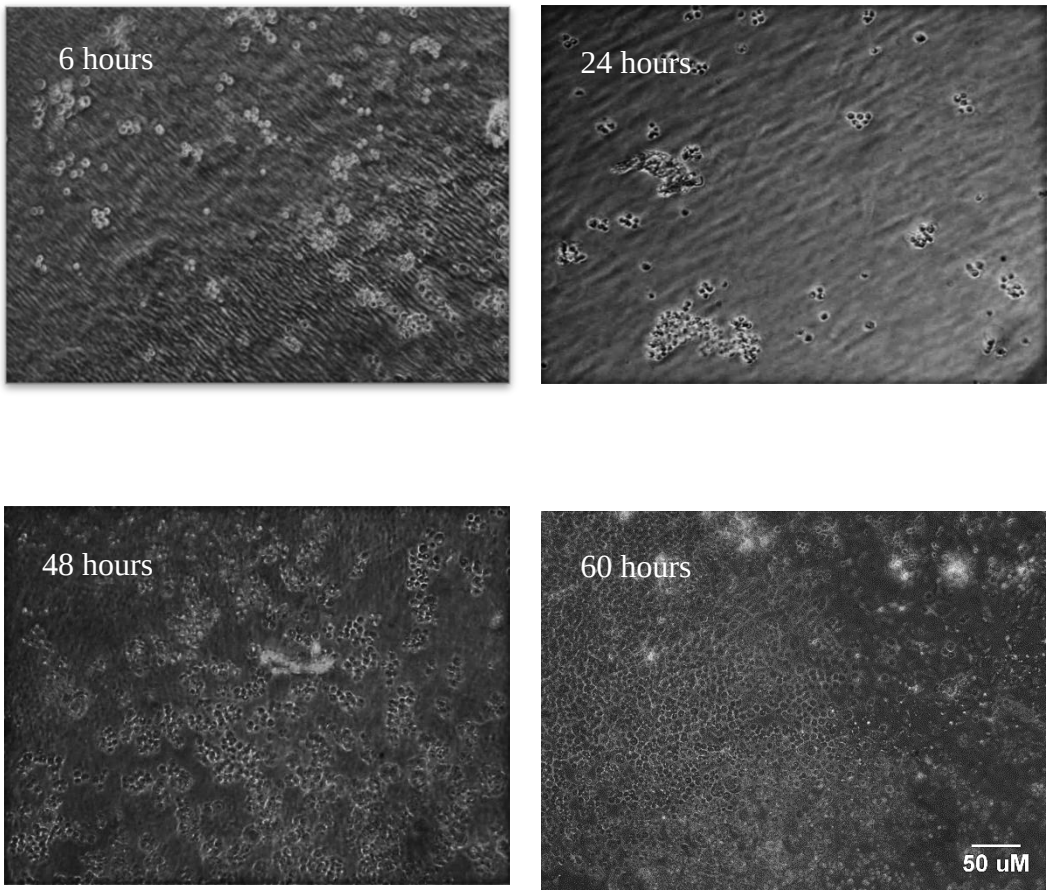


Figure 14 Representative images of Ishikawa endometrial cancer cells on (-ve)pMA at 6, 24, 48 and 60 hours.

4.5.1.2 Ishikawa Endometrial Cancer Cell Morphology on Flat, Negative and Positive Bioimprint Polystyrene Slides

Next, Ishikawa endometrial cancer cells were cultured on pST flat and Bioimprint slides. Again, cell morphology at 6, 24, 48 and 60 hours was examined to check the cell spreading. Similar to cells on tissue culture grade pST (Figure 12), cells on pST slides, both flat and Bioimprints, started to show flattened adherent morphology after 6 hours of seeding and grew to confluency at 48 hours (Figure 15, 16 and 17). At 6 hours, most of the Ishikawa cells were still in cell suspension and not attached on surface, hence the cells were seen as circular cells. The background Bioimprint was not seen at this focal plane that captured the cells. However, at 24, 48 and 60 hours, the cells were not distinguishable from the Bioimprints because the focal plane that looked at the attached cells was the same as the focal plane that focused the background Bioimprint. But at this early stage, it was speculated that cells that contained vacuoles (which were seen as white spots) were the real cells (indicated in figures with red arrows). This indistinction indicated that the cells were well-spread on pST microscope slide surfaces. For the remaining experiments, cell staining was used to provide certain information regarding cell position and spreading.

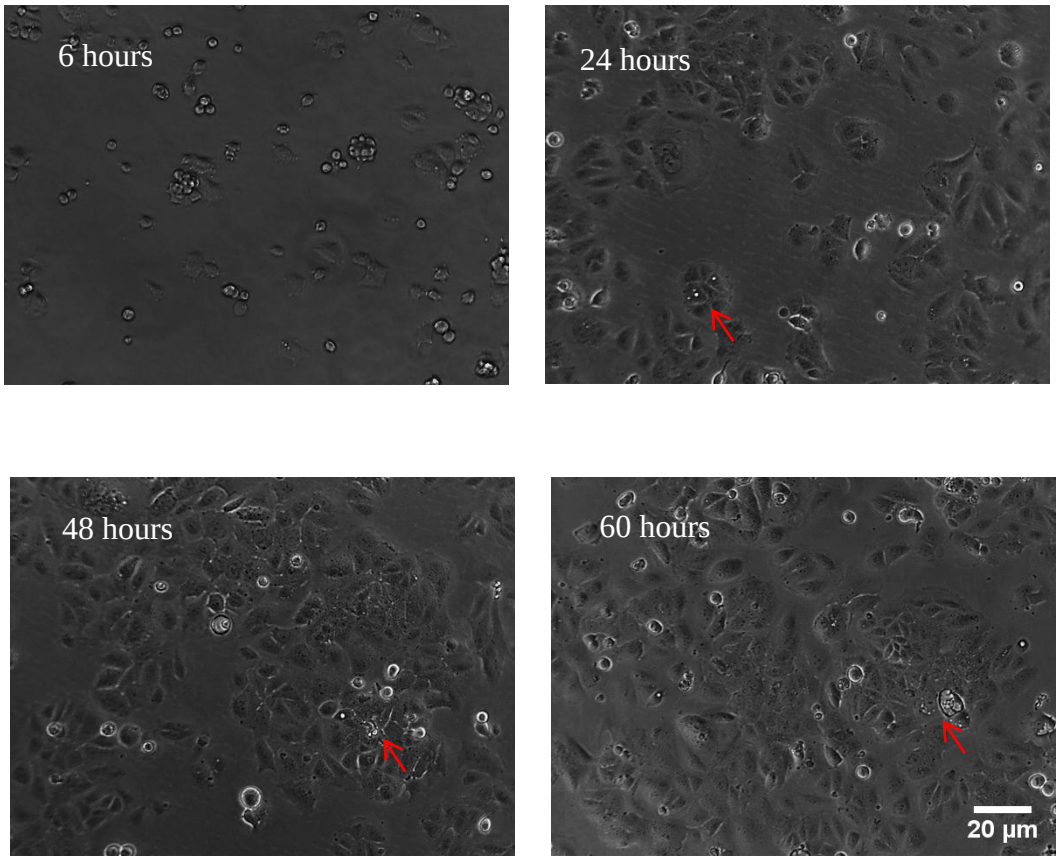


Figure 15 Representative images of Ishikawa endometrial cancer cells on (f)pST at 6, 24, 48 and 60 hours.

Red arrows indicate real cells with vacuoles.

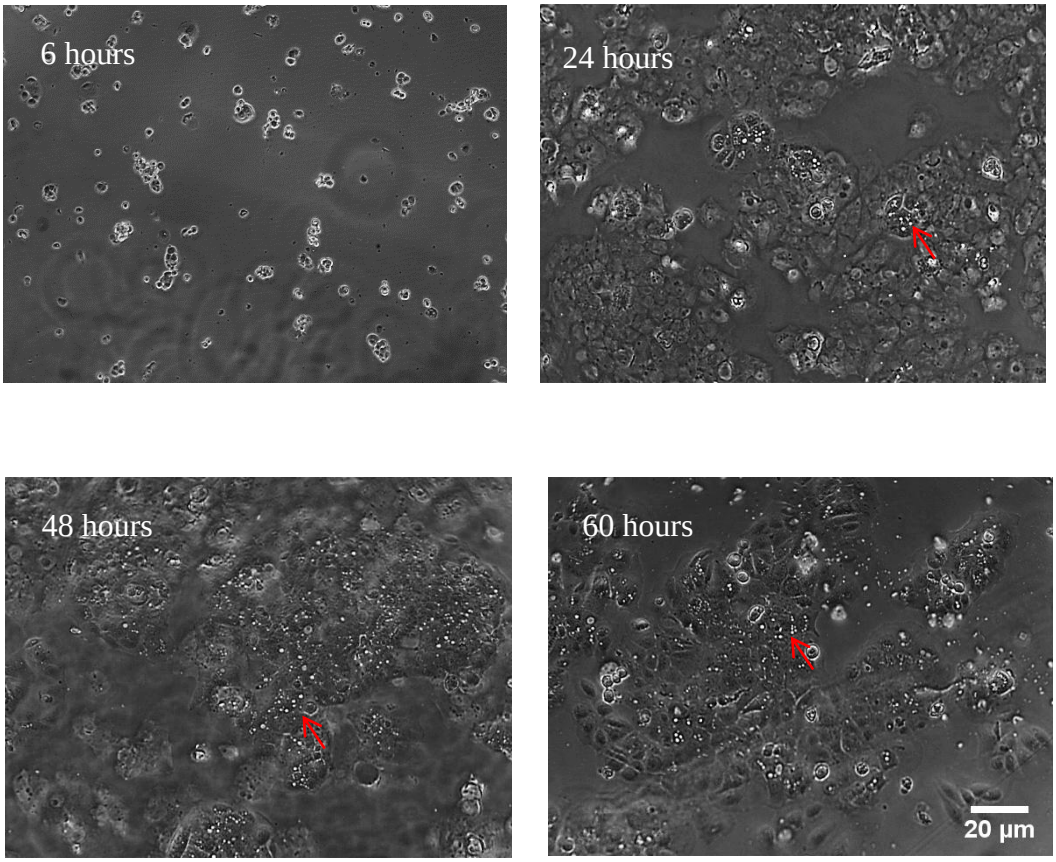


Figure 16 Representative images of Ishikawa endometrial cancer cells on (-ve)pST at 6, 24, 48 and 60 hours.

Red arrows indicate real cells with vacuoles.

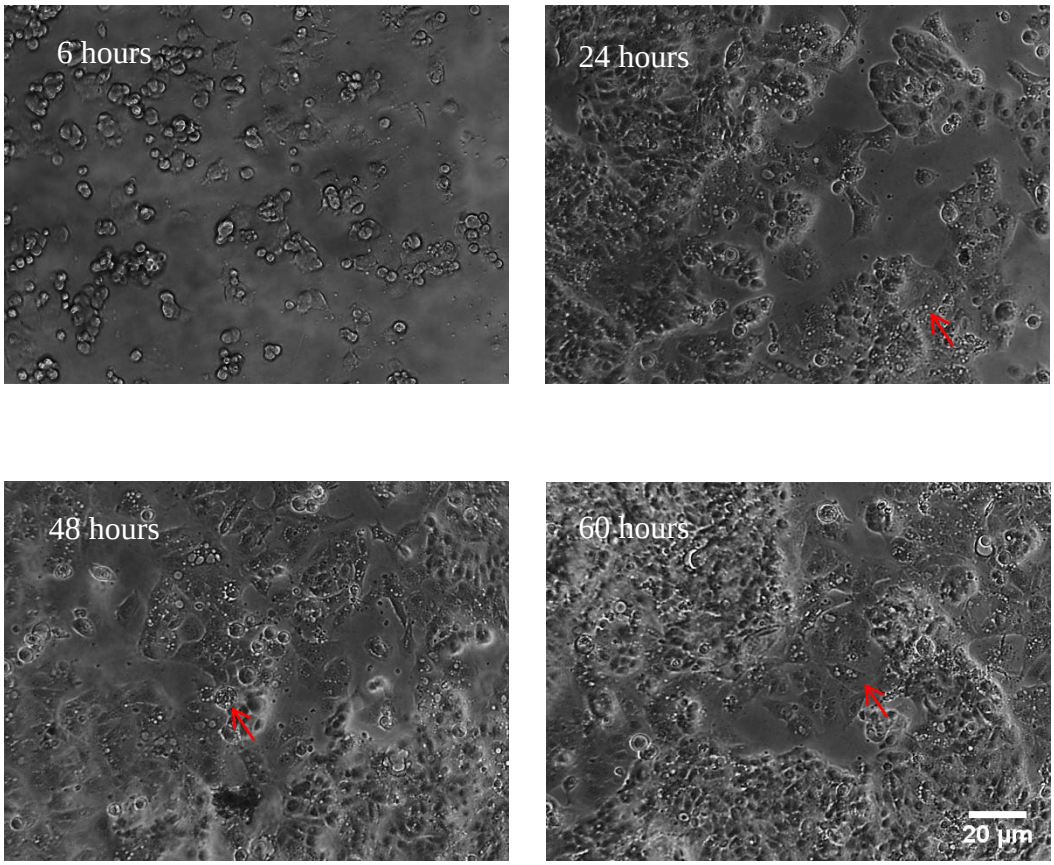


Figure 17 Representative images of Ishikawa endometrial cancer cells on (+ve)pST at 6, 24, 48 and 60 hours.

Red arrows indicate real cells with vacuoles.

4.5.2 Ishikawa Endometrial Cancer Cell Cytoskeleton

4.5.2.1 Ishikawa Endometrial Cancer Cell Cytoskeleton on Glass and Tissue Culture Grade Polystyrene, Polymethacrylate Flat and Bioimprint Culture Substrates

In addition to observing cell morphology with an inverted microscope, the cell actin filaments and Cytokeratin-18 were also stained to observe their alignment on different substrates. Cell cytoskeleton functions to support the cells on the surface hence a linear-type cytoskeleton structure indicates "well-spread" behaviour. Actin filaments were chosen to be stained since they are known to be responsive to the mechanical signal from the surroundings; also, Cytokeratin-18 was stained because it supports cell structure and defines cell size.

Ishikawa endometrial cancer cells cultured on glass and tissue culture grade pST had similar actin filaments and Cytokeratin-18 arrangement. They had well-spread cytoskeleton across both surfaces (Figure 18).

Cell actin filaments and Cytokeratin-18 staining on pMA substrates showed rounded spreading (Figure 18); when compared to cells on glass and tissue culture grade pST (Figure 18). Further, cells on (-ve)pMA biomprint had slightly more spread out cell actin and Cytokeratin-18 compared to cells on (f)pMA (Figure 18), indicated by yellow arrow).

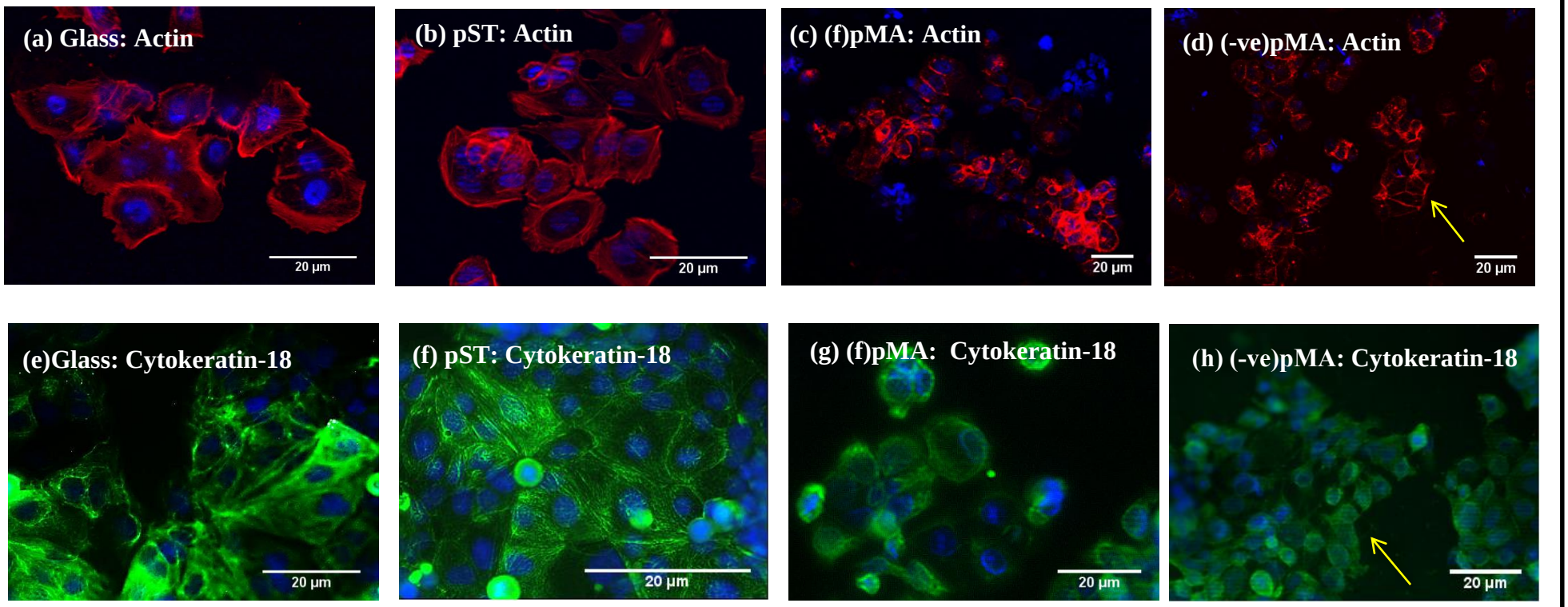


Figure 18 Representative images of Ishikawa endometrial cancer cell actin filaments and Cytokeratin-18 staining on glass, pST, (f)pMA and (-ve)pMA.

Ishikawa cell actin filament was stained red with Texas Red-X phalloidin, cell Cytokeratin-18 was stained green with Alexa Fluor 488-tagged Cytokeratin-18 antibody. and the cell nucleus was stained blue on (a)& (e) glass, (b)& (f) tissue culture grade pST, (c)& (g) (f)pMA and (d) & (h) (-ve)pMA. Yellow arrows show examples of cells that had well-spread (d) actin filament and (h) cell Cytokeratin-18 on (-ve)pMA.

4.5.2.2 *Ishikawa Endometrial Cancer Cell Cytoskeleton on Flat, Negative and Positive Bioimprint Polystyrene Slides*

In agreement with the observed well-spread behaviour of cells on pST Bioimprints in section 4.5.1.2, an examination of fluorescently stained cell cytoskeleton again showed that cells on pST surfaces: (f), (-ve) and (+ve)pST Bioimprints all had well-spread morphology (Figure 19).

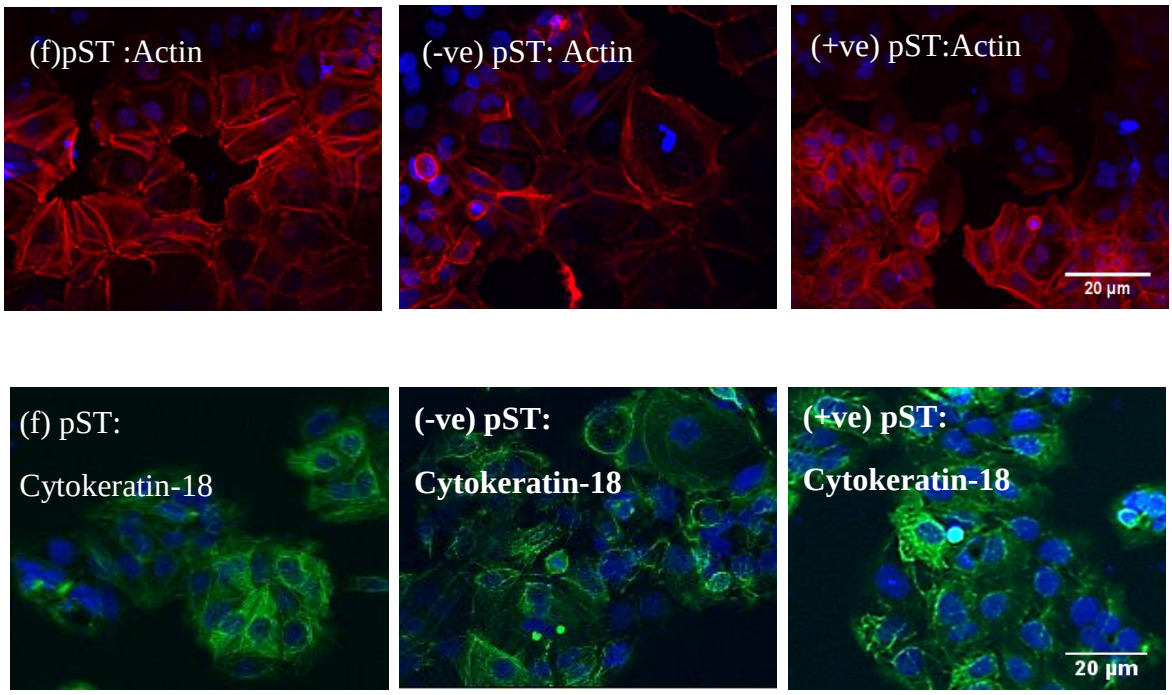


Figure 19 Representative images of Ishikawa endometrial cancer cell actin filaments and Cytokeratin-18 staining on (f), (-ve) and (+ve)pST.

Ishikawa cell actin filament was stained red with Texas Red-X phalloidin, cell Cytokeratin-18 was stained green with Alexa Fluor 488-tagged Cytokeratin-18 antibody. and the cell nucleus was stained blue on (from left to right) (f)pST, (-ve)pST and (+ve)pST Bioimprints.

4.5.3 Ishikawa Endometrial Cancer Cell Spreading Area and Circularity

4.5.3.1 Ishikawa Endometrial Cancer Cell Spreading Area and Circularity on Glass, Tissue Culture Grade Polystyrene, Polymethacrylate Flat and Bioimprint Culture Substrates

After the preliminary observation that cells had different morphologies between substrates made of conventional cell culture substrates versus pMA; and between (f)pMA versus (-ve)pMA; no observable difference was seen between (f)pST versus either (+ve) or (-ve)pST. Next, to quantify cell morphology, the cell cytoskeleton spreading area was measured to determine the effects of material and topography on cell structure.

Cells showed larger cytoskeleton spreading area on glass and tissue culture grade pST surfaces, which paralleled the observation that cells had well-spread morphology on these two surfaces. Whereas for cells on pMA surfaces, in which cells appeared to be circular on both the flat and the Bioimprint surfaces, cells had smaller spreading area compared to cells on glass and tissue culture grade pST. Nonetheless, cells on (-ve)pMA had larger spreading area compared to cells on (f)pMA (Figure 20).

Furthermore, cell circularity measurement showed that cells on pMA substrates were significantly more circular than cells on glass and tissue culture grade pST, and comparison between (f)pMA and (-ve)pMA showed that cells were less circular on (-ve)pMA; interestingly, circularity of cells on tissue culture grade pST versus (-ve)pMA was not significantly different (Figure 21).

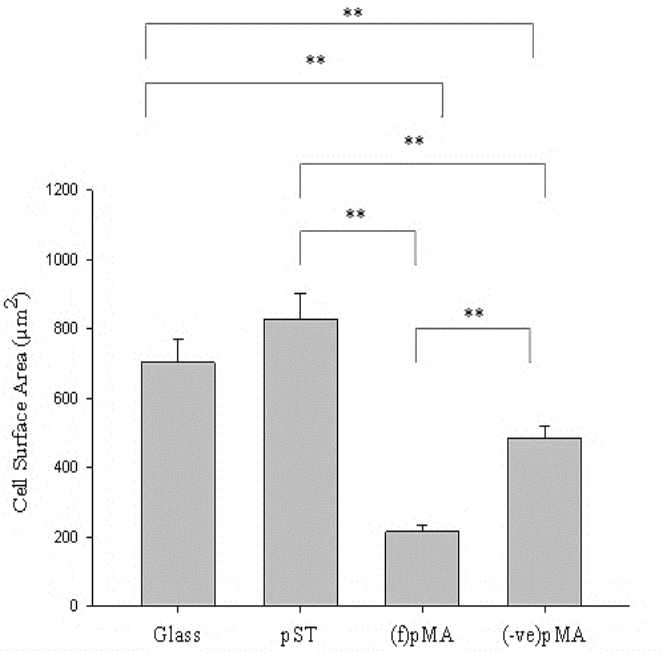


Figure 20 Ishikawa endometrial cancer cell spreading area on glass, tissue culture grade pST, (f)pMA and (-ve)pMA.

Ishikawa cells were cultured for 60 hours, followed by cell fixing and Cytokeratin-18 staining. The cell images were then taken from four corners of a culture chamber. Then at least 20 cells were chosen from each corner for cell surface area measurement. Data are presented as cell surface area mean ± SEM of at least 80 Ishikawa cells. **, p<0.01.

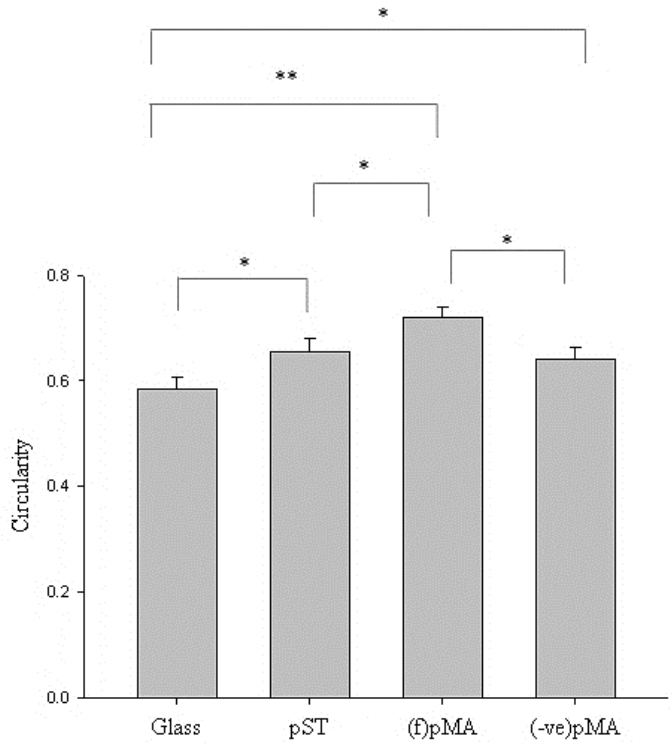


Figure 21 Ishikawa endometrial cancer cell circularity on glass, tissue culture grade pST, (f)pMA and (-ve)pMA.

Ishikawa cells were cultured for 60 hours, followed by cell fixing and Cytokeratin-18 staining. The cell images were taken from four corners of a culture chamber. Then at least 20 cells were chosen from each corner for cell circularity measurement. Data are presented as cell circularity mean ± SEM of at least 80 Ishikawa cells. **, p<0.01; *p<0.05.

4.5.3.2 Ishikawa Endometrial Cancer Cell Spreading Area and Circularity on Flat, Negative and Positive Bioimprint Polystyrene Slides

For pST microscope slides, even though there was no observable difference in cell morphology, quantification of cell cytoskeleton spreading showed that cells on (f)pST had a larger surface area compared to cells on (-ve) and (+ve)pST (Figure 22).

Furthermore, cells on (-ve)pST were less circular than cells on (f)pST and (+ve)pST, and no statistical difference between cells on (f)pST and (+ve)pST was observed (Figure 23).

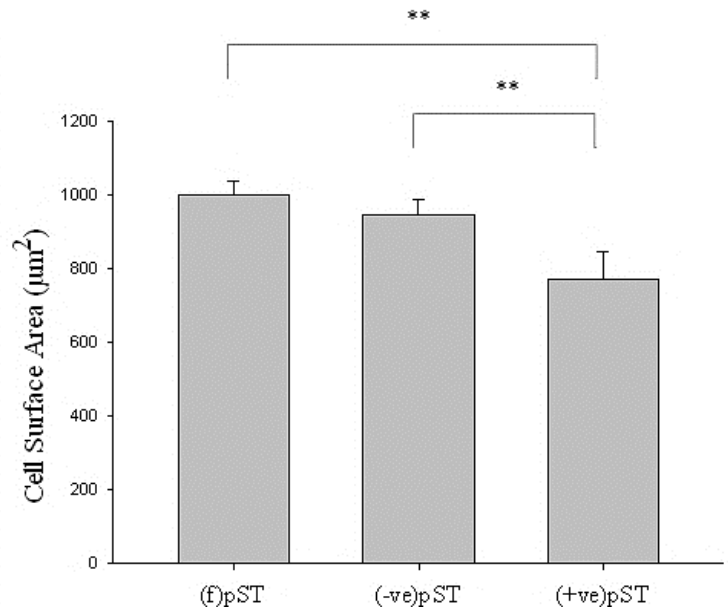


Figure 22 Ishikawa endometrial cancer cell spreading area on (f)pST, (-ve)pST and (+ve)pST imprint. Ishikawa cells were cultured for 60 hours, followed by cell fixing and Cytokeratin-18 staining. Cell images were taken from four corners of a culture chamber. Then at least 20 cells were chosen from each corner for cell surface area measurement. Data are presented as cell surface area mean ± SEM of at least 80 Ishikawa cells. **, p<0.01.

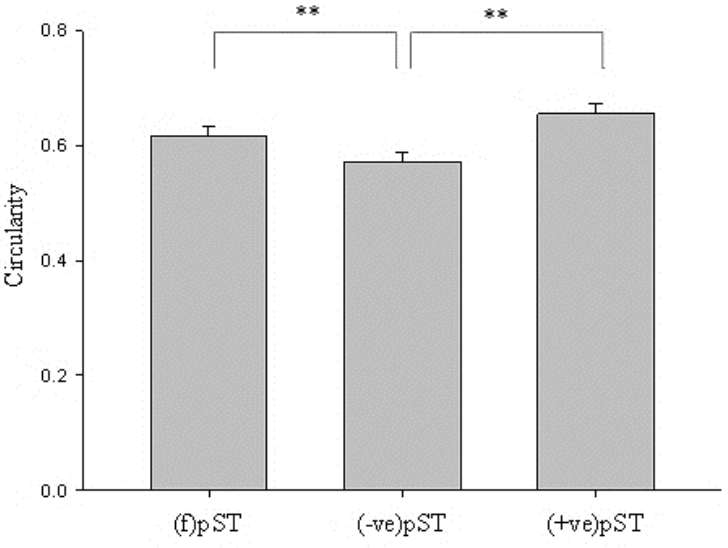


Figure 23 Ishikawa endometrial cancer cell circularity on (f)pST, (-ve)pST and (+ve)pST imprint.

Ishikawa cells were cultured for 60 hours, followed by cell fixing and Cytokeratin-18 staining. Cell images were taken from four corners of a culture chamber. Then at least 20 cells were chosen from each corner for cell circularity measurement. Data are presented as cell circularity mean ± SEM of at least 80 Ishikawa cells. **, p<0.01

.

4.5.4 Specificity of Ishikawa Endometrial Cancer Cell Alignment on Surface Topography

4.5.4.1 Ishikawa Endometrial Cancer Cells on Ishikawa Polystyrene Microscope Slide Bioimprints

Previously works in our lab observed that there was preferential attachment on imprinted areas on (-ve)pMA compared to flat areas (Murray et al., 2014). Here cell deposition on pST flat or Bioimprint areas was quantitatively measured with the methods described in Chapter 2 Section 2.7. The measured cell area was then compared to the proposed cell area.

Ishikawa cells were observed to have selectively grown on a substrate negatively imprinted with Ishikawa cells. No selective binding was observed on the substrate that was positively imprinted (Figure 24).

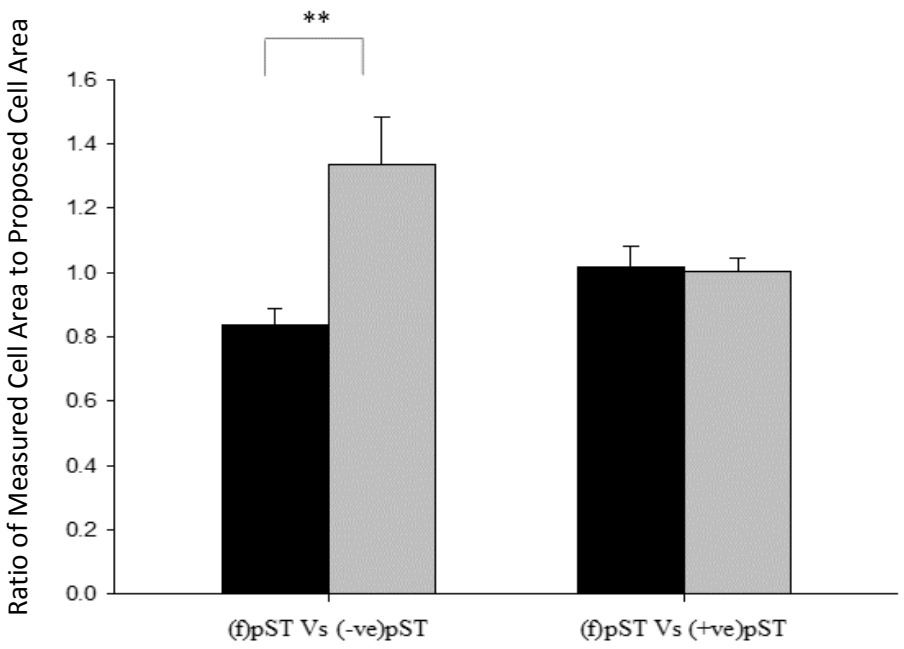


Figure 24 Ratio of the measured Ishikawa cell area to the proposed cell area on respective surfaces.

Data are presented as fraction of cells mean ± SEM of 5 independent experiments in quadruplicate.**, $p<0.01$.

4.5.4.2 *Ishikawa Endometrial Cancer Cells on C2C12 Murine Myoblast Polystyrene Microscope Slide Bioimprints*

me procedure was performed using an imprint of C2C12 mouse myoblast cells as substrate for the endometrial cancer cells to investigate the possibility that the preference was a result of a non-specific effect of surface patterning. In contrast to Ishikawa cells cultured on Ishikawa cell imprints, Ishikawa cells cultured on a substrate negatively imprinted with C2C12 cells showed no preferential attachment on imprinted area. Further, there was again no selection on a substrate positively imprinted with C2C12 cells (Figure 25).

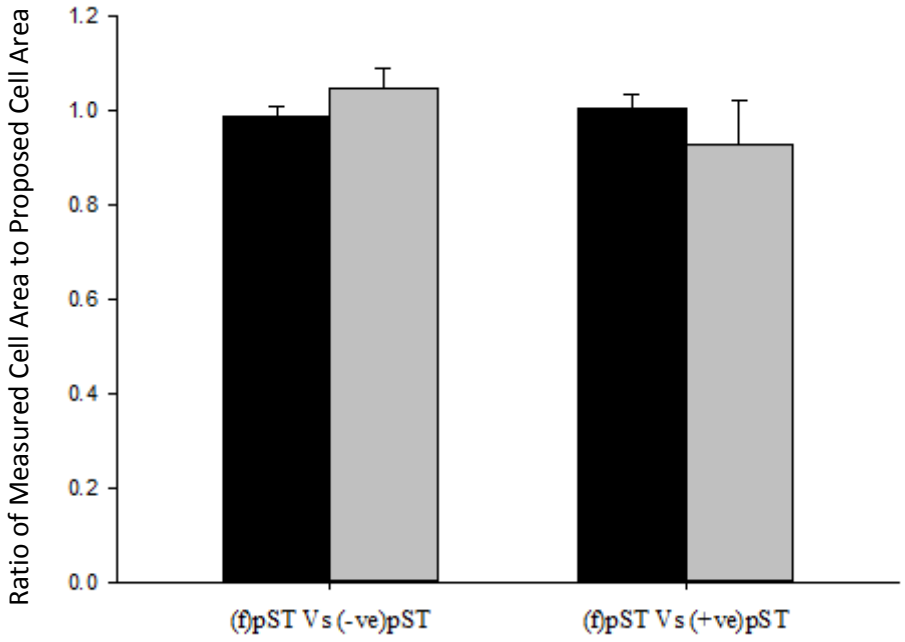


Figure 25 Ratio of the measured Ishikawa cell area to the proposed cell area on respective surfaces.

Data are presented as fraction of cells mean ± SEM of 5 independent experiments in quadruplicate.

4.6 Discussion

4.6.1 Ishikawa Endometrial Cancer Cell on Glass, Tissue Culture Grade Polystyrene and Polymethacrylate Flat and Bioimprint Culture Substrates

Ishikawa endometrial cancer cells adhered on glass and tissue culture grade pST flat surfaces in a very short time and adhered very well to these surfaces. This is not surprising since glass and tissue culture grade pST are both substrates that support cell adhesion which makes them commonly used for cell culture. Glass was the very first material used for cell culture in the early 20th century; and is now mainly used for experiments involving microscopy imaging. In the mid-20th century, the culture substrate shifted from glass to the more convenient disposable pST. pST itself is not a favourable substrate for cell adhesion because of its charge-neutral and hydrophobic surface, hence it needs surface treatments such as corona discharge and plasma treatment. Surface treatments on pST surface incorporate oxygen ions onto surfaces to make it hydrophilic and negatively charged. In this project, two sources of treated pST were used for studies that involved comparison between tissue culture grade flat pST and pMA (the source was the Nunc Omni polystyrene tray), and for comparison between (f)pST and pST Bioimprints (the source was the Ted Pella polystyrene microscope slide); these pST substrates may have been differently surface-treated, or have differences in their compositions. However, there were no differences in the effects that were observed.

The reasons behind the difference in cell adhesion on glass, tissue culture grade pST and pMA substrates are related to the surface properties including wettability and surface charges of these substrates. The glass has a negatively charged surface due to dissociation of terminal silanol groups in aqueous conditions, while the treated tissue culture grade pST has a negatively charged surface in solution due to the presence of oxygenated functional groups on surfaces. These negatively charged surfaces may have facilitated protein deposition from either the serum or cell secretions, that in turns assists cell adhesion. Instead, pMA has a charge-neutral surface that may promote poor protein deposition and so resulting in lower cell adhesion compared to glass and tissue culture grade pST surfaces.

Moreover, each of these materials has different contact angles. Glass, tissue culture grade pST and pMA each has been reported to exhibit angles of wettability of 26-45, 35-68 and 65-80 degrees, respectively (Saltzman & Kyriakides, 2007), which are the contact angle ranges that allow cell adhesion (Figure 26). In our laboratory, contact angles for glass and tissue culture grade pST were observed to be 23.935˚ and 58.295˚, respectively (Murray et al., 2014).

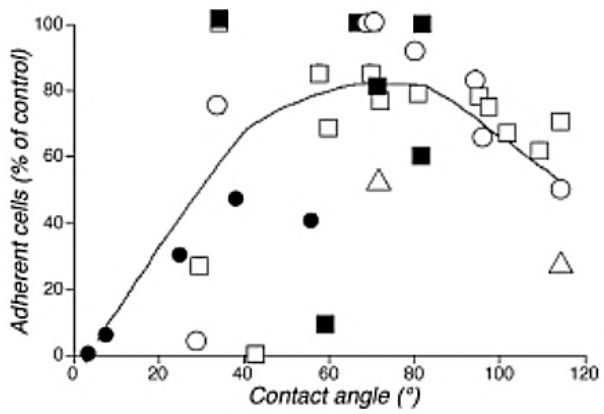


Figure 26 Cell adhesion at different contact angle. Fibroblasts (open squares); L cells (open circles) and endothelial cells (open triangles and filled circles).

Adapted from Saltzman, W. M., & Kyriakides, T. R. (2007). Chapter Twenty-Cell interactions with polymers. In R. L. L. Vacanti (Ed.), Principles of Tissue Engineering (Third Edition) (pp. 279-296). Burlington: Academic Press.

It has been found that moderate wettability gave cells the optimum cell adhesiveness (Saltzman & Kyriakides, 2007). Hence, glass and treated pST are both ideal cell culture substrates since their surfaces are negatively charged and the surface contact angles are close to the optimum culture wettability range. On the other hand, pMA is a biocompatible substrate, yet it is not a very favourable cell culture substrate because of the slightly high surface contact angle and its neutral surface.

The influence of substrate material characteristics on cells was shown in our observations that Ishikawa cells appeared circular and smaller on both (f) and (-ve)pMA than on glass and tissue culture grade pST, using inverted light microscopic examination, cell

cytoskeleton staining and cell circularity measurement. Nonetheless, by comparing between (f)pMA and (-ve)pMA, Ishikawa cells were bigger in size and less circular if the Bioimprint was present. This implies that even on a non-favourable substrate, the presence of cell-like surface topography helps cells to spread better.

4.6.2 Ishikawa Endometrial Cancer Cell on Flat, Negative and Positive Bioimprint Polystyrene Slides

On the other hand, on pST, which is a substrate optimized for cell adhesion, the Bioimprint, especially the positive Bioimprint may restrict cells to spread, which can be seen from smaller cell size and higher circularity on (+ve)pST compared to (f)pMA.

For pST microscope slides, Ishikawa cells also showed preferential attachment on (-ve)pST but not on (+ve)pST; which was supported by the previous observation that cells showed preferential attachment on (-ve)pMA (Murray et al., 2014). This difference between (-ve)pST and (+ve)pST may be because of gravitational effect of pulling cells down into the pit, or gravitational effect on the deposition of proteins. To test this hypothesis, Ishikawa cells were cultured on a different type of Bioimprint: C2C12 murine myoblast Bioimprint. Here C2C12 murine myoblast cells were chosen because this cell line has different morphology from that of Ishikawa cells. Hence, C2C12 murine myoblast Bioimprint was a culture platform that similarly had pit-and hump-like topography, but the topography shape was different from the seeding Ishikawa cells.

Ishikawa cells did not show similar preferential attachment on C2C12 (-ve)pST Bioimprint. Hence, the presence of negative Bioimprint is not the reason for the observed preferential attachment but the shape of the Bioimprint is influential.

4.7 Conclusion

The results in this chapter favour our hypothesis that the spreading behaviour of Ishikawa endometrial cancer cells can be influenced by physical microenvironment. Ishikawa cells had well-spread morphology, larger spreading area and were less circular on glass and tissue culture grade pST, compared to pMA substrates. In addition to substrate materials, the presence of cell-like topography, both on pMA and pST substrates, has changed the cell spreading and morphology. On pMA substrates, the Bioimprint improved cell spreading as shown by larger cell spreading area and less circularity on (-ve)pMA than on (f)pMA whereas on pST microscope slide substrates, (-ve) and (+ve) Bioimprints both may have limited cell spreading.

Moreover, Ishikawa endometrial cancer cells had preferential attachment on (-ve)pST than on (f)pST, which paralleled with previous observations that cells had preferential attachment on (-ve)pMA. Most importantly, this preferential attachment was not seen on (+ve)pST nor on (-ve)pST Bioimprints made from a different cell type.

These observations imply that surface topography, which was able to be studied independently from the substrate material, is influential on the area of cell spreading, morphology and preferential adhesion. Since cells were seen to respond to different substrate materials and topographies in terms of cell spreading and morphology, the adherence and growth of Ishikawa endometrial cancer cells on substrates of different materials with or without the Bioimprint were investigated. In the next chapter, the cell structure was characterised further by looking at the expression and behaviours of adhesion molecules and cytoskeleton in Ishikawa endometrial cancer cells.

Chapter 5 Influences of Substrate Material and Topography on Ishikawa Endometrial Cancer Cell Adhesion Molecules and Cell Cytoskeleton

5.1 Introduction

Ishikawa endometrial cancer cells morphology and spreading were observed to be different in response to different physical microenvironments in the previous chapter. Here in this chapter, the results that further characterize the cell adhesion and cytoskeleton behaviours in response to culture substrate material and topography are presented.

Ishikawa cells were observed to have different morphologies which indicated that they spread differently on distinct substrates of different materials and topographies. This brought the project to the next question of whether or not the expression of cell adhesion molecules was also affected. For this, the expression of the cell adhesion receptor, β1 integrin, and the activation of a downstream kinase FAK were quantified. Further, because the cell adhesion molecules were known to influence cell cytoskeleton arrangement and density that ultimately changed the cell spreading, the expression levels of actin and Cytokeratin-18 were investigated.

5.5.1 Integrins

Integrins (Figure 27) are transmembrane hetero-dimer receptors consisting of an α subunit and a β subunit. There are 18 α subunits and 8 β subunits that give rise to 24 possible combinations of integrin receptors. Integrins were first described in 1986 and marked a

major breakthrough in the field of biomechanical study (Tamkun et al., 1986). The extracellular part of the integrin binds to ECM components, such as to fibronectin through Arg-Gly-Asp (RGD) tripeptide sequences. Whereas the intracellular part of the integrin is attached to adaptor proteins including talin, vinculin and FAK, forming a focal adhesion (FA), which in turn is connected to actin cytoskeleton. In short, integrin is the bridge between ECM and intracellular cytoskeleton and proteins. The function of integrin is to work as a sensor to physical environment changes. The physical environment changes can be either endogenously or exogenously initiated. Integrin senses the changes and then conveys the force signal bi-directionally. Integrin can be activated extracellularly, which then changes the cell signalling intracellularly. Alternatively, integrin can also be activated intracellularly, which alters the integrin's affinity to ligands extracellularly. For example, integrin has been shown to be activated by ligand mimetic peptide or Mn^{2+} extracellularly, and altered its conformation from the inactive form to the active structure (Takagi et al., 2002). On the other hand, integrin can also be activated by talin in the intracellular compartment, and then changed from the inactivate clasped structure to the activate unclasped conformation (Vinogradova et al., 2002).

The activated integrins cluster together with a number of adaptor proteins intracellularly and form FA (Galbraith et al., 2002; Paszek et al., 2005). In this activated form, integrin changes the composition and movement of the intracellular adaptor proteins and/or changes the network lattice of the intracellular cytoskeleton, which ultimately changes the cell behaviours. The next section discusses the role of FA in mechanical signalling.

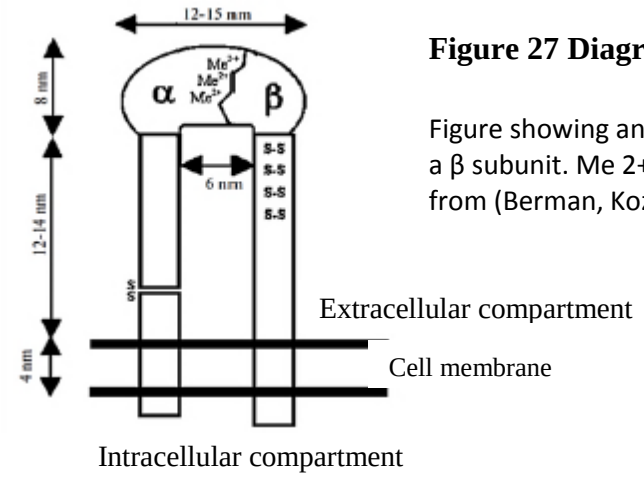


Figure 27 Diagram of hetero-dimer integrin.

Figure showing an integrin molecule consisting of an α and a β subunit. Me 2+: methyl 2+, S-S: disulfide bond. Adapted from (Berman, Kozlova, & Morozevich, 2003, p. 1286).

5.1.2 Focal Adhesion (FA)

Integrin clustering is followed by a formation of cell-matrix adhesion complex or focal complex (FX) that matures and turns into FA by recruiting more adaptor proteins. FA formation is controlled by mechanical signals. The assembly of proteins and integrins to FA is controlled by the direction of the cell tensional force (Ballestrem et al., 2001; Besser & Safran, 2006). Moreover, FA sites are not static; FAs are able to assemble and disassemble accordingly in response to signals from the surroundings (Schwarza et al., 2006).

At the mature FA sites, FAK is one of the main kinases that modulate downstream signalling. Activation of FAK occurs through phosphorylation at tyrosine 397 and this is followed by clustering of more integrins and adaptor proteins to the FA site (Kornberg et al., 1992; Kornberg et al., 1991; Shi & Boettiger, 2003). The activated FAK also activates Src, Ras-related C3 botulinum toxin substrate 1 (Rac-1), Cell division control protein 42 (Cdc 42), Rho GTPases and so on. These activated biomolecules will then change the behaviours of cell cytoskeleton or signalling biomolecules. For example, the activated Rho GTPases restructured actin cytoskeleton and increased the tensional force of the actin filaments (Nobes & Hall, 1995). Hence, FA has a strong relationship with the cell stress fibres and the tensional force the cell exerts on the ECM. Due to its effects on the cellular stress fibres, mechanical signal control of FA behaviours is partly through changing the features of the cell stress fibres, including the arrangement, density, localization or the cell stress fibres' association with other biomolecules.

5.1.3 Cell Cytoskeleton

Biological cells are described as a tensegrity model which is an energy model in which cells maintain their shape by tensile force. This model is based on the architecture of cells in which the cells maintain their structural stability through cytoskeleton. Cytoskeleton, which literally means the skeleton of a cell, is a force-bearing structure that supports the cell, defines cell shape and controls cell movement through remodelling itself. Components of

cytoskeleton include microtubules, intermediate filaments (IF) and actin filaments, each of them having different roles in force transmission. Compression stress experienced by cells is tolerated by microtubules whereas tensional stress is borne by the actin microfilaments and the intermediate filaments (Dennerll et al., 1988; Stamenović & Coughlin, 1999; Stamenović et al., 1996; Wang et al., 1993; Wang et al., 2001). These three cytoskeleton types are connected to each other forming a network through cross-linking proteins.

Actin filaments or filamentous-actin (F-actin) are made of globular actin (G-actin) and have a polar structure with two ends termed the plus and minus ends. The plus end grows towards the cell membranes and the minus end connects with microtubules. The structure of actin filaments can vary from highly oriented filament bundles or randomly arranged filaments. Different arrangements of actin filaments possess distinct functions. The function of each was shown clearly in a study done using endothelial cells: the organized structure anchored cells on substrate or was associated with cell-cell contacts whereas randomly arranged actins were involved in cell motility or cellular microstructure movement such as movement of projections during phagocytosis (Gipson & Anderson, 1979). Cells respond to extracellular forces through re-distributing and remodelling their actin filaments, which then alters the intracellular tensile force, resulting in shape or cell stiffness changing. For example, actin stress fibres can behave like viscoelastic cables and polymerize upon sensing exogenous forces to elevate intracellular tensional force, allowing cells to adhere and pull on ECM protein fibres (Bellows et al., 1982; Chrzanowska-Wodnicka & Burridge, 1996; Ehrlich et al., 1991; Forscher & Smith, 1988; Grinnell et al., 1998; Miyata et al., 1999; Paterson et al., 1990). The ability of actin filaments to carry out these functions is because actin filaments are associated with myosin motors that actively convert chemical energy adenosine triphosphate (ATP) to mechanical energy, generating a tensional force to support cells.

Another cell cytoskeleton protein that was of interest was Cytokeratin-18 which is an IF. IFs form an extensive network inside cells and link the cell membrane or organelles to the nuclear membrane or nucleoplasm. Due to their extensive network within cells, they are involved in directing intracellular organelle positioning and organization. Further,

Cytokeratin-18 has been reported to be involved in maintaining cell structure and plays a role in adhesion and spreading (Bordeleau et al., 2010; Bordeleau et al., 2012).

In this project, the culturing of Ishikawa cells on substrates of different materials and different topographies exposed the cells to different physical signals. To study the cell responses to these substrates the expression and distribution of β1 integrin were first investigated as β1 integrin is the main β subunit and forms dimers with at least 12 α subunits. Then, the expression of FAK and phosphorylated-FAK (pFAK) were studied. Furthermore, the expression levels of actin and Cytokeratin-18 were measured to see the changes of these molecules in response to the Bioimprint.

5.1.4 Nitric Oxide Secretion

Nitric oxide (NO) is one of the compounds secreted in response to mechanical stimulation through modulation of the F-actin and G-actin ratio in the cell. NO is one of the few gaseous biological signalling messengers and is synthesized by NO synthases (NOS). There are three types of NOS: neuronal NOS (nNOS), endothelial NOS (eNOS) and inducible NOS (iNOS). NO synthesized by nNOS acts as a neurotransmitter, NO synthesized by eNOS is involved in vasodilation, smooth muscle cell proliferation, inhibition of platelet aggregation and apoptosis, whereas NO made by iNOS is required in macrophage-related immunity. NO has also been linked to cancer occurrence, in which it can promote or inhibit cancer. NO generated by macrophages has been reported to be apoptotic to cells and reduced metastasis of cancer cells (Li et al., 1991; Xie et al., 1995). Nonetheless, NO has also been shown to promote tumorigenesis (Mordan et al., 1993) and angiogenesis through increasing VEGF secretion (Ambs et al., 1998).

It has been observed that vascular endothelium cell stiffness determined the NO secretion level, where softer cells secreted more NO compared to stiff cells (Fels et al., 2010). Further study showed that the stiffness of endothelial cells was modulated by cortical-F actin in

which depolymerisation of cortical F-actin to G-actin softened the cells and released NO (Fels et al., 2012).

Aldosterone, which is a mineralocorticoid hormone, was shown to be able to transiently soften endothelial cells, thereby increasing NO secretion (Fels et al., 2010). At a longer incubation time, aldosterone, on the other hand, has different influence on cell NO secretion, in which the effect depended on the NO synthase that was involved. For example, aldosterone has been reported to decrease NO secretion through inhibiting iNOS activity in rat neonatal cardiomyocytes (Chun et al., 2003), yet in another report, aldosterone enhanced NO secretion through eNOS activation (Mutoh et al., 2008).

Here, in addition to looking at NO secretion of Ishikawa endometrial cancer cells between (f), (-ve) and (+ve)pST, aldosterone was used to change the cell stiffness through altering the Ishikawa cell actin filaments, both after transient incubation (7 minutes treatment) and longer time incubation (24 hours), and we hypothesized that cells on different culture substrates would have different responses to aldosterone treatment due to difference in their actin structure.

5.2 Hypotheses

In this chapter, our hypotheses are:

1. Cell adhesion is mediated through β1 integrin.
2. The expression levels of adhesion molecule β1 integrin, downstream signalling kinase FAK and pFAK and cell cytoskeleton actin filaments and Cytokeratin-18 are different on glass, tissue culture grade pST and pMA substrates; and between (f)pMA and (-ve)pMA as well as among (f)pST, (-ve)pST and (+ve)pST.
3. FAK activation, as measured by pFAK/FAK ratio, is linked to β1 integrin and these two biomolecules exist in the same cell compartment in cells.
4. Cell nitric oxide secretion, that is mediated through actin structure, with or without aldosterone, will be different on (f)pST, (-ve)pST and (+ve)pST.

5.3 Aims

In this chapter, we aim to

1. Quantify the expression levels of adhesion molecule β1 integrin and downstream signalling kinase FAK and pFAK.
2. Quantify abundance levels of pFAK and calculate the ratio of pFAK/FAK as an indication of FAK activation.
3. Observe the interaction of β1 integrin and pFAK by immunofluorescent double staining.
4. Quantify the expression levels of cell cytoskeleton actin filaments and Cytokeratin-18.
5. Examine the effect of β1 integrin blockage on cell initial adhesion.
6. Examine cell actin filaments structure with or without aldosterone treatment.
7. Quantify cell nitric oxide secretion with or without aldosterone treatment.

5.4 Experimental Approach

Western blot was used to semi-quantify β1 integrin, FAK, pFAK, actin and Cytokeratin-18 protein levels. For β1 integrin blockage, L-arginylglycyl-L-α-aspartyl-L-serine (RGDS), which is a β1 integrin recognition peptide sequence, was used to bind to β1 integrin of suspended cells hence preventing them from binding to culture surfaces. The number of cells that bind to surfaces was calculated after 3 hours of RGDS treatment.

For co-localisation of β1 integrin and pFAK, immunofluorescent double staining was performed. Immunofluorescence was also used to examine the cell actin structure in a study using aldosterone. Last, cell nitric oxide secretion levels were measured using a commercial NO assay kit.

5.5 Results

5.5.1 Ishikawa Endometrial Cancer Cell β1 integrin Expression

5.5.1.1 Cell β1 Integrin Expression on Glass, Tissue Culture Polystyrene and Polymethacrylate Polymer Flat and Bioimprint Culture Substrates

First cell β1 integrin expression was examined as it is involved in cell adhesion on surfaces. It was found that cells on conventional culture substrates expressed more β1 integrin than cells on pMA substrates. Additionally, compared to (f)pMA, cells on (-ve)pMA had higher expression of β1-Integrin. Further, although cells on tissue culture grade pST showed a trend of expressing higher β1-Integrin than cells on the glass platform, the difference was not statistically significant (p=0.084) (Figure 28).

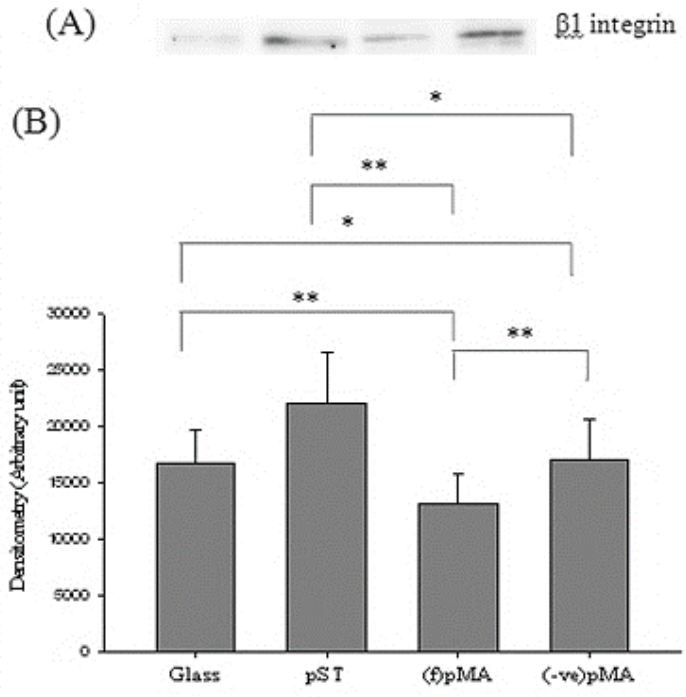


Figure 28 Ishikawa endometrial cancer cell β1 integrin expression on glass, tissue culture grade pST, (f)pMA and (-ve)pMA.

(A) (From left to right: glass, tissue culture grade pST,(f)pMA and (-ve)pMA) a representative example of β1 integrin western blot protein band.

(B) Bar chart showing densitometry of β1 integrin of cells cultured on respective surfaces.

Western blot data are presented as densitometry mean ± SEM of 5 independent experiments in triplicate. **, p<0.01; *, p<0.05.

5.5.1.2 Cell β1 Integrin Expression on Flat, Negative and Positive Bioimprint Polystyrene Slides

Similarly, for cells on pST microscope slides, cells on (-ve)pST and (+ve)pST also had higher expression of β1 Integrin than those of (f)pST (Figure 29).

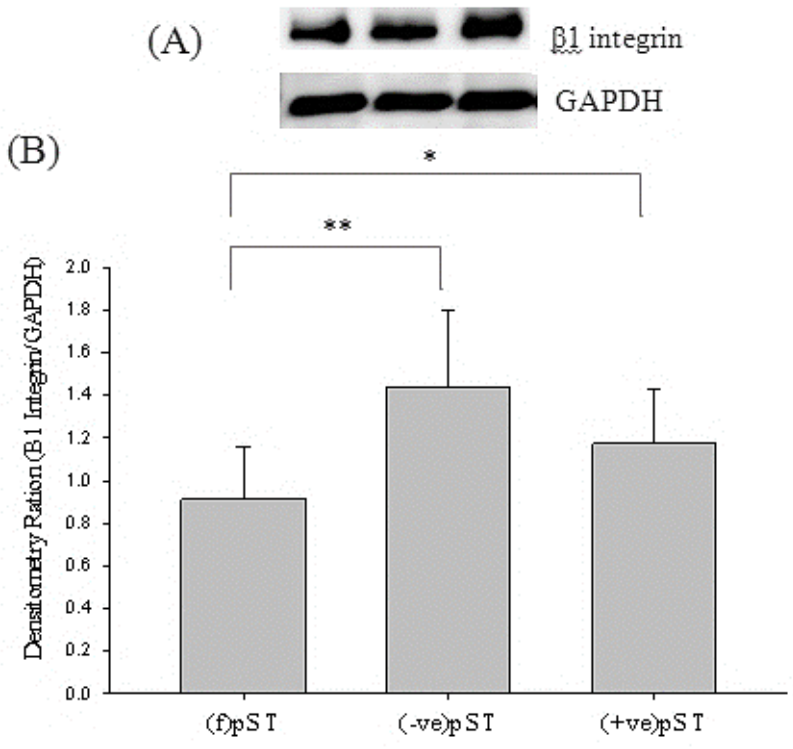


Figure 29 Ishikawa endometrial cancer cell β1 integrin expression on (f), (-ve) and (+ve)pST.

(A) (From left to right: (f)pST, (-ve)pST, (+ve)pST) representative examples of β1 integrin (Upper row) and GAPDH (bottom row) western blot protein bands.

(B) Densitometry ratio of β1 integrin/GAPDH of cells cultured on (f)pST, (-ve)pST and (+ve)pST.

Data are presented as β1 integrin densitometry normalized with GAPDH densitometry mean ± SEM of 11 independent experiments in quadruplicate. **, $p<0.01$; *, $p<0.05$.

5.5.2 Ishikawa Endometrial Cancer Cell FAK Expression and Activation (pFAK/FAK Ratio) and pFAK Distribution

5.5.2.1 Cell FAK Expression and Activation (pFAK/FAK Ratio) on Glass, Tissue Culture Polystyrene and Polymethacrylate Polymer Flat and Bioimprint Culture Substrates

Western blot analysis revealed that cells cultured on conventional culture substrates especially on tissue culture grade pST expressed high levels of FAK. Then again, (-ve)pMA imprint exhibited higher FAK expression than cells on the (f)pMA (Figure 30).

FAK activation, as indicated by the ratio of phosphorylated-FAK (pFAK) to total FAK levels, in constrast was lower on tissue culture grade pST compared to glass. Also, there was a lower activation on (-ve)pMA compared to (f)pMA (Figure 31).

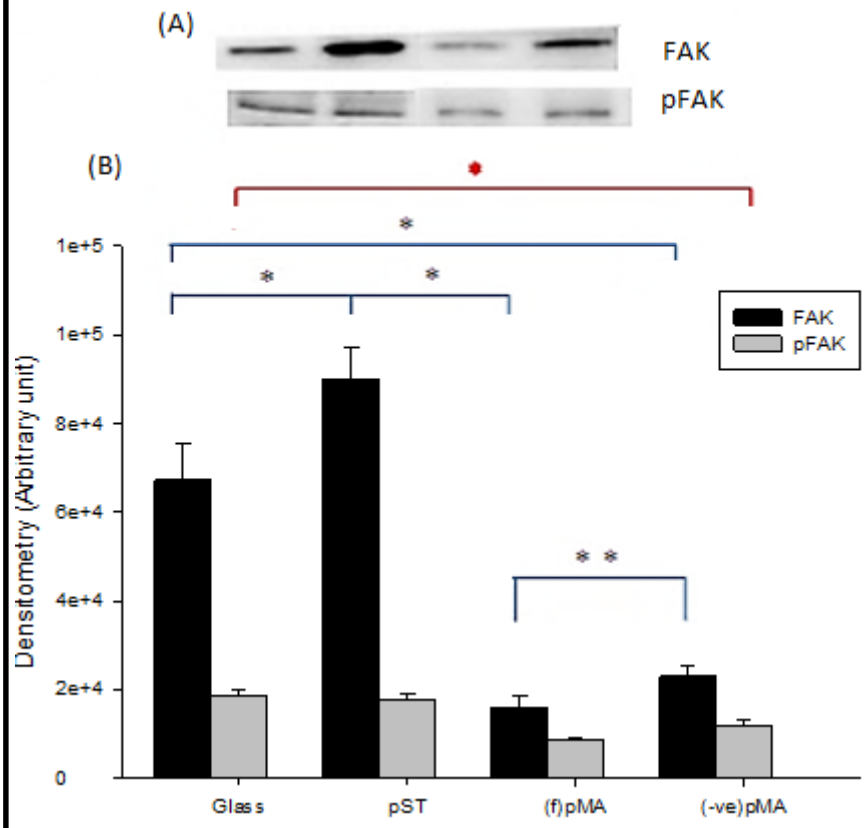


Figure 30 Ishikawa endometrial cancer cell expression levels of FAK and pFAK on glass, tissue culture grade pST, (f)pMA and (-ve)pMA.

(A) (From left to right: glass, tissue culture grade pST,(f)pMA and (-ve)pMA) representative examples of FAK (upper row) and pFAK (bottom row) western blot protein bands.

(B) Bar chart showing densitometry of FAK and pFAK of cells cultured on respective surfaces. Data are presented as densitometry mean ± SEM of 6 independent experiments in triplicate. **, p<0.01; *, p<0.05. (blue *: FAK; red *: pFAK).

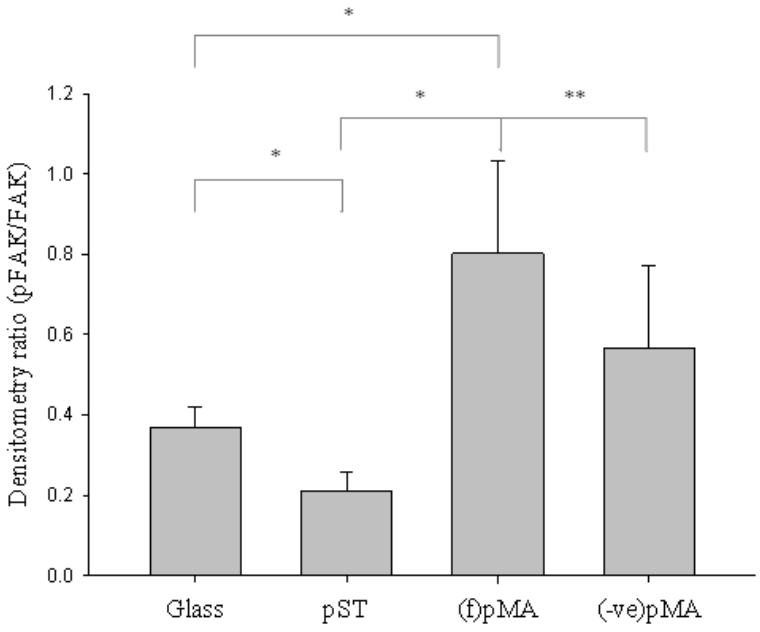


Figure 31 Ishikawa endometrial cancer cell FAK activation on glass, tissue culture grade pST, (f)pMA and (-ve)pMA.

Data are presented as densitometry ratio mean of pFAK/FAK ± SEM of 6 independent experiments in triplicate.
**, p<0.01; *, p<0.05.

5.5.2.2 Cell FAK Expression and Activation (pFAK/FAK Ratio) on Flat, Negative and Positive Bioimprint Polystyrene Slides

For cells on pST microscope slides, cells on (-ve)pST imprint had no difference in FAK expression and activation (pFAK/FAK ratio) detected compared to cells on f(pST). Further, an increase in FAK expression was observed in cells cultured on (+ve)pST imprint compared to cells on (f) and (-ve)pST (Figure 32). Further, there was a lower ratio of pFAK/FAK on (+ve)pST compared to (f)pST (Figure 33).

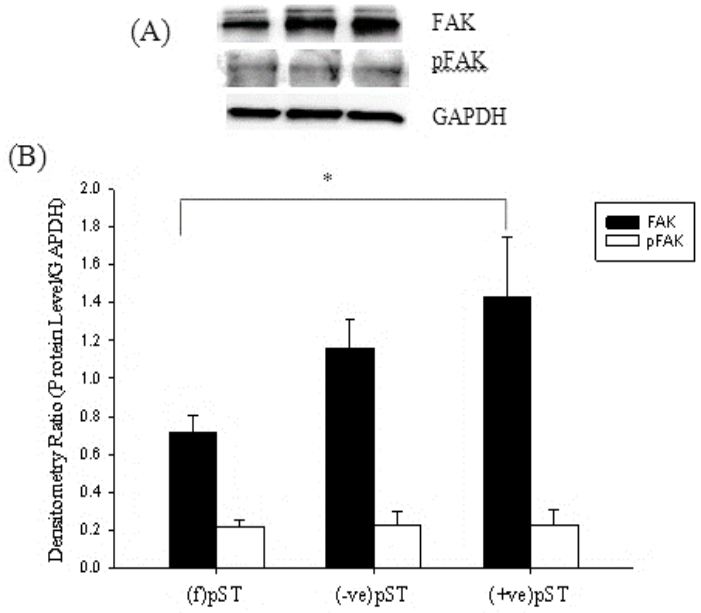


Figure 32 Ishikawa endometrial cancer cell FAK and pFAK expression on (f), (-ve) and (+ve)pST.

(A) (From left to right: (f)pST, (-ve)pST, (+ve)pST) representative examples of FAK(upper row), pFAK(middle row) and GAPDH(bottom row) western blot protein bands.

(B) Densitometry ratio of FAK/GAPDH (black bar) and pFAK/GAPDH (white bar).

Data are presented as FAK and pFAK densitometry normalized with GAPDH densitometry mean ± SEM of 6 independent experiments in quadruplicate. *, p<0.05.

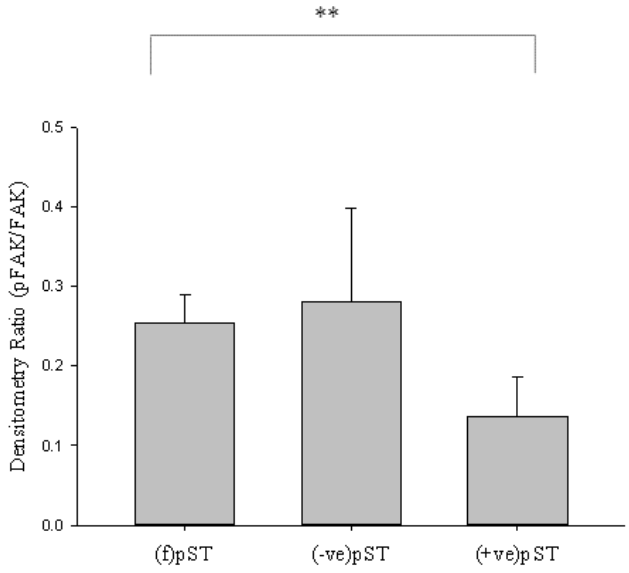


Figure 33 Ishikawa endometrial cancer cell pFAK/FAK on (f), (-ve) and (+ve)pST.

Data are presented as densitometry ratio mean of pFAK/FAK ± SEM of 6 independent experiments in quadruplicate. **, p<0.01.

pFAK and β1 integrin were both shown to be in the cell cytoplasm in the same cell, suggesting possible interaction on all culture substrates that were tested (Figure 36 and 37). However, the pFAK level was not related proportionally to β1 integrin. Moreover, pFAK levels fluctuated among samples especially on the (-ve)pST. Some studies have shown that pFAK is an unstable molecule and the phosphorylation and dephosphorylation processes occur within a short period (Baillat et al., 2008). Hence, FAK and pFAK levels were examined again at 3 hours for cells on pST microscope slide substrates.

FAK still showed a trend toward increased expression on (-ve) and (+ve)pST compared to the (f)pST, though this was not significant. Similarly pFAK did not show any significant change (Figure 34). At 3 hours, FAK activation, as determined by the ratio of pFAK/FAK, was not significantly different among topographies (Figure 35).

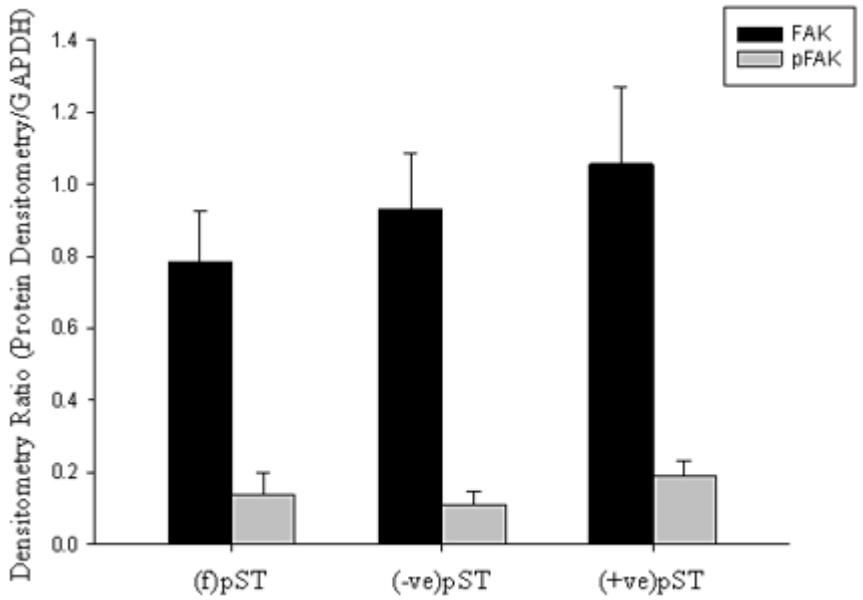


Figure 34 Ishikawa endometrial cancer cell FAK and pFAK expression on (f), (-ve) and (+ve)pST at 3 hours.

Figure showing densitometry ratio of FAK/GAPDH (black bar) and pFAK/GAPDH (white bar). Data are presented as FAK and pFAK densitometry normalized with GAPDH densitometry mean ± SEM of 4 independent experiments in quadruplicate.

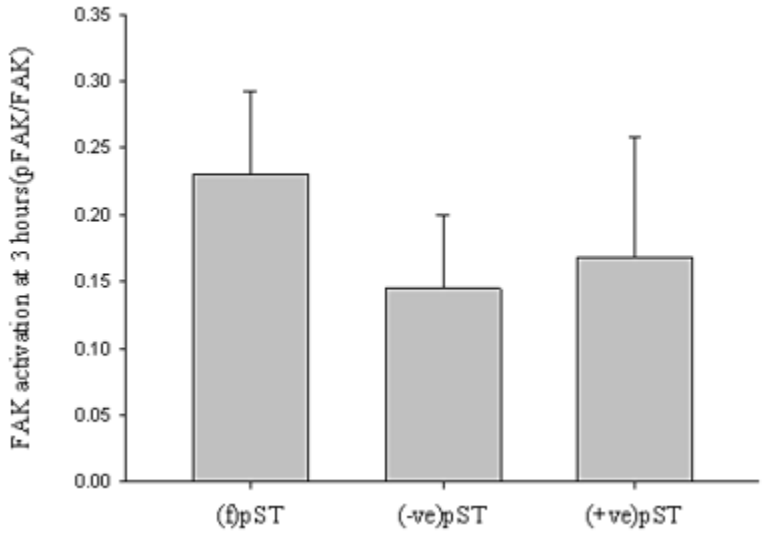


Figure 35 Ishikawa endometrial cancer cell pFAK/FAK on (f), (-ve) and (+ve)pST at 3 hours.

Data are presented as densitometry ratio mean of pFAK/FAK ± SEM of 4 independent experiments in quadruplicate.

5.5.3 Ishikawa Endometrial Cancer Cell β1 integrin Co-exists with pFAK in cell cytoplasm

5.5.3.1 β1 Integrin co-exists with pFAK in same cell cytoplasm on Glass, Tissue Culture Polystyrene and Polymethacrylate Polymer Flat and Bioimprint Culture Substrates

Upon aggregation with β1integrin, FAK will be auto-phosphorylated at Y397 into pFAK. Auto-phosphorylation at Y397 triggers phosphorylation at other sites of FAK, and this creates binding sites for FA proteins such as vinculin, talin, and kinases of the Src family, hence activating signalling pathways.

Our immunofluorescent staining results demonstrated that pFAK and β1 integrin were both present in the cytoplasm of the cells (Figure 36), indicating potential interaction.

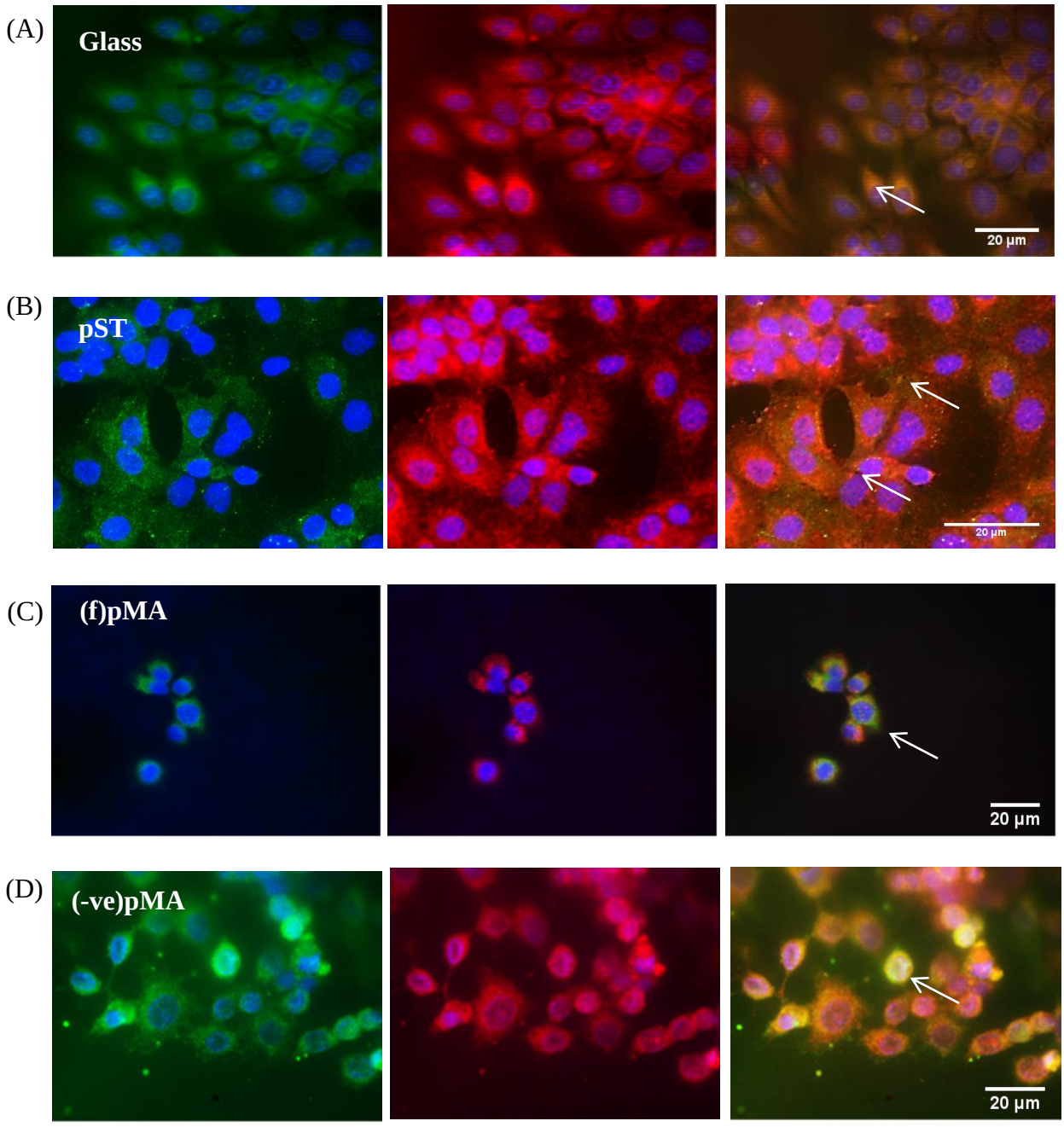


Figure 36 Representative images of double-staining of β1 integrin and pFAK in cells cultured on (A) glass (B) tissue culture grade pST (C) (f)pMA (D) (-ve)pMA.

Figures showing immunofluorescent staining of β1 integrin (green, left), pFAK (red, middle) and superimposed images of the β1 integrin and pFAK(right). Examples of β1 integrin and pFAK co-existence in a same cell compartment are indicated by white arrows. Cell nuclei were co-stained with Hoechst 33342(blue).

5.5.3.2 *Cell β1 integrin co-exists with pFAK in the cell cytoplasm on Flat, negative and positive bioimprint polystyrene slides*

Similarly, co-existance of β1 integrin and pFAK in the cell cytoplasm was observed in cells on (f), (-ve) and (+ve)pST, as indicated by arrows in the figure below (Figure 37).

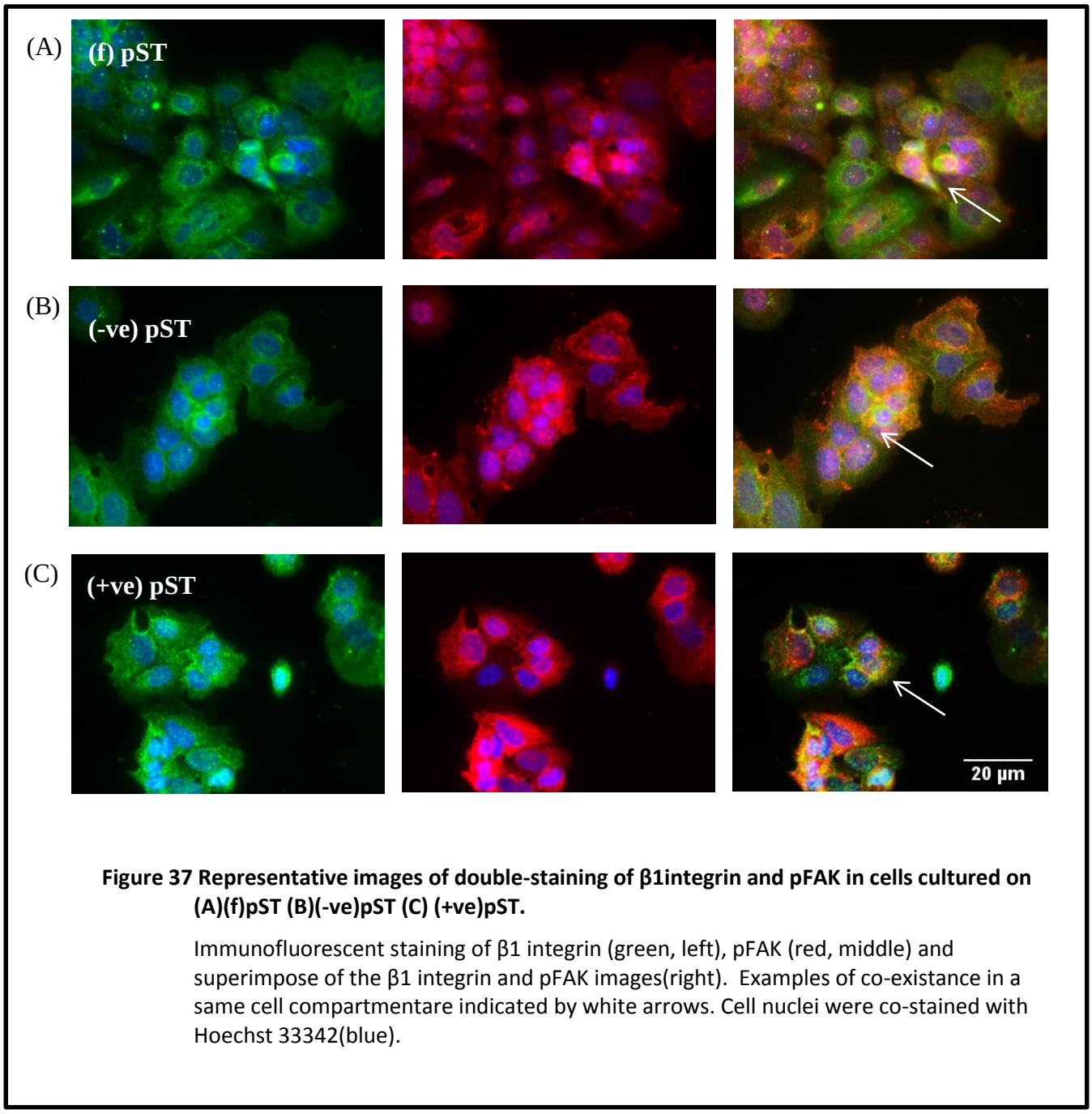


Figure 37 Representative images of double-staining of β1integrin and pFAK in cells cultured on (A)(f)pST (B)(-ve)pST (C) (+ve)pST.

Immunofluorescent staining of β1 integrin (green, left), pFAK (red, middle) and superimpose of the β1 integrin and pFAK images(right). Examples of co-existance in a same cell compartmentare indicated by white arrows. Cell nuclei were co-stained with Hoechst 33342(blue).

5.5.4 Ishikawa Endometrial Cancer Cell Actin Expression

5.5.4.1 Cell Actin Expression on Glass, Tissue Culture Polystyrene and Polymethacrylate Polymer Flat and Bioimprint Culture Substrates

Actin is recruited to FA in response to biomechanical stimulation and modifies its structure to subsequently transmit information for relevant gene activation. Ishikawa cells on (-ve)pMA had more elongated actin filaments than cells on (f)pMA (Figure 18).

By quantifying expression levels of actin, actin expression was observed to be lower on tissue culture grade pST than glass, and expression on tissue culture grade pST was similar to that on (-ve)pMA, which is higher than (f)pMA (Figure 38).

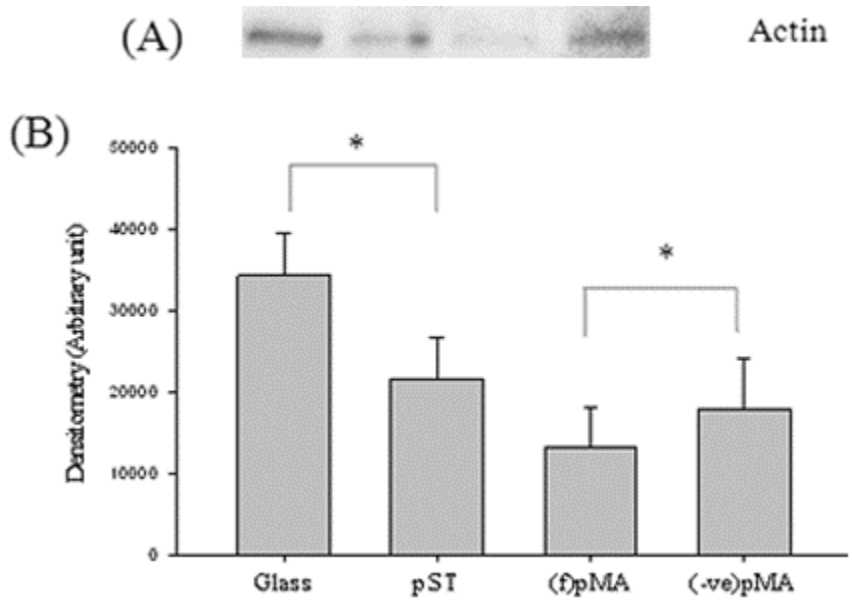


Figure 38 Ishikawa endometrial cancer cell actin expression on glass, tissue culture grade pST and (f)pMA and (-ve)pMA.

(A) (From left to right: glass, tissue culture grade pST,(f)pMA and (-ve)pMA) a representative example of actin western blot protein band.

(B) Bar chart showing densitometry of actin of cells cultured on respective surfaces.

Data are presented as densitometry mean ± SEM of 7 independent experiments in triplicate. *, $p<0.05$.

5.5.4.2 *Cell Actin Expression on Flat, Negative and Positive Bioimprint Polystyrene Slides*

In contrast, cells on pST had no observable difference in actin arrangement between cells on (-ve)pST and (+ve)pST surfaces from those on (f)pST (Figure 19) and actin expression was similar on the three pST substrates (Figure 39).

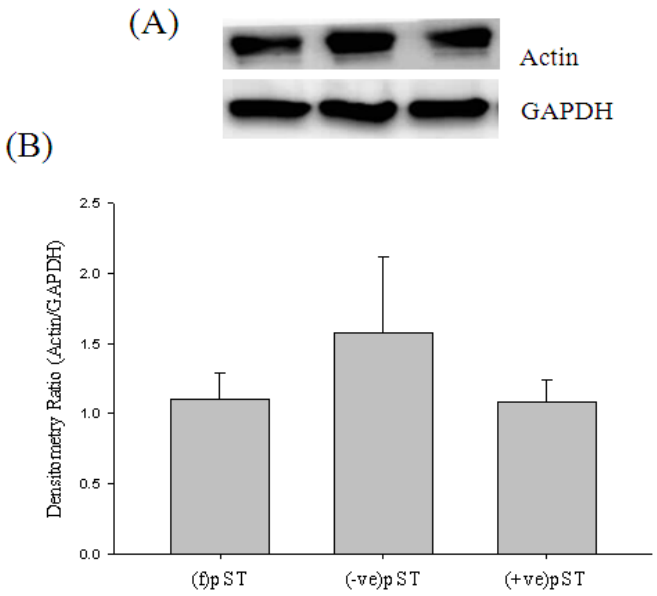


Figure 39 Ishikawa endometrial cancer cell actin expression on (f), (-ve) and (+ve)pST.

(A) (From left to right: (f)pST, (-ve)pST, (+ve)pST) representative examples of actin (upper row) and GAPDH (bottom row) western blot protein bands.

(B) Densitometry ratio of actin/GAPDH of cells cultured on (f)pST, (-ve)pST and (+ve)pST imprint.

Data are presented as actin densitometry normalised with GAPDH densitometry mean ±SEM of 5 independent experiments in quadruplicate.

5.5.5 Ishikawa Endometrial Cancer Cell Cytokeratin-18 Expression

5.5.5.1 Cell Cytokeratin-18 Expression on Glass, Tissue Culture Polystyrene and Polyethacrylate Polymer

Cells grown on (-ve)pMA imprint had elongated Cytokeratin-18 alignment compared to cells on (f)pMA, which was different from the responses of cells on glass and tissue culture grade pST (Figure 18), and western blotting showed that there was higher expression of Cytokeratin-18 in cells on (-ve)pMA imprint than (f)pMA and higher expression of cell Cytokeratin-18 on tissue culture grade pST than on glass (Figure 40).

Notably, Cytokeratin-18 expression had a similar pattern to that of the cell spreading area on conventional culture substrates and pMA substrates (Figure 40).

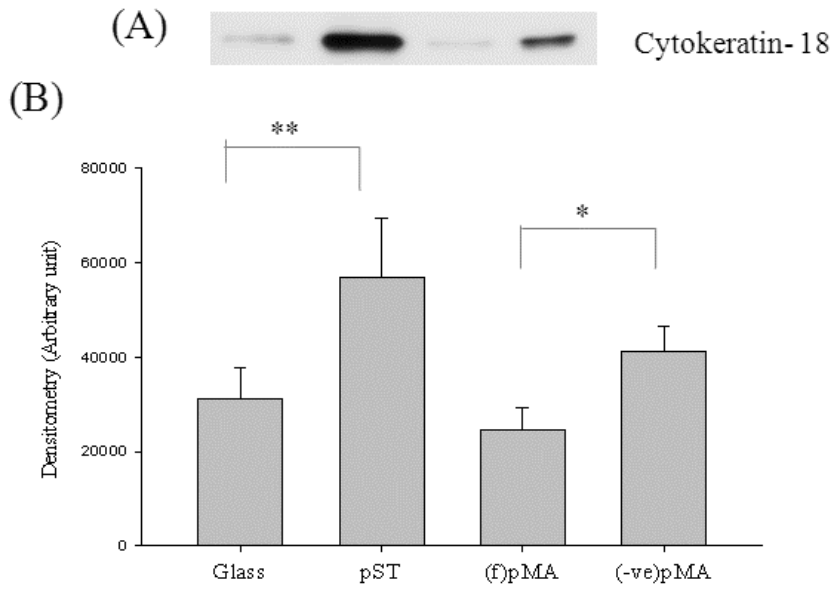


Figure 40 Ishikawa endometrial cancer cell Cytokeratin-18 expression on glass, tissue culture grade pST and (f)pMA versus (-ve)pMA.

(A) (From left to right: glass, tissue culture grade pST,(f)pMA and (-ve)pMA) a representative example of Cytokeratin-18 western blot protein band.

(B) Bar chart showing densitometry of Cytokeratin-18 of cells cultured on respective surfaces. Data are presented as densitometry mean ± SEM of 7 independent experiments in triplicate. **, $p<0.01$; *, $p<0.05$.

5.5.5.2 *Cell Cytokeratin-18 Expression on Flat, Negative and Positive Bioimprint Polystyrene Slides*

On the contrary, immunofluorescence showed that there was no clear difference observed between Cytokeratin-18 arrangement in cells on the pST surfaces (Figure 19), yet the expression in cells on both (-ve)pST and (+ve)pST imprint was higher than on (f)pST substrates (Figure 41).

The trend of Cytokeratin-18 expression was opposite to the trend of the cell spreading area (Figure 22 and 41) among cells on pST microscope slide substrates. This indicated that there may be a change in Cytokeratin-18 density, yet without affecting the Cytokeratin-18 arrangement between cells on different substrates.

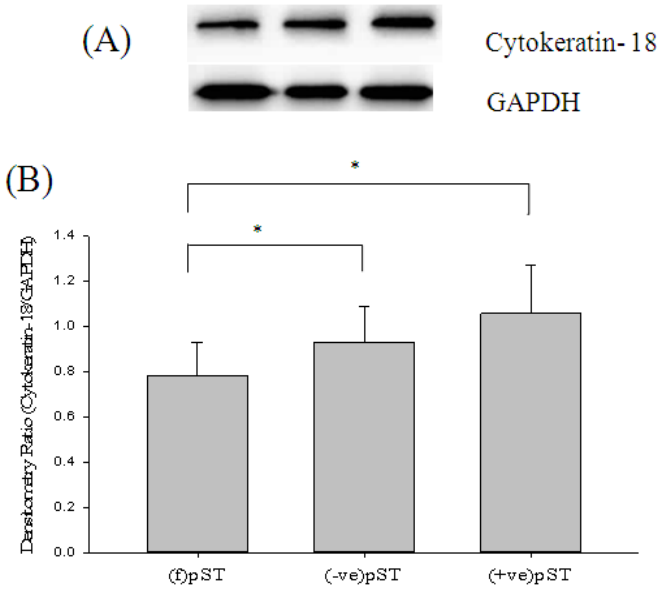


Figure 41 Ishikawa endometrial cancer cell Cytokeratin-18 expression on (f), (-ve) and (+ve)pST.

(A) (From left to right: (f)pST, (-ve)pST, (+ve)pST) representative examples of Cytokeratin-18 (upper row) and GAPDH (bottom row) western blot protein bands.

(B) Densitometry ratio of Cytokeratin-18/GAPDH of cells cultured on (f)pST, (-ve)pST and (+ve)pST.

Data are presented as Cytokeratin-18 densitometry normalized with GAPDH densitometry mean ±SEM of 12 independent experiments in quadruplicate. *, $p<0.05$.

5.5.6 Ishikawa Endometrial Cancer Cell β1 Integrin Blocking

RGDS is a tetra-peptide found in fibronectin and fibrinogen that interacts with β1 integrin in cell adhesion. β1 integrin expression was shown to be affected by the topography of the substrate (Figure 28 and 29), which suggested that β1 integrin was involved in cell responses to the physical environment. Therefore, to confirm the role of β1 integrin in cell adhesion on pST the effect of RGDS binding to β1 integrin, which blocks the β1 integrin from binding to the pST surface, was investigated. The initial binding of cells (determined with cell counting method described in section 2.2.3) to pST substrate was indeed blocked by RGDS (Figure 42). Control peptide arginyl-glycyl-glutamyl-serine (RGES), in which Asp3 is replaced by Glu3, had no effect on adhesion which is consistent with the hypothesis of an early involvement of β1 integrin in the adhesion of cells to distinct topographies.

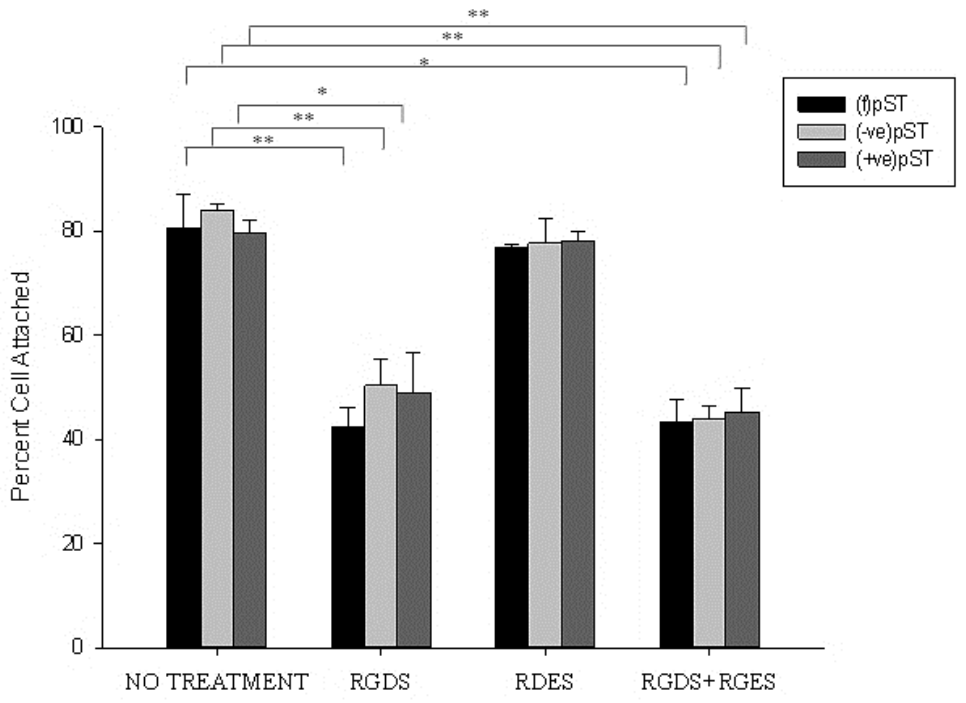


Figure 42 Effects of β1 blockage on cell initial adhesion.

Cells were grown on respective substrates with No Treatment, RGDS, RGES, or RGDS + RGES for 3 hours. Data are presented as mean ± SEM of measurements of 3 independent experiments in quadruplicate. **, $p<0.01$; *,$p<0.05$.

5.5.7 Ishikawa Endometrial Cancer Cell Nitric Oxide Secretion

5.5.7.1 Aldosterone Effects on Cell Cortical Actin at Different Concentrations

The aldosterone concentration was first chosen using immunofluorescent staining based on the hypothesis that aldosterone would disrupt cell cortical actin structure. Cortical actins refer to the actin filaments adjacent or underneath the cell membrane. A disruption of cortical actin can be seen as discontinuity of the filamentous actin structure (Figure 43, spots of disrupted cortical actin indicated by yellow arrows).

Ishikawa cells were treated with 1nM, 10nM and 100nM aldosterone for 7 mins and then the cells' cortical actin filaments were examined with Texas Red-X phalloidin. The cells' cortical actin filaments were seen to have depolymerised at 10nM and 100nM aldosterone (Figure 43). The final aldosterone concentration chosen for the experiment here was 10nM. This concentration has also been used by Fels et al. on endothelial cells (Fels et al., 2010).

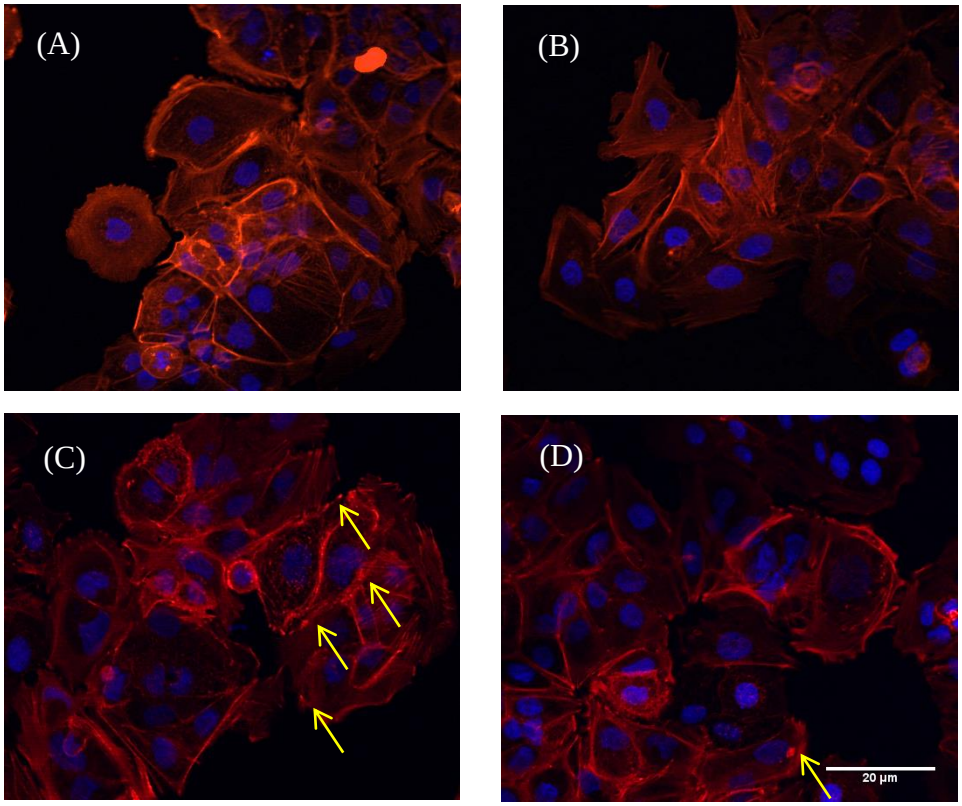


Figure 43 Representative images of Ishikawa endometrial cancer cell actin filaments staining.

Ishikawa cell actin filaments were stained with Texas Red-X phalloidin (red), and the cell nuclei were stained with Hoechst 33342 stained (blue) on (f)pST. Cells were treated for 7mins with (A) No treatment and (B) 1 nM (C) 10 nM (D) 100 nM aldosterone. Examples of fragmented cortical actin filaments are indicated by yellow arrows.

5.5.7.2 Cell Cortical Actin Filaments on Flat, Negative and Positive Bioimprint Polystyrene Slide with or without Aldosterone Treatment

By examining the structure of cortical actin filaments with or without aldosterone treatment, some distortion of the cortical actin structures was observed in cells with 7 mins aldosterone treatment (Figure 44(D)-(F), yellow arrows) but not in cells with no aldosterone treatment (Figure 44(A)-(C)). There was less distortion in cells on (+ve)pST compared to cells on (f) and (-ve)pST.

At 24 hours, all cells with and without treatment showed dense actin filaments (Figure 44(G)-(L)), indicating that the aldosterone effect on cell cortical actin filaments occurred transiently.

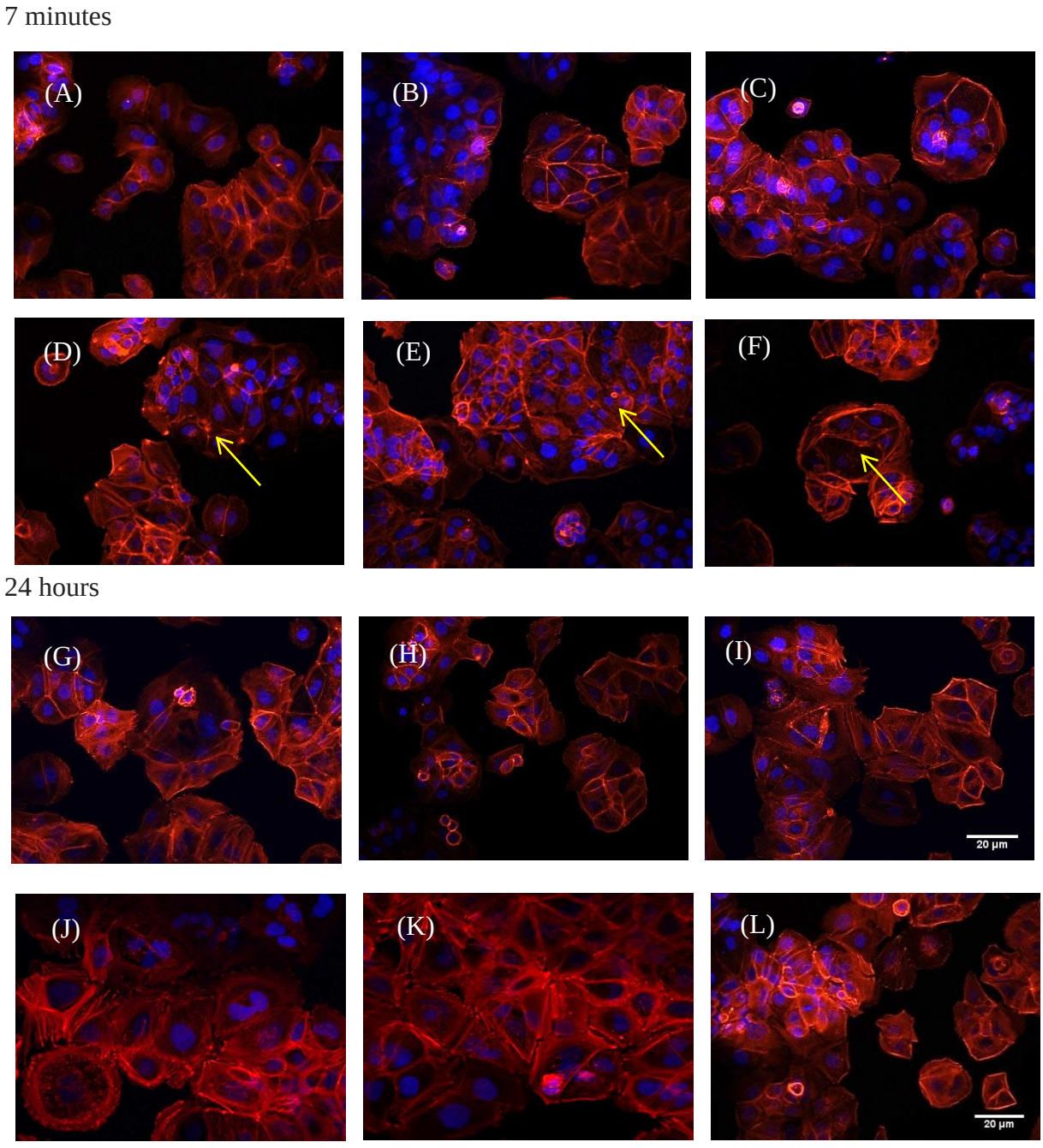


Figure 44 Representative images of Ishikawa endometrial cancer cell actin filaments staining.

Ishikawa cell actin filaments were stained with Texas Red-X phalloidin (red), and cell nuclei were stained with Hoechst 33342 (blue). Cells on (A),(G):(f) pST (B),(H):(-ve)pST and (C),(I): (+ve)pST were the control cells without aldosterone treatment. Cells on (D),(J):(f) pST (E),(K):(-ve)pST and (F),(L): (+ve)pST were the cells with 10 nM aldosterone treatment. The time indicates when the cells were fixed and stained. Examples of fragmented cortical actin filaments are indicated by yellow arrows.

5.5.7.3 Cell Nitric Oxide Secretion on Flat, Negative and Positive Bioimprint Polystyrene Slide with or without Aldosterone Treatment

At 7 mins and without any treatment, Ishikawa endometrial cancer cells showed similar NO secretion on all substrates. Whereas at 24 hours without the addition of aldosterone, cells on (-ve)pST had significantly higher NO level compared to cells on (f) and (+ve)pST (Figure 45). This was similar to the observation that there may be an increase in actin filaments expression on (-ve)pST compared to (f) and (+ve)pST (Figure 39). More repetitions are needed for statistical robustness in quantifying the actin expression. Further experiments are also needed to more specifically quantify the cell stiffness. The higher actin filaments may be an indication of higher cell stiffness thus resulting in higher NO secretion.

Aldosterone did not have an effect in increasing NO release in the short term treatment. Aldosterone treatment for 24 hours decreased NO secretion significantly in cells on (-ve)pST as compared to the cells without treatment. No significant effect was observed for cells on (f) and (+ve)pST with aldosterone treatment at 24 hours (Figure 45).

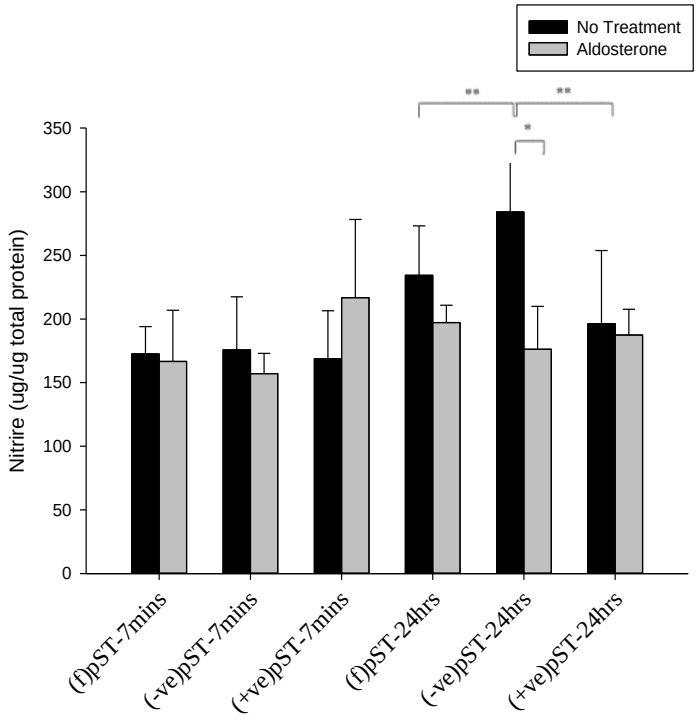


Figure 45 Ishikawa endometrial cancer cell NO secretion at 7mins and 24 hours with or without aldosterone on (f), (-ve) and (+ve)pST.

NO level measurement was normalised with total protein. Data are presented as NO μg/μg total protein mean ± SEM of measurements of 4 independent experiments in quadruplicate. *, p<0.05; **, p<0.01.

5.6 Discussion

5.6.1 Cell Culture on Glass, Tissue Culture Grade Polystyrene and Polymethacrylate Flat and Bioimprint Culture Substrates

In this chapter, the influence of culture substrate material and topography on cell expression of β1 integrin, activation of FAK and expression of actin and Cytokeratin-18 were studied. Cells on glass and tissue culture grade pST have been observed to have well-spread morphology and the cells on pMA substrate had a circular morphology, and that in the presence of the Bioimprint, cells were more spread out compared to (f)pMA (Figure 11, 12, 13, 14 and 18). The expression of β1 integrin and FAK were in parallel to the observed cell spreading behaviour. Initially, Ishikawa cells on glass and tissue culture grade pST were shown to have higher expression of β1 integrin and FAK when compared to cells on pMA substrate. Hence, the well-spread behaviour on glass and tissue culture grade pST is most probably due to an increase in expression of β1 integrin and FAK. This may be because the surface wettability allows efficient adsorption of serum protein especially fibronectin onto surfaces (Lampin et al., 1997), which encourages cell adhesion and spreading through activating β1 integrin and increasing FAK expression.

The cells on glass showed no significant difference in β1 integrin expression compared to the cells on the tissue culture grade pST. This may be because glass and tissue culture grade pST are both surfaces that support cell adhesion and growth. There is still a non-significant difference in β1 integrin expression between cells on glass and tissue culture grade pST, which may be due to the different wettabilities, surface functional groups and charges between the two surfaces, where the serum protein may have adsorped better on the tissue culture grade surface and encouraged cell adhesion and increased β1 integrin expression.

When compared between (f) and (-ve)pMA, β1 integrin expression was higher in cells on (-ve)pMA than (f)pMA. Similarly, FAK expression level was higher in cells on (-ve)pMA compared to (f)pMA. The presence of the Bioimprint increased cell expression of β1 integrin and FAK, an effect similar to cell spreading area, this indicates surface topography also plays a role in affecting cell spreading through β1 integrin and FAK.

In parallel to the observation that cells on glass and tissue culture grade pST spread better than cells on pMA substrates, actin and Cytokeratin-18 both showed a trend of higher expression in cells on glass and tissue culture grade pST compared to cells on pMA substrates. Moreover, comparison between cells on (f) and (-ve)pMA substrates showed a higher expression on the (-ve)pMA than on (f)pMA. This suggests not only substrate material (glass versus tissue culture grade pST) but topography (between (f)pMA and (-ve)pMA) can affect cell cytoskeleton expression which in turn modifies the cell spreading.

5.6.2 Cell Culture on Flat, Negative and Positive Bioimprint Polystyrene Slides

The topography effect can be further seen between pST microscope slide substrates, i.e. (f)pST, (-ve)pST and (+ve)pST. The expression levels of β1 integrin and Cytokeratin-18 were again higher on pST Bioimprints than on (f)pST, moreover, the expression level of FAK was higher on (+ve)pST compared to cells on (f)pST. These observations further indicating that surface topography could alter cell expression levels of β1 integrin, FAK and Cytokeratin-18.

Unlike the comparison between (f) and (-ve)pMA, in which there was an increase in actin expression on (-ve)pMA compared to (f)pMA; on pST substrates, there was no significant difference in actin expression between (f)pST and both (-ve) and (+ve)pST. However, the cell actin architecture (changing between a filamentous actin structure to a globular actin structure) was altered as shown from the NO measurement. This suggests that the culture substrate topography itself is not the only factor in the microenvironment that affects cell behaviours, but the culture substrate materials are also important in affecting cells.

Even though immunofluorescent examination of β1 integrin and pFAK showed that these two molecules were located in the cell cytoplasm of the same cell (Figure 36 and 37), which provides them potential to interact, an examination of the ratio of pFAK/FAK showed that there was a non-parallel change in β1 integrin and FAK activation (as indicated by the pFAK/FAK ratio). A physical topographical effect on lowering FAK activation was

observed between (f) and (-ve)pMA and between (f), (-ve) and (+ve)pST microscope slide substrates. One possible reason may be due to the temporal dynamic of cellular phosphorylation, in which phosphorylation and dephosphorylation occur over time. For this, we examined the activation of FAK at 3 hours on pST microscope slide substrates, which showed no difference between substrates of different materials. Hence, β1 integrin may have an inhibition effect on FAK activation, which requires further investigation.

Notably, pFAK and actin expression levels fluctuated in cells on (-ve)pST (Figure 46). There was a possibility that the wide mean distribution was due to the presence of outliers, although the same lysates had more compact ranges for other compounds, and in the same culture set the (f) and (+ve)pST substrates did not have excessive variation, hence the wide distribution warrants further investigation.

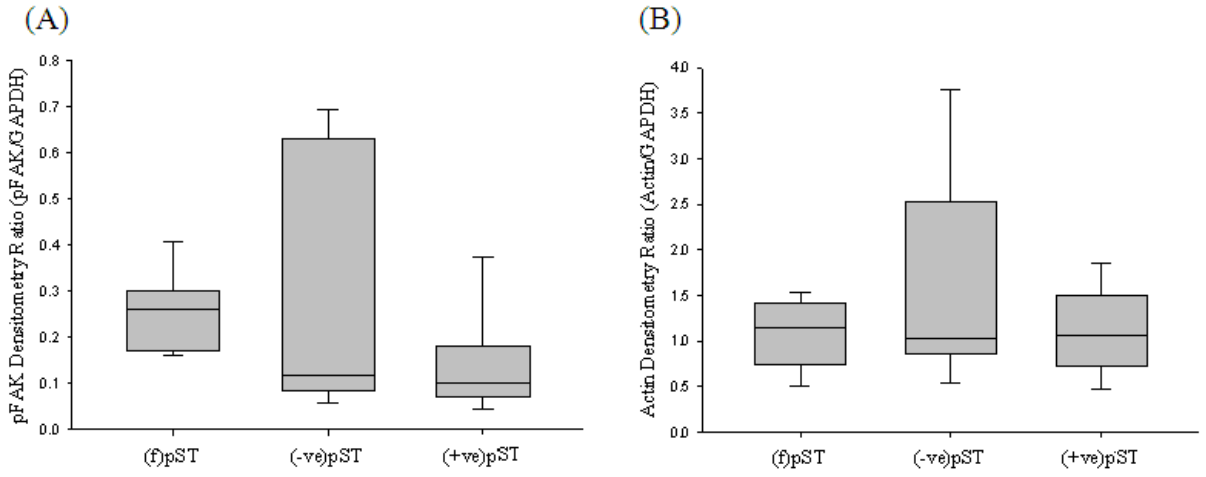


Figure 46 Boxplots of (A) pFAK and (B) Actin expression levels.

Boxplots of pFAK (A) and actin (B) densitometry measurement of expression level. Box=25th and 75th percentiles; median= dark line in the box; bar=minimum and maximum values; n=6 for pFAK and 5 for actin.

Aldosterone treatment at 7min did not increase NO secretion of cells. This was different from Fels' report in which aldosterone was reported to increase NO secretion (Fels et al., 2010). A possible reason could be due to the different cell types used which involve different nitric oxide synthase and hence difference responses to aldosterone treatment. Fels'

study was on endothelial cells that mainly used eNOS for NO secretion (Kirsch et al., 2013). However, in cancer cells, iNOS may be more influential than eNOS (Crowell et al., 2003; Lechner et al., 2005). The involvement of different NOS also explained the observation of decreased NO secretion at 24 hours of aldosterone treatment. For example, a study on smooth muscle cells showed that aldosterone decreased iNOS activity at 24 hours treatment (Godfrey et al., 2011), and another report showed that aldosterone decreased NO secretion by reducing iNOS activity (Chun et al., 2003). Hence, different cell types would have different responses to aldosterone modulation of NO secretion due to the involvement of the different NOS.

Here, a decrease in NO secretion at 24 hours with aldosterone treatment was observed; it is speculated that iNOS may be involved in Ishikawa endometrial cancer cell NO secretion. More studies to examine the expression levels of different nitric oxide synthases will certainly be required. Nonetheless, aldosterone only showed an effect in decreasing NO level on (-ve)pST but not on (f) and (+ve)pST. This indicates that surface topography may have changed the cells' actin activity, which affects the cell response to aldosterone.

Without any treatment, cells on (-ve)pST had higher NO secretion compared to cells on (f) and (+ve)pST at 24 hours. Previous western blot measurements of actin expression level showed no significant difference among the three substrates. However, an examination of the raw data showed that actin expression on (-ve)pST had a wide distribution in which 3 out of 6 samples of cells on (-ve)pST showed high actin expression level. Hence, the actin expression may fluctuate for cells on (-ve)pST (Figure 39 and 46B). Besides, when the cell size was compared between cells on different substrates, the cells on (-ve)pST were smaller than cells on (f)pST (Figure 22), hence, some cells on (-ve)pST may have more actin packed into a smaller cell area, which may result in stiffer cells and thus higher NO secretion.

Further studies that examine the expression of different types of NOS as mentioned above, and also studies to measure the stiffness of cells would be needed to interpret the results presented here. Nonetheless, these preliminary observations showed that cells growing on

different physical topographies altered their NO secretion pattern, which may be partly due to different activity of actin filaments.

5.6.3 Summary

The results showed that the integrin receptor expression was affected by the physical topography. Cells on (-ve)pMA imprint and both (-ve) and (+ve)pST imprint exhibited a higher expression of integrin than cells on flat surfaces. Further, we showed that the interaction between Ishikawa cells and different culture surfaces during adhesion was through an RGD moiety. As a result, cell interaction with substrate surfaces is at least partly through fibronectin that may be deposited from culture serum and secreted by the cells themselves. Further, physical topography also affected cell FAK expression and phosphorylation, which may be partly through β1 integrin.

Ishikawa cells on all imprints (pMA and pST) showed a higher expression of Cytokeratin-18 expression than the cells on respective flat surfaces. In contrast, actin did not. This may indicate that the cell-like topography influence on cells is more prominently modulated by Cytokeratin-18 than actin. Alternatively or additionally, changes in actin may be involved in the changes in actin dynamics, i.e. alteration of ratio of F-actin to G-actin, which can be inferred indirectly from the different NO secretion between cells on (f), (-ve) and (+ve)pST.

5.7 Conclusion

The results in this chapter favour our hypothesis that the adhesion molecules and cytoskeleton of Ishikawa endometrial cancer cell can be modulated by physical microenvironment. Comparisons between (-ve)pMA to (f)pMA and among (-ve)pST or (+ve)pST to (f)pST confirmed that cell-like topography, independent from culture substrate material, increased cell expression of β1 integrin (an adhesion receptor), FAK (a downstream kinase) and Cytokeratin-18. On the other hand, comparison between glass,

tissue culture grade pST and pMA substrates suggests that cells also responded to culture substrate material, and examination of cell responses to pMA Bioimprint and pST Bioimprints showed that cell's responses to physical topography were influenced by substrate material. In short, physical topography and culture substrate material, may work alone or together to modulate the expression of Ishikawa cell adhesion molecules and cytoskeleton.

Next Ishikawa endometrial cancer cell growth was examined by quantifying cell number and semi-quantifying cell growth biomolecule expression level. The results are presented in the next chapter.

Chapter 6 Influences of Substrate Material and Topography on Ishikawa Endometrial Cancer Cell Adhesion, Growth and Activation of MAPK/ERK and PI3K /AKT Pathways

6.1 Introduction

As discussed in chapters 4 and 5, Ishikawa endometrial cancer cells changed their spreading and adhesion behaviours in response to their physical environment. Investigations of Ishikawa cell growth on substrates of different materials and topographies were then carried out since cell growth can be influenced by cell spreading. The results are presented in this chapter.

Regulation of cell growth through modulating cell shape and size has been reported as long ago as 1978. Folkman and Moscona reported that cell shape regulated cell DNA synthesis, where DNA synthesis was reduced as cells became rounded, and DNA synthesis was only initiated when the cells reached a certain size (Folkman & Moscona, 1978). Another study in cell cycle regulation by cell shape demonstrated that cells that were prevented from spreading failed to progress from the G1 to S phase, and this was due to the failure of cyclin D1 levels to increase, resulting in the downregulation of $p27^{Kip1}$, and phosphorylation of the retinoblastoma protein (Huang et al., 1998).

This cell shape regulation of growth is reported to be through actin filaments. A recent report of cell shape regulation of a growth-related transcription factor, NFκB was through modulation of actin filaments (Sero et al., 2015). Another example was shown in a study reported by Ingber et al. who used cytochalasin D to inhibit actin polymerization; they

observed that there was a dose-dependent inhibition of cell spreading, nuclear extension as well as DNA synthesis (Glushankova & Vasil'ev Iu, 1986; Ingber et al., 1995).

Previously a change in cell morphology and cell size of Ishikawa cells growing on substrates of different materials (glass, tissue culture grade pST and pMA) and between flat and the Bioimprint substrates (Figure 11, 12, 13, 14, 20 and 21) was observed. It was also observed that there was an alteration in cell actin distribution and expression between cells growing on glass, tissue culture grade pST and pMA substrates (Figure 18 and 38). Although no significant alteration in actin expression and arrangement between cells on (f), (-ve) and (+ve)pST (Figure 19 and 39) was seen, a difference in cell NO secretion on these substrates (Figure 45) indicated that there may be a difference in cell actin dynamics (change of F-actin to G-actin ratio) on (-ve)pST compared to (f)pST and (+ve)pST. Therefore, the growth of cells on those substrates further was investigated.

The cell number was first counted, and then the cell cyclins D2, B1 and B2 and a proliferation marker proliferating cell nuclear antigen (PCNA) expression levels were quantified. Cyclin D2 is involved in cell cycle G1/S transition by coupling with CDK4 or CDK6, whereas cyclin B interacts with Cdc 42 and is required for the late phase of mitosis. Hence measuring the expression levels of cyclins D and B, as well as PCNA may indicate the growth of cells growing on different substrates.

Further, the activation of signalling molecules on two proliferation pathways was observed: mitogen-activated protein kinase/extracellular signal-regulated kinases (MAPK/ERK) and Phosphoinositide 3-kinase/protein kinase B (PI3K/AKT). Studies have shown that these two pathways are activated by mechanical signals. For example, integrin clusters have been shown to activate MAPK/ERK-and Rho-dependent pathways (Paszek et al., 2005). Growth related epidermal growth factor (EGF)-dependent MAPK/ERK activation was found to be higher in a stiff tissue environment, and MAPK/ERK activity was sustained only when FAs formed (Paszek et al., 2005), which indicates that MAPK/ERK pathway is one of the modulators of mechanical signals. Moreover, it has been shown that cyclic mechanical strain induced the PI3K/AKT pathway through actin cytoskeleton-related signalling

(Horiuchi, Akimoto, Hong, & Ushida, 2012). ECM stiffness was also found to stimulate the assembly of the vinculin-talin-actin complex at FA which then activated the PI3K pathway (Rubashkin et al., 2014). Furthermore, nicotine-promoted NSCLC cell proliferation as discussed above (Chapter 1 section 1.4) occurred through the MAPK/ERK and PI3K/mTOR pathways (Zheng et al., 2007).

6.2 Hypotheses

1. Ishikawa endometrial cancer cells cultured on glass, tissue culture grade pST and pMA substrates, and cells between (f)pMA and (-ve)pMA have different early adhesion, growth, and expression of cyclin D2 and signalling molecules of the MAPK/ERK pathway.
2. Ishikawa endometrial cancer cells cultured on (f)pST, (-ve)pST and (+ve)pST have different early adhesion, growth, and expression of cyclin B and D2, PCNA and signalling molecules of the MAPK/ERK and PI3K/AKT pathways.

6.3 Aims

Among culture substrates that are made of different materials, i.e. glass, tissue culture grade pST and pMA; and between (f)pMA versus (-ve)pMA as well as (f)pST, (-ve)pST and (+ve)pST, we aim to:

1. Quantify cell adhesion and cell growth by measuring the number of adherent and non-adherent live and dead cells on different surfaces at 6 and 60 hours.
2. Quantify cell cycle D2 expression levels.
3. Investigate activation of the MAPK/ERK pathway.

Further, for Ishikawa cells cultured on (f)pST, (-ve)pST and (+ve)pST, we aim to

1. Quantify cell cycle B and PCNA expression levels.
2. Examine activation of the PI3K/AKT pathway.

6.4 Experimental Approach

To measure cell numbers at 6 and 60 hours, two different methods were used for quantification; trypan blue exclusion cell count was used for cells cultured on glass, tissue culture grade pST and pMA substrates whereas coomassie blue staining was used for cells seeded on pST flat and the Bioimprint substrates; the rationale for using the two different methods was discussed in Chapter 2 section 2.5.

Western blot was used to quantify the expression levels of the cell cycle regulator, PCNA, ERK, phosphorylated ERK (pERK), AKT and phosphorylated-AKT (pAKT). The relative activation of each pathway was measured by calculating the ratio of pERK/ERK and pAKT/AKT, respectively.

6.5 Results

6.5.1 Ishikawa Endometrial Cancer Cell Adhesion and Growth

6.5.1.1 Ishikawa Endometrial Cancer Cell Adhesion and Growth on Glass, Tissue Culture Grade Polystyrene and Polymethacrylate Flat and Bioimprint Culture Substrates

By quantifying the cell numbers at 6 hours and 60 hours, it was found that there were less cells adhered on pMA substrates at 6 hours (Figure 47) compared to cells on glass and pST substrates. The cell adhesion was measured at 6 hours, so it is not related to cell growth. To look at cell growth, cell number was measured at 60 hours. The cells on pMA had lower growth at 60 hours than cells on glass and tissue culture grade pST (Figure 48). Nonetheless, cells on (-ve)pMA imprint had higher growth rate than cells on (f)pMA (Figure 48).

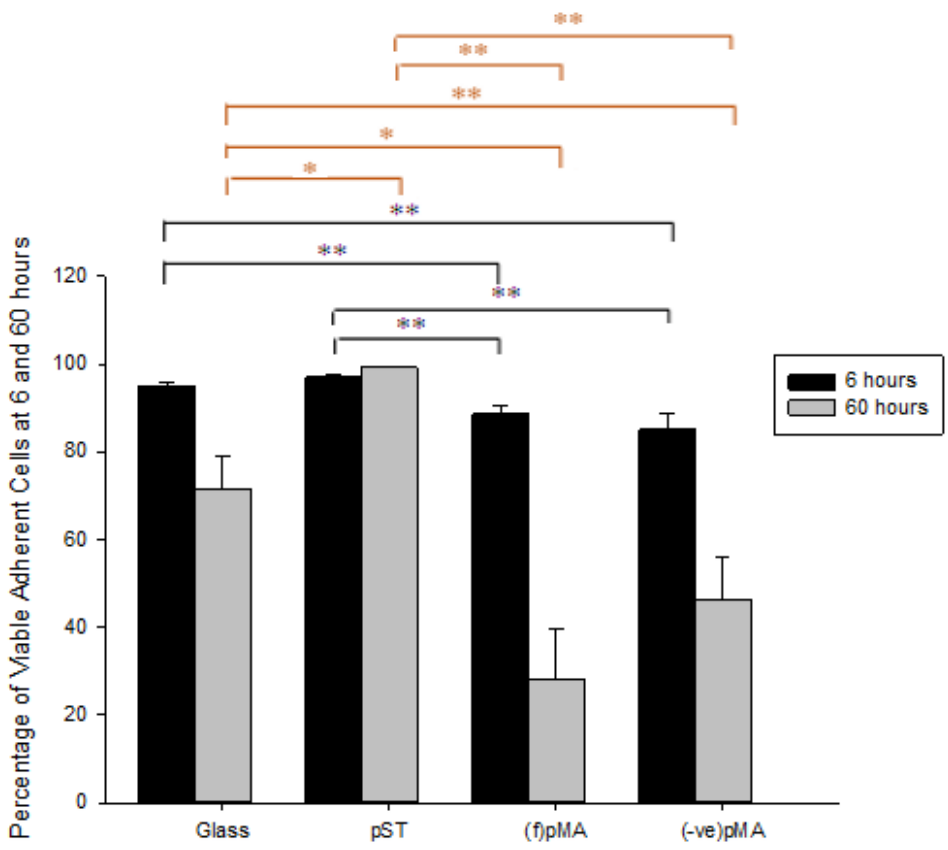


Figure 47 Percentage of adherent Ishikawa cells on glass, tissue culture grade pST, flat and (-ve)pMA at 6 and 60 hours.

Data are presented as mean ± SEM of 3 independent experiments in triplicate.

*, p<0.05; **, p<0.01 (black *: 6 hours; red *: 60 hours).

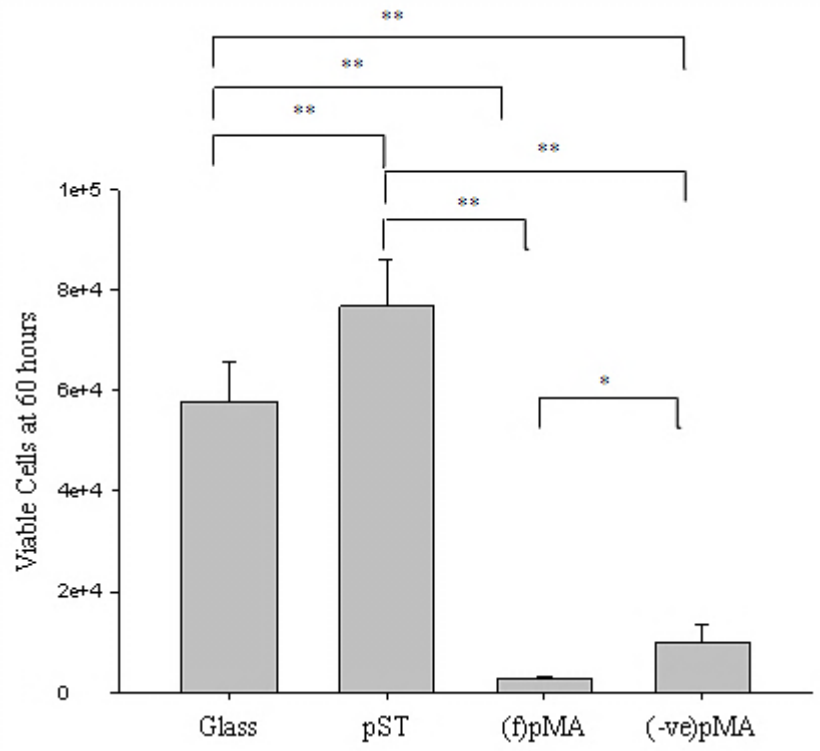


Figure 48 Number of Ishikawa cells on glass, tissue culture grade pST, flat and (-ve)pMA at 60 hours.

Data are presented as mean ± SEM of 3 independent experiments in triplicate. **, $p<0.01$; *, $p<0.05$.

6.5.1.2 *Ishikawa Endometrial Cancer Cell Adhesion and Growth on Flat, Negative and Positive Bioimprint Polystyrene Slides*

For cells cultured on the (f), (-ve) and (+ve)pST, cells on (-ve) and (+ve)pST showed lower growth at 60 hours than cells on the (f)pST (Figure 49).

The cell number measurements were performed on adherent cells at 6 and 60 hours. There was no difference in the non-adherent cells among pST substrates at 6 hours (percentages of non-adherent cells: 5% on (f)pST, 7% on (-ve)pST and 6% on (+ve)pST; data not shown).

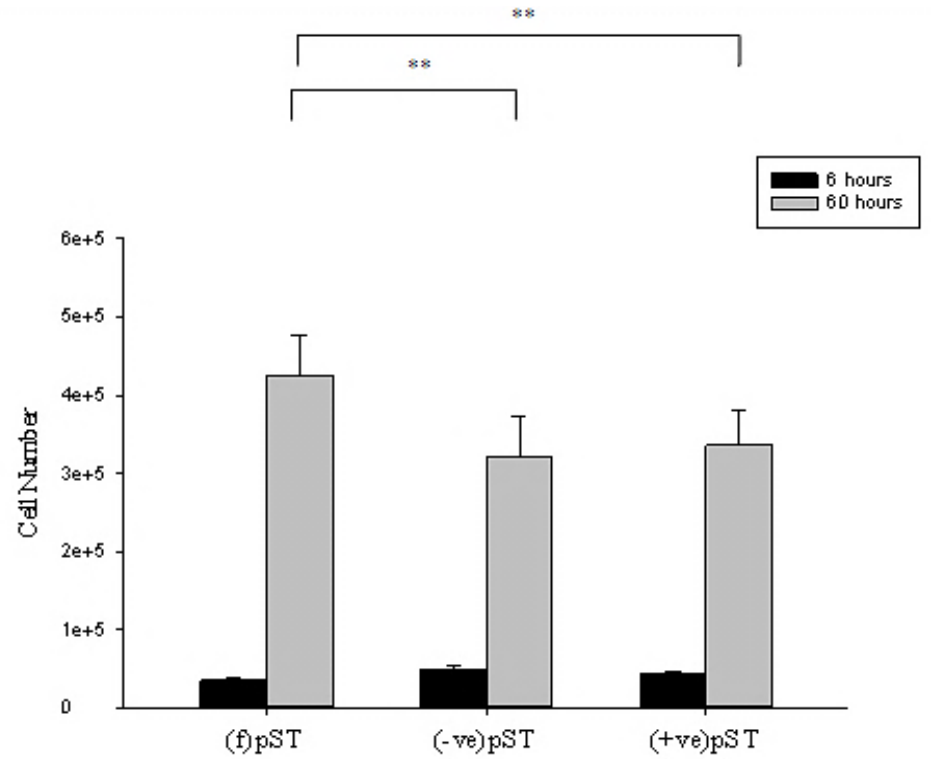


Figure 49 Ishikawa cell numbers on (f)pST, (-ve)pST and (+ve)pST at 6 and 60 hours.

Data are presented as mean ± SEM of 7 independent experiments in quadruplicate. **, $p<0.01$.

6.5.1.3 Time Point of Analyses

The time point of analysis in this project was chosen as 60 hours unless otherwise stated. There were insufficient cells on pMA subsrates at 48 hours whereas there was too low cell survival on pMA substrates at 72 hours. Hence, 60 hours was chosen because this was the optimum time point where sufficient viable cell number was available for all end point analysis on all culture substrates.

6.5.1.4 Ishikawa Endometrial Cancer Cell Growth on Flat, Negative and Positive Human Dermal Microvascular Endothelial Cell Bioimprint Polystyrene Slides

To investigate the possibility that the differential cell growth was a result of a non-specific effect of surface patterning, here another non-cancerous human dermal microvascular endothelial cell line: HMEC-1, was used to make the Bioimprint. Ishikawa endometrial cancer cells were then cultured on HMEC-1 (-ve) and (+ve)pST Bioimprints, and their cell growth at 60 hours was examined. The HMEC-1 cell line was chosen here because it has originated from a human source. In contrast to Ishikawa cells cultured on Ishikawa cell imprints, Ishikawa cells cultured on HMEC-1 (-ve) and (+ve)pST showed no difference in cell numbers at 60 hours, indicating there was no difference in growth behaviour on different pST substrates (Figure 50).

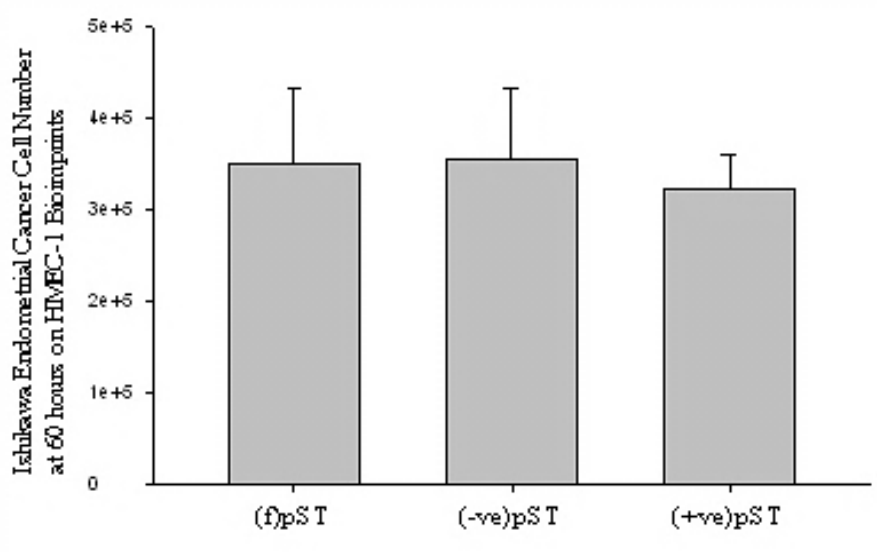


Figure 50 Ishikawa cell numbers on (f)pST, (-ve)pST and (+ve)pST of human dermal microvascular endothelial cell 60 hours.

Data are presented as mean ± SEM of 3 independent experiments in quadruplicate.

6.5.2 Ishikawa Endometrial Cancer Cell Cycle Biomolecules and Proliferation Marker Expression

Since substrate material and surface topography affected cell growth, cyclin D2 expression was then quantified, and for cells on pST microscope slide substrates, cyclin B1, B2 and PCNA were measured.

Results showed that cells on (f)pMA had a trend for lower expression of cyclin D2 compared to cells on glass, tissue culture grade pST and (-ve)pMA, which paralleled the result of cell growth at 60 hours (Figure 48) though there was no statistical difference. Further studies may be required to increase the sample size for statistical verification.

6.5.2.1 Cell Cyclin D2 Expression on Glass, Tissue Culture Polystyrene and Polymethacrylate Polymer Flat and Bioimprint Culture Substrates

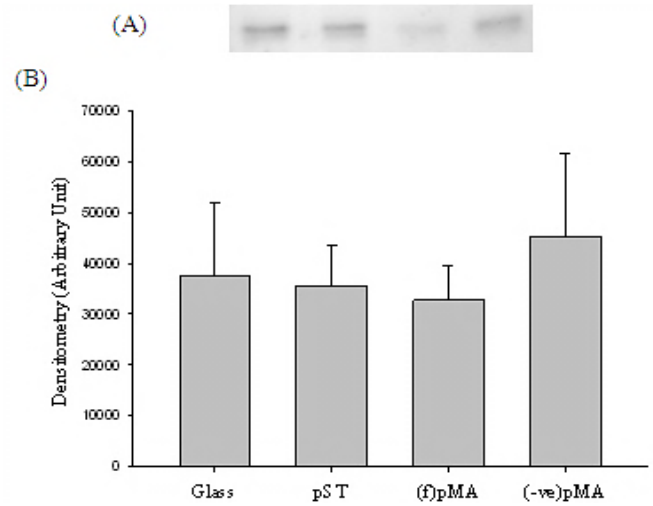


Figure 51 **Ishikawa endometrial cancer cell cyclin D2 expression on glass, tissue culture grade pST, (f)pMA and (-ve)pMA.**

(A) (From left to right: glass, tissue culture grade pST,(f)pMA and (-ve)pMA) a representative example of cyclin D2 western blot protein band.

(B) Densitometry of cyclin D2 of cells cultured on glass, tissue culture grade pST, (f)pMA and (-ve)pMA.

Data are presented as densitometry mean ±SEM of 3 independent experiments in triplicate.

6.5.2.2 Cell PCNA, Cyclin D2, B1 and B2 Expression on Flat, Negative and Positive Bioimprint Polystyrene Slides

For cells cultured on pST microscope slide substrates, cells on (-ve)pST had lower expression of PCNA compared to (+ve)pST and (f)pST (Figure 52), with no statistical difference between (+ve)pST and (f)pST, which may be the reason for the observed lower cell growth on (-ve)pST compared to cell growth on (f)pST (Figure 49). Further, cells on (+ve)pST showed significantly lower expression of cyclin B2 (Figure 53 B) compared to cells on (f) and (-ve)pST, which again agreed with the result of cell growth at 60 hours (Figure 49). Cells on (+ve)pST showed a trend toward lower cyclin D2 compared to cells on (f) and (-ve)pST but the difference was not statiscally significant (Figure 53 C). There was no difference in cyclin B1 expression (Figure 53 A).

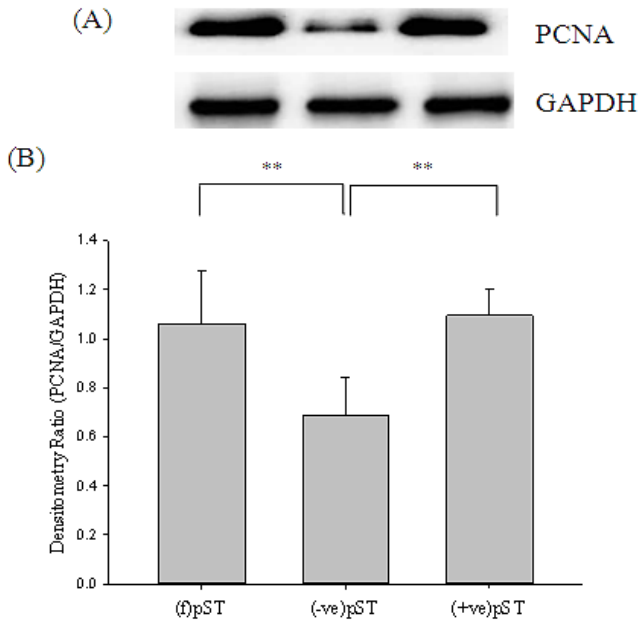


Figure 52 Ishikawa endometrial cancer cell PCNA expression on (f), (-ve) and (+ve)pST.

(A) (From left to right: (f)pST, (-ve)pST, (+ve)pST imprints) representatives examples of PCNA (upper row) and housekeeping protein GAPDH (bottom row) western blot protein bands.

(B) Densitometry ratio of PCNA/GAPDH of cells cultured on (f)pST, (-ve)pST and (+ve)pST imprint.

Data are presented as PCNA densitometry normalized with GAPDH densitometry mean ±SEM of 10 independent experiments in quadruplicate. **, $p<0.01$.

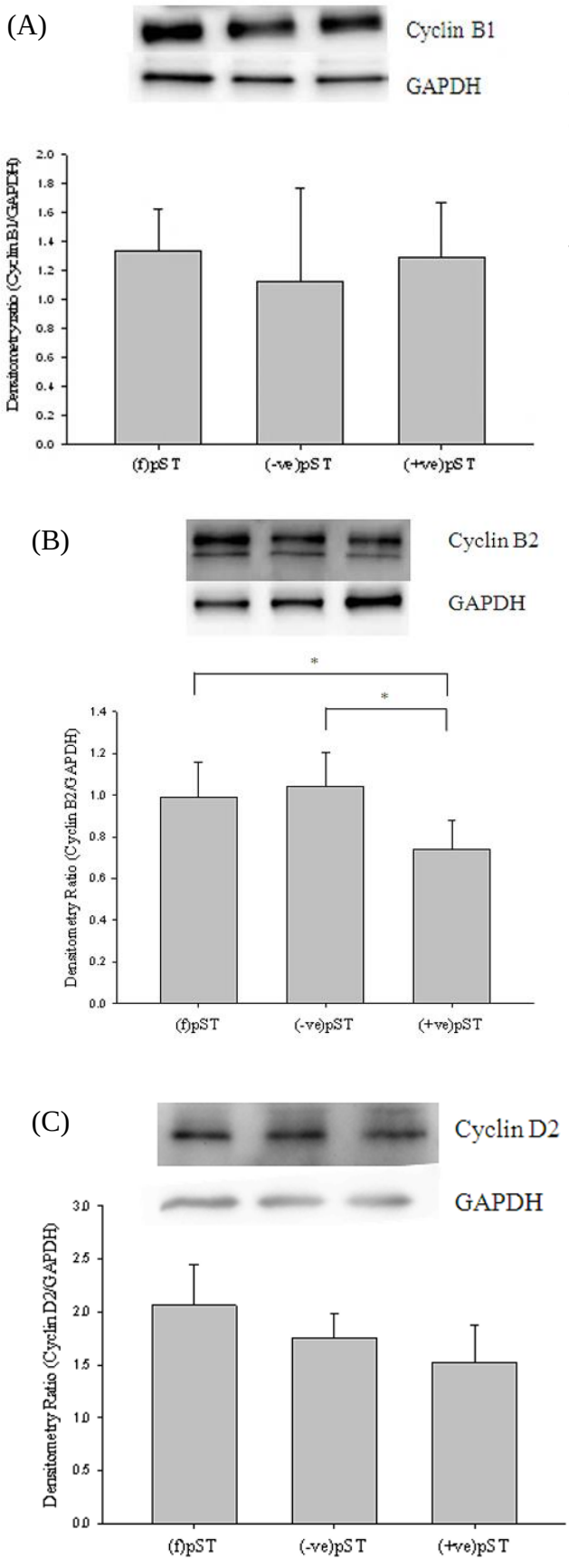


Figure 53 Ishikawa endometrial cancer cell (A) cyclin B1, (B) B2 and (C) D2 expression on (f), (-ve) and (+ve)pST.

[Top] (From left to right: (f)pST, (-ve)pST, (+ve)pST). (Upper rows) Examples of (A) cyclin B1, (B) B2 and (C) D2 and (bottom rows) housekeeping protein GAPDH of western blot protein bands.

[Bottom] Densitometry ratio of cyclin (A) B1/GAPDH, (B) cyclin B2/GAPDH and (C) cyclin D1/GAPDH of cells cultured on (f)pST, (-ve)pST and (+ve)pST imprint.

Data are presented as densitometry normalized with GAPDH densitometry mean ±SEM of 4 independent experiments in quadruplicate. *,p<0.05.

6.5.3 Ishikawa Endometrial Cancer Cell ERK Signalling

6.5.3.1 Cell ERK/pERK Ratio on Glass, Tissue Culture Polystyrene and Polymethacrylate Polymer Flat and Bioimprint Culture Substrates

Next, to further study the control of cell behaviours, the expression of ERK and phosphorylated ERK kinases were investigated to examine if the pathway was involved in cell responses to culture substrate material and topography. No significant difference between cells growing on different materials (between glass, tissue culture grade pST and pMA substrates) as well as between (f)pMA and (-ve)pMA were detected. Although there may be a lower expression ratio of pERK/ERK on (f)pMA compared to cells on glass, tissue culture grade pST and (-ve)pMA, this was not statistically significant (Figure 54).

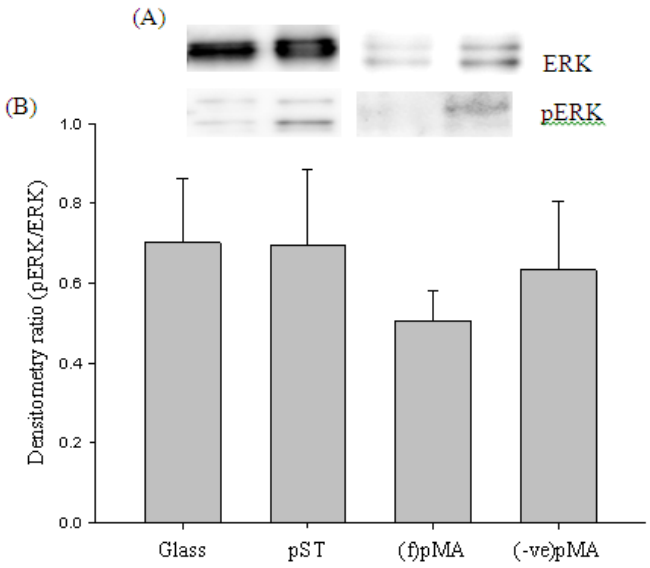


Figure 54 Ishikawa endometrial cancer cell pERK/ERK on glass, tissue culture grade pST, (f)pMA and (-ve)pMA.

(A) (From left to right: glass, tissue culture grade pST,(f)pMA and (-ve)pMA) representative examples of ERK (upper row) and pERK (bottom row) western blot protein bands.

(B) Densitometry ratio of ERK and pERK of cells cultured on glass, tissue culture grade pST, (f)pMA and (-ve)pMA.

Data are presented as densitometry ratio mean ±SEM of 3 independent experiments in triplicate.

6.5.3.2 Cell pERK/ERK ratio on Flat, Negative and Positive Bioimprint Polystyrene Slides

Similar to the cells on glass, tissue culture grade pST and pMA substrates, there was no significant difference observed among cells grown on (f), (-ve) and (+ve)pST (Figure 55).

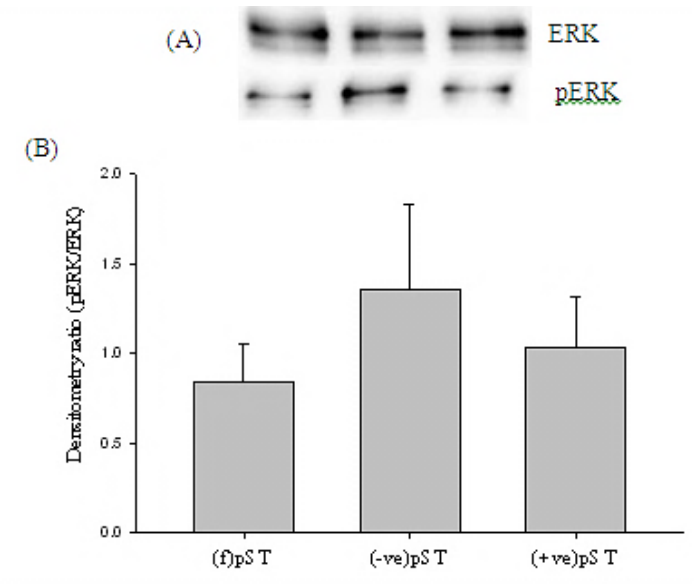


Figure 55 Ishikawa endometrial cancer cell ERK/pERK on (f), (-ve) and (+ve)pST.

(A) (From left to right: (f)pST, (-ve)pST, (+ve)pST) representative examples of ERK (upper row) and pERK (bottom row) western blot protein bands.

(B) Densitometry ratio of ERK and pERK of cells cultured on (f)pST, (-ve)pST and (+ve)pST imprint.

Data are presented as densitometry ratio mean ±SEM of 12 independent experiments in quadruplicate.

6.5.4 Ishikawa Endometrial Cancer Cell PI3K/AKT Signalling

6.5.4.1 Cell AKT/pAKT Ratio on Flat, Negative and Positive Bioimprint Polystyrene Slides

For pST microscope slide substrates, the PI3K/AKT pathway was also studied, another pathway involved in cell growth regulation that is also mechano-sensitive. Yet again, no significant difference was observed (Figure 56).

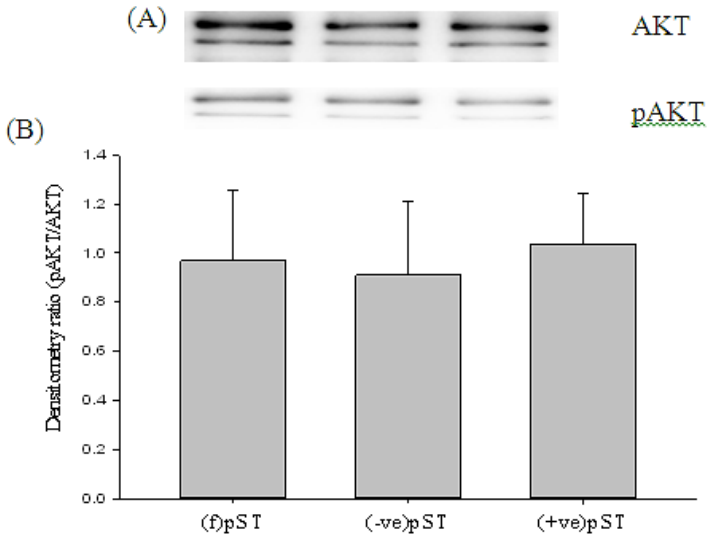


Figure 56 Ishikawa endometrial cancer cell AKT/pAKT on (f), (-ve) and (+ve)pST.

(A) (From left to right: (f)pST, (-ve)pST, (+ve)pST) representative examples of AKT (upper row) and pAKT (bottom row) western blot protein bands.

(B) Densitometry ratio of AKT and pAKT of cells cultured on (f)pST, (-ve)pST and (+ve)pST imprint.

Data are presented as densitometry ratio mean ±SEM of 9 independent experiments in quadruplicate.

6.6 Discussion

Table 4 Summary of Results from Section 6.5.1.1, 6.5.2.1, 6.5.3.1. A table showing the comparative level of the measured parameters between Ishikawa endometrial cancer cells on glass, tissue culture grade pST, (f)pMA and (-ve)pMA. The numbers relate to the comparative measurements (cell number and western blot desitometry); 1=lowest value and 4=highest value. The "-" symbol indicates no statistically significant difference between the compared groups.

	Glass	Tissue Culture Grade pST	Polymethacrylate	
			(f)pMA	(-ve)pMA
Cell adherence at 6 hrs	2	2	1	1
Cell adherence at 60 hrs	2	3	1	1
Cell Number	3	4	1	2
Cyclin D2	-	-	-	-
pERK/ERK	-	-	-	-

Table 5 Summary of Results from Section 6.5.1.2, 6.5.2.2, 6.5.3.2, 6.5.4.1. A table showing the comparative level of the measured parameters between Ishikawa endometrial cancer cells on (f)pST, (-ve)pST and (+ve)pST. The numbers relate to the comparative measurements (cell number and western blot densitometry); 1=lowest value and 4=highest value. The "-" symbol indicates no statistically significant difference between the compared groups.

	(f)pST	(-ve)pST	(+ve)pST
Cell Number at 6 hrs	-	-	-
Cell Number at 60 hrs	2	1	1
PCNA	2	1	2
Cyclin B1	-	-	-
Cyclin B2	2	2	1
Cyclin D2	-	-	-
pERK/ERK	-	-	-
pAKT/AKT	-	-	-

The growth effect of incubating cells on glass, tissue culture grade pST and pMA substrates was investigated. Glass and pST are both conventional cell culture substrates; pMA, however, is not a common cell culture substrate although it is biocompatible. There was

only a small difference in initial adherence from that on conventional pST culture surfaces (approximately 89% on (f)pMA compared to approximately 97% on (f)pST; $p<0.05$). When cells were incubated for a longer period (60hours), the cells on pMA substrate showed lower growth than cells on glass and tissue culture grade pST; this may be partly due to the hydrophobic and charge-neutral surface of pMA; that had affected cell membrane interactions with the substrate surface which reduced the cell shape and size (Figure 20 and 21). This size reduction then may have influenced the cell DNA synthesis rate, as suggested by Folkman's study (Folkman & Moscona, 1978), or have altered the cell NFκB signalling (Sero et al., 2015). The observation that cells cultured on pMA surfaces had lower populations is consistent with the sparing use of polymethacrylate in *in vitro* culture studies and corresponding wide use of glass and tissue culture grade pST that are well-characterized for cell growth and maintenance.

Next, when the effect of the cell-like topography was investigated; the topographical influence depended on the substrate material. On the pMA substrate, in which the material is not the optimized cell culture material, the presence of the Bioimprint helped in cell adhesion and enhanced cell growth. On the contrary, on pST, a material that supports maximized cell growth, the presence of the Bioimprint acted instead to restrict cell spread, hence reducing the cell growth as compared to the flat surface.

The effect of pMA Bioimprint on enhanced cell growth may likely be through increasing cell adhesion and spreading by increasing β1 integrin and cell Cytokeratin-18 expression, and probably through cyclin D2. On the other hand, on pST Bioimrprint, the decreased cell growth may also be mediated by β1 integrin and cell Cytokeratin-18 modulated mechanisms that involved PCNA on (-ve)pST and cyclin B2 on (+ve)pST.

Further, by using the Bioimprint made of different cell lines, it has been clearly shown that different physical topographies carried different physical signals. Here the results demonstrated that Ishikawa endometrial cancer cells only reduced growth on their own Bioimprint. Even a cell Bioimprint using other cells of human origin did not result in a

change in Ishikawa cell growth. This suggests that the shape of the topography is important in directing cell behaviours.

Moreover, influences of the substrate material and physical topography on cell growth were not related to either the activation of the MAPK/ERK or PI3K/AKT pathways. In fact, iTRAQ analysis suggested that other pathways may be involved in our context, for instance, the c-JUN pathway or NFκB or signal transducer and activator of transcription 3 (STAT3) related signalling pathways (discussed in Chapter 7 section 7.5.3). Futhermore, Ishikawa endometrial cancer cells are cells with a phosphatase and tensin homolog (PTEN) mutation. PTEN is a tumour suppressor protein that suppresses cancer cell growth by negatively regulating the PI3K/AKT pathway (Stambolic et al., 1998). Hence, the PTEN mutation in Ishikawa cells may have limited the cells' response to surface topography through modulation of PI3K/AKT pathway.

Further studies have yet to be done to look at the proliferation of cells growing on pMA substrates, and instead of measuring the proliferation biomarker expression level, the rate of DNA synthesis may be a better indicator of cell growth in all cases since the cell size effect on growth may be more pronounced at the DNA synthesis level.

6.7 Conclusion

The results in this chapter favour our hypothesis. The observations discussed in this chapter have demonstrated that the Ishikawa endometrial cancer cell growth can be affected by different substrate materials and surface topography. On a less favourable surface, cell number was reduced compared to cells on a surface that supports cell growth. Notably, on the less favourable surfaces, the cell-like topography acted to assist cell growth whereas on a surface that supported cell growth, the topography instead restricted the cells' ability to spread and grow.

Furthermore, different substrate materials and topographies regulate cell growth by different mechanisms. Comparison between cells growing on the glass, tissue culture grade pST and pMA substrates showed that the MAPK/ERK signalling molecules were not involved in the observed distinct growth characteristics. However, β1 integrin, cell Cytokeratin-18, and probably cyclin D2 were likely to be involved in cell proliferation regulation.

Cell growth on (f), (-ve) and (+ve)pST may involve other pathways that were also cell spreading-related. It is also clearly shown that the presentation of topography (both positive and negative) is also important in determining the expression of cell growth-related biomolecules. The 'hump' like topography affected the cell cyclin B2, which reduced cell number, whereas the 'pit' like topography influenced the cell PCNA expression with reduced cell number.

Also, on all culture substrate materials and topographies the MAPK/ERK and PI3K/AKT pathways were not involved in cell growth regulation. Other proliferation pathways suggested above are worthy of further exploration.

Here in this chapter Ishikawa endometrial cancer cells were shown to have different growth behaviours in response to culture substrate of different materials and topographies. In the next chapter, the results obtained from iTRAQ are presented. iTRAQ is a technique that profiles the protein expression in Ishikawa cells to further characterize the cell behaviours that are changed in response to surface topography.

Chapter 7 Proteomic Analysis of Ishikawa Endometrial Cancer Cell on Flat, Negative and Positive Bioimprint Polystyrene Slides

7.1 Introduction

In the last few chapters Ishikawa endometrial cancer cells were observed to have responded to physical microenvironments by changing their morphology, spreading, adhesion and growth. Here the iTRAQ technique was utilised to further characterize the protein expression in Ishikawa endometrial cancer cells.

Proteomics is the large-scale qualitative and quantitative analysis of proteins, or, in other words, profiling the entire set of proteins present in the specimens analysed. In addition to 2-dimensional electrophoresis (2-DE), iTRAQ is another method in proteomics study. In particular, iTRAQ enables comparative analysis of several samples. Also, the chemical-based labelling of samples allows iTRAQ to be done on any biological specimens such as cell or tissue lysates.

iTRAQ involves digestion of different protein samples to peptides. Peptides in each sample of cells from the same topography are tagged with a specific isotope to the N-terminus and the side chain amines. All samples are then pooled and fractioned by nano-liquid chromatography and the fragments are next identified and quantified by tandem mass spectrometry. The tandem mass spectrometry fragments are searched through a fragmentation database. The tagging will identify from which sample each peptide was derived. Thence the ratio of levels of a tagged peptide from a pair of original paired samples can be calculated (i.e. (+ve)pST / (f)pST or (-ve)pST / (f)pST or (+ve)pST / (-ve)pST).

iTRAQ is a discovery-based methodology to determine the pattern of protein expression of the tested specimens. iTRAQ was used here to compare protein expression in cells that were cultured on (f), (-ve)pST or (+ve)pST, and thence to study the proteins that were affected by physical topography. This allowed formulation of possible hypotheses regarding the Ishikawa endometrial cancer cell behaviours that were influenced by surface topography.

7.2 Aim

In this chapter, we utilize iTRAQ technique aiming to profile the proteins presence in Ishikawa endometrial cancer cells cultured on (f)pST, (-ve)pST and (+ve)pST.

7.3 Experimental Approach

iTRAQ was performed by The Centre for Protein Research of The University of Otago in Dunedin, New Zealand. The cell culture and cell lysate preparation were done in Laboratory of Cell and Protein Regulation in Christchurch, New Zealand and sent to Dunedin. Details of samples preparation were described in Section 2.13. Each iTRAQ sample was pooled from 16 wells of cultures on a substrate type and iTRAQ analysis was done twice independently.

Proteins that were potentially sensitive to topography were selected by including only proteins that had an expression ratio, x, that were $x \leq 0.8$ or $1.2 \leq x$. However, proteins that showed opposite direction of difference in the two iTRAQ analysis runs were excluded. Further, the values of the ratios obtained in the analysis varied between peptides from a protein and these, as percentages, formed the basis of a variability confidence level. Proteins that had mean variability confidence levels of > 17 % were excluded. Proteins that complied with both of these criteria were identified as those being most likely to be potentially sensitive to physical topography.

Proteins are presented in Table 6. Each protein is listed under a functional group the protein belongs to; the functions of the protein are obtained from a literature search. In the discussion section, a more detailed discussion of those proteins' functions is presented (Table 7 to Table 12). Under each functional group, the proteins are ranked from high to lower ratio of the compared samples.

7.4 Results

7.4.1 Identification of Changed Proteins

The expression of a total of thirty-four proteins was identified to be sensitive to the topography of the substrates. With nineteen up-regulated and six down-regulated in cells on (+ve)pST compared to (f)pST; four up-regulated and five down-regulated in cells on (-ve)pST compared to (f)pST, and fifteen up-regulated and one down-regulated in cells on (+ve)pST compared to (-ve)pST (Table 6). The functions of these proteins were searched through literature.

Table 6 List of proteins that were up-regulated or down-regulated in comparisons between (+ve) / (f)pST, (-ve) / (f)pST and (+ve) / (-ve)pST.

The number in parentheses: upper row: ratio, $\bar{x}$= mean of ratio from two individual iTRAQ tests; bottom row: % of the variability, $\bar{y}$ =mean of % of the variability from two individual iTRAQ tests. Highlighted cells indicate proteins' $\bar{x}$ of $\geq$ 1.2 or $\leq$ 0.8 and $\bar{y}$ of $\leq$ 17.0%.

Functional Group	Proteins Identified from iTRAQ	(+ve)/(f) pST	(-ve)/(f) pST	(+ve)/(-ve) pST
DNA Structure, Transcription	histone H1.0	(1.2,2.0; ***$\bar{x}$=1.6***) (16.1,7.0; $\bar{y}$ =11.5)	(1.2,1.3; ***$\bar{x}$=1.2***) (29.4,2.2; $\bar{y}$ =15.8)	(1.0,1.6; ***$\bar{x}$=1.3***) (18.9,7.5; y=13.2)
	SRA stem-loop-interacting RNA-binding protein, mitochondrial isoform 3 precursor	(1.2,1.6; ***$\bar{x}$=1.4***) (8.1,18.3; $\bar{y}$ =13.2)	(1.0,1.0; ***$\bar{x}$=1.0***) (8.9,15.9; $\bar{y}$ =12.4)	(1.2,1.5; ***$\bar{x}$=1.4***) (7.2,13.0; $\bar{y}$ =10.1)
	ATP-dependent RNA helicase DDX18	(1.1,1.4; ***$\bar{x}$=1.3***) (8.6,13.5; $\bar{y}$ =11.1)	(1.1,1.2; ***$\bar{x}$=1.1***) (12.8,18.6; $\bar{y}$ =15.7)	(1.0,1.2; ***$\bar{x}$=1.1***) (5.4,4.4; $\bar{y}$ =4.9)
	non-histone chromosomal protein HMG-14	(1.3,0.6; ***$\bar{x}$=0.9***) (30.5,98.3; $\bar{y}$ =64.4)	(1.4,1.2; ***$\bar{x}$=1.3***) (10.2,3.8; $\bar{y}$ =7.0)	(0.9,0.5; ***$\bar{x}$=0.7***) (18.9,103.3; $\bar{y}$ =61.1)
	SWI/SNF complex subunit SMARCC1	(0.9,0.8; ***$\bar{x}$=0.9***) (22.2,36.9; $\bar{y}$ =29.6)	(0.8,0.8; ***$\bar{x}$=0.8***) (9.9,9.3; $\bar{y}$ =9.6)	(1.0,1.0; ***$\bar{x}$=1.0***) (24.6,47.1; $\bar{y}$ =71.7)
Extracellular Matrix Proteins, Cell Structural and Cell Migration	UBX domain-containing protein 4	(1.0,4.1; ***$\bar{x}$=2.5***) (13.5,13.4; $\bar{y}$ =13.5)	(1.1,1.5; ***$\bar{x}$=1.3***) (25.0,26.4; $\bar{y}$ =25.7)	(0.9,2.5; ***$\bar{x}$=1.7***) (12.6; $\bar{y}$ =12.6)
	spondin-1 precursor	(1.0,1.4; ***$\bar{x}$=1.2***) (5.2,12.6; $\bar{y}$ =8.9)	(1.1,0.9; ***$\bar{x}$=1.0***) (12.9,11.2; $\bar{y}$ =12.0)	(0.9,1.5; ***$\bar{x}$=1.2***) (7.9,21.4; $\bar{y}$ =14.7)
	thyroid receptor-interacting protein 6 (TRIP6)	(1.0,1.3; ***$\bar{x}$=1.2***) (14.9,16.0; $\bar{y}$ =15.4)	(0.9,1.0; ***$\bar{x}$=1.0***) (24.5,7.0; $\bar{y}$ =15.8)	(1.2,1.3; ***$\bar{x}$=1.2***) (10.0,22.7; $\bar{y}$ =16.4)
Signalling Pathways	nodal modulator 2 isoform 2 precursor	(1.0,1.8; ***$\bar{x}$=1.4***) (4.3,24.3; $\bar{y}$ =14.3)	(1.0,1.2; ***$\bar{x}$=1.1***) (16.6,18.7; $\bar{y}$ =17.6)	(1.0,1.5; ***$\bar{x}$=1.3***) (15.4,22.3; $\bar{y}$ =18.9)
	COP9 signalosome complex subunit 5 (CSN5)	(1.0,1.3; ***$\bar{x}$=1.2***) (15.4,15.2; $\bar{y}$ =15.3)	(1.0,0.9; ***$\bar{x}$=0.9***) (8.6,13.0; $\bar{y}$ =10.8)	(1.1,1.4; ***$\bar{x}$=1.3***) (14.9,2.3; $\bar{y}$ =8.6)
	signal transducer and activator of transcription 3 (STAT3) isoform 3	(0.9,1.2; ***$\bar{x}$=1.0***) (1.7,3.5; $\bar{y}$ =2.6)	(0.8,0.8; ***$\bar{x}$=0.8***) (1.1,7.6; $\bar{y}$ =4.3)	(1.1,1.3; ***$\bar{x}$=1.2.***) (0.3,6.8; $\bar{y}$ =3.6)
Energy Modulation	complement component 1 Q subcomponent-binding protein, mitochondrial precursor	(1.0,2.0; ***$\bar{x}$=1.5***) (16.1,15.0; $\bar{y}$ =15.5)	(1.1,1.0; ***$\bar{x}$=1.1***) (16.2,16.9; $\bar{y}$ =16.5)	(1.0,2.0; ***$\bar{x}$=1.5***) (16.7,0.2; $\bar{y}$ =8.5)
	adenylate kinase 2, mitochondrial isoform c	(1.3,1.1; ***$\bar{x}$=1.2***) (10.8,,11.4; $\bar{y}$ =11.1)	(1.1,0.9; ***$\bar{x}$=1.0***) (13.8,14.1; $\bar{y}$ =14.0)	(1.2,1.2; ***$\bar{x}$=1.2***) (12.8,25.0; $\bar{y}$ =18.9)
	uridine 5'-monophosphate synthase	(0.9,1.5; ***$\bar{x}$=1.2***) (14.2,17.7; $\bar{y}$ =16.0)	(0.9,1.0; ***$\bar{x}$=0.9***) (12.1,18.6; $\bar{y}$ =15.3)	(1.0,1.4; ***$\bar{x}$=1.2***) (25.1,4.7; $\bar{y}$ =14.9)
	inorganic pyrophosphatase 2, mitochondrial isoform 1 precursor (PPi)	(1.0,0.7; ***$\bar{x}$=0.8***) (8.7,25.4; $\bar{y}$ =17.1)	(1.0,0.9; ***$\bar{x}$=0.9***) (13.0,14.2; $\bar{y}$ =13.6)	(1.0,0.7; ***$\bar{x}$=0.9***) (10.4,20.5; $\bar{y}$ =15.5)
	1,4-alpha-glucan-branching enzyme	(0.8,0.7; ***$\bar{x}$=0.7***) (11.5,8.7; $\bar{y}$ =10.1)	(0.7,1.1; ***$\bar{x}$=0.9***) (28.1,6.8; $\bar{y}$ =17.4)	(1.2,0.7; ***$\bar{x}$=1.0***) (27.5,25.1; $\bar{y}$ =26.3)
Cell Viability	apoptosis regulator BAX isoform sigma	(0.8,0.8; ***$\bar{x}$=0.8***) (16.9,2.5; $\bar{y}$ =9.7)	(1.2,0.9; ***$\bar{x}$=1.1***) (17.7,14.7; $\bar{y}$ =16.2)	(0.7,0.8; ***$\bar{x}$=0.8***) (35.1,17.3; $\bar{y}$ =26.2)
	puromycin-sensitive aminopeptidase	(0.9,1.6; ***$\bar{x}$=1.3***) (7.0,14.6; $\bar{y}$ =10.8)	(0.9,0.8; ***$\bar{x}$=0.9***) (7.0,22.4; $\bar{y}$ =14.7)	(0.9,1.7; ***$\bar{x}$=1.3***) (13.4,17.8; $\bar{y}$ =10.6)

Innate Immune Response (also in Cell Growth Regulation)	macrophage migration inhibitory factor (MIF)	(1.0,0.9; $\bar{x}$=1.0) (28.0,8.5; ȳ =18.2)	(0.8,0.8; $\bar{x}$=0.8) (12.9,11.2; ȳ =12.0)	(1.2,1.1; $\bar{x}$=1.2) (23.2,14.5; ȳ =18.9)
Protein Synthesis, Processing, Degradation and Transportation	endoplasmic reticulum resident protein 29 isoform 1 precursor	(1.1,1.6; $\bar{x}$=1.3) (6.0,24.3; ȳ =15.1)	(1.0,1.1; $\bar{x}$=1.0) (6.9,5.0; ȳ =6.0)	(1.0,1.4; $\bar{x}$=1.2) (5.3,24.4; ȳ =14.9)
	selenide, water dikinase 1 isoform 2	(1.2,1.6; $\bar{x}$=1.4) (15.4,24.9; ȳ =20.1)	(1.1,1.1; $\bar{x}$=1.1) (3.4,14.5; ȳ =8.9)	(1.1,1.4; $\bar{x}$=1.3) (8.9,18.0; ȳ =13.5)
	long-chain fatty acid transport protein 4	(1.0,1.4; $\bar{x}$=1.2) (14.3,1.9; ȳ =8.1)	(0.9,1.1; $\bar{x}$=1.0) (8.0,1.2; ȳ =4.6)	(1.1,1.1; $\bar{x}$=1.1) (5.5,1.0; ȳ =3.3)
	26S protease regulatory subunit 4	(1.1,1.4; $\bar{x}$=1.2) (5.2,18.6; ȳ =11.9)	(1.0,1.1; $\bar{x}$=1.1) (6.7,10.3; ȳ =8.5)	(1.0,1.1; $\bar{x}$=1.1) (7.2,15.0; ȳ =11.1)
	E3 ubiquitin-protein ligase CHIP	(1.0,1.2; $\bar{x}$=1.1) (19.2,2.8; ȳ =11.0)	(0.9,0.9; $\bar{x}$=0.9) (10.8,6.5; ȳ =8.7)	(1.1,1.3; $\bar{x}$=1.2) (12.5,5.1; ȳ =8.8)
	phosphoacetylglucosamine mutase isoform 2	(0.8,0.8; $\bar{x}$=0.8) (13.3,43.4; ȳ =28.3)	(0.8,0.8; $\bar{x}$=0.8) (21.3,9.3; ȳ =15.3)	(1.2,0.9; $\bar{x}$=1.1) (11.2,48.7; ȳ =30)
	eukaryotic translation initiation factor 3 subunit M	(0.8,0.6; $\bar{x}$=0.7) (20.6,11.7; ȳ =16.2)	(1.0,1.1; $\bar{x}$=1.0) (2.0,20.0; ȳ =11.0)	(0.9,0.5; $\bar{x}$=0.7) (20.9,19.7; ȳ =20.3)
Ribosomal Protein, RNA Processing	U2 small nuclear ribonucleoprotein A'	(1.0,1.7; $\bar{x}$=1.3) (7.6,10.7; ȳ =9.1)	(1.1,1.1; $\bar{x}$=1.1) (6.5,8.4; ȳ =7.4)	(1.0,1.4; $\bar{x}$=1.2) (8.5,10.3; ȳ =9.4)
	60S ribosomal protein L35	(1.1,3.4; $\bar{x}$=2.2) (12.4,40.9; ȳ =26.7)	(1.3,1.3; $\bar{x}$=1.3) (4.9,15.0; ȳ =10.0)	(0.8,2.5; $\bar{x}$=1.7) (8.2,29.1; ȳ =18.7)
	pre-mRNA 3'-end-processing factor FIP1 isoform 3	(1.0,1.5; $\bar{x}$=1.2) (18.6,14.0; ȳ =16.3)	(0.9,,0.8; $\bar{x}$=0.9) (17.0,4.5; ȳ =10.8)	(1.1,1.7; $\bar{x}$=1.4) (36.3,15.0; ȳ =25.7)
Lipid Transport and Metabolism	enoyl-CoA delta isomerase 1, mitochondrial isoform 2 precursor	(0.9,,1.9; $\bar{x}$=1.4) (8.2,18.3; ȳ =13.3)	(0.9,1.1; $\bar{x}$=1.0) (18.2,24.2; ȳ =21.3)	(1.0,1.7; $\bar{x}$=1.4) (22.0,16.9; ȳ =19.5)
	oxysterol-binding protein 1	(1.2,3.1; $\bar{x}$=2.1) (20.2,50.1; ȳ =35.2)	(1.1,1.3; $\bar{x}$=1.2) (12.4,16.2; ȳ =14.3)	(1.0,2.2; $\bar{x}$=1.6) (13.3,38.6; ȳ =26)
Calcium-Mediated Processes	copine-1 isoform c	(0.9,1.6; $\bar{x}$=1.2) (18.3,2.7; ȳ =10.5)	(0.9,1.0; $\bar{x}$=1.0) (13.4,13.5; ȳ =13.4)	(0.9,1.5; $\bar{x}$=1.2) (10.8,5.7; ȳ =8.3)
Vesicles And Organelles Movement	cytoplasmic dynein 1 light intermediate chain 2	(1.1,0.8; $\bar{x}$=0.9) (22.7,19.3; ȳ =21.0)	(1.0,0.6; $\bar{x}$=0.8) (13.7,11.7; ȳ =12.7)	(1.0,1.3; $\bar{x}$=1.2) (8.6,28.3; ȳ =18.5)
Golgi apparatus Functions	ADP-ribosylation factor-like protein 1	(1.0,0.7; $\bar{x}$=0.8) (26.7,7.5; $\bar{y}$=17.1)	(1.1,1.0; $\bar{x}$=1.0) (9.1,4.6; $\bar{y}$=6.8)	(0.8,0.6; $\bar{x}$=0.7) (27.0,7.1; $\bar{y}$=17.1)
Accelerate Apoptosis	apoptosis regulator BAX isoform sigma	(0.8,0.8; $\bar{x}$=0.8) (16.9,2.5; $\bar{y}$=9.7)	(1.2,0.9; $\bar{x}$=1.1) (17.7,14.7; $\bar{y}$=16.2)	(0.7,0.8; $\bar{x}$=0.8) (35.1,17.3; $\bar{y}$=26.2)
Bone Mineral Phase	alpha-2-HS-glycoprotein preproprotein	(0.9,0.4; $\bar{x}$=0.7) (16.1,15.0; $\bar{y}$=15.6)	(1.0,0.6; $\bar{x}$=0.8) (19.0,29.0; $\bar{y}$=24.0)	(1.0,0.7; $\bar{x}$=0.9) (6.5,23.0; $\bar{y}$=14.8)

7.5 Discussion

The proteins are grouped into different functional groups and are discussed below. The order of proteins in each functional group is the same as the order in Table 6.

7.5.1 DNA Condensation

Table 7 The proteins under the functional group of DNA condensation.

Proteins Identified from iTRAQ	**Functions**
Histone H1.0	-A linker histone (LH) that connects DNA between nucleosome chains. -Organizes and condenses the nucleosome chains into high order chromatin structure. -Compact chromatin has limited DNA transcription and replication. It has been shown that dissociation of H1 histone from chromatin structure increased transcription activities (Zlatanova et al., 2000).
SRA stem-loop-interacting RNA-binding protein, mitochondrial	-Binds to SRA RNA and acts as a nuclear receptor corepressor that mediates certain transcriptional repression
ATP-dependent RNA helicase DDX18	-RNA-dependent helicase that functions to unpackage an organism's genes.
non-histone chromosomal protein HMG-14	-Maintains actively transcriptable genes in an accessible chromatin structure -Stimulates transcriptional process through stimulating RNA polymerase II elongation
SWI/SNF complex subunit SMARCC1	- Regulates transcriptional activation and repression of genes through remodeling chromatin. - Involved in neural development and dendrite growth.

There were five proteins belong to the functional group of DNA structure and gene transcription regulation. Three were up-regulated on (+ve)pST compared to cells on (f)pST while two were also up-regulated compared to cells on the (-ve)pST. There were two proteins up-regulated on (-ve)pST compared to cells on (f)pST whereas only one protein was down-regulated on (-ve)pST compared to (f)pST.

Histone H1.0 was the only protein that was up-regulated on both (+ve) and (-ve)pST compared to (f)pST. A higher expression of histone H1.0 on (+ve)pST and (-ve)pST compared to cells on (f)pST may imply a more compact chromatin structure in cells on pST Bioimprints, and therefore explain the lower growth of cells on these substrates.

Moreover, SRA stem-loop-interacting RNA-binding protein, a protein that functions as a nuclear receptor corepressor that represses gene transcription, showed an increased expression on (+ve)pST compared to cells on (f)pST, this may also explain the lowered cell growth on (+ve)pST than on flat substrate.

Further, we observed that the non-histone chromosomal protein HMG-14 had a higher expression on (-ve)pST compared to cells on (f)pST and (+ve)pST. This protein functions to maintain actively transcriptable genes in an accessible chromatin structure and it stimulates transcriptional process through stimulating the rate of RNA polymerase II elongation (Ding et al.,1994). A higher expression of this protein on (-ve)pST compared to cells on (f)pST and (+ve)pST may explain a less reduction effect on cell proliferation by the negative cell-like topography compared to the positive topography. Though there was a less reduction effect on cell proliferation on the (-ve)pST than (+ve)pST, the cells still showed lower growth compared to (f)pST, probably due to a down-regulation of SWI/SNF complex subunit SMARCC1.

There have been studies that reported that mechanical signals can change a cell chromosome structure and alter the cell transcription. For example, the assembly of DNA and histone octamer into an individual nucleosome (Mihardja et al., 2006) and assembly and disassembly

of nucleosomes into chromatins (Leuba et al., 2003) were shown to be reversible and inducible by mechanical force. Furthermore, distortions of nucleus and chromatin structures were observed with an application of force (Bloom et al., 1996; Le Beyec et al., 2007; Maniotis et al., 1997). Also, it was observed that following cytoskeletal restructuring, fibroblast nuclei and nucleus lamina were shrunk. This change of cell nucleus morphology limited accessibility of transcription factors to certain chromosomal segments, hence gene expression was reduced and eventually the fibroblast adhesion patterns and shapes were altered (Dalby et al., 2007). All these force-dependent modifications of DNA structures suggest that the accessibility of DNA for transcription and replication can be manipulated mechanically, and cell-like topography may have changed gene expression through histone condensation of chromatin.

7.5.2 Extracellular Matrix Proteins, Cell Structural and Cell Migration

Table 8 The proteins under the functional group of extracellular matrix proteins, cell structural and cell migration.

Proteins Identified from iTRAQ	Functions
UBX domain-containing protein	-Associated with Rho-GTPase and restructured cell actin filaments (Katoh et al., 2002).
Spondin-1 (or F-spondin and vascular smooth muscle growth factor)	-Cell secreted ECM protein that regulates cell adhesion and cell spreading. -Attached cells to basement membrane through interacting with integrin (Woo et al., 2008). -Inhibits angiogenesis by inhibiting spreading and FAK phosphorylation of endothelial cells. -It has been shown to mature existing neo-vessel by stimulating the growth of vascular smooth muscle cells (Terai et al., 2001).
Thyroid receptor-interacting protein 6 (TRIP6)	-Localized to focal adhesion (FA) and transmits signals from the cell surface to the nucleus, then disintegrates adherens junctions,

	reorganizes actin cytoskeleton and promotes cell migration and invasion.

Three proteins identified were involved in cell-ECM protein secretion and cell adhesion regulation. All these proteins were up-regulated in cells on (+ve)pST compared to cells on (f)pST. The observation of different expression of proteins associated with ECM and cell adhesion is consistent with the hypothesis that cells may respond to physical features by modulating the cell neighbourhood to alter cell spreading and growth.

UBX domain-containing protein was expressed higher on both Bioimprint compared to the flat platform. It has been shown that this protein was associated with Rho-GTPase and restructured cell actin filaments (Katoh et al., 2002). Rho-GTPase is a well-known protein family involved in mechanical signals sensing and responding. Hence endometrial cancer cells may respond to the surface topography through modulating UBX domain-containing protein regulation of Rho-GTPase and actin filaments.

On the other hand, spondin-1 (or F-spondin and vascular smooth muscle growth factor) is a cell secreted ECM protein that regulates cell adhesion and cell spreading. It has been shown on human umbilical vein endothelial cells (HUVECS) that it reduced cells spreading on extracellular matrix through functional blocking of with integrin (Woo et al., 2008; Terai et al., 2001) and inhibiting FAK phosphorylation (Terai et al., 2001). We observed smaller cell size (Figure 22), and up-regulation of β1 integrin (Figure 29) but down-regulation of pFAK/FAK (Figure 33) in cells on (+ve)pST compare to flat culture substrate, it is speculated spondin-1 may have increased adherence of cells on substrate surface through integrin, and then limited cell spreading by lowering FAK phosphorylation.

On the other hand, TRIP6 that is localised to FA showed an up-regulation in cells on (+ve)pST compared to cells on (f)pST and (-ve)pST; this is consistent with previously observed higher FAK expression in cells on (+ve)pST than cells on (-ve)pST (Figure 34),

which suggests a potential role of TRIP6 in responding to physical topography through association with FAK.

7.5.3 Signalling Pathways

Table 9 The proteins under the functional group of signaling pathway.

Proteins Identified from iTRAQ	**Functions**
Nodal modulator 2 isoform 2 precursor	-Antagonizes Nodal signalling.
COP9 signalosome complex subunit 5 (CSN 5)	-Involved in phosphorylation of tumor protein p53 (TP53/p53), c-JUN, NFκB, inositol-tetrakisphosphate 1-kinase (ITPK1) and Interferon regulatory factor 8 (IRF8) pathways. -Overexpressed in cells in response to UV irradiation (Wei et al., 2008). -Regulates DNA-damage repair. -It has been correlated to resistance to chemotherapy and radiotherapy (Pan et al., 2013). -Has an important role in cell growth, as seen in studies that showed that down-regulation of CSN reduced cell growth through decreasing cell cycle regulator S-phase-associated protein (Skp-2) levels (Denti, Fernandez-Sanchez, Rogge, & Bianchi, 2006) and insufficient down-regulation of p27 in cell cycle (Tomoda et al., 2004).
signal transducer and activator of transcription 3 isoform 3 (STAT3)	-A transcription factor and a regulator of cell growth and apoptosis. -Activated by receptor-associated kinase or cytokines such as interferons, epidermal growth factor (EGF), Interleukin -5 and -6. -Binds to small GTPase and Rac-1 (two of the well-known mechano-responsive biomolecules).

Thyroid receptor-interacting protein 6 (TRIP6)	-Transcriptional co-activator for NF-kappa-B and c-JUN pathways.

Four proteins that were involved in signalling pathways were identified to be possibly changed on Bioimprints compared to flat substrate. Three had higher expression on (+ve)pST than on (f)pST and/or (-ve)pST whereas one of these signalling molecules was down-regulated in cells on (-ve)pST compared to cells on flat substrate.

Nodal modulator 2 isoform 2 precursor showed an increased expression on the (+ve)pST than on (f)pST, this protein involves in Nodal signalling that plays a part in pattern formation and differentiation during embryo development. The role of Nodal signalling in embryonic pattern formation and differentiation suggests that this signalling may also involve in mechanical signalling because embryonic development involves mechanical changes. The endometrial cancer cells may possibly alter this signalling in response to the physical topography which requires further investigation.

COP9 signalosome complex subunit 5 (CSN 5) regulates DNA-damage repair has an important role in cell growth, as seen in studies that showed that down-regulation of CSN reduced cell growth through decreasing cell cycle regulator S-phase-associated protein (Skp-2) levels (Denti et al., 2006) and insufficient down-regulation of p27 in cell cycle (Tomoda et al., 2004). Though an increased expression of CSN 5 may seem contradict to the reduced growth of cells on (+ve)pST compared to cells on flat substrate (Figure 49), CSN5 may play a role in cells survival response to the (+ve)pST.

On the other hand, signal transducer and activator of transcription 3 isoform 3 (STAT3) showed reduced expression on (-ve)pST than cells on (f)pST. STAT3 is a transcription factor and a regulator of cell growth and apoptosis that binds to small GTPase and Rac-1. A decreased expression of those signalling proteins may explain the reduced growth of endometrial cancer cells on the negative Bioimprint.

Further, TRIP6 that involves in cell migration is also involved in the cell NF-kappa-B and c-JUN pathways regulation. iTRAQ analysis suggests an involment of these two signalling pathways in Ishikawa cells response to the topography through TRIP6.

iTRAQ analysis may explain the reason for no significant difference being observed for MAPK/ERK and PI3K/AKT pathways between cells on different substrates (Sections 6.5.3.2 and 6.5.4). As shown by the proteins identified by iTRAQ analysis, the pathways that were most likely affected by the Bioimprint on Ishikawa endometrial cancer cells were the Nodal signalling, JAK/STAT3, NFκB and CSN 5. JAK/STAT3 and NFκB also have been linked to mechanical signalling previously (Kumar & Boriek, 2003; Leychenko et al., 2011; MacKenna et al., 1998; Pan et al., 1999).

An identification of alteration of these signalling molecules suggests that the physical topography may alter cell signalling molecules that regulate cell growth and cell survival.

7.5.4 Energy Modulation

Table 10 The up-regulated proteins under the functional group of cell energy modulation.

Proteins Identified from iTRAQ	**Functions**
Complement component 1 Q subcomponent-binding protein	-Involved in oxidative phosphorylation (OxPhos) pathway by binding to p32 which was part of OxPhos regulation (Muta et al., 1997). -Interacted with β1 integrin in endothelial cells and mediated cell adhesion and spreading (Feng et al., 2002).

Adenylate kinase 2	-Participates in cellular energy homeostasis by catalysing the reversible transfer of the phosphate group between ATP and adenosine monophosphate (AMP).
Uridine 5'-monophosphate synthase	-Catalyses the formation of uridine monophosphate which is the energy source for many biosynthetic pathways.
inorganic pyrophosphatase 2, mitochondrial isoform 1 precursor (PPi)	-Part of ATP biosynthesis: butyrate + ATP + CoA ⇌ butyryl-CoA +PPi +AMP -Involved in maintaining the balance of thermodynamic process of ATP biosynthesis and usage (Harold, 1962) by driving the above equilibrium equation from right to left. -Restored ATP biosynthesis (Mansurova et al., 1975).
1,4-alpha-glucan-branching enzyme	-Synthesizes glycogen, which is a form of energy storage in cells.

iTRAQ analysis suggests that the cells responded to (+ve)pST by adjusting the cell energy homeostasis because five proteins that were up- or down-regulated were related to cell energy generation. Three proteins in this functional category were up-regulated in cells on (+ve)pST compared to the cells on (f)pST, and two of them showed higher expression compared to cells on (-ve)pST. On the other hand, there were two proteins down-regulated on (+ve) compared to cells on (f)pST, the down-regulation of these proteins were associated with generation of more energy. This suggests that cells on the (+ve)pST may require more energy for cell growth and function.

Complement component 1 Q subcomponent-binding protein, a protein that is involved in oxidative phosphorylation (OxPhos) pathway (Muta et al., 1997) has been shown to interact with β1 integrin in endothelial cells and mediated cell adhesion and spreading (Feng et al., 2002). An elevated β1 integrin expression in cells on (+ve)pST was observed previously (Figure 29), so it is reasonable to propose that complement component 1 Q subcomponent-binding protein may be altered by surface topography in association with β1 integrin to increase cell energy production.

There were two down-regulated proteins in cells on (+ve)pST and (-ve)pST compared to (f)pST: 1,4-alpha-glucan-branching enzyme and inorganic pyrophosphatase 2 (PPi). 1,4-alpha-glucan-branching enzyme involves in the process of synthesizing glycogen, which is a form of energy storage in cells. The detection of a down-regulation of 1,4-alpha-glucan-branching enzyme proposes that the cells reduce the energy storage to produce more energy for spreading and adhesion on Bioimprints. Further, an identification of PPi, which is a molecule part of ATP biosynthesis and is involved in maintaining the balance of thermodynamic process of ATP biosynthesis and usage (Harold, 1962), suggests that the cells on (+ve)pST may have consumed PPi for ATP generation.

The alteration of these proteins in cells on (+ve) compared to (f)pST suggests the requirement of more energy to grow on (+ve)pST. This may explain our previous observation of no preferential adhesion on (+ve)pST (Figure 24). We propose that cells have preference to adhere and grow on surfaces that require less energy. Essentially cellular energy conversion is apparently one of the cellular responses to the positive topography, where Ishikawa cells may require more kinetic energy from ATP phosphate bond chemical energy to spread on (+ve)pST. Moreover, even when the cells are in a static state, cell actin filaments that are associated with myosin motors will still actively convert chemical energy (ATP) to mechanical energy to pre-stress the actin filaments and generate tensional force to support cells (Lodish et al., 2000). Hence, an increase in cellular energy requirement suggests that Ishikawa cells may be generating more tensional force to support them to adhere on the Bioimprints.

The modification of energy-related peptides is not predicted, but the hypothesis that topography and the associated physical signals are important components of cell regulation readily links to schemes that incorporate differential energy usage.

7.5.5 Cell growth and viability

Table 11 The proteins under the functional group of cell growth and viability.

Apoptosis regulator BAX isoform sigma	- Accelerates programmed cell death
Puromycin-sensitive aminopeptidase	- Regulates proteolytic events that are part of cell growth and viability processes
Macrophage migration inhibitory factor (MIF)	- Pro-inflammatory cytokine, regulates the innate immune response to bacterial pathogens

Apoptosis regulator BAX isoform sigma, was identified to be down-regulated on (+ve)pST compared to cells on (f)pST. The apoptosis regulator BAX isoform sigma is a protein that accelerates apoptosis process, the mechanism of how the positive topography reduces apoptosis is unclear, it may be that the endometrial cancer cells defended against the growth reduction effect of the positive topography through reducing the cell apoptosis.

Two of the proteins that are part of the cell innate immune response regulation also play a role in regulating cell growth. Puromycin-sensitive aminopeptidase was upregulated on (+ve)pST compared to the cells on (-ve) and (f)pST, and MIF was downregulated in cells on the (-ve)pST compared to cells on (f)pST. MIF has been reported to have increased expression in cancer cells and it has been related to tumour growth (Nishihira, 2000). Further, MIF has been shown to increase the expression of αvβ3 integrin in Ishikawa endometrial cancer line (Bondza, 2008) and also in chondrosarcoma cells through the PI3K and NF-κB pathways (Lee et al., 2012). A decreased MIF expression on (-ve)pST may be responsible for the reduced growth (Figure 49) on this substrate.

The observation of different expression of proteins associated with cell apoptosis and growth regulation is consistent with the hypothesis that the physical microenvironment may modulate cells growth and survival.

7.5.6 Proteins involved in intermediary functions

Table 12 The proteins with intermediary functions.

Golgi apparatus functions	
ADP-ribosylation factor-like protein 1	- Maintains the function of of the Golgi apparatus.
Calcium-mediated intracellular processes	
Copine-1 isoform c	- Regulates calcium-mediated intracellular precesses such as neuronal progenitor cell differentiation; induces neurite outgrowth, membrane trafficking, TNF-alpha-induced NF-kappa-B transcriptional repression
Lipid transport and metabolism	
Oxysterol-binding protein 1	- Involved in the transportation of lipid between the Golgi complex and membranes of the endoplasmic reticulum, regulates sterol degradation, regulates cholesterol efflux
Enoyl-CoA delta isomerase 1, mitochondrial isoform 2 precursor	- Involved in fatty acid beta-oxidation pathway, which is part of lipid metabolism
Protein synthesis, processing, degradation and transportation	
Selenide, water dikinase 1 isoform 2	- Synthesizes selenophosphate
Endoplasmic reticulum resident protein 29 isoform 1 precursor	- Involved in the protein folding within the endoplasmic reticulum (ER)
E3 ubiquitin-protein ligase CHIP	- Involved in proteasomal degradation of misfolded chaperone substrates and regulate certain proteins' polyubiquitination.
Phosphoacetylglucosamine mutase isoform 2	- Catalyzes the conversion of GlcNAc-6-P into GlcNAc-1-P.
26S protease regulatory subunit 4	- ATP-dependent degradation of ubiquitinated proteins.
Long-chain fatty acid transport protein 4	- Regulates long-chain fatty acids translocation across the plasma membrane, formation of the epidermal barrier, inhibits light-induced degeneration of rods and cones
Eukaryotic translation initiation factor 3 subunit M	- Initiation of protein synthesis
Ribosomal protein, RNA processing	
60S ribosomal protein L35	- A ribosomal protein.

U2 small nuclear ribonucleoprotein A'	- Associated with sn-RNP U2. It helps the A' protein to bind stem loop IV of U2 snRNA.
Pre-mRNA 3'-end-processing factor FIP1 isoform 3	- Involved in pre-mRNA processing.
Bone mineral phase	
Alpha-2-HS-glycoprotein preproprotein	- Regulates the bone's mineral phase. Shows affinity for calcium and barium ions.
Innate immune response	
Macrophage migration inhibitory factor (MIF)	- Pro-inflammatory cytokine, regulates the innate immune response to bacterial pathogens
Puromycin-sensitive aminopeptidase	- Involves in antigen-processing pathway for MHC class I molecules
Intracellular vesicles and organelles movement	
Cytoplasmic dynein 1 light intermediate chain 2	- Regulates movement of vesicles and organelles along microtubules, binding of dynein to membranous organelles or chromosomes.

In addition to cell energy homeostasis, a change in the cell physical microenvironment also potentially altered other cell functions. These processes were protein synthesis, processing and transportation and RNA processing. An alteration in these processes proposes a change in the cell functions including cell growth, cell spreading and cell metabolism in response to the physical microenvironment.

The initiation of cell defence activities can also be seen from a change in the proteins that have the function in regulation of innate immune response. This response may function to enhance cell survival though further studies are required to examine the exact roles of these proteins.

Though iTRAQ analysis is not a confirmative experiment that definitely identifies the responsive proteins in Ishikawa cells to surface topography, it is a method that is designed to enable us to search for potential responsive proteins. We reported that cells on (+ve)pST showed more alterations in protein expression than the cells on (-ve)pST as compared to cells on (f)pST). Further, the proteins identified were all in functional categories that fitted our hypothesis that Ishikawa cells responded to surface topography by altering cell structure,

signalling and ECM proteins secretion. This again suggests that Ishikawa cells are responsive to surface topography. On the other hand, iTRAQ analysis generates two other hypotheses in which Ishikawa cells may also have modified their nuclear structure in response to surface topography, moreover, Ishikawa cells' energy modulation may also be affected by the surface topography.

There is a limitation of this iTRAQ analysis because there were only two pooled samples used for the analysis. However, there were filters in place so moderately reliable data are presented in this thesis. Further, the iTRAQ results are being followed up in our lab by doing western blot analysis on a few targeted proteins.

iTRAQ analysis screened the cell's whole set of proteins. Certain criteria were applied to select the proteins that were likely being regulated by the cell's physical microenvironment. And the proteins that were neither up or down were the proteins that may not be involving in the mechanical responses. However, further detailed analysis on potentially changed protein are certainly required to confirm this due to the limitation of the number of repetition used in this project.

7.6 Conclusion

Though iTRAQ analysis is not an experiment that definitely identified the responsive proteins in Ishikawa cells to surface topography, it is a method that is designed to enable us to search for potential responsive proteins, i.e., iTRAQ is rather a hypothesis generating experiment. The fact that the identified proteins were all in functional categories that fitted our hypothesis that Ishikawa cells responded to surface topography by altering cell signalling molecules, structure and ECM proteins secretion again suggests that Ishikawa cells are responsive to surface topography. On the other hand, iTRAQ analysis generates two other hypotheses in which Ishikawa cells may also have modified their nuclear structure in response to surface topography, and also, Ishikawa cells' energy modulation may also be affected by surface topography.

Cells on (+ve)pST showed more alteration in protein expression than cells on (-ve)pST (as compared to cells on (f)pST), and this together with the observation that cells may possibly require more energy to spread over the hump-like topography, may explain the reason of no preferential adhesion on (+ve)pST (Figure 24). We propose that cells have preference to adhere and grow on surfaces that require less energy. Further, lower growth on (+ve)pST and an upregulation of CSN5 suggest that cells respond to the reduced growth by activating a DNA repairing system, a mechanism that has been correlated to drug resistance development. This suggests that (+ve)pST may be an *in vitro* model that has the ability to trigger cell responses that have been masked by the unnatural spreading on flat culture surface. Though fewer regulated proteins have been identified in cells on (-ve)pST, the proteins identified nonetheless suggested different transcription activities, ribosome homeostasis, lipid metabolism and most importantly, different ECM protein (hyaluronan) synthesis when compared to cells on (f)pST.

Taken altogether, surface topography affects endometrial cancer cells protein synthesis, and the presentation of topography (positive versus negative topographies) determines the degree of influence on cells. The proteins that were suggested to have changed in response to physical topography are functioning in alteration of nucleus structure, cell adhesion, ECM protein synthesis, cell cytoskeleton-related behaviours, growth behaviours and cell energy generation. Moreover, a greater response in cells on (+ve)pST compared to cells on (-ve)pST agreed with results from other experiments. Cells on (+ve)pST changed their protein expression from those of cells on flat surfaces to a larger extent than cells on (-ve)pST. These results from iTRAQ studies provide preliminary evidence that cell biochemistry is responsive to the physical environment. The influence of cell-like topography on Ishikawa cell nucleus structure, the type and the amount of cell ECM protein secretion, cell energy pathways and modulation of STAT3 and CSN5 signalling pathways are worthy of further study.

This chapter presents the results from iTRAQ analysis in which the data obtained agreed with our previous observations that Ishikawa endometrial cancer cells responded to physical microenvironment. In the next chapter the experiments that investigated Ishikawa cells VEGF secretion and the cell response to chemotheraphy drugs are presented: cisplatin and paclitaxel, on culture substrates of different topographies.

Chapter 8 Influences of Substrate Material and Topography on Endometrial Cancer Cell VEGF Secretion and Responses to Cancer Therapeutic Drugs

8.1 Introduction

Following the previous chapters that discussed the influence of the cell's physical microenvironment on Ishikawa cells behaviours, here in this chapter the VEGF secretion of these cells (which is the key mediator in cancer angiogenesis) and cellular response to chemotheraphy drugs are investigated.

In this introduction, first the linkage between VEGF and cancer is discussed, especially the mechanical signals modulation of VEGF secretion, followed by discussion of a potential anti-cancer agent, EGCG, and a hypoxia mimicking agent, $CoCl_2$, in cancer VEGF secretion studies. Then a discussion on the two clinical chemotherapy drugs, cisplatin and paclitaxel follows. Finally, studies that demonstrated differential cell responses to chemical treatments due to mechanical influences are noted, leading us to study the effects of culture substrate materials and cell-like topography on Ishikawa endometrial cancer cell responses to cisplatin and paclitaxel.

Cancer has been associated with the overexpression of VEGF because an abnormally growing tumour requires adequate blood and oxygen supplies to form new blood vessels. VEGF modulation may occur partly through mechanical factors. VEGF secretion has been reported to be regulated by cellular tension (Faure et al., 2008). Also, it has been shown that chondrocytes responded to mechanical signals and increased VEGF secretion (Perera et al., 2010). In cancer cells, VEGF secretion was stimulated by fluid shear stress which then

promoted chondrosarcoma invasion (Wang et al., 2014). Furthermore, cancer cells growing in a 3D culture model had different VEGF secretion pattern than cells growing on 2D monolayer (Chitcholtan et al., 2012).

There are a number of natural compounds that have been reported to have an impact on regulating cell VEGF secretion. One of these natural compounds is (−)-epigallocatechin-3-gallate (EGCG), an extract from green tea. Green tea, which is derived from the plant *Camellia sinensis*, contains polyphenolic compounds such as (−)-epigallocatechin (EGC), (−)-epicatechin-3-gallate (ECG), and (−)-epicatechin (EC) in addition to EGCG. EGCG is the most potent antioxidant and anti-cancerous polyphenol due to the presence of the gallic acid group. EGCG has been shown to reduce angiogenesis (Gu et al., 2013; Rodriguez et al., 2006). This is partly through EGCG inhibition of VEGF secretion that has been observed *in vitro* (Luo et al., 2014; Sartippour et al., 2002; Zhu et al., 2011) and through down-regulating hypoxia induced factor (HIF-1α) that has been reported *in vivo* (Gu et al., 2013).

Alternatively, $CoCl_2$ works conversely to EGCG which induced HIF-1α and increased cell expression of cyclooxygenase-2 (Cox-2) which then increased VEGF secretion (Liu et al., 1999).

Here, the VEGF secretion of endometrial cancer cells on different substrates was measured, and then the cells were treated with $CoCl_2$ and EGCG and their stimulation and suppression effects on cell VEGF secretion were studied, respectively, as a positive and negative control on cell VEGF secretion.

In addition to $CoCl_2$ and EGCG, Ishikawa cells were also treated with cisplatin and paclitaxel. Cisplatin and paclitaxel are both clinical chemotherapy drugs. Cisplatin is an alkylating agent that attacks DNA by attaching an alkyl group to the guanine base of DNA. This crosslinks the DNA double strand and causes a halt in cell division and eventually cells undergo apoptosis. The cisplatin mechanism of action is not cell cycle specific, and therefore

differs from paclitaxel. Paclitaxel is a cytotoxic plant alkaloid with a cell-cycle specific mechanism of action. Paclitaxel has been shown to promote cells to enter the mitotic phase and then cells at the mitosis checkpoint by binding to microtubules to prevent them from separation during mitosis, which eventually induced cell apoptosis (Yang et al., 2009).

It has been shown that cell responses to drugs are partly modulated by mechanical signals. This has been demonstrated where cells in 3D culture responded to drugs differently than cells in a 2D culture model. For example, human epithelial carcinoma cells showed higher sensitivity to tirapazamine (TPZ) when cultured as a 3D model compared to the 2D culture (Tung et al., 2011). Moreover, JIMT1 breast cancer cells growing as a 2D monolayer, clustered on poly-2-hydroxyethyl methacrylate (polyHEMA) and 3D structure in Matrigel each showed a different response to the drugs. The cells in Matrigel showed higher responsiveness to drugs which were similar to drug responsiveness in a xenograft model (Hongisto et al., 2013). However, the increased sensitivity to drugs in 3D culture is not always the case, for example, in the same study done by Tung as stated above, the human epithelial carcinoma cells were less sensitive to the anticancer drug 5-fluorouracil (5-FU) (Tung et al., 2011). A study performed in our lab also showed less sensitivity to doxorubicin in 3D culture model than in a 2D cell monolayer (Chitcholtan et al., 2012). These observed differences may be due to the different cell lines and the different drugs used. Nonetheless, it is clear that cells grown as 3D culture, which closely represents the real cell living microenvironment, show different responses to drugs compared to cells that are grown on an unnatural 2D culture substrate.

Based on the reports that cancer cell VEGF secretion and cell responses to anticancer agents can be influenced by mechanical signals, we questioned if the culture substrate materials and cell-like topography would have any effect on cell VEGF secretion. Further, if Ishikawa cell responses to cisplatin and paclitaxel would be affected by culture substrate material and topography.

The effects of cisplatin and paclitaxel on cells cultured on (f), (-ve) and (+ve)pST studied were cell VEGF secretion, and cell growth by quantifying cell number and expression of the

cell proliferation marker, PCNA and also the cell cycle modulators, cyclins B and D2. For paclitaxel treatment, cyclin B and cyclin D2 were studied as reports had shown that increased cyclin B stability (Giovinazzi et al., 2012) and up-regulation of cyclin D2 (Liu et al., 2012) had been associated with increased cell resistance to paclitaxel. Also, cyclin B1 inhibition enhanced the effect of paclitaxel treatment (Androic et al., 2008; Yuan et al., 2005). Hence, a study on the expression level of cyclin B and D2 may indicate the efficacy of paclitaxel on cells growing on different substrates. The cisplatin working mechanism is not cell cycle specific; here the expression of cyclin B and D2 in Ishikawa cells with cisplatin treatment were determined as an additional indication of influence of cisplatin on cell growth.

8.2 Hypotheses

1. Ishikawa endometrial cancer cell VEGF secretion differs among cells cultured on glass, tissue culture grade pST and pMA substrates, and also differs between cells cultured on (f) and (-ve)pMA. Also, Ishikawa cells show a different extent of responses to $CoCl_2$ and EGCG treatments by increasing and reducing their VEGF secretion, respectively.
2. Ishikawa endometrial cancer cell VEGF secretion differs among cells cultured on (f)pST, (-ve)pST and (+ve)pST, and exhibit a different extent of responses to $CoCl_2$, EGCG, cisplatin and paclitaxel treatments in altering their VEGF secretion.
3. Ishikawa endometrial cancer cells grown on (f)pST, (-ve)pST or (+ve)pST will reduce their growth, cyclin B1, B2, D2 and PCNA expression in response to cisplatin and paclitaxel treatments. The extents of reductions are different among cells on different culture substrates.

8.3 Aims

VEGF secretion was studied in cells growing on glass, tissue culture grade pST, (f)pMA and (-ve)pMA as well as cells growing on (f), (-ve) and (+ve)pST. Further, EGCG and $CoCl_2$ influences on cell VEGF secretion were investigated.

Furthermore, the effects of cisplatin and paclitaxel on cells on (f), (-ve) and (+ve)pST with regard to cell VEGF secretion, cell growth and cell PCNA, cyclin B1,B2 and D2 were studied.

8.4 Experimental Approach

VEGF secretion level was measured using an R&D System ELISA Duo Set kit.

Cell proliferation markers and cell cycle regulators expression levels were measured by western blot methods.

8.5 Results

8.5.1 Cell VEGF Secretion

8.5.1.1 Cell VEGF Secretion on Glass, Tissue Culture Polystyrene and Polymethacrylate Flat and Bioimprint Culture Substrates

The control cells without any treatment showed that the VEGF secretion level was the highest in cells on (f)pMA compared to cells that were grown on glass and tissue culture grade pST, and the presence of (-ve)pMA Bioimprint significantly lowered the cell VEGF secretion. When $CoCl_2$ was added, VEGF levels were increased on all culture substrates, but the elevation was not significant on (f)pMA and (-ve)pMA compared to respective no treatment cells; whereas when EGCG was added, VEGF secretion was lowered on glass and tissue culture grade pST, and significantly on glass. EGCG did not reduce the VEGF secretion of cells cultured on pMA substrates (Figure 57).

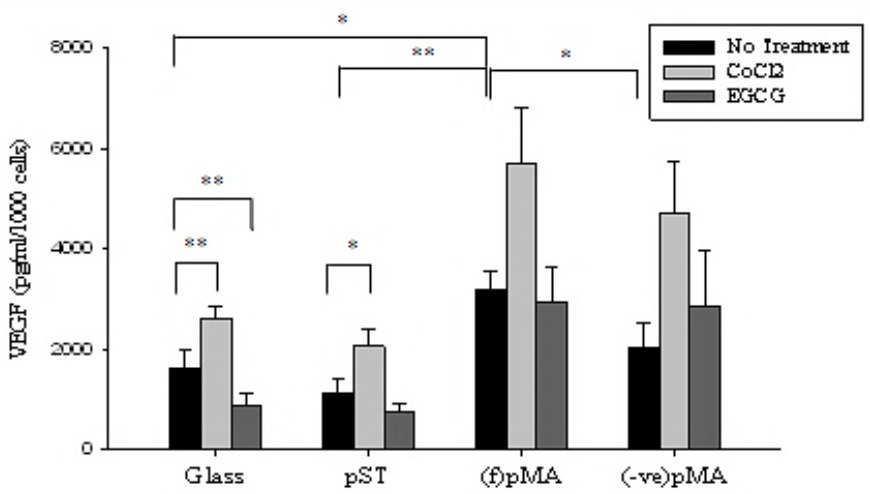


Figure 57 Ishikawa endometrial cancer cell VEGF secretion with or without $CoCl_2$ and EGCG Treatments on glass, tissue culture grade pST, (f)pMA and (-ve)pMA.

VEGF level measurement was normalised with cell number. Data are presented as VEGF (pg/ml)/cell of 4 independent experiments in triplicate. *, $p<0.05$; **, $p<0.01$.

8.5.1.2 Cell VEGF Secretion on Flat, Negative and Positive Bioimprint Polystyrene Slides

On the other hand, for cells on pST microscope slides, VEGF secretion was similar among non-treated (f), (-ve) and (+ve)pST cells (Figure 58 (A) and (B)).

The effects of cisplatin and paclitaxel on cell VEGF secretion were next investigated, along with the influence of $CoCl_2$ and EGCG on cell VEGF secretion. There was no significant decrease in VEGF secretion level with either cisplatin or paclitaxel treatments and there was no substrate topographic effect on cell VEGF secretion level with cisplatin and paclitaxel treatments (Figure 58 (A)).

When $CoCl_2$ was added, VEGF level showed a significant increase in cells grown on (f)pST compared to non-treated cells. Whereas with EGCG treatment, no significant reduction of VEGF secretion was observed on all substrates, though among EGCG treated cells on (f), (-ve) and (+ve)pST, the cells on (f)pST showed significantly lower VEGF secretion compared to cells on (+ve)pST (Figure 58 (B)).

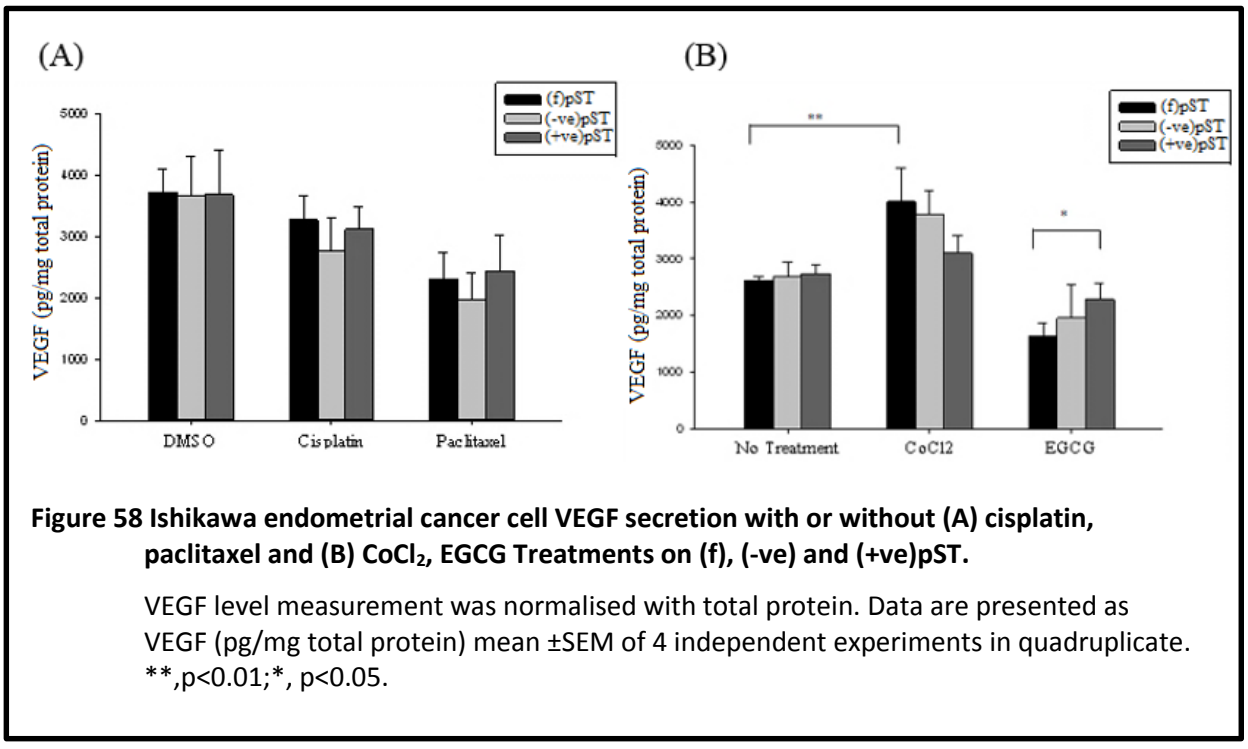


Figure 58 Ishikawa endometrial cancer cell VEGF secretion with or without (A) cisplatin, paclitaxel and (B) $CoCl_2$, EGCG Treatments on (f), (-ve) and (+ve)pST.

VEGF level measurement was normalised with total protein. Data are presented as VEGF (pg/mg total protein) mean ±SEM of 4 independent experiments in quadruplicate. **,p<0.01;*, p<0.05.

8.5.2 Cisplatin and Paclitaxel Treatments for Cells on Flat, Negative and Positive Bioimprint Polystyrene Slides

8.5.2.1 Cell Proliferation

Ishikawa cell numbers on (f), (-ve) and (+ve)pST with the treatment of cisplatin and paclitaxel were quantified. Cisplatin and paclitaxel reduced cell growth on all substrates. The reductions of cell number were significant in cells on (f) and (+ve)pST as compared to the DMSO-treated cells (Figure 59).

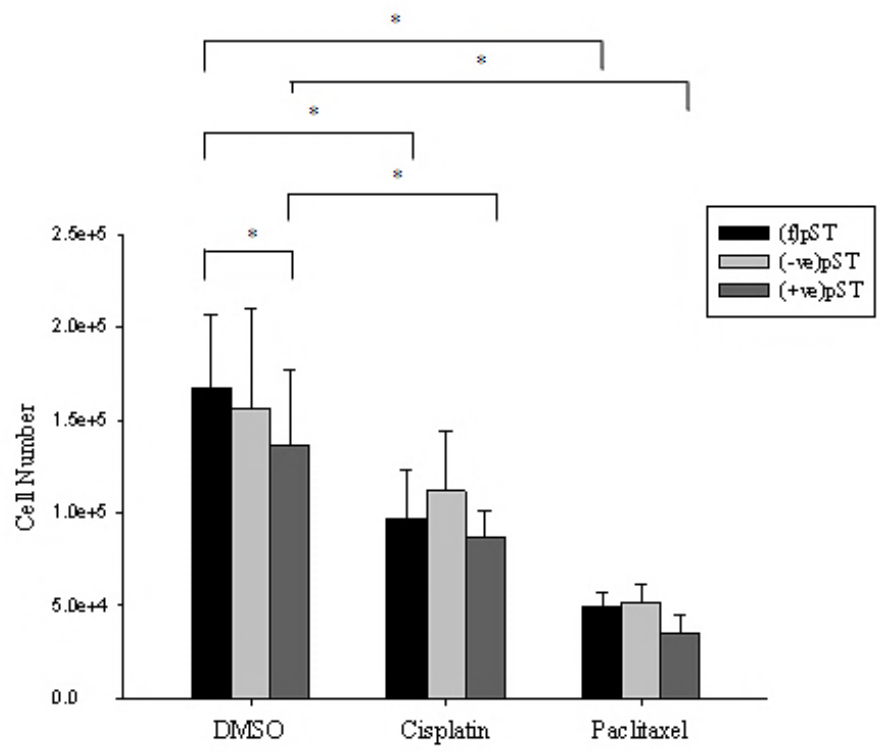


Figure 59 Ishikawa endometrial cancer cell number with or without cisplatin and paclitaxel treatments on (f), (-ve) and (+ve)pST.

Ishikawa cell numbers on (f)pST, (-ve)pST and (+ve)pST with DMSO (control), cisplatin or paclitaxel treatment. Data are presented as mean ± SEM of 4 independent experiments in quadruplicate. *, $p<0.05$.

8.5.2.2 Expression of Cell PCNA

Following cell number quantification, the expression level of the cell proliferation marker, PCNA, and also the cell cycle regulators: cyclin B1, B2 and D2 (section 8.5.2.3) were measured. Cisplatin and paclitaxel had no significant effect in reducing Ishikawa cell PCNA expression compared to control cells. Within the group of cells with paclitaxel treatment, there was a significant difference in PCNA expression level between cells on (f) and (+ve)pST (Figure 60).

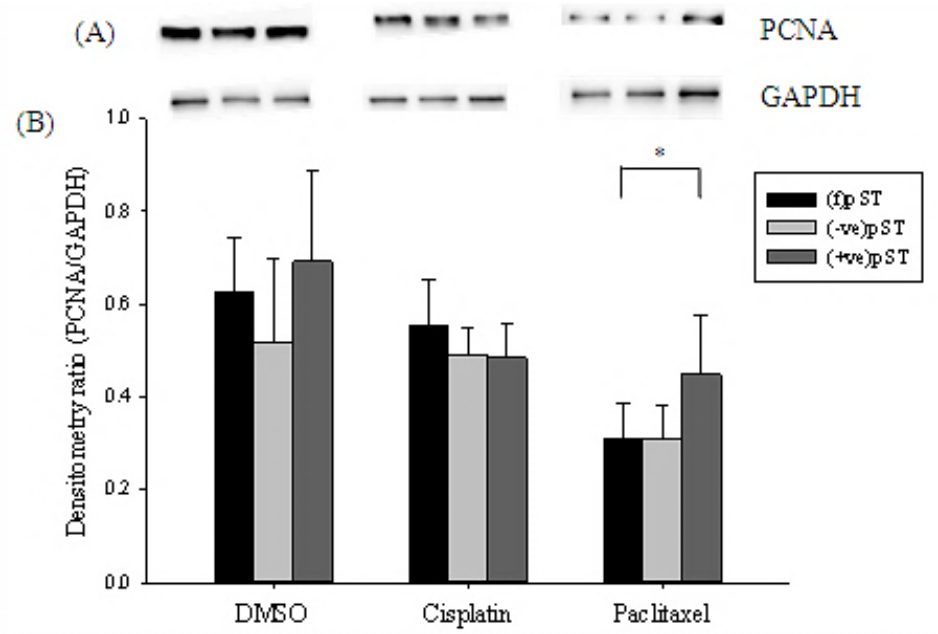


Figure 60 Ishikawa endometrial cancer cell PCNA expression with or without cisplatin and paclitaxel treatments on (f), (-ve) and (+ve)pST.

(A) Representative examples of PCNA (upper row) and GAPDH (bottom row) western blot protein bands of cells grown on (f)pST, (-ve)pST and (+ve)pST imprint with DMSO (control), cisplatin or paclitaxel treatment.

(B) Densitometry ratio of PCNA/GAPDH of cells cultured on (f)pST, (-ve)pST and (+ve)pST imprint with DMSO (control), cisplatin or paclitaxel treatment.

Data are presented as PCNA densitometry normalized with GAPDH densitometry mean ±SEM of 3 independent experiments in quadruplicate. *, $p<0.05$.

8.5.2.3 Expression of Cell Cyclin B1, B2 and D2

Cisplatin and paclitaxel treatments both reduced the expression of cyclin B1 and B2 in cells on all substrates although the reduction was not significant (Figure 61 A and B).

Furthermore, cisplatin and paclitaxel treatments both reduced the expression of cyclin D2 in cells on all substrates. Paclitaxel treatment reduced cyclin D2 significantly in cells on (f)pST and (+ve)pST compared to respective DMSO-treated cells but not on (-ve)pST. Moreover, there was significantly lower cyclin D2 expression in cells with paclitaxel treatment on (f)pST compared to cells with paclitaxel treatment on (+ve)pST. Cisplatin reduced cyclin D2 expression on all substrates, but the effect was not significant (Figure 61 C).

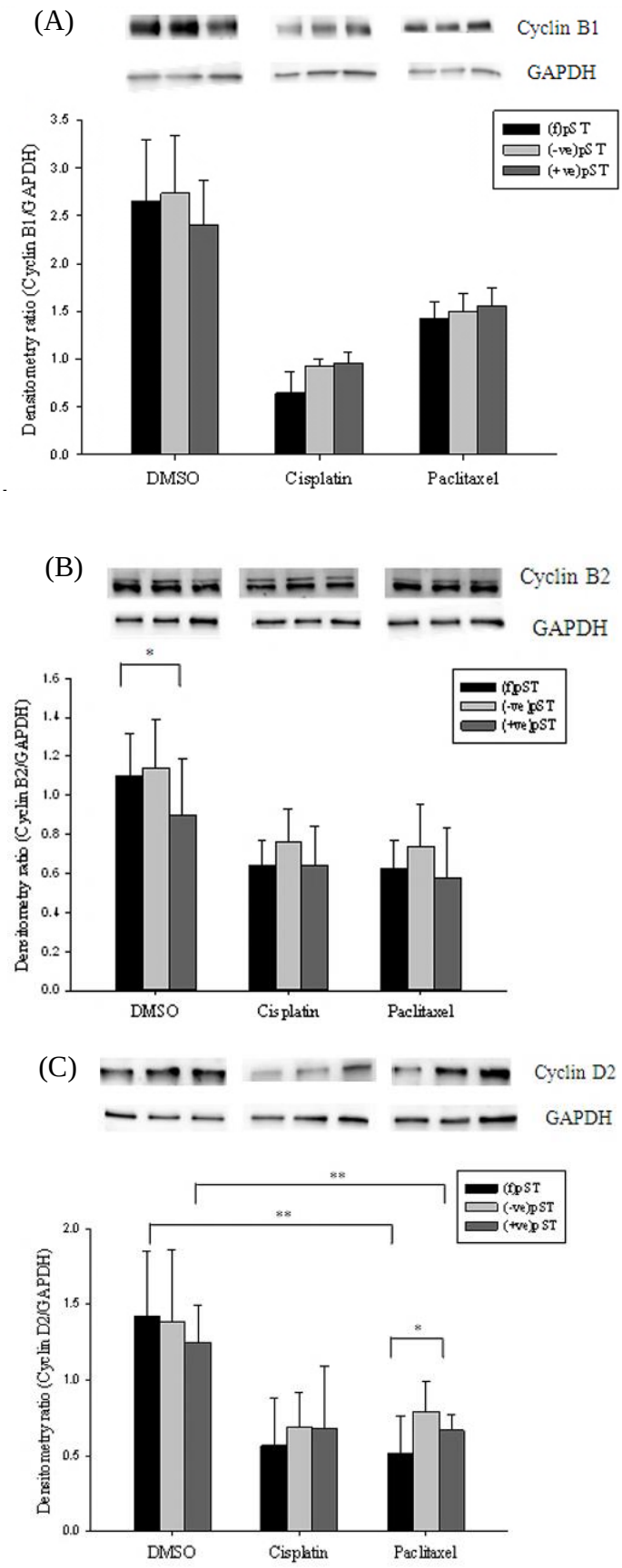


Figure 61 Ishikawa endometrial cancer cell (A) cyclin B1, (B) B2 and (C) D2 expression on (f), (-ve) and (+ve)pST with or without cisplatin and paclitaxel treatments.

[Top] (From left to right: (f)pST, (-ve)pST, (+ve)pST with DMSO (control), cisplatin or paclitaxel treatment) (upper rows) representative examples of (A) cyclin B1, (B)B2 and (C) D2 and (bottom rows) housekeeping protein GAPDH of western blot protein bands.

[Bottom] Densitometry ratio of cyclin (A) B1/GAPDH, (B) cyclin B2/GAPDH and (C) cyclin D2/GAPDH of cells cultured on (f)pST, (-ve)pST and (+ve)pST imprints with DMSO (control), cisplatin or paclitaxel treatment.

Data are presented as densitometry normalized with GAPDH densitometry mean ±SEM of 4 independent experiments in quadruplicate. **, $p<0.01$; *, $p<0.05$.

8.6 Discussion

8.6.1 VEGF Secretion in Cells Growing on Glass, Tissue Culture Polystyrene and Polymethacrylate Flat and Bioimprint Culture Substrates

For the cells that were grown on glass, tissue culture grade pST and pMA substrates, the cell VEGF secretion was studied. The cells secreted less VEGF on glass and tissue culture grade pST compared to cells on pMA substrates. VEGF secretion may be one of the cell self-protection responses to the less-favourable substrate (pMA), as the VEGF secretion level was found to be tightly correlated with various cell stresses (Østergaard et al., 2009; Storkebaum & Carmeliet, 2004). The stress from pMA culture substrate discussed here could be due to the charge-neutral surface that does not encourage cell spreading or the non-optimum cell spreading contact angle of this material (as discussed in Chapter 4 section 4.6). The presence of the Bioimprint with cell-like features, however, may have reduced the stress on cells which then reduced VEGF secretion. This observation was consistent with our previous findings that more cells grew on (-ve)pMA than on (f)pMA (Figure 48).

$CoCl_2$ increased VEGF levels on all substrates. Yet EGCG was less effective on pMA substrates in suppressing VEGF levels compared to its effect on cells on glass and tissue culture grade pST. The cell stress resulting from pMA material may not be able to be counteracted by EGCG.

8.6.2 VEGF Secretion in Cells Growing on Flat, Negative and Positive Bioimprint Polystyrene Slides

On a favourable cell culture material (pST), an addition of cell-like topography did not have any effect on cell VEGF secretion. Further, Ishikawa cells with cisplatin and paclitaxel treatments did not have a significant reduction in their VEGF secretion on all substrates. However, there was a trend that both $CoCl_2$ and EGCG were most effective on cells cultured on (f)pST.

For cells that were cultured on (f), (-ve) and (+ve)pST , $CoCl_2$ increased VEGF secretion significantly in cells on (f)pST but not significantly in cells on pST Bioimprints. This may indicate greater responses in cells grown on (f)pST to $CoCl_2$ than cells on (-ve) and (+ve)pST.

Alternatively, EGCG did not have a significant effect in reducing cell VEGF secretion, but among the cells with EGCG treatment on (f), (-ve) and (+ve)pST, the cells on (f)pST showed a significantly lower VEGF level than cells on (+ve)pST, which may again indicate a greater response in cells grown on (f)pST to EGCG than cells on (+ve)pST.

There are several possible explanations for the observed differential effects of $CoCl_2$ and EGCG on cells grown on different substrates. These reasons are related to the mechanism of actions of $CoCl_2$ and EGCG.

The anti-cancerous activity of EGCG has been reported to be through various mechanisms. One of these mechanisms was by interacting with vimentin (Ermakova et al., 2005). Vimentin is an intermediate filament that has been reported to function to maintain cell shape, cell motility and in regulating FAs (Mendez et al., 2010). Since differing cell spreading area (Figure 22) and different cell FAK expression and pFAK/FAK ratio (Figure 32 and 33) were observed between cells cultured on different topographical substrates, the

cell vimentin may be influenced by the cell-like topography. Hence, EGCG that works by interacting with vimentin will be influenced by the different vimentin behaviours among these cells.

Then again, a study showed that treatment with $CoCl_2$ had an indirect effect on the cell actin filaments by upregulating cofilin-1 (Østergaard et al., 2009). Cofilin-1 binds to actin and regulates assembly and disassembly of actin filament. In our study, we postulate the possibility that there is a difference in actin dynamicity (by alteration of F-actin and G-actin ratio), by our observation that there was a difference in NO secretion between cells on (f), (+ve)pST and (-ve)pST (Figure 45). Hence, $CoCl_2$ influences on cells on (f), (-ve) and (+ve)pST, through cofilin-1, may be different due to dissimilarity in their actin behaviours.

In short, the physical topography may have altered the cell responses to $CoCl_2$ and EGCG treatments through altering cell cytoskeleton molecules: vimentin and actin filaments.

8.6.3 Cisplatin and Paclitaxel Influence on Cell Growth on Flat, Negative and Positive Bioimprint Polystyrene Slides

Table 13 Summary of results of section 8.5.2.

A table summarizing the extent of cell responsiveness to cisplatin and paclitaxel treatments on (f), (-ve) and (+ve)pST as compared to control DMSO-treated cells. The direction of arrows indicates down-regulation of measured endpoints. The number of the arrows relates to the extent of responsiveness, as compared among (f), (-ve) and (+ve)pST. The "-" symbol indicates no statistically significant difference between the compared groups.

	(f)pST		**(-ve)pST**		**(+ve)pST**	
	Cisplatin	**Paclitaxel**	**Cisplatin**	**Paclitaxel**	**Cisplatin**	**Paclitaxel**
Cell Number	↓	↓	-	-	↓	↓
PCNA	-	↓	-	-	-	-
CyclinB1	-	-	-	-	-	-
CyclinB2	-	-	-	-	-	-
CyclinD2	-	↓↓	-	-	-	↓

When Ishikawa endometrial cancer cells were treated with cisplatin and paclitaxel, generally cells showed a greater response to paclitaxel compared to cisplatin. There was a trend that cells on (f)pST were slightly more responsive to paclitaxel compared to cells on (+ve) and (-ve)pST, as shown by the significant difference of measured parameters between DMSO-treated control cells and paclitaxel-treated cells on (f)pST, and between cells on (f) and (+ve)pST within the paclitaxel treated group. Notably, on (-ve)pST, all the measured parameters showed a trend of reduction similar to cells on (+ve)pST, although there were not significant differences compared to the control cells.

Cells on (f) and (+ve)pST with cisplatin and paclitaxel treatments showed a significant reduction in cell number compared to control cells. Although cells on (-ve)pST showed no significant reduction in cell number with either cisplatin or paclitaxel treatments, there was a trend to reduce cell number. By comparing among cells growing on different surface topographies, results with regard to cell number support a topographical effect on cell

responses to cisplatin and paclitaxel although further studies are needed to confirm these statistics.

For cisplatin and paclitaxel treatments, although there was no significant reduction in PCNA expression level between treated cells to control cells, within the group of paclitaxel treated cells, cells on (f)pST showed significantly less PCNA expression compared to cells on (+ve)pST. This indicated a significantly greater response to paclitaxel in cells on (f)pST compared to cells on (+ve)pST.

Further, for cells with paclitaxel treatment, there was a non-significant reduction in cell cyclin D2 on (-ve)pST compared to control cells. Whereas there was a significant reduction of cyclin D2 in cells on (f) and (+ve)pST compared to control cells. The cells on (f)pST had significantly lower cyclin D2 expression level compared to the cells on (+ve)pST within the group of paclitaxel treatment, which again indicates less sensitivity of cells on pST Bioimprints to paclitaxel.

The observed different drug efficacies on cells on different culture substrates may be linked to the cell responses to physical topography, which in turn affected the drug mechanism of actions.

The paclitaxel mechanism of action is the cell cycle and is M phase specific; paclitaxel binds to cell microtubules and prevents them from separation during cell division. Cells on (+ve) and (-ve)pST had lower growth activity (Figure 49). Paclitaxel, which works on fast-dividing cancer cells, may have less dividing cells on (-ve) and (+ve)pST to target, resulting in the difference in paclitaxel efficacy observed between cells on (f), (-ve) and (+ve)pST.

Ishikawa cells were less responsive to cisplatin compared to paclitaxel. Further; no topographical effect on cell responses to cisplatin treatment was observed.

Ishikawa endometrial cancer cells cultured on (f), (-ve) and (+ve)pST showed responses to chemotherapy drugs, in which they showed a reduction in their expression of PCNA and some of the cyclins. Moreover, results showed that on different substrate topographies, there was a slight difference in the extent of the cell responses to paclitaxel.

8.7 Conclusion

The results in this chapter favour our hypothesis that culture substrate material and surface topography alter Ishikawa endometrial cancer cell responses to potential anti-cancer agents, both natural products and synthetic drugs. These results agreed with other findings that the physical environment can change the cell sensitivity to drug treatments. The use of the Bioimprint that can provide the cell with different physical microenvironment signals, compared to the flat culture substrate and is potentially a valuable and reliable culture substrate in drug studies.

All the observations presented in previous chapters were obtained from Ishikawa cells cultured in medium with FBS. The next chapter will present the results obtained from culture in medium without FBS.

Chapter 9 Influences of Substrate Topography on Ishikawa Endometrial Cancer Cell in Culture Medium without FBS Factors

9.1 Introduction

Ishikawa endometrial cancer cell responses to physical topography in culture medium with FBS were presented in chapters four to eight. Here in this chapter the observations obtained from cell culture in medium without FBS are presented. Thus the involvement of biological source of serum chemical factors in cell-surface interactions was investigated.

In vitro culture medium often requires a supplement of serum that can be from different animals and of adult, newborn or fetal origins. Some examples of serum are the adult horse, goat, swine and bovine or fetal bovine serum (FBS). The most commonly used serum is of fetal origin because this source provides a few advantages. First, fetal serum has a low concentration of antibodies due to the non-fully developed immune system. Second, to support growth, fetal serum is rich in growth factors, and this makes it ideal for maintaining cells in culture.

FBS consists of macromolecules, cell adhesion and spreading factors, low molecular weight nutrients, hormones and growth factors. FBS often enhances cell growth, survival, adhesion and spreading, minimizes protease activities, maintains culture pH and detoxifies the culture medium. However, there are some disadvantages of adding FBS into culture medium, mainly because of its poorly defined composition and batch-to-batch variation.

This project is a study of cell interaction with culture substrate topography, and we hypothesized that the cell adhesion factors in FBS may influence the cell responses to topography factors.

It has been shown that cell adhesion is affected by the FBS in the culture medium. For example, by quantifying the attachment of cells cultured in medium with or without FBS, it was reported that 74% ±3% of Chinese hamster ovary (CHO) cells attached on surfaces in serum-free medium whereas 98% ±2% of cells attached on surfaces in FBS-containing medium. Also, even 1% of serum concentration was shown to be enough for maximum cell adhesion strength (Yildirim & Whish, 1997). Moreover, it has been reported that osteoblasts formed FAs on substrate surfaces in medium with FBS, yet without FBS, the cell-substrate adhesion bonds involved no FAs formation (Verdanova et al., 2012).

A study showed that cell adhesion was partly controlled by competitive adsorption of fibronectin, vitronectin or collagen (either from cell secretion or contained in serum) with albumin and globulin that were present in serum (Dewez et al., 1997; Dewez et al., 1998). The adsorption of serum proteins on the substrate surface could delay or promote cell adhesion, depending on the cultured cell types and the proteins adsorbed. The rate and the type of proteins adsorbed on a solid surface are in turn controlled by the interphase free energy between the solid surface and the culture medium.

It has been observed that the FBS influence on cell adhesion depends on the solid surface wetting property. For example, BSA was found to be more easily adsorbed onto hydrophobic surfaces. Hence, FBS lowered cell adhesion on a hydrophobic surface which may be due to the adsorption of BSA, which inhibits cell attachment, from FBS onto the culture surface (Carré & Lacarrière, 2010). On the other hand, fibronectin, which is from serum or secreted by cells, has been reported to be deposited on a hydrophilic surface more easily than on a hydrophobic surface (Grinnell & Feld, 1981). Hence, FBS assists cell adhesion on hydrophilic surfaces. In short, cell adhesion is influenced by protein adsorption on culture surfaces, which in turn is determined by the protein content in culture solutions, and the type of culture substrate and its surface free energy.

In this chapter, the effect of pST topography on Ishikawa endometrial cancer cells in culture medium without FBS was studied, whereas the examination of topography influence on Ishikawa cells, in the presence of FBS was presented and discussed in Chapter 4-8.

9.2 Hypothesis

We hypothesize that Ishikawa endometrial cancer cells cultured on (f)pST, (-ve)pST and (+ve)pST in medium without FBS would exhibit different characteristics compared to cells cultured in medium with FBS.

9.3 Aims

The purpose of the experiments in this chapter was to study the responses of Ishikawa endometrial cell to surface topographies in the absence of FBS.

9.4 Experimental Approach

All these experiments were done at the same time as the respective experiments of cells cultured in medium with FBS described above.

9.5 Results

9.5.1 Ishikawa Endometrial Cancer Cell Morphology in Serum-Free Culture Medium

Inverted microscope images are shown for cells on (f)pST at 6 and 60 hours (Figure 62), and for cells on (-ve) and (+ve)pST the cell morphology was studied with immunofluorescent staining, which will be shown in section 9.5.2 .

Ishikawa endometrial cancer cells cultured in the serum-free medium had similar attachment rate compared to cells cultured in medium supplemented with FBS. At 6 hours, a few cells started to have flattened morphology (red arrow), indicating that the cells may have started to attach onto surfaces. At 60 hours, there was more cell debris observed compared to cells cultured in medium with FBS (cell culture in medium with FBS:Figure 15. Cell culture in medium without FBS:Figure 62, the yellow arrow indicates cell debris), indicating that cells may be under stress and a number of cells were unable to survive.

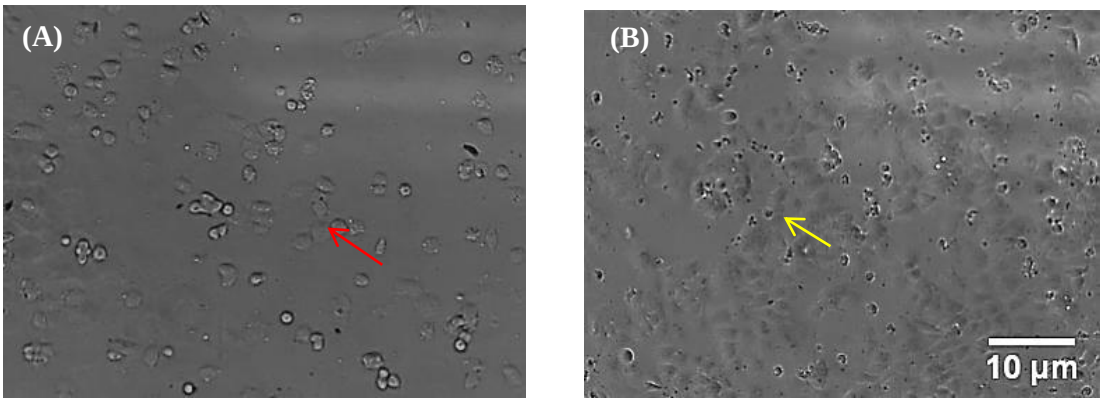


Figure 62 Representative images of Ishikawa endometrial cancer cell morphology in culture medium without FBS.

(A) Cells on (f)pST at 6 hours (B) Cells on (f)pST at 60 hours. Red arrow shows an example of flatten cell; the yellow arrow shows an example of cell debris.

9.5.2 Ishikawa Endometrial Cancer Cell Cytoskeleton in Serum-Free Culture Medium

Ishikawa endometrial cancer cells in culture medium without FBS showed smaller actin cytoskeleton and Cytokeratin-18 spreading (Figure 63) compared to cells cultured in medium with FBS (Figure 19). The cells in medium without FBS on (f)pST were more spread out compared to cells on (-ve) and (+ve)pST which were more clumped (yellow arrows) (Figure 63).

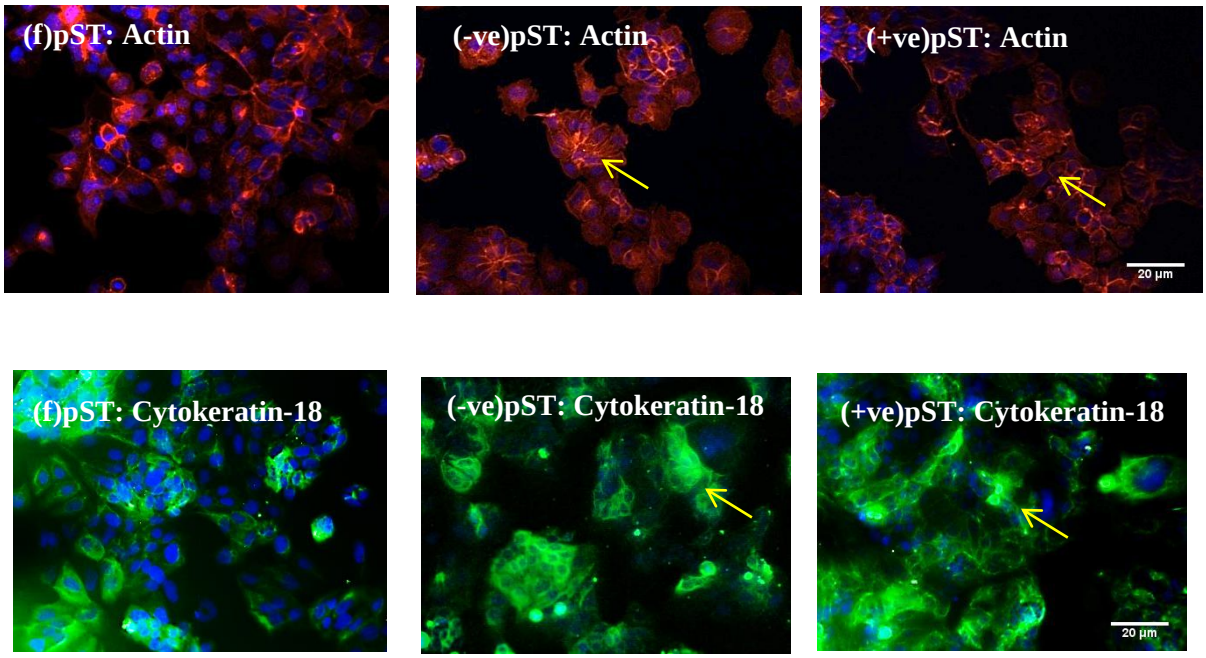


Figure 63 Representative images of Ishikawa endometrial cancer cell actin filaments and Cytokeratin-18 staining.

Ishikawa endometrial cancer cell actin filament was stained withTexas Red-X phalloidin (red, upper row), the cell Cytokeratin-18 was stained with Alexa Fluor 488-tagged Cytokeratin-18 antibody (green, bottom row), and the cell nucleus was stained with Hoestch 33342 (blue) on (f)pST (left), (-ve)pST and (+ve)pST (right). Yellow arrows indicate a few examples of clumped cells.

9.5.3 Ishikawa Endometrial Cancer Cell Spreading Area and Circularity on Flat, Negative and Positive Bioimprint Polystyrene Slides in Serum-Free Culture Medium

When Ishikawa endometrial cancer cells were cultured in medium without FBS, the cell spreading area on (f), (-ve) and (+ve)pST followed a similar trend to the cell spreading area in medium with FBS (Figure 22 and 23), in which cells were smallest on (+ve)pST and had more spherical morphology on (+ve)pST compared to (-ve)pST (Figure 64).

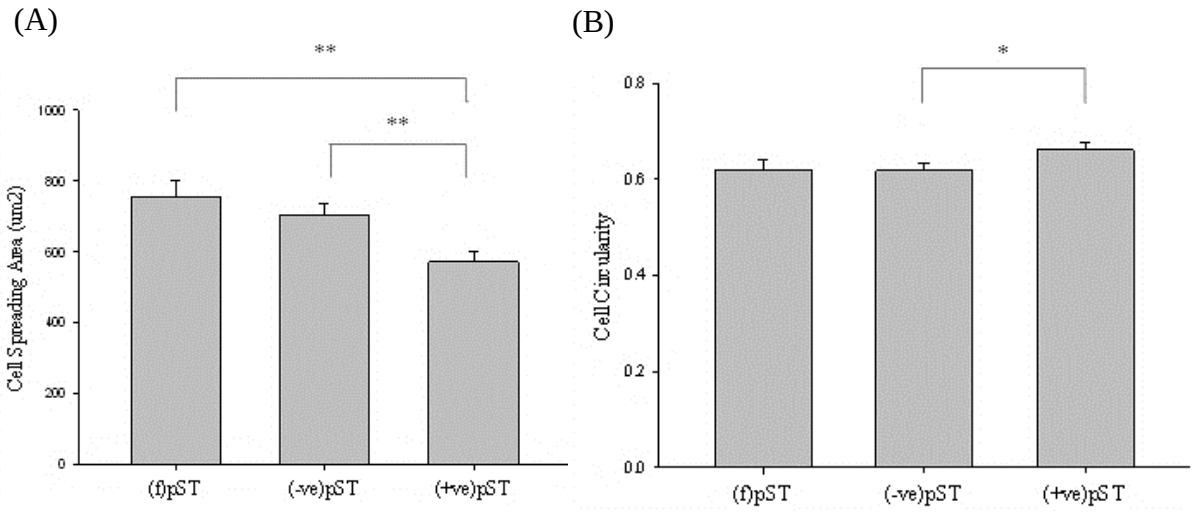


Figure 64 Ishikawa endometrial cancer cells (A) spreading area and (B) circularity on (f)pST, (-ve)pST and (+ve)pST in medium without FBS.

Ishikawa cells were cultured for 60 hours, followed by cell fixing and Cytokeratin-18 staining. The cell images were taken from four corners of a culture chamber. Then at least 25 cells were chosen for cell surface area measurement. Data are presented as (A) cell surface area and (B) cell circularity measured from at least 100 Ishikawa cells. **, $p<0.01$; *,$p<0.05$.

9.5.4 Ishikawa Endometrial Cancer Cell β1 Integrin Expression on Flat, Negative and Positive Bioimprint Polystyrene Slides in Serum-Free Culture Medium

Although Ishikawa endometrial cancer cells that were cultured in medium without FBS had similar cell spreading pattern on (f), (-ve) and (+ve)pST, as compared to cells cultured in medium with FBS, they were different in their β1 integrin expression and the subsequent FAK activation. When cells were cultured in medium without FBS, there was no significant difference in the β1 integrin expression between (f)pST and either (-ve) or (+ve)pST (Figure 65 compared to Figure 29). Moreover, the initial binding did not involve β1 integrin as RGDS did not have any effect on blocking the initial attachment of Ishikawa endometrial cancer cells (Figure 66 compared to Figure 42).

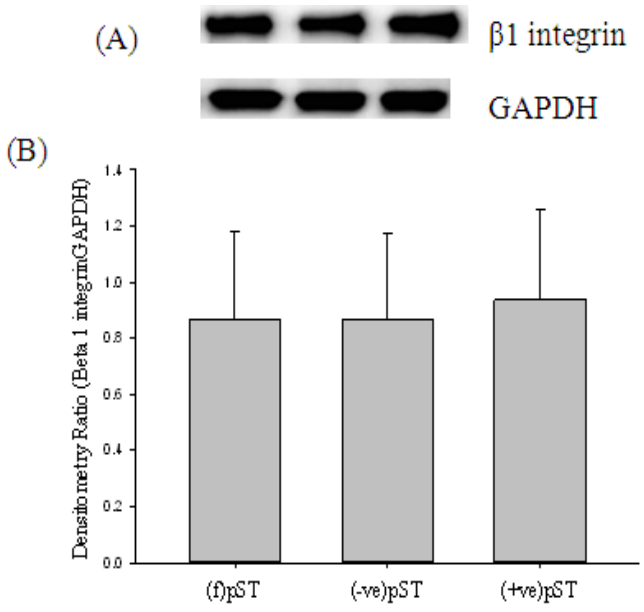


Figure 65 Ishikawa endometrial cancer cell β1 integrin expression on (f), (-ve) and (+ve)pST, in medium without FBS.

(A) (From left to right: (f)pST, (-ve)pST, (+ve)pST) representative examples of β1 integrin (Upper row) and GAPDH (bottom row) western blot protein bands.

(B) Densitometry ratio of β1 integrin/GAPDH of cells cultured on (f)pST, (-ve)pST and (+ve)pST imprint.

Data are presented as β1 integrin densitometry normalized with GAPDH densitometry mean ± SEM of 11 independent experiments in quadruplicate.

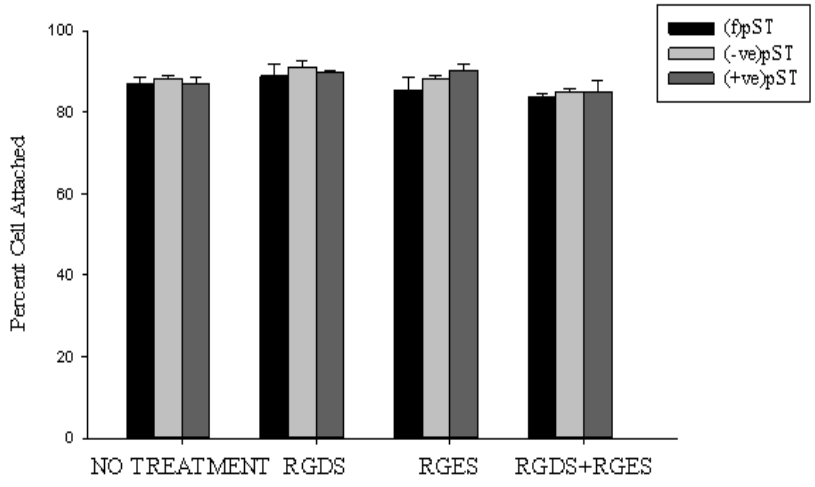


Figure 66 Effects of β1 blockage on cell initial adhesion in serum-free culture medium.

Data are presented as mean ± SEM of measurements of 3 independent experiments in quadruplicate.

9.5.5 Ishikawa Endometrial Cancer Cell FAK Expression and Activation (pFAK/FAK) on Flat, Negative and Positive Bioimprint Polystyrene Slides in Serum-Free Culture Medium

In addition to the different expression of β1 integrin, FAK activation (as indicated by the ratio of pFAK to total FAK levels) was also different in cells cultured in medium with FBS from those cultured in medium without FBS. Cells cultured in medium without FBS did not have higher FAK expression on the imprinted substrates (Figure 67) but have elevated FAK activation (as indicated by pFAK/FAK ratio) at 60 hours (Figure 68). Furthermore, FAK expression and activation at 3 hours were not significantly different among (f), (-ve) and (+ve)pST (Figure 69 and 70), though there was a trend of increased activation on (-ve) and (+ve)pST compared to (f)pST (Figure 70).

These were different from cells in medium with FBS, in which cells on imprinted surfaces had higher expression of β1 integrin and FAK (Figure 29 and 32) but had lower pFAK/FAK ratio compared to cells on (f)pST (Figure 33).

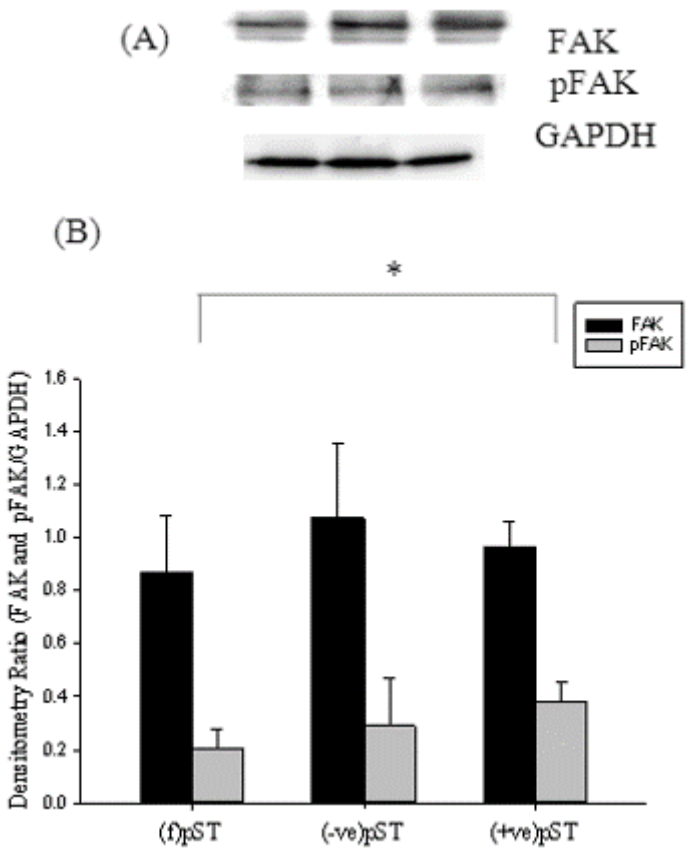


Figure 67 Ishikawa endometrial cancer cell (B) FAK and pFAK expression and (C) pFAK/FAK on (f)pST, (-ve)pST and (+ve)pST in serum-free culture medium.

(A) (From left to right: (f)pST, (-ve)pST, (+ve)pST) representative examples of FAK (upper row), pFAK (middle row) and GAPDH (bottom row) western blot protein bands.

(B) Densitometry ratio of FAK/GAPDH (black bar) and pFAK/GAPDH (grey bar).

Data are presented as FAK and pFAK densitometry normalized with GAPDH densitometry mean ± SEM of 4 independent experiments in quadruplicate. *, $p<0.05$.

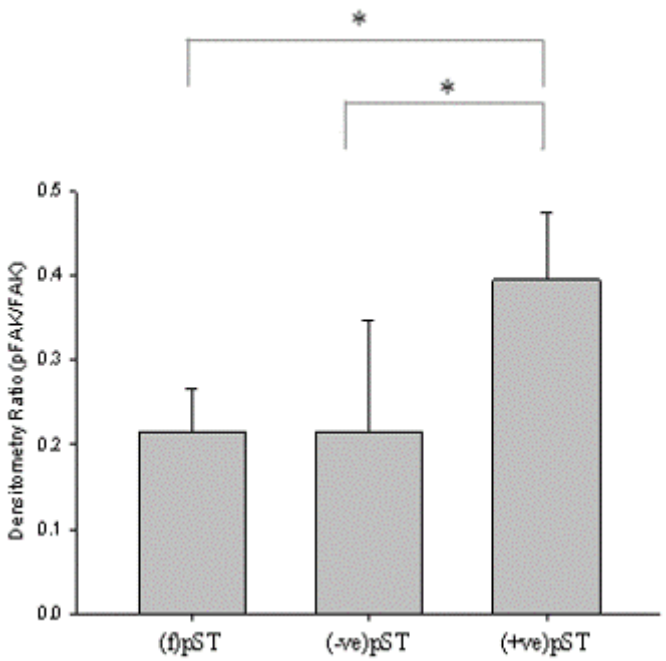


Figure 68 Ishikawa endometrial cancer cell pFAK/FAK on (f), (-ve) and (+ve)pST.

Data are presented as densitometry ratio mean of pFAK/FAK ± SEM of 4 independent experiments in quadruplicate. *, $p<0.05$.

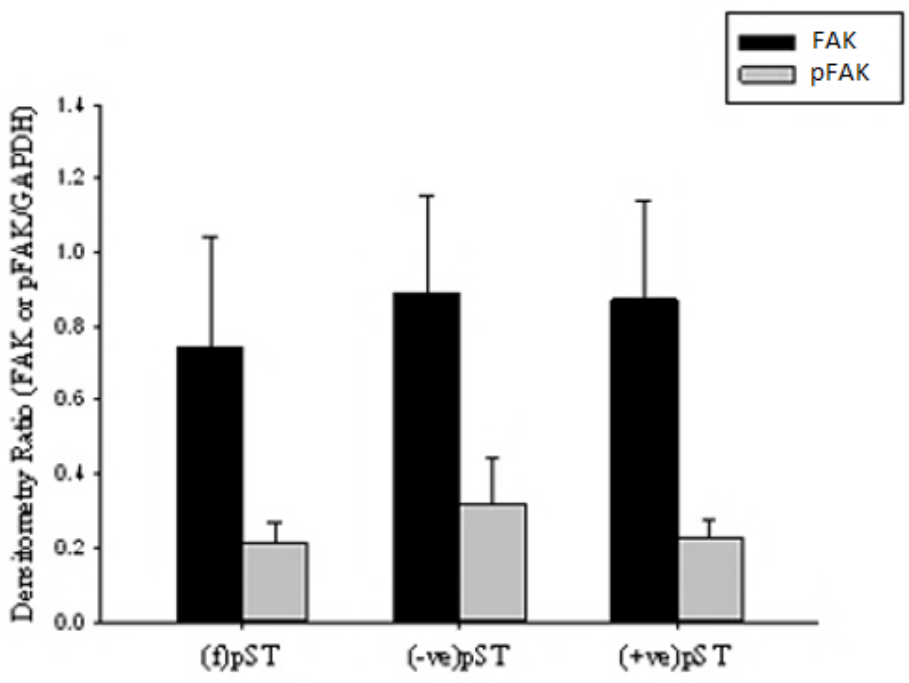


Figure 69 Ishikawa endometrial cancer cell FAK and pFAK expression and on (f)pST, (-ve)pST and (+ve)pST in serum-free culture medium at 3 hours.

Figure showing the densitometry ratio of FAK/GAPDH (black bar) and pFAK/GAPDH(grey bar). Data are presented as FAK and pFAK densitometry normalized with GAPDH densitometry mean ± SEM of 4 independent experiments in quadruplicate.

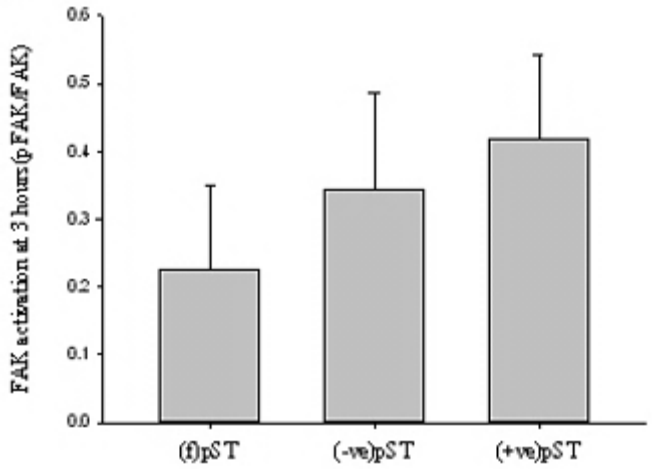


Figure 70 Ishikawa endometrial cancer cell pFAK/FAK on (f), (-ve) and (+ve)pST at 3 hours.

Data are presented as densitometry ratio mean of pFAK/FAK ± SEM of 4 independent experiments in quadruplicate.

9.5.6 Ishikawa Endometrial Cancer Cell Cytoskeleton Expression and Nitric Oxide Secretion on Flat, Negative and Positive Bioimprint Polystyrene Slides in Serum-Free Culture Medium

9.5.6.1 Ishikawa Endometrial Cancer Cell Actin and Cytokeratin-18 Expression on Flat, Negative and Positive Bioimprint Polystyrene Slides in Serum-Free Culture Medium

Ishikawa endometrial cancer cells cultured in medium without FBS had distinct cell cytoskeleton responses to surface topography compared to cells cultured in medium with FBS. Previously it was observed that cells cultured in medium with FBS had a higher Cytokeratin-18 expression on both (-ve) and (+ve)pST compared to a flat substrate (Figure 41). Cells in medium without FBS, on the other hand, had no significant difference in cell Cytokeratin-18 expression (Figure 72).

Similar to cells cultured in medium with FBS, there was no change in actin filaments expression (Figure 71 compared to Figure 39), though there was a trend of decreased actin expression on (+ve)pST compared to (f) and (-ve)pST (Figure 71). The smaller cell spreading area in medium without FBS was therefore apparently not related to the cell Cytokeratin-18 expression and may be linked to actin expression.

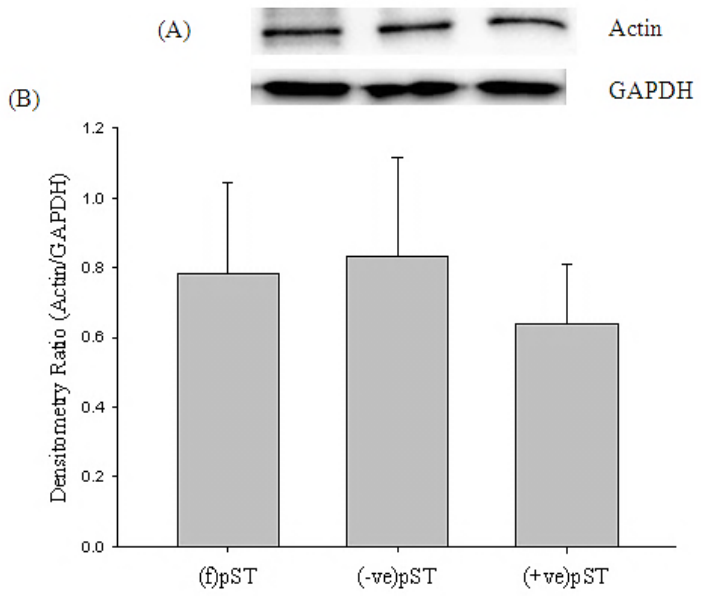


Figure 71 Ishikawa endometrial cancer cell actin expression on (f)pST, (-ve)pST and (+ve)pST in serum-free culture medium.

(A) (From left to right: (f)pST, (-ve)pST, (+ve)pST) representative examples of actin western blot protein bands.

(B) Densitometry ratio of actin/GAPDH of cells cultured on (f)pST, (-ve)pST and (+ve)pST imprint.

Data are presented as actin densitometry normalized with GAPDH densitometry mean ±SEM of 5 independent experiments in quadruplicate.

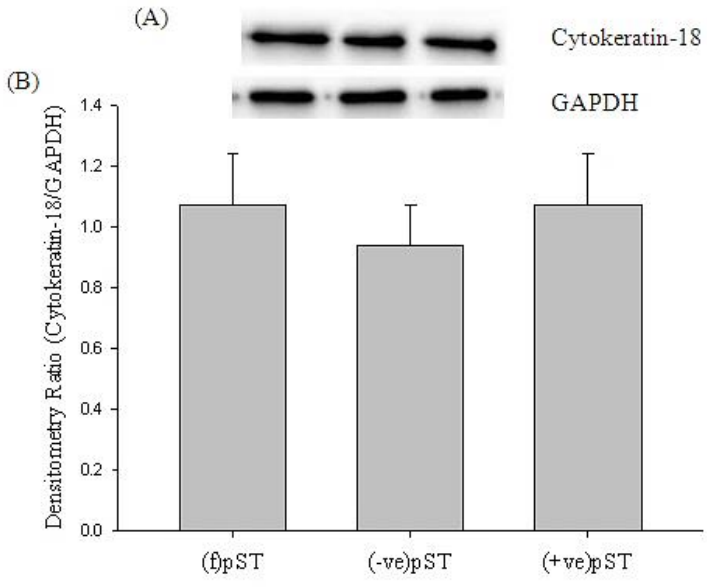


Figure 72 Ishikawa endometrial cancer cell Cytokeratin-18 expression on (f)pST, (-ve)pST and (+ve)pST in serum-free culture medium.

(A) (From left to right: (f)pST, (-ve)pST, (+ve)pST) representative examples of Cytokeratin-18 western blot protein bands.

(B) Densitometry ratio of Cytokeratin-18/GAPDH of cells cultured on (f)pST versus (-ve)pST, (+ve)pST imprint.

Data are presented as Cytokeratin-18 densitometry normalized with GAPDH densitometry mean ±SEM of 9 independent experiments in quadruplicate.

9.5.6.2 Ishikawa Endometrial Cancer Cell Cortical Actin Filaments on Flat, Negative and Positive Bioimprint Polystyrene Slides in Serum-Free Culture Medium with or without Aldosterone Treatment

By examining the cortical actin filaments structure with or without aldosterone treatment, some distortion of the cortical actin structures could be observed after 7 mins of aldosterone treatment (Figure 73, yellow arrows). However, less distortion of cortical actin filaments was observed in cells cultured in medium without FBS (Figure 73) compared to cells in medium with FBS (Figure 44).

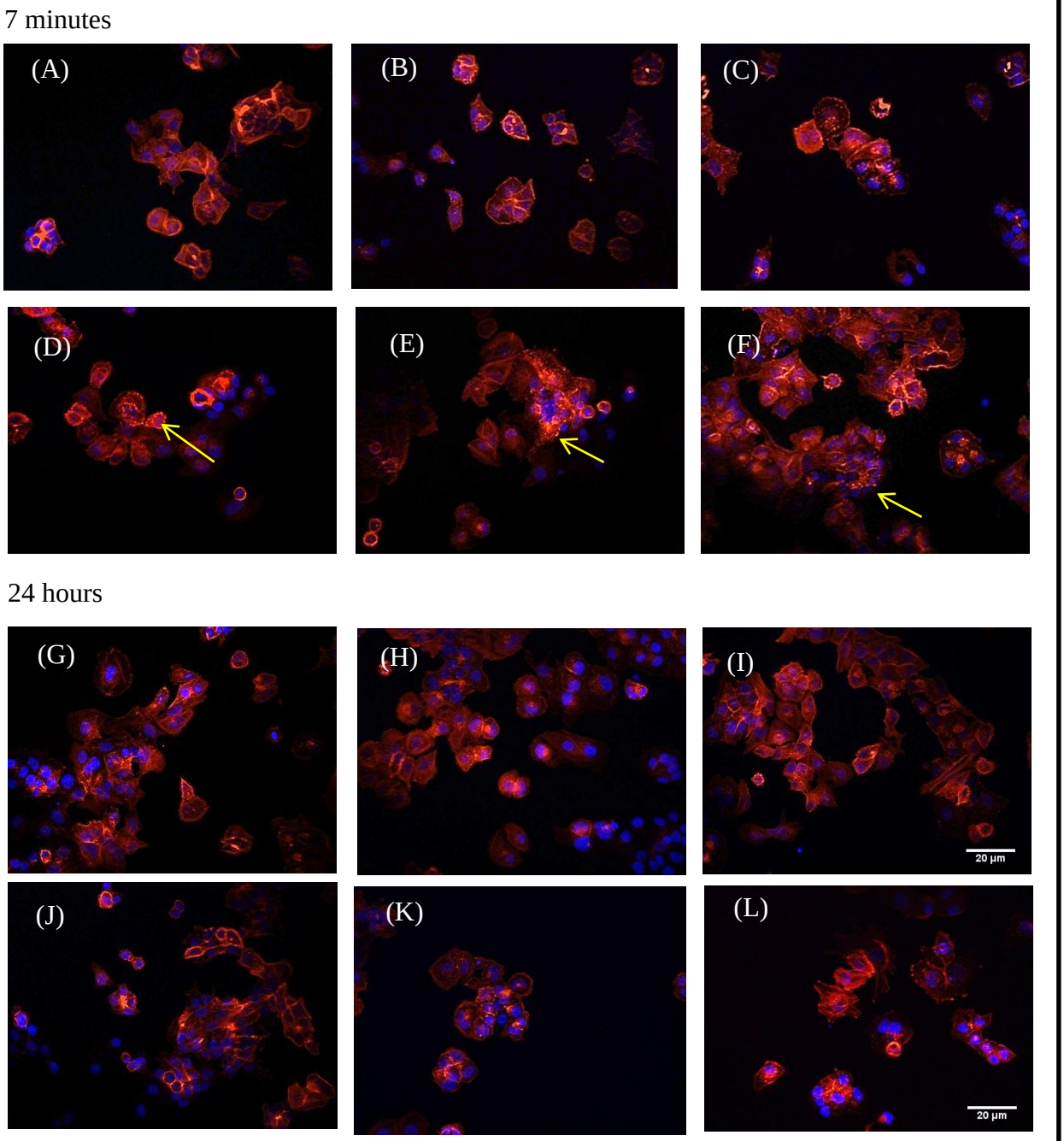


Figure 73 Representative images of Ishikawa endometrial cancer cell actin filaments staining.

Ishikawa cell action filament was stained with Texas Red-X phalloidin (red), and cell nucleus was stained with Hoechst 33342 (blue). Cells on (A),(G):(f) pST (B),(H):(-ve)pST and (C),(I): (+ve)pST were the control cells without aldosterone treatment. Cells on (D),(J):(f) pST (E),(K):(-ve)pST and (F),(L): (+ve)pST were the cells with 10 nM aldosterone treatment. The time indicates when the cells were fixed and stained. Examples of fragmented cortical actin filaments are indicated by yellow arrows.

9.5.6.3 *Ishikawa Endometrial Cancer Cell Nitric Oxide Secretion on Flat, Negative and Positive Bioimprint Polystyrene Slides in Serum-Free Culture Medium*

NO secretion, a cell activity that is partly regulated by actin, showed different responses to topography by cells in the presence of FBS compared to those cultured in medium without FBS. Cells in the serum-free medium had less NO secretion (Figure 74) compared to cells cultured in medium with FBS (Figure 45). Further, there was no difference in NO secretion among cells on (f), (-ve) and (+ve)pST in culture medium without FBS (Figure 74). This was different from cells in medium with FBS in which the cells without aldosterone treatment on (-ve)pST at 24 hours showed higher NO secretion than cells on (f) and (+ve)pST (Figure 45). This may be because of the less well-spread cell morphology with more densely-packed actin filaments (Figure 63 and 73) and the compaction of actin filaments in cells on all topographies may have caused the no difference in NO secretion.

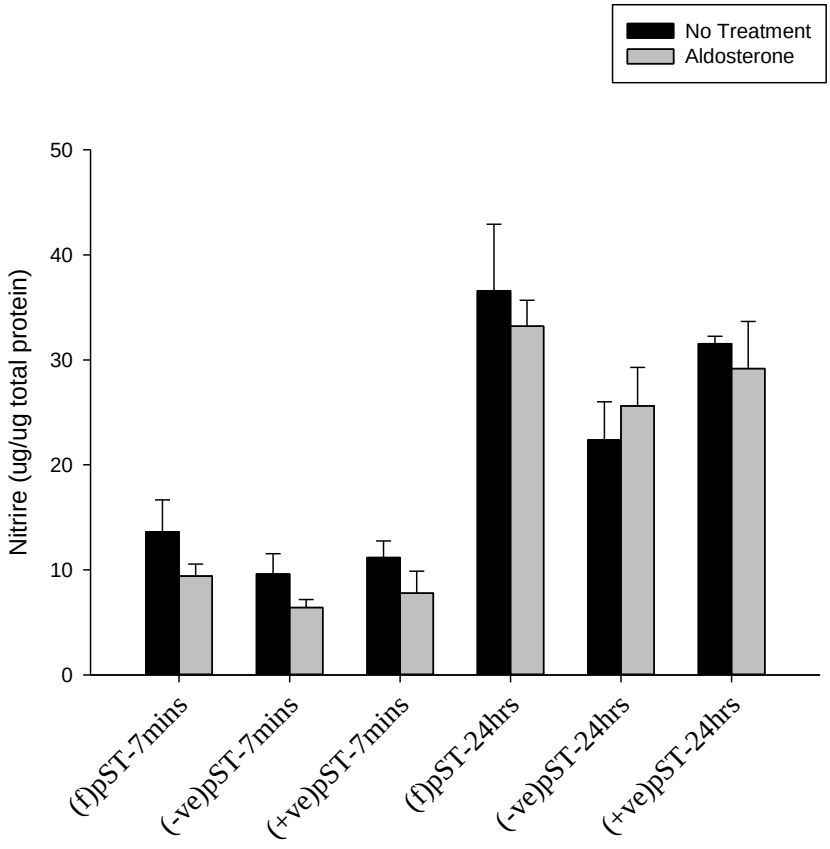


Figure 74 Ishikawa endometrial cancer cell NO secretion in serum-free medium with or without aldosterone at 7min and 24 hours.

NO level measurement was normalised with total protein. Data are presented as NO µg/µg total protein mean ± SEM of measurements of 3 independent experiments in quadruplicate.

9.5.7 Ishikawa Endometrial Cancer Cell Growth and Expression of Proliferation Marker and Cell Cycle Molecules on Flat, Negative and Positive Bioimprint Polystyrene Slides in Serum-Free Culture Medium

To examine Ishikawa endometrial cancer cell growth behaviour in culture medium without FBS, the cell number was quantified at 6 and 60 hours, and the expression of PCNA and cyclin B2, because there were significant changes of these parameters in the experiments with cells in medium with FBS (Figure 49, 52 and 53 B). Cyclin D2 expression was also studied because previously there was a trend of decreased cyclin D2 expression (Figure 53 C) in Ishikawa cells in response to physical topography.

Ishikawa endometrial cancer cells growing in serum-free medium showed similar growth behaviours compared to cells growing in medium with FBS on all substrates. Cells similarly showed fewer number at 60 hours on (+ve)pST and a trend of fewer cells on (-ve)pST when compared to (f)pST (Figure 75 compared to Figure 49). Moreover, similar to cells grown in medium with FBS (Figure 53 B), cells on (+ve)pST have reduced cyclin B2 expression compared to (-ve)pST (Figure 77 A). Additionally, there was no significant difference in cell cyclin D2 expression between cells growing on different topographies (Figure 77 B compared to Figure 53 C).

Cells in medium without FBS, however, responded differently, compared to cells in culture medium with FBS with regard to cell PCNA expression. The PCNA expression in cells without FBS exhibited no significant difference among different substrates (Figure 76), unlike cells in medium with FBS in which cells on (-ve)pST had lower PCNA expression compared to cells on (f) and (+ve)pST (Figure 52).

9.5.7.1 *Ishikawa Endometrial Cancer Cell Numbers on Flat, Negative and Positive Bioimprint Polystyrene Slides in Serum-Free Culture Medium*

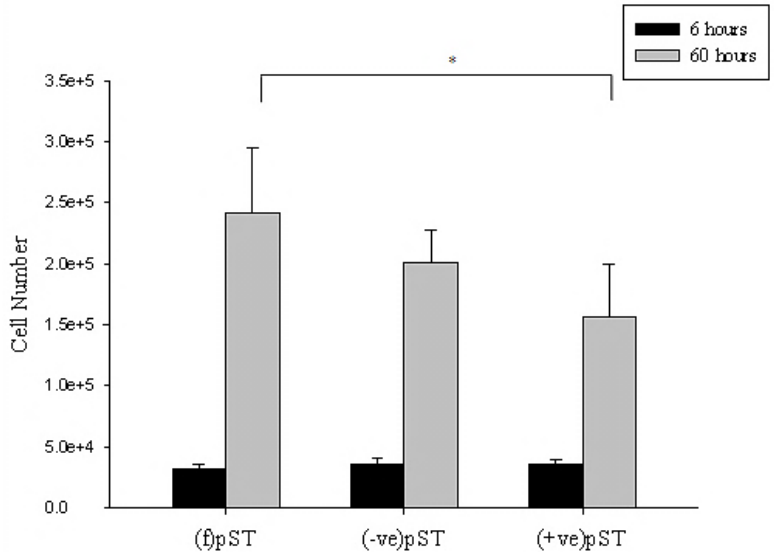


Figure 75 Ishikawa cell numbers on (f)pST, (-ve)pST and (+ve)pST in serum-free medium at 6 and 60 hours.

Data are presented as mean ± SEM of 6 independent experiments in quadruplicate. *, $p<0.05$.

9.5.7.2 *Ishikawa Endometrial Cancer Cell Cyclin PCNA and B2, D2 Expression on Flat, Negative and Positive Bioimprint Polystyrene Slides in Serum-Free Culture Medium*

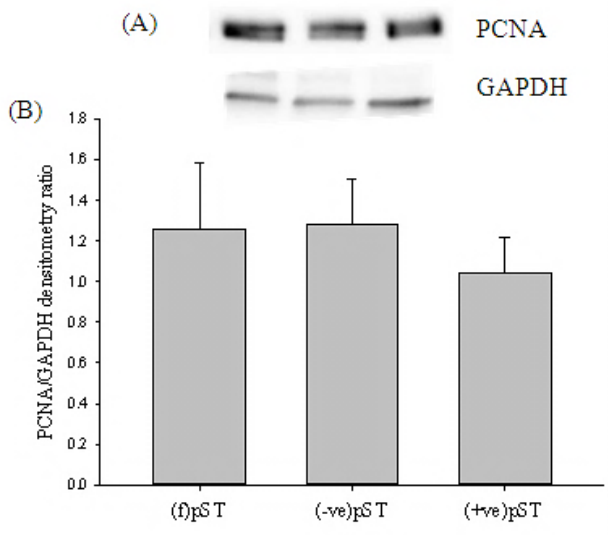


Figure 76 Ishikawa endometrial cancer cell PCNA expression on (f)pST, (-ve)pST and (+ve)pST in serum-free culture medium.

(A) (From left to right: (f)pST, (-ve)pST, (+ve)pST) representative examples of PCNA (upper row) and housekeeping protein GAPDH (bottom row) western blot protein bands.

(B)Densitometry ratio of PCNA/GAPDH of cells grown on (f)pST, (-ve)pST and (+ve)pST imprint.

Data are presented as PCNA densitometry normalized with GAPDH densitometry mean ±SEM of 5 independent experiments in quadruplicate.

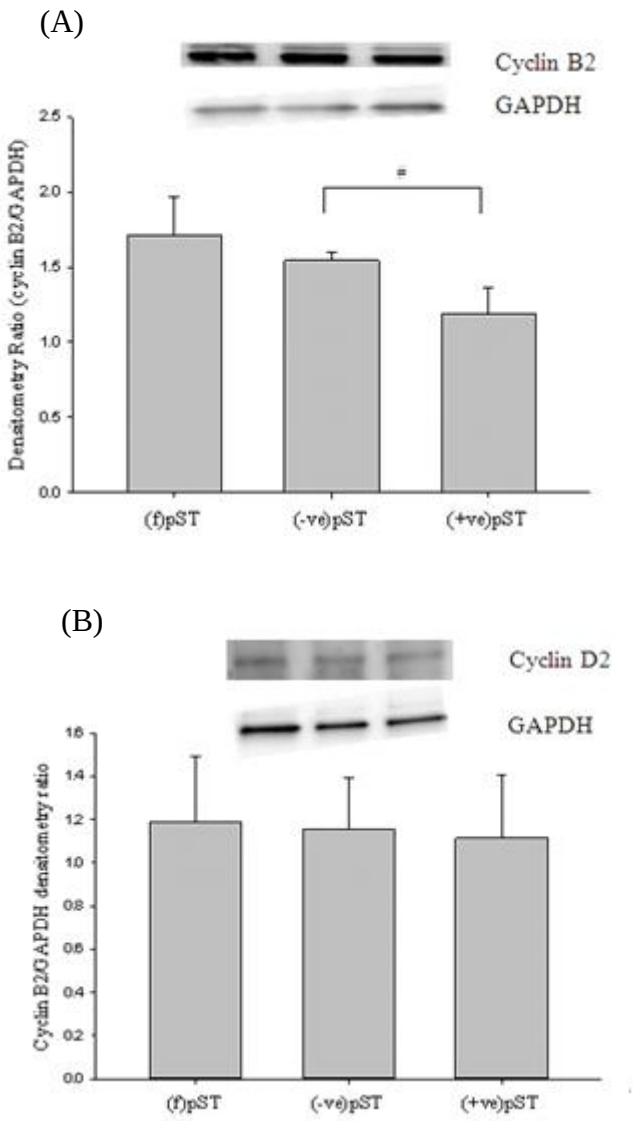


Figure 77 Ishikawa endometrial cancer cell (A) cyclin B2 and (B) D2 expression on (f), (-ve) and (+ve)pST in serum-free culture medium.

[Top] (From left to right: (f)pST, (-ve)pST, (+ve)pST)(Upper rows) representative examples of (A) cyclin B2 and (B) D2 and (bottom rows) housekeeping protein GAPDH of western blot protein bands.

[Bottom] Densitometry ratio of (A) cyclin B2/GAPDH and (B) cyclin D2/GAPDH of cells cultured on (f)pST, (-ve)pST and (+ve)pST imprint.

Data are presented as densitometry normalized with GAPDH densitometry mean ±SEM of 4 independent experiments in quadruplicate. $p<0.05$.

9.5.8 Ishikawa Endometrial Cancer Cell Proteomic Analysis on Flat, Negative and Positive Bioimprint Polystyrene Slides in Serum-Free Culture Medium

9.5.8.1 Identification of Changed Proteins

Without the effect of serum in culture medium, Ishikawa endometrial cancer cells responded to surface topography differently from those in culture with FBS with regard to the modulation of their protein expression. Thirty-two proteins were identified to be sensitive in cells by surface topography in serum-free culture medium, twenty four of which were upregulated and eight were down-regulated in cells on either (+ve) or (-ve)pST compared to cells on (f)pST. These proteins are listed in Table 14.

Cells cultured in serum-free medium had a relatively similar number of differently expressed proteins on (+ve)pST and (-ve)pST compared to (f)pST. This was in constrast to cells cultured in medium with FBS that had more proteins with different expression in cells on (+ve)pST than cells on (-ve)pST, compared to cells on (f)pST. Most of these proteins identified here were involved in cell proliferation, survival, and cell cytoskeleton. One difference between cells cultured in serum-free medium from those in medium with FBS was that none of the proteins detected, from this iTRAQ analysis, were linked to cell energy homeostasis. Another difference was that cells cultured in medium without FBS had more alteration of proteins related to cell stress responses.

The proteins were selected based on the same criteria as discussed in Chapter 7 section 7.1 and each protein was listed under a functional group the protein belongs to; the functions of the protein were obtained from a literature search. In the discussion section, a more detailed discussion of those proteins' functions are presented (Table 16 to Table 21). Under each functional group, the proteins are ranked from high to lower ratio of the compared samples.

Table 14 List of proteins that were up-regulated or down-regulated in comparisons between (+ve) / (f)pST, (-ve) / (f)pST and (+ve) / (-ve)pST.

Cells were in culture medium without FBS. The number in parentheses: upper row: ratio, $\bar{x}$= mean of ratio from two individual iTRAQ tests; bottom row: % of the variability, $\bar{y}$ =mean of % of the variability from two individual iTRAQ tests. Highlighted cells indicate proteins' $\bar{x}$ of $\geq$ 1.2 or $\leq$ 0.8 and $\bar{y}$ of $\leq$ 17.0%.

Cell Stress Responses	dnaJ homolog subfamily B member 1	(1.0,2.1; ***$\bar{x}$=1.6***) (14.5; $\bar{y}$ =14.5)	(1.1,2.0; ***$\bar{x}$=1.5***) (9.9; $\bar{y}$ =9.9)	(1.0,1.0; ***$\bar{x}$=1.0***) (11.7; $\bar{y}$ =11.7)
	peroxiredoxin-4 precursor	(1.1,1.7; ***$\bar{x}$=1.4***) (9.9,32.6; $\bar{y}$ =21.3)	(1.1,1.6; ***$\bar{x}$=1.4)*** (0.5,31.1; $\bar{y}$ =15.8)	(1.0,1.0; ***$\bar{x}$=1.0***) (6.0,3.4; $\bar{y}$ =4.7)
	ubiquitin-conjugating enzyme E2 N	(1.2,1.4; ***$\bar{x}$=1.3***) (16.4,17.1; $\bar{y}$ =16.8)	(1.0,1.4; ***$\bar{x}$=1.2***) (10.5,15.8; $\bar{y}$ =13.2)	(1.2,1.0; ***$\bar{x}$=1.1***) (16.7,5.8; $\bar{y}$ =11.3)
	thioredoxin-related transmembrane protein 2 isoform 2	(1.0,1.2; ***$\bar{x}$=1.1***) (14.3,29.2; $\bar{y}$ =21.8)	(1.3,1.3; ***$\bar{x}$=1.3***) (19.9,6.4; $\bar{y}$ =13.2)	(0.8,0.9; ***$\bar{x}$=0.9***) (13.1,23.0; $\bar{y}$ =18.1)
	reticulon-3 isoform a	(0.8,2.1; ***$\bar{x}$=1.5***) (1.0,24.2; $\bar{y}$ =11.6)	(0.9,1.3; ***$\bar{x}$=1.1***) (11.0,9.1; $\bar{y}$ =10.1)	(0.8,1.6; ***$\bar{x}$=1.2***) (1.3,28.3; $\bar{y}$ =14.8)
Cell Epigenetic Regulation	nucleolin	(1.2,,1.4; ***$\bar{x}$=1.3***) (4.3,28.2; $\bar{y}$=16.3)	(1.1,1.3; ***$\bar{x}$=1.2***) (3.3,27.6; $\bar{y}$=15.5)	(1.1,1.0; ***$\bar{x}$=1.1***) (3.5,2.2; $\bar{y}$=2.9)
	SWI/SNF-related matrix-associated actin-dependent regulator of chromatin subfamily A member 5 (SMARCA5)	(1.2,1.2; ***$\bar{x}$=1.2***) (11.9,16.3; $\bar{y}$ =14.1)	(1.1,1.1 ***$\bar{x}$=1.1***) (30.0,19.0; $\bar{y}$ =25)	(1.1,1.0; ***$\bar{x}$=1.1***) (22.0,10.6; $\bar{y}$ =16.3)
	histone deacetylase 1	(0.9,0.7; ***$\bar{x}$=0.8***) (2.6,22.3; $\bar{y}$ =12.5)	(0.9,0.7; ***$\bar{x}$=0.8***) (14.8,8.1; $\bar{y}$ =11.5)	(1.0,0.9; ***$\bar{x}$=1.0***) (10.7,13.9; $\bar{y}$ =12.3)
	histone deacetylase 2	(0.8,0.7; ***$\bar{x}$=0.8***) (9.0,14.9; $\bar{y}$ =12)	(0.8,0.7; ***$\bar{x}$=0.8***) (10.9,6.1; $\bar{y}$ =9)	(1.0,0.9; ***$\bar{x}$=1.0***) (12.0,8.5; $\bar{y}$ =10.3)
Cell Growth	kinesin-like protein KIF23 isoform 2	(1.2,1.8; ***$\bar{x}$=1.5***) (11.7; $\bar{y}$ =11.7)	(1.5; ***$\bar{x}$=1.5***) (68.8; $\bar{y}$ =68.8)	(1.3,1.2; ***$\bar{x}$=1.3***) (17.3,11.7; $\bar{y}$ =14.5)
	cysteine-rich protein 2 isoform 1	(1.5,0.8; ***$\bar{x}$=1.2***) (19.4,43.1; $\bar{y}$ =31.1)	(1.0,0.7; ***$\bar{x}$=0.9***) (36.0,47.4; $\bar{y}$ =41.7)	(1.5,1.1; ***$\bar{x}$=1.3***) (18.1,11.4; $\bar{y}$ =14.8)
	nuclear migration protein nudC	(1.0,1.5; ***$\bar{x}$=1.3***) (19.4,27.7; $\bar{y}$=23.6)	(1.1,1.4; ***$\bar{x}$=1.3***) (7.6,22.1; $\bar{y}$=14.9)	(1.0,1.0; ***$\bar{x}$=1.0***) (17.2,8.8; $\bar{y}$=13)
Cell Cytoskeleton	kinectin isoform c	(1.1,1.4; ***$\bar{x}$=1.3***) (9.6,21.6; $\bar{y}$ =15.6)	(1.0,1.3; ***$\bar{x}$=1.2***) (30.4,19.6; $\bar{y}$ =25)	(1.1,1.0; ***$\bar{x}$=1.1***) (15.0,5.6; $\bar{y}$ =10.3)
	keratin, type II cytoskeletal 1	(1.1,0.9; ***$\bar{x}$=1.0***) (15.9,25.7; $\bar{y}$=20.8)	(0.9,0.8; ***$\bar{x}$=0.9***) (27.3,27.8; $\bar{y}$=27.6)	(1.4,1.1; ***$\bar{x}$=1.3***) (20.1,5.7; $\bar{y}$=12.9)
	tubulin alpha-1C chain	(1.0,1.4; ***$\bar{x}$=1.2***) (8.9,18.8; $\bar{y}$=13.9)	(1.0,1.3; ***$\bar{x}$=1.2***) (5.4,21.7; $\bar{y}$=13.6)	(1.0,1.0; ***$\bar{x}$=1.0***) (4.7,2.8; $\bar{y}$=3.8)

	keratin, type II cytoskeletal 2 epidermal	(1.2,1.1; $\bar{x}$=1.2) (12.6,38.3; $\bar{y}$=25.5)	(0.9,1.0; $\bar{x}$=1.0) (9.9,46.4; $\bar{y}$28.2)	(1.3,1.1; $\bar{x}$=1.2) (13.4,5.5; $\bar{y}$=9.5)
Cell Signalling Biomolecules	GDP-fucose protein O-fucosyltransferase 1 isoform 1 precursor	(1.0,1.5; $\bar{x}$=1.3) (22.1,2.0; $\bar{y}$ =6.0)	(1.0,1.5; $\bar{x}$=1.3) (15.8,3.2; $\bar{y}$ =10)	(1.1,1.0; $\bar{x}$=1.1) (26.3,0.1; $\bar{y}$ =13.2)
	epidermal growth factor receptor isoform a precursor	(0.9,0.8; $\bar{x}$=0.9) (28.4,15.5; $\bar{y}$ =22)	(0.8,0.8; $\bar{x}$=0.8) (13.9,9.5; $\bar{y}$ =6.7)	(1.2,1.0; $\bar{x}$=1.1) (41.0,7.3; $\bar{y}$ =24.2)
Innate Immune Responses (also in Cell Growth Regulation)	macrophage migration inhibitory factor (MIF)	(1.1,1.2; $\bar{x}$=1.2) (13.8,13.8; $\bar{y}$ =13.8)	(1.1,1.4; $\bar{x}$=1.3) (10.4,6.3; $\bar{y}$ =8.4)	(1.0,0.8; $\bar{x}$=0.9) (9.4,7.0; $\bar{y}$ =8.2)
Ribosomal Protein, RNA Processing	60S ribosomal protein L27a	(1.0,1.4; $\bar{x}$=1.3) (7.1,12.5; y=9.8)	(1.0,1.1; $\bar{x}$=1.1) (4.0,9.2; $\bar{y}$ =6.6)	(1.1,1.2; $\bar{x}$=1.2) (8.3,9.4; $\bar{y}$ =8.9)
	40S ribosomal protein S20 isoform 2	(0.8,0.8; $\bar{x}$=0.8) (10.0,21.1; $\bar{y}$ =15.6)	(0.8,0.7; $\bar{x}$=0.8) (14.9,19.4; $\bar{y}$ =17.2)	(1.0,1.1; $\bar{x}$=1.1) (13.7,3.5; $\bar{y}$ =8.6)
Protein Synthesis, Processing, Degradation and Transportation	ATPase ASNA1	(1.1,1.3; $\bar{x}$=1.2) (15.2,16.0; $\bar{y}$ =15.6)	(1.1,1.2; $\bar{x}$=1.2) (11.4,21.0; $\bar{y}$ =16.2)	(1.0,1.0; $\bar{x}$=1.0) (18.8,7.0; $\bar{y}$ =12.9)
	prolyl endopeptidase	(0.8,0.7; $\bar{x}$=0.8) (14.0,17.3; $\bar{y}$ =15.7)	(0.9,0.8; $\bar{x}$=0.9) (10.3,20.0; $\bar{y}$ =15.2)	(0.9,0.9; $\bar{x}$=0.9) (19.0,12.1; $\bar{y}$ =15.6)
Pre- mRNA Splicing	U4/U6.U5 tri-snRNP-associated protein 2 isoform 4	(0.9,1.7; $\bar{x}$=1.3) (24.0,11.6; $\bar{y}$ =17.8)	(1.0,1.8; $\bar{x}$=1.4) (7.5,5.1; $\bar{y}$ =6.3)	(0.9,0.9; $\bar{x}$=0.9) (28.8,9.1; $\bar{y}$ =19)
	probable ATP-dependent RNA helicase DDX46	(0.9,0.7; $\bar{x}$=0.8) (21.8,8.1; $\bar{y}$ =15)	(1.0,0.9; $\bar{x}$=1.0) (24.0,5.0; $\bar{y}$ =15)	(1.0,0.8; $\bar{x}$=0.9) (34.9,4.4; $\bar{y}$ =19.7)
Enzymatic Activity	glyoxylate reductase/hydroxypyruvate reductase	(0.9,1.7; $\bar{x}$=1.3) (19.0,11.6; $\bar{y}$ =15.3)	(1.1,1.8; $\bar{x}$=1.5) (28.5,18.8; $\bar{y}$ =23.7)	(1.0,0.9; $\bar{x}$=1.0) (37.0,11.6; $\bar{y}$ =24.3)
	isochorismatase domain-containing protein 1	(0.9,0.7; $\bar{x}$=0.8) (4.6,15; $\bar{y}$ =9.8)	(1.0,0.7; $\bar{x}$=0.9) (32.5,17.6; $\bar{y}$ =25.1)	(1.0,1.0; $\bar{x}$=1.0) (27.2,2.8; $\bar{y}$ =15)
Translation	eukaryotic translation initiation factor 3 subunit M	(1.1,1.6; $\bar{x}$=1.4) (27.4,18.4; $\bar{y}$ =22.9)	(1.1,1.6; $\bar{x}$=1.4) (7.1,21.9; $\bar{y}$ =14.5)	(1.1,1.0; $\bar{x}$=1.1) (10.0,11.8; $\bar{y}$ =10.9)
Catabolism	nicotinate-nucleotide pyrophosphorylase [carboxylating] precursor	(1.0,0.5; $\bar{x}$=0.8) (12.1; $\bar{y}$=12.1)	(1.1,0.6; $\bar{x}$=0.9) (4.0; $\bar{y}$=4.0)	(1.0,0.9; $\bar{x}$=1.0) (13.8; $\bar{y}$=13.8)
Golgi apparatus Functions	ADP-ribosylation factor-like protein 1	(1.0,1.7; $\bar{x}$=1.4) (7.9,24.4; $\bar{y}$ =16.2)	(1.2,1.6; $\bar{x}$=1.4) (13.6,15.7; $\bar{y}$ =14.7)	(0.6,1.0; $\bar{x}$=0.8) (36.0,17.5; $\bar{y}$ =26.8)
mRNA Degradation	m7GpppX diphosphatase	(1.3,1.0; $\bar{x}$=1.2) (27.1,12.4; $\bar{y}$ =19.8)	(1.0,0.9; $\bar{x}$=1.0) (22.2,8.2; $\bar{y}$ =15.2)	(1.3,1.1; $\bar{x}$=1.2) (8.4,9.8; $\bar{y}$ =9.1)

9.5.9 Cisplatin and Paclitaxel Treatments on Ishikawa Endometrial Cancer Cells on Flat, Negative and Positive Bioimprint Polystyrene Slides in Serum-Free Culture Medium

9.5.9.1 Cisplatin and Paclitaxel Effects on Ishikawa Endometrial Cancer Cell VEGF Secretion on Flat, Negative and Positive Bioimprint Polystyrene Slides in Serum-Free Culture Medium

VEGF secretion was studied. Cells incubated in medium without FBS secreted significantly higher VEGF on (f)pST compared to cells on (-ve) and (+ve)pST (Figure 78). This was different from cells incubated in medium with FBS supplemented, in which the cells had similar VEGF secretion on all culture substrates (Figure 58).

Furthermore, the responses to cisplatin and paclitaxel treatments were different to the cell responses to these chemotherapy drugs in incubations with FBS. In the presence of FBS, both cisplatin and paclitaxel reduced VEGF secreted by cells on all substrates, with a greater reduction in cells with paclitaxel treatment, though the VEGF reduction was not significant (Figure 58). However without FBS in the culture medium, VEGF secretion showed a trend of elevation when treated with cisplatin and paclitaxel as compared to DMSO-treated control cells, though the increment was not significant. The cells on (+ve)pST with paclitaxel treatment had significantly lower VEGF secretion compared to cells on (f) and (-ve)pST (Figure 78).

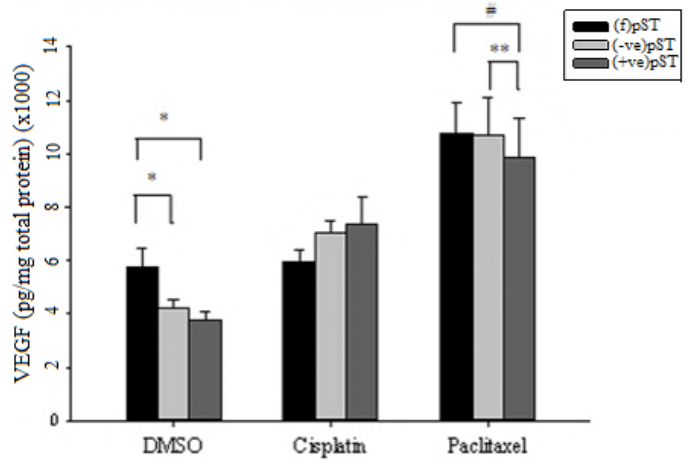


Figure 78 Ishikawa endometrial cancer cell VEGF secretion with or without cisplatin and paclitaxel treatment on (f)pST, (-ve)pST and (+ve)pST in serum-free culture medium.

Data are presented as VEGF (pg/mg total protein) mean ±SEM of 4 independent experiments in quadruplicate. *,p<0.05;**,p<0.01; #,p=0.06.

9.5.9.2 *Cisplatin and Paclitaxel Effects on Ishikawa Endometrial Cancer Cell Growth on Flat, Negative and Positive Bioimprint Polystyrene Slides in Serum-Free Culture Medium*

The chemotherapy drug effects on cell growth were similar between cultures in the presence and absence of FBS in culture medium. Without FBS added in the culture medium, cisplatin and paclitaxel had no robust effect on reducing cell number and the reduction was not significant on all substrates (Figure 79 compared to Figure 59).

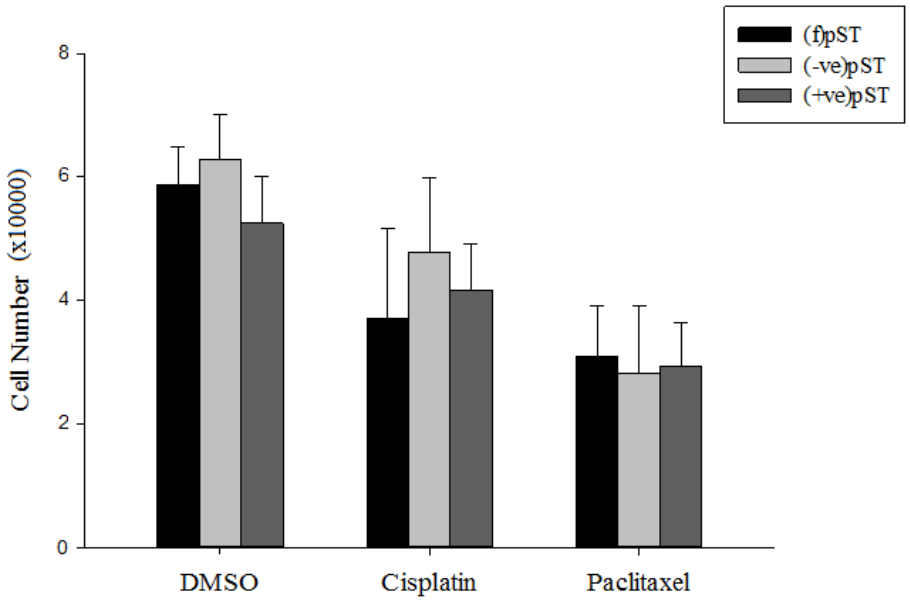


Figure 79 Ishikawa endometrial cancer cell number with or without cisplatin and paclitaxel treatments on (f)pST, (-ve)pST and (+ve)pST in serum-free culture medium.

Ishikawa cell numbers on (f)pST, (-ve)pST and (+ve)pST with DMSO (control), cisplatin or paclitaxel treatment. Data are presented as mean ± SEM of 4 independent experiments in quadruplicate.

9.5.9.3 *Cisplatin and Paclitaxel Effects on Ishikawa Endometrial Cancer Cell PCNA and Cycle Regulators Expression on Flat, Negative and Positive Bioimprint Polystyrene Slides in Serum-Free Culture Medium*

Cell cycle regulators and cell proliferation marker expression were studied without an addition of FBS. The effects of cisplatin and paclitaxel treatments on Ishikawa endometrial cancer cell expression of PCNA and cyclin B1, B2 and D2 were examined. Ishikawa cells with cisplatin and paclitaxel treatments showed a trend of reduced expression level for all measured parameters on all substrates; however, the reduction was only significant on certain substrates, which suggested a more consistent effect of cisplatin and paclitaxel on those substrates.

For cells with cisplatin and paclitaxel treatments, the expression level of PCNA in cells on (-ve)pST was significantly lower compared to control cells. No significant effect was seen in cells on (f) and (+ve)pST compared to respective control cells (Figure 80 compared to Figure 60).

Now considering cyclin B1, for cells treated with paclitaxel, only the level of cyclin B1 in cells on (f)pST was significantly lower compared to control cells. Moreover, within the group of paclitaxel treatment, there was a significant difference between cells on (f)pST and cells on (-ve)pST. On the other hand, within the group of cisplatin treatment, there was a significant difference in cyclin B1 level between cells on (f)pST and cells on (+ve)pST (Figure 81 A compared to Figure 61 A).

Besides, for both cisplatin and paclitaxel treatments, there was a significant reduction of cyclin B2 in cells on (f)pST. Also, within the cisplatin treatment group, cells on (f)pST had a significantly lower cyclin B2 level than cells on (-ve)pST (Figure 81 B compared to Figure 61 B).

Cisplatin and paclitaxel treatments both reduced cyclin D2 expression significantly in cells growing on (f)pST and (-ve)pST, but had no significant influence on cells on (+ve)pST, as compared to respective DMSO-treated control cells. Further, within the group of cisplatin treatment, cells on (-ve)pST had a significantly lower cyclin D2 level compared to cells on (+ve)pST (Figure 81 C compared to Figure 61 C).

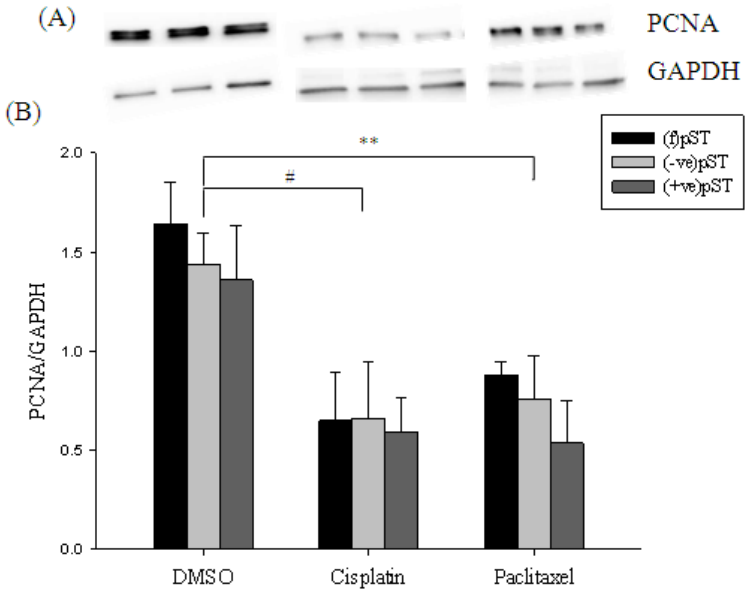


Figure 80 Ishikawa endometrial cancer cell PCNA expression with or without cisplatin and paclitaxel treatments on (f)pST, (-ve)pST and (+ve)pST in serum-free culture medium.

(A) Representative examples of PCNA (upper row) and GAPDH (bottom row) western blot protein bands of cells grown on (f)pST, (-ve)pST and (+ve)pST imprint with DMSO (control), cisplatin or paclitaxel treatment.

(B) Densitometry ratio of PCNA/GAPDH of cells cultured on (f)pST, (-ve)pST and (+ve)pST imprint with DMSO (control), cisplatin or paclitaxel treatment.

Data are presented as PCNA densitometry normalized with GAPDH densitometry mean ±SEM of 3 independent experiments in quadruplicate. **, $p<0.01$; #, $p=0.06$

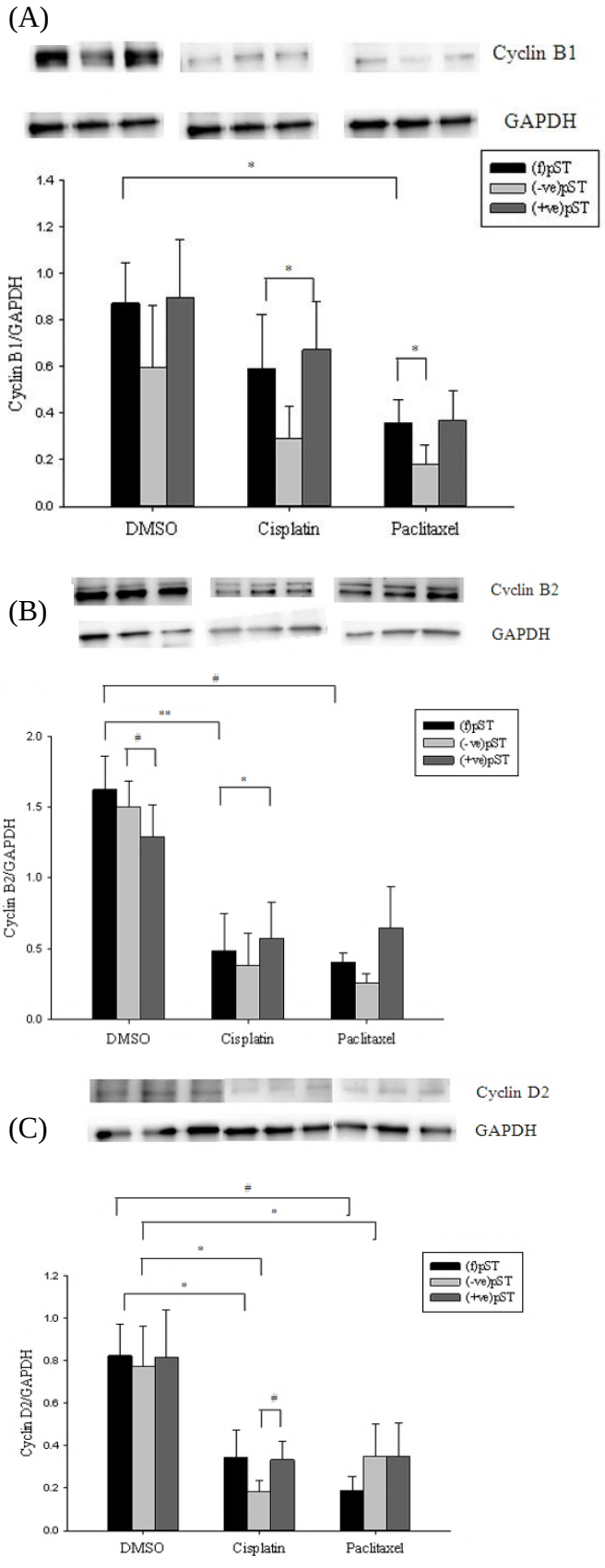


Figure 81 Ishikawa endometrial cancer cell (A) cyclin B1, (B) B2 and (C) D2 expression on (f), (-ve) and (+ve)pST with or without cisplatin and paclitaxel treatments.

[Top] (From left to right: (f)pST, (-ve)pST, (+ve)pST with DMSO (control), cisplatin or paclitaxel treatment) (Upper rows) representative examples of (A) cyclin B1, (B) B2 and (C) D2 and (bottom rows) housekeeping protein GAPDH of western blot protein bands.

[Bottom] Densitometry ratio of (A) cyclin B1/GAPDH, (B) cyclin B2/GAPDH and (C) cyclin D2/GAPDH of cells cultured on (f)pST, (-ve)pST and (+ve)pST imprint with DMSO (control), cisplatin or paclitaxel treatment.

Data are presented as densitometry normalized with GAPDH densitometry mean ±SEM of 4 independent experiments in quadruplicate. **, p<0.01; *, p<0.05; #, p=0.06.

9.6 Discussion

9.6.1 Ishikawa Endometrial Cancer Cell Initial Attachment and Morphology in Culture Medium without FBS

When compared to cells that were cultured in medium with FBS, the cells in medium without FBS were similarly attached to the cultured substrate at 6 hours after seeding. Hence, initial attachment by Ishikawa endometrial cancer cells does not seem to be affected by FBS.

On the other hand, cell spreading area was the smallest on (+ve)pST and cells were the most circular on (+ve)pST compared to cells on (f) and (-ve)pST, which was similar to cells growing in medium with FBS. This indicates that the cell spreading behaviour is largely affected by surface topography independent of serum factors. A smaller cell size may be associated with a reduced cell number on (+ve)pST as compared to (f)pST. This relationship has been noted previously (Figure 22 and 49), i.e. topography modulates cell size which modulates cell proliferation.

9.6.2 Ishikawa Endometrial Cancer Cell Expression of Cell Cytoskeleton and Adhesion Molecules in Culture Medium without FBS

FBS affected the cell β1 integrin, Cytokeratin-18 and FAK activities in response to surface topography. This leads to speculation that FBS in the culture medium may have a role in activating β1 integrin. This is because in culture medium without FBS, RGD peptide had no effect in inhibiting initial adhesion of Ishikawa cells onto culture substrates, which indicates that β1 integrin is not involved in the process of cell adhesion via fibronectin (an RGD-containing peptide) in medium without FBS.

Moreover, without the effect of FBS, the cell actin filaments and Cytokeratin-18 were not affected by physical topography. First, Cytokeratin-18 was not changed in response to topography. Hence, in an absence of FBS, the topographic factor may not be influential on

the cell Cytokeratin-18 but instead on another family of cytokeratin (cytokeratin type II on (+ve)pST and microtubule on (+ve) and (-ve)pST, as suggested by iTRAQ analysis (Table 14 and 19). Furthermore, actin expression and actin-regulated activity (NO secretion) were not affected by the topography factor in an absence of FBS. This was opposite to cells in medium with FBS in which Ishikawa cell Cytokeratin-18 expression level and cell NO secretion were affected by surface topography.

In contrast to cells cultured in medium with FBS, the cells cultured on imprints in medium without FBS showed higher FAK activation. This implies that the topography factor, without the involvement of FBS, activates FAK by a process not mediated by β1 integrin.

Altogether the results again indicate that cell-like surface topography influences cell behaviour. The topographical factor influence on cells is itself affected by chemical factors. Thus each of them determines the type of signaling molecules to be activated, and the combination of all the effects determines cell behaviour.

9.6.3 Ishikawa Endometrial Cancer Cell Growth in Culture Medium without FBS

Table 15 Summary of Results from Section 9.5.7.

A table showing the comparative level of the measured parameters between Ishikawa endometrial cancer cells on (f)pST, (-ve)pST and (+ve)pST in serum-free culture medium (comparing to Table 5). The numbers relate to the comparative measurements (cell number and western blot densitometry); 1=lowest value and 4=highest value. The "-" symbol indicates no statistically significant difference between the compared groups.

	(f)pST	(-ve)pST	(+ve)pST
Cell Number at 6 hrs	-	-	-
Cell Number at 60 hrs	2	-	1
PCNA	-	-	-
Cyclin B2	-	2	1
Cyclin D2	-	-	-

By comparing to cells that were cultured in medium with FBS, we observed a lower growth of cells in medium without FBS on all substrates. When compared between surfaces with different topographies, cells on (+ve)pST at 60 hours had a lower number than on (f)pST; this implies that the topography factor could affect cell growth. And that this may be through the reduction of cell spreading area and a reduction in cyclin B2.

Ishikawa cells cultured in medium with FBS on (-ve)pST had lower PCNA expression level compared to cells on (f) and (+ve)pST (Figure 52). In contrast, when FBS was not supplemented, cells on (-ve)pST had similar PCNA expression compared to (f) and (+ve)pST. The expression of PCNA in cells on (-ve)pST when FBS was not supplemented may be the reason for the non-significant decrease in cell number when compared to cell number on (f)pST (Figure 76). PCNA is not only functioning in DNA replication, it also has a role in DNA repair (Kelman, 1997). Hence, one possible reason for the observed difference could be that cells on (-ve)pST responded to no-FBS-starvation by activating cell stress responses that involved a change of cell PCNA expression in order to activate the DNA repairing system, and this activation of cell survival pathways may have compensated for the growth reduction of cells on (-ve)pST. This was also supported by the altered proteins identified from the iTRAQ analysis in which a number of altered proteins on (-ve)pST had functions in cell stress responses (Table 14 and 16).

9.6.3.1 Summary

By comparing the results between cell culture in medium with and without FBS, it is clear that the topography factor could act on certain behaviours independently of serum factors. Topography influenced the cell spreading area, which then reduced cell growth through reducing cell cyclin B2. And similar to the culture in medium with FBS, the positive 'hump-like' topography has a greater effect on cell behaviours compared to the negative 'pit-like' topography, in which Ishikawa cells on (+ve)pST had lowest cell number and lowest expression level of cyclin B2 compared to cells on (f) and (-ve)pST.

Ishikawa cell β1 integrin was not involved in the cell response to surface topography in the absence of FBS supplemented in the medium. When FBS was absent, other integrins may be involved in cell attachment on surfaces, and FAK activation was elevated due to the influence of physical topography. Hence, surface topography functions along with the microenvironment chemical factor in modulating cell behaviours.

9.6.4 Ishikawa Endometrial Cancer Cell Protein Profile in Culture Medium without FBS

9.6.4.1 Cell Stress Responses

Table 16 The proteins under the functional group of cell stress response.

Proteins Identified from iTRAQ	**Functions**
DnaJ homolog subfamily B member 1	-Involved in the repair responses to DNA damage (Kultz, 2005). -Associated with Heat Shock Protein 70, which is a molecule involved in the mitochondrial responses to oxidative stress (Landriscina et al., 2009).
Peroxiredoxin-4 precursor	- Involved in the activation of cell ROS adaptive responses to protect cells against oxidative stress
Ubiquitin-conjugating enzyme E2 N	-Regulates cell transcription. -Regulates error-free DNA repair pathway -Maintains cell survival after DNA damage through NFκB pathways.
Thioredoxin-related transmembrane protein 2 isoform 2	- Involved in the activation of cell Reactive Oxygen Species (ROS) adaptive responses to protect cells against oxidative stress (Kultz, 2005; Landriscina et al., 2009).
Reticulon-3 isoform	-Involved in membrane trafficking of cell secretion events between ER (endoplasmic reticulum) and Golgi apparatus. -Reduces apoptosis or responds to ER stress by enhancing Bcl-2 inhibition of apoptosis.

iTRAQ analysis suggests that Ishikawa endometrial cancer cells experience cellular stress when incubated in medium without FBS. This is not surprising because cells may be deprived of some amino acids and glucose in medium without FBS. However, the activation of cell defence responses to the stress experienced varied on different culture substrates. Among the proteins that were involved in cell stress responses or cell survival regulation, four were more highly expressed in cells on (+ve)pST compared to cells on a flat surface, and one of them, together with two other different stress-related proteins, were up-regulated on (-ve)pST.

In the real tumour environment, cells are exposed to various kinds of stresses constantly. The possibility of stimulation of cell stress-responses using surface topography may indicate that the culture substrate with cell-like topography more closely mimics the real cancer cell microenvironment, and cell behaviours may be more like those in *in vivo* conditions.

An identification of stress molecules in the iTRAQ analysis on culture without FBS agrees to the hypothesis that Ishikawa cells respond to the physical microenvironment differently from those in culture medium with FBS because none of the proteins identified were involved in cell stress regulation in culture medium with FBS (Table 6).

9.6.4.2 Cell Epigenetic Regulation

Table 17 The protein under the functional group of cell epigenetic regulation.

Proteins Identified from iTRAQ	Functions
Nucleolin	- Induces chromatin decondensation - Involved in pre-rRNA transcription - Involved in ribosome assembly and in the process of transcriptional elongation.
SWI/SNF-related matrix-associated actin-dependent regulator of chromatin subfamily A member 5 (SMARCA5)	-Part of WSTF-ISWI chromatin remodelling (WICH) complex that is involved in maintaining and the remodelling of chromatin and transcription. -A component of nucleolar remodelling complex (NoRC) that forms heterochromatin and plays a role in modulating transcription silencing.
Histone deacetylase 1 and 2	-Involved in histone deacetylation process -Histone acetylation or deacetylation is one of the mechanisms in epigenetics, which is a phenomenon of heritable gene expression alteration without changing the gene sequences. -Deacetylase of histone marks the epigenetic repression and enables histones to wrap the DNA tighter, which reduces cell transcription. -It has been reported that HDAC 1 and 2 knock-out or inhibition reduced cell proliferation and HDAC 1 and 2 were required for cell cycle progression and chromosome segregation (Jamaladdin et al., 2014).

Nucleolin was up-regulated on both (+ve) and (-ve)pST whereas SMARCA5 was up-regulated on (+ve)pST, compared to (f)pST. An elevation of expression of nucleolin and SMARCA5 suggests a potential role of these poteins in the cell response to physical topography through regulation at the transcription level.

Histone deacetylase 1 and 2 (HDAC 1 and 2) were decreased on both (+ve) and (-ve)pST compared to cells on (f)pST, which propose a role of this protein in response to physical topography.

Cell responses to mechanical signals involving epigenetic modification are supported by other findings. It has been shown that the levels of histone deacetylation 4 and 5 increased in endothelial cells that were exposed to shear forces; further, phosphorylation and stabilizing of histone deacetylation 3 were mechanisms of endothelial cell survival (Zhou et al., 2011). Also, it has been observed that interaction between ECM and a cell could modify the epigenetic pattern and subsequently determine gene expression patterns and manipulate cell characteristics and functions (Leli èvre et al., 1998; Plachot & Leli èvre, 2004). In addition, it was observed that rounding up of cells resulted in global histone deacetylation, chromatin condensation and reduced gene expression in human epithelial cells, independent from biochemical signals (Le Beyec et al., 2007).

iTRAQ analysis suggested that physical topography reduced the expression of HDAC 1 and 2, which may result in wrapped DNA, reduced cell transcription and may also partly explain the lower cell growth observed on (-ve) and (+ve)pST compared to (f)pST.

This result again supports our hypothesis that the physical topography may change a cell's behaviour which may be partly through altering the cell at the nuclear level. Further, different biomolecules were involved in the cell response between culture with FBS and without FBS (Table 6 and **7**).

9.6.4.3 Cell Growth

Table 18 The proteins under the functional group of cell growth.

Proteins Identified from iTRAQ	Functions
Kinesin-like protein KIF23 isoform 2	-A component of central spindlin complex that is required in cytokinesis. -Involved in Rho-mediated signalling and direct movement of microtubule during cytokinesis.
Cysteine-rich protein 2 isoform 1	-A component of ADA2A-containing (ATAC) complex that has histone acetyltransferase activity. -Increases gene transcription and is required in cell progression from G1 to G2/M phases.
Nuclear migration protein nudC	-Regulates cytokinesis, mitosis and ensures correct formation of mitotic spindles and chromosome separation.
Macrophage migration inhibitory factor (MIF)	- A pro-inflammatory cytokine that regulates the innate immune response to bacterial pathogens

A number of proteins that iTRAQ suggested to be differently expressed were involved in cell growth. There were four up-regulated proteins in this functional category: kinesin-like protein KIF23 isoform 2 and cysteine-rich protein 2 isoform 1 were up-regulated in cells on (+ve)pST compared to cells on (-ve)pST or (f)pST, and MIF was up-regulated on both (+ve)pST and (-ve)pST compared to (f)pST. On the other hand, nuclear migration protein nudC was up-regulated in cells on (-ve)pST compared to cells on (f)pST.

Meanwhile, HDAC 1 and 2, which have been discussed above in section 9.6.4.2 were down-regulated on (+ve)pST or on both (-ve) and (+ve)pST.

Although there were a number of up-regulated cell stress response proteins and cell growth proteins in cells on (-ve) and (+ve)pST, the cells on (-ve) and (+ve)pST still showed lower growth compared to cells on (f)pST (Figure 75). This could suggest that the activated cell adaptive responses may still be inadequate to counteract the effect of physical topography on cell growth, hence resulting in lower cell growth on (-ve) and (+ve)pST compared to cells on (f)pST.

Alternatively or additionally, there was a decrease in expression of HDAC 1 and 2 on both (+ve) and (-ve)pST compared to (f)pST. This may cause a decreased cell growth on (-ve) and (+ve)pST compared to cell growth on (f)pST, with a more pronounced decrease on (+ve)pST compared to (-ve)pST.

The observation of different expression of proteins associated with cell stress and growth regulation agrees with the hypothesis that cells may respond to physical features by modulating the cell survival and growth functions. Further, there was only one overlap biomolecule between the culture with FBS and without FBS (discussed in section 9.6.4.7) suggests a role of FBS in modulating Ishikawa cell response to the physical topography.

9.6.4.4 Cell Cytoskeleton

Table 19 The proteins under the functional group of cell cytoskeleton structure.

Proteins Identified from iTRAQ	**Functions**
Kinectin isoform c	-Binds to kinesin -Kinesin is one of the cellular motor components that moves along microtubule filaments and has a role in mitosis, meiosis and protein trafficking in cells.
Keratin type II cytoskeletal 1 and 2	-Components of cell cytoskeleton.

Tubulin alpha-1C chain	-A main component of microtubule.

From the protein list, four cell cytoskeleton-related proteins were identified, three of which were up-regulated on (+ve)pST and one was up-regulated in cells on (-ve)pST compared to cells on (f)pST. Keratin type II cytoskeletal 1 and 2 and kinectin isoform c were up-regulated in cells on (+ve)pST compared to cells on (f)pST or (-ve)pST. On the other hand, tubulin alpha-1C chain was up-regulated in cells on (-ve)pST compared to cells on (f)pST.

The observation that there was a change in cell cytoskeleton is consistent with the hypothesis that cells growing on surfaces with cell-like topography may change their cell cytoskeleton. Also, these identified cell cytoskeleton molecules were not detected in the culture in medium with FBS (Table 6), proposing an influence of FBS in the cell response to physical topography.

9.6.4.5 Cell Signalling Biomolecules

Table 20 The proteins under the functional group of cell signaling biomolecules.

Proteins Identified from iTRAQ	**Functions**
GDP-fucose protein O-fucosyltransferase 1	-A catalyser involved in the NOTCH signalling pathway. -NOTCH signalling has been previously reported to be linked to Rho GTPase signalling (Redmond & Ghosh, 2001). Furthermore, NOTCH signalling has been related to lung, skin, cervical, breast, epithelial and lymphoma cancer development. Its role in cancer development is however debating in different studies (for review: (Allenspach et al., 2002)),

Epidermal growth factor receptor isoform a precursor	EGFR is a receptor tyrosine kinase for EGF family which has been well-studied in cancer research. An overexpression and over-activation of EGFR has been related to cancers in which it promotes uncontrolled cell division to eventually form a tumour. converts extracellular signals to activate signalling intracellular pathways such as MAPK/ERK, PI3K/AKT, phosphorylation of phospholipase-Cγ-protein kinase C (PLCγ-PKC), STATs modules and NFκB pathways.

There were two proteins involved in cell signalling. One, EGFR receptor isoform a precursor was down-regulated consistently on (–ve)pST compared to (f)pST.

Another protein was GDP-fucose protein O-fucosyltransferase 1 isoform 1 precursor which was found to increase on both (-ve) and (+ve)pST compared to (f)pST.

Surface topography may potentially influence cell signalling molecules. The fact that the altered signalling molecules of culture in medium with FBS (Table 6 and 9) were different between those of culture without FBS proposes that surface topography factor works along with chemical or nutrient supplement factors, which ultimately determine the cell behaviours.

9.6.4.6 Proteins involved in intermediatery functions

Table 21 The proteins with intermediary functions.

Ribosomal protein, RNA processing	
60S ribosomal protein L27a	- A ribosomal protein.
40S ribosomal protein S20 isoform 2	- A ribosomal protein.
Protein synthesis, processing, degradation and transportation	
ATPase ASNA1	- Involved in protein transportation, insulin signaling.
Prolyl endopeptidase	- Involved in peptide cleavage.

Pre- mRNA splicing	
Probable ATP-dependent RNA helicase DDX46	- Plays an essential role in splicing, either prior to, or during splicing A complex formation.
U4/U6.U5 tri-snRNP-associated protein 2 isoform 4	- Involved in pre-mRNA splicing and regulates AURKB mRNA levels.
Enzymatic activity	
Isochorismatase domain-containing protein 1	- Catalysis of a biochemical reaction
Glyoxylate reductase/hydroxypyruvate reductase	- Enzyme with hydroxy-pyruvate reductase, glyoxylate reductase and D-glycerate dehydrogenase activities.
Translation	
Eukaryotic translation initiation factor 3 subunit M	- Component of the eukaryotic translation initiation factor 3 (eIF-3) complex, which is required for several steps in the initiation of protein synthesis.
Catabolism	
Nicotinate-nucleotide pyrophosphorylase [carboxylating] precursor	- Involved in the catabolism of quinolinic acid (QA).
Vesicles formation	
Clathrin light chain B isoform a	- Clathrin is the major protein of the polyhedral coat of coated pits and vesicles.
Golgi apparatus functions	
ADP-ribosylation factor-like protein 1	- Allosteric activator of the cholera toxin catalytic subunit, an ADP-ribosyltransferase. - Activate phospholipase D with very low efficiency. Involved in maintaining normal function of the Golgi apparatus.
mRNA degradation	
m7GpppX diphosphatase	- mRNA decapping - Involved in the first intron splicing of pre-mRNAs.
Innate immune response	
Macrophage migration inhibitory factor(MIF)	- Expressed at inflammation sites. - A pro-inflammatory cytokine and is part of the innate immune responses to bacterial pathogens

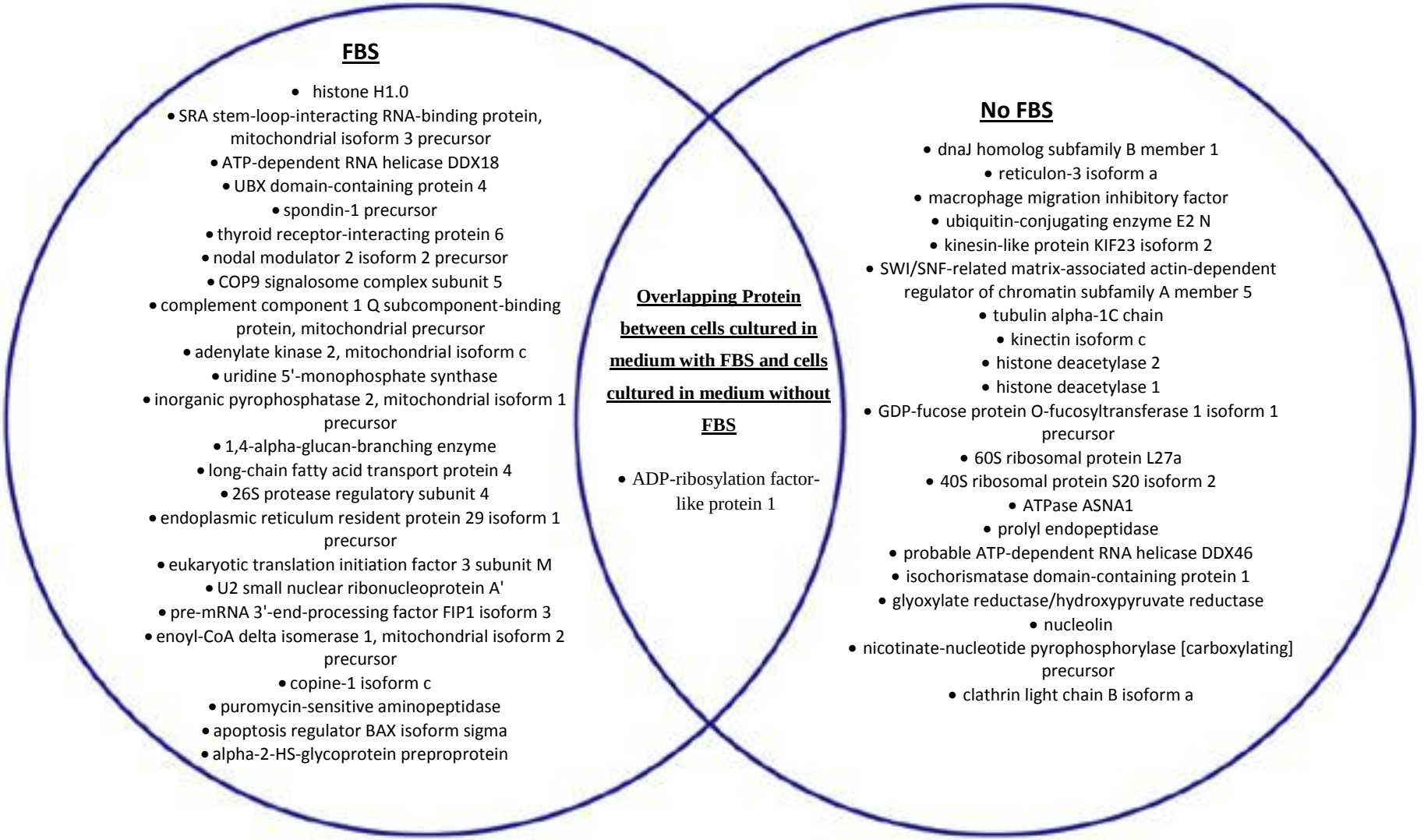
There were a number of proteins involved in intermediatery functions such as regulation of vesicle formation, Glogi apparatus function, mRNA and in innate immune response. An alteration in these proteins suggests a potential role of physical microenvironment in altering cell functions. Further study is needed to further characterize the role of these functions in response to physical topography.

Almost all proteins with intermediatory functions identified in culture medium without FBS were different from the culture in medium with FBS (Table 12), suggesting again the role of FBS in regulation of cell response to the physical microenvironment.

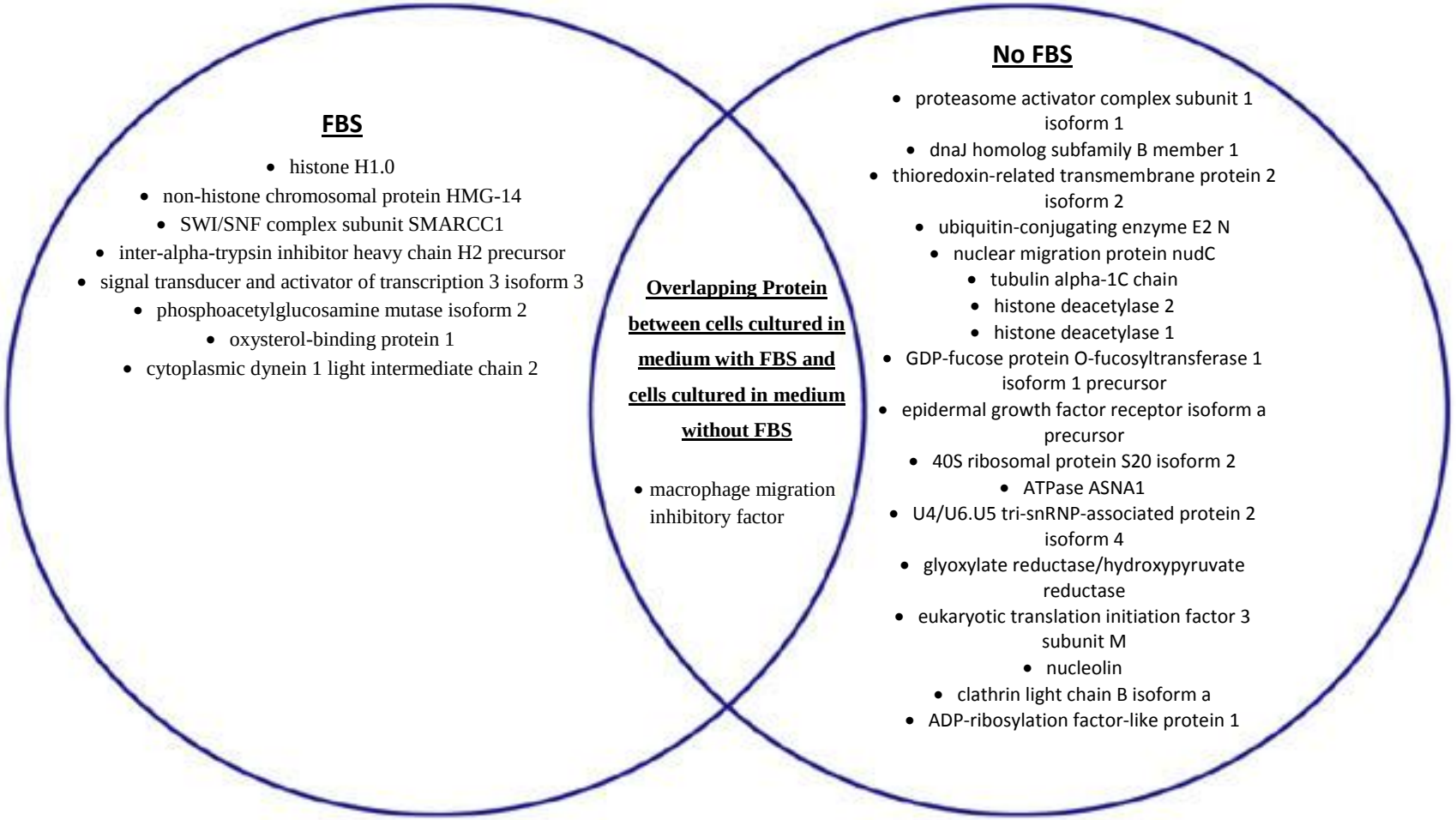
There were two proteins identified to be potentially altered in both culture with and without FBS, and the discussion of this is presented in the next section.

9.6.4.7 Venn diagram of all significant proteins in culture medium with and without FBS conditions

(a)



(b)


FBS
histone H1.0
non-histone chromosomal protein HMG-14
SWI/SNF complex subunit SMARCC1
inter-alpha-trypsin inhibitor heavy chain H2 precursor
signal transducer and activator of transcription 3 isoform 3
phosphoacetylglucosamine mutase isoform 2
oxysterol-binding protein 1
cytoplasmic dynein 1 light intermediate chain 2
Overlapping Protein between cells cultured in medium with FBS and cells cultured in medium without FBS
macrophage migration inhibitory factor
No FBS
proteasome activator complex subunit 1 isoform 1
dnaJ homolog subfamily B member 1
thioredoxin-related transmembrane protein 2 isoform 2
ubiquitin-conjugating enzyme E2 N
nuclear migration protein nudC
tubulin alpha-1C chain
histone deacetylase 2
histone deacetylase 1
GDP-fucose protein O-fucosyltransferase 1 isoform 1 precursor
epidermal growth factor receptor isoform a precursor
40S ribosomal protein S20 isoform 2
ATPase ASNA1
U4/U6.U5 tri-snRNP-associated protein 2 isoform 4
glyoxylate reductase/hydroxypyruvate reductase
eukaryotic translation initiation factor 3 subunit M
nucleolin
clathrin light chain B isoform a
ADP-ribosylation factor-like protein 1

(c)

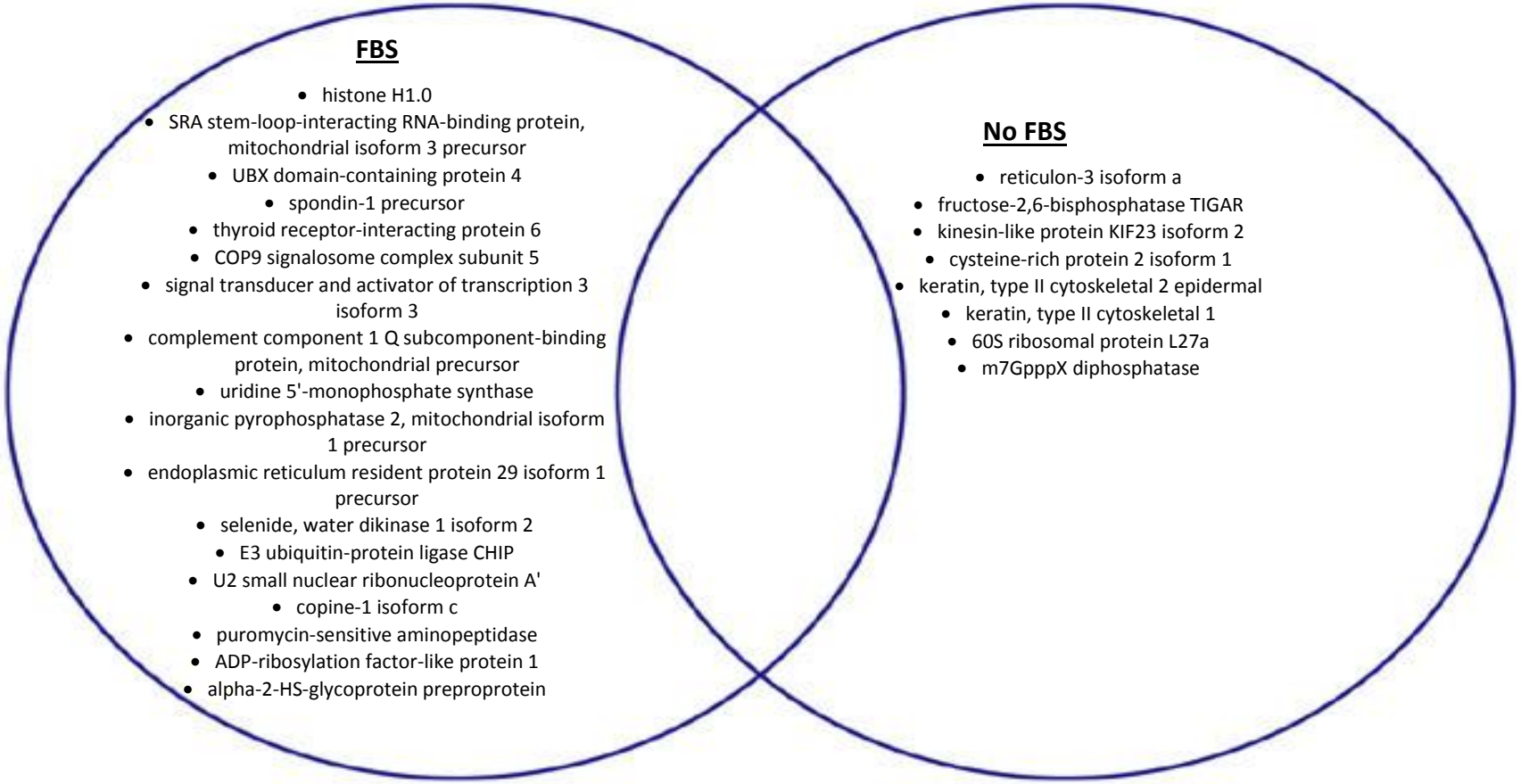


Figure 82 Venn diagrams of proteins identified from iTRAQ analysis of samples of culture with FBS and without FBS and the intersect protein between these samples.

(a) Venn diagram of comparison between (+ve)pST to (f)pST

(b) Venn diagram of comparison between (-ve)pST to (f)pST

(c) Venn diagram of comparison between (+ve)pST to (-ve)pST

The ADP-ribosylation factor-like protein 1 was down-regulated on the (+ve)pST compared to the cells on (-ve) and (f)pST in culture medium with FBS but it was up-regulated on both (+ve)pST and (-ve)pST compared to (f)pST when the cells were cultured in medium without FBS. The ADP-ribosylation factor-like protein 1 is involved in maintaining the Golgi apparatus functions. Golgi apparatus functions in processing, sorting and distributing cell secretion, lipid transportation and lysosome formation. Golgi apparatus has also been related to cellular mechanical response previously (Egea & Serra-Peinado, 2014). The iTRAQ analysis suggests that Golgi apparatus may be responsive to the cell-like topography, and the response depends on the availability of culture serum.

MIF was down-regulated in cells on the (-ve)pST compared to cells on (f)pST in the presence of FBS whereas it was up-regulated on both (+ve) and (-ve)pST compared to (f)pST in serum-free culture medium. The role of MIF in cancer cell growth and its interaction with the integrin has been discussed in section 7.5.5 β1 integrin has been shown to be differently regulated in culture with or without FBS (Figure 29 and 65). This may be the reason for the observed different regulation of MIF in culture medium with or without FBS. However, the involvement of other types of integrin in the interaction with MIF on different topographies, and the more targeted study on this molecule are needed to characterize the role of MIF on the cell-like topography, in culture medium with or without FBS.

Further, iTRAQ suggested that SWI/SNF complex subunit SMARCC1 was down-regulated on the (-ve)pST compared to (f)pST in culture medium with FBS supplement and SMARCA5 was up-regulated on the (+ve)pST compared to (f)pST in serum free culture medium. These two proteins are in the family of SWI/SNF-related matrix-associated actin-dependent regulator of chromatin (SMARC) which is part of the SWI/SNF chromatin remodelling complexes. Mutations of different subunits of SMARC have been related to different type to cancers (Wilson & Roberts, 2011) and some family members of this family were reported to be located at regions that are associated with somatic rearrangements in human cancers (Ring et al., 1998). For example, genetic variant of this family has been associated with hepatocellular carcinoma risk (Zhong et al., 2014). Although different subunits were altered on different topographies with or without FBS, the potential

involvement of SMARC-family in cell response to physical topography through modulating chromatin structure and transcription is worth further studied.

9.6.4.8 Summary

iTRAQ study in Ishikawa cells cultured on surfaces with different physical topography in medium without FBS again suggested alterations of proteins in functional categories that fitted our hypothesis: Ishikawa cells responded to surface topography by altering cell growth-related biomolecules, signalling molecules, cytoskeleton and ECM protein secretion. On the other hand, iTRAQ analysis generates two hypotheses; Ishikawa cells may have modified their nuclear structure in response to physical topography, and also, the activation of stress response in serum-free medium by Ishikawa cells may be affected by physical topography. Future exploration of the influence of physical microenvironment on cell nucleus structure and cell stress pathways is needed.

Although iTRAQ identified a few potential proteins that were responsive to the physical topography, further study is needed to look into the potential proteins because of the limitation of this iTRAQ analysis that only two pooled samples were used for the analysis.

9.6.5 Ishikawa Endometrial Cancer Cell Responses to Cisplatin and Paclitaxel in Culture Medium without FBS

Table 22 Summary of Results from Section 9.5.9.

A table summarizing the extent of cell responsiveness to cisplatin and paclitaxel treatments on (f), (-ve) and (+ve)pST as compared to control DMSO-treated cells, in serum free culture medium (comparing to Table 13).The direction of arrows indicates down-regulation of measured endpoints. The number of the arrows relates to the extent of responsiveness, as compared among (f), (-ve) and (+ve)pST. The "-" symbol indicates no statistically significant difference between the compared groups.

	(f)pST		**(-ve)pST**		**(+ve)pST**	
	Cisplatin	**Paclitaxel**	**Cisplatin**	**Paclitaxel**	**Cisplatin**	**Paclitaxel**
VEGF	-	↑↑	-	↑↑	-	↑
Cell Number	-	-	-	-	-	-
PCNA	-	-	↓	↓	-	-
Cyclin B1	-	↓	-	-	-	-
Cyclin B2	↓	↓	-	-	-	-
Cyclin D2	↓	↓	↓	↓	-	-

9.6.5.1 Cisplatin and Paclitaxel Treatments Effects on Cell VEGF Secretion in Culture Medium without FBS

The control Ishikawa endometrial cancer cells incubated in medium without FBS and without cisplatin or paclitaxel treatments showed highest VEGF secretion on (f)pST compared to cells on (-ve) and (+ve)pST.

Cells are exposed to stress when grown in medium without FBS, and it has been reported that deprivation of amino acid and glucose resulted in an increase in VEGF secretion in cells (Abcouwer et al., 2002). The observation that Ishikawa cells on (f)pST secreted more VEGF than cells on (-ve) and (+ve)pST suggests that cells on (f)pST may experience greater stress, or cells on (f)pST do not up-regulate stress-related proteins as much as cells on (-ve) and (+ve)pST do. Moreover, cells on (+ve)pST secreted significantly lower VEGF than cells on (f) and (-ve)pST within the paclitaxel treatment group. This again suggests that cells on

(+ve)pST may have up-regulated stress-related proteins that may have reduced the cell VEGF response to paclitaxel. This was supported by iTRAQ analysis in which a number of the up-regulated stress-related proteins were observed in cells on (-ve) and (+ve)pST compared to cells on (f)pST.

When cisplatin and paclitaxel were added, cells secreted more VEGF, as compared to the non-treated control cells. VEGF has been reported to assist ovarian cancer cells in developing resistance against cisplatin treatment (Hu et al., 2003). A study that examined VEGF secretion also reported that an increase in the expression of VEGF was one of the cell adaptive stress responses to chemotherapy (Fan et al., 2008). Hence, an increase in VEGF level may be a cell response to stress to enhance cell survival.

In short, in culture medium without FBS, Ishikawa endometrial cancer cell VEGF secretion was affected by surface physical topography. Further, Ishikawa endometrial cancer cells increased the VEGF secretion in response to cisplatin and paclitaxel treatments, and there was no topographical effect in the cell responses to cisplatin. Morever, cells responded to paclitaxel differently on different physical topographies.

9.6.5.2 Cisplatin and Paclitaxel Effects on Cell Growth in Culture Medium without FBS

Ishikawa cells on all substrates with both chemotherapy drugs showed a trend of modestly reduced cell number and expression levels in PCNA, cyclin B1, B2 and D2. However, the chemotherapy drugs may have more consistent effects on Ishikawa cells on (f)pST and (-ve)pST compared to cells on (+ve)pST. A consistency of effect in this context underpins the significant difference observed between treated and control cells, whereas an inconsistency of response is a possible reason for a non-significant observation although a trend of reduction was observed.

Cells on (+ve)pST, in culture medium without FBS and without any treatments had lower growth compared to cells on (f)pST. Hence, paclitaxel, that is cell cycle specific (as discussed in Chapter 8, section 8.6.3) may have less dividing cells to target, resulting in inconsistent efficacy on cells on (+ve)pST compared to cells on (f) and (-ve)pST. Moreover, an activation of cellular stress responses (as shown by iTRAQ analysis, Table 14) may contribute to decreased cellular sensitivity to chemotherapy drugs. This may be because cell stress responses function to minimize any exogenous damage to cell homeostasis and to increase cell recovery from any damage. Any activated self-protection system may also protect cells against chemotherapy drugs treatment. For example, increased heat shock protein (HSP) and NFκB pathway activation (Table 14) are related to resistance to chemotherapy drugs (Ciocca & Calderwood, 2005; Li et al., 2005; Vargas-Roig et al., 1998). Hence, an increase in activities of cell stress response-related proteins may contribute to reduced effectiveness of drugs on cells growing on (+ve)pST compared to cells on (f) and (-ve)pST.

A similar trend of more consistent efficacies of cisplatin and paclitaxel on cells on (f)pST compared to cells on pST culture substrate with cell-like topography was observed in this experiment, compared to previous experiments involving culture medium with FBS supplemented. This implies that surface physical topography, without an additional effect from culture serum, is sufficient to change cell behaviours and cell responses to drug treatments.

9.6.5.3 Cisplatin and Paclitaxel Effects on Cell Growth on Negative Polystyrene Microscope Slide Bioimprint

The cells on (-ve)pST in medium without FBS were more responsive to chemotherapy drugs than cells on (+ve)pST compared to control cells, with regard to the reduction of PCNA and cyclin B2 by both drugs. This was different from cells cultured on (-ve)pST in medium with FBS, in which the cells in medium with FBS showed inconsistent responses to any of the tested chemotherapy drugs.

One possible reason may be that cells on (-ve)pST showed decreased expression of epidermal growth factor receptor isoform a precursor as shown by iTRAQ analysis (Table 14 and 20), which is a tyrosine kinase receptor. An activation of tyrosine kinase signal has been related to cell survival, down-regulation of pro-apoptotic pathways, and resistance to chemotherapy drugs, through activation of NFκB pathway and PI3K/AKT pathway (Kuroda et al., 2010; Lien et al., 2014; Tanaka et al., 2011). Hence, a decreased expression of epidermal growth factor receptor isoform a precursor may have reduced the resistance to drugs in cells growing on (-ve)pST. This resulted in greater responses to cisplatin and paclitaxel.

These observations that there were differences in the cell responses to chemotherapy drugs between cells cultured in medium with or without FBS suggest that cell culture medium serum is important in determining cell behaviours, by activating certain pathways, which then modulate the cell responses to other stimuli. The physical microenvironment, on the other hand, has a role in influencing the pathways that are involved, as shown in our comparisons between cells on (-ve) and (+ve)pST. Most importantly, Ishikawa cells on (f) and (-ve) pST showed slightly more consistent responsiveness to cisplatin and paclitaxel treatments compared to cells on (+ve)pST, even in an absence of FBS factor. This indicates that the cell-like topography with incorporation of physical microenvironment signals modulates cell behaviours and cell responses to external stimuli.

9.7 Conclusion

In an absence of FBS, the cells showed similar spreading behaviours compared to the cells in culture medium with FBS, in which the spreading behaviours were different on different culture substrates with different topographies, indicating a role of surface physical topography in determining cell spreading. Further, similar to the culture in medium with FBS, cells also had lower cell number after 60 hours on pST Bioimprints compared to (f)pST. On (+ve)pST particularly, cells had the lowest cell number compared to (-ve)pST and (f)pST. Also, cells on (+ve)pST showed significantly lower cyclin B2 compared to cells on (f) and (-ve)pST. Combining these results with the above observations from the cell culture in medium with FBS, it may be concluded that the surface topography, especially the (+ve)pST has a

role in modulating the cell spreading area, which then alters the cell biomolecules (cyclin B2) and then changes the cell growth behaviour.

There are some cell behaviours that were differently modulated between culture medium with and without FBS. To begin with, the activation of β1 integrin was not observed in cells cultured in medium without FBS. This may be largely due to a lack of deposition of fibronectin onto the surface, as shown by no RGDS blocking of β1 integrin. Without an activation of β1 integrin, the influences from physical topography were different from those observed in cells cultured in medium with FBS. First, the cell Cytokeratin-18 was not altered, but instead the cell actin showed a trend of decreasing, especially on (+ve)pST compared to (f) and (-ve)pST. Moreover, an activation of FAK was observed on only the (+ve)pST compared to (f) and (-ve)pST. Altogether these observations imply that surface topography has a role in determining cell behaviours, and the topographical effects on cells are in turn influenced by the chemical factors.

Not surprisingly, proteomic analysis suggested that cells cultured in medium without FBS may have activated stress response molecules due to deprivation of cell metabolism-related factors. Unlike cells in medium with FBS in which some energy-related proteins were suggested to have been regulated by surface physical topography, here none of the changed proteins identified were related to energy homeostasis, from our iTRAQ analysis. This is not too surprising since the cells may have been deprived of an energy source that normally is found in FBS. However, the physical topography may have modulated the stress responses that the cells activated.

A different activation of cell stress responses may then have a role in regulating the cell responses to clinical drugs, namely cisplatin and paclitaxel. Cells on (f)pST again showed more consistent responses to chemotherapy drugs than the cells on (+ve)pST. In contrast to cell culture in medium with FBS, the cells on (-ve)pST also showed more consistent significant responses to the drugs. Again, clearly the surface topography and microenvironment chemistry works in conjunction to determine cell behaviours. The cell responses to physical topography depend on the energy and nutrient reservoirs available,

which in turn depend on the source from the cell microenvironment, and also on the intracellular energy and nutrient consumptions.

The results presented in this chapter in culture medium without FBS further favour our hypothesis that surface cell-like physical topography has a role in modulating cell behaviours. Notably, positive topography had a greater impact than negative topography on cells, both in media with and without FBS, which may be due to the more physiologically relevant presentation of this topography.

Chapter 10 Conclusion

Mechanical signal modulation of tissue development, cell alignment and differentiation have been well-studied in the fields of embryonic development, tissue implantation and wound healing. Nevertheless, mechanical influence on cancer development and progression is a relatively new concept in oncology research. The idea that cancer development is also modulated by mechanical signals was initiated from the observation that cancer cell growth and development *in vivo* were very different from *in vitro* conditions (Dolberg & Bissell, 1984; Howlett et al, 1995; Wang et al., 1998), and these phenomena were postulated to be in part due to difference in the physical microenvironment the cancer cells encountered. This idea is also well supported by the fact that a tumour is a stiff tissue (Levental et al., 2009; Paszek et al., 2005; Provenzano et al., 2006), but metastasis cancer cells are softer than non-metastasis cancer cells (Lekka et al., 1999). In fact, it has been suggested that the modest efficiency of current chemotherapy is partly due to a lack of attention to cancer-related physical mechanical signals. Yet the physical factors are generally neglected due to a lack of a satisfactory study model that incorporates this concept in laboratory settings. More recently, 3D cell culture has become more commonly used, and there are an increasing number of studies that particularly examine the effect of culture substrate stiffness on cancer cell behaviours. Relatively fewer studies investigated the influence of physical topography on cancer cells, and these studies examined the effect of regular geometry on cancer cells. Nonetheless, all those few reports showed that cancer cells do respond to surrounding mechanical signals, including physical topography.

Here, we reported the use of a platform with cell-like topography to study Ishikawa endometrial cancer cell behaviours. Further, we studied the effect of cell-like topography separately or incorporated with chemical factors. The chemical factors we studied here were the culture substrate material and and the biological source of chemical factors: the FBS supplement in culture medium. We speculated here that endometrial cancer cells modulated their adhesion, spreading, growth, expression of selected proteins and responses to chemotherapy drugs on culture substrates with cell-like topography. Moreover, chemical factors were joined to physical topography in affecting cell behaviours.

A comparison between glass, tissue culture grade pST and pMA supports our hypothesis that substrate material regulates cell behaviours, and that physically imprinting with cell-like topography alters cell behaviours too. Here, we showed that Ishikawa endometrial cancer cells spread and grew better on hydrophilic and negatively charged glass and tissue culture grade pST surfaces when compared to the more hydrophobic and charge-neutral pMA surface.

When the pMA surface was imprinted with cell-like topography, the physical cell-like features assisted Ishikawa cells to spread and grow better compared to cells on flat pMA. This improved cell spreading was likely through modulating cell adhesion molecule β1 integrin and cell cytoskeleton actin filaments and Cytokeratin-18, associated with an inhibition of FAK activation, and all these may enter an integrated network and eventually enhance growth. Further, we observed that Ishikawa cells increased their VEGF secretion on pMA substrates compared to cells on glass and tissue culture grade pST. An addition of cell-like topography on pMA substrate decreased cell VEGF secretion significantly. Thus topography altered distinct pathways but their interconnections are not yet defined.

Then we fabricated the cell-like topography on a more commonly used culture material, pST. On this favourable cell culture substrate, the topographical effect worked oppositely to restrict Ishikawa cell spreading and growth relative to cells on a flat surface, a process that was also mediated through β1 integrin, cell Cytokeratin-18, and inhibition of FAK activation. The difference in effects between substrates with different physical properties but the same topography raises questions regarding details of the signalling pathways on flat and imprinted surfaces. On pST, the Bioimprint was made in two forms: a pit-like topography, (-ve)pST, versus a hump-like topography, (+ve)pST. A comparison between these two showed that Ishikawa endometrial cancer cells responded to each of these topographies differently. Relative to cells on a flat surface cells on (+ve)pST reduced growth through cyclin B2 whereas cells on (-ve)pST decreased cell growth through lowering PCNA expression. Thus it appears cells are sensitive to nano- or micro- details of substrate topography.

With EGCG, $CoCl_2$, cisplatin and paclitaxel treatments, we observed variation in response to treatments in Ishikawa cells growing on either (+ve)pST or (-ve)pST, compared to cells on (f)pST. These results agreed with other findings that the physical environment can change the cell sensitivity to drug treatments. Moreover, iTRAQ analysis suggested a change in protein expression in response to cell-like topography compared to flat substrate. The proteins identified were mainly involved in alteration of cell nucleus structure, cell energy generation, cell adhesion, ECM proteins, cell cytoskeleton-related and growth behaviours. Notably, some proteins identified by iTRAQ analysis were involved in modulation of cell histone structure and acetylation that controls cell transcription and replication activities. An alteration of those proteins suggests that the physical topography may have changed Ishikawa endometrial cancer cell behaviours through altering the cells' gene expression.

Ishikawa endometrial cancer cells were shown to have preferential attachment on (-ve)pST rather than on (f)pST, which agreed with the previous observation that cells had preferential attachment on (-ve)pMA. A non-preferential attachment on the positive topography may probably be due to the requirement of more energy to spread over the hump-like topography, as suggested by iTRAQ analysis. Most importantly, this preferential activity was not seen on (+ve)pST nor on negative Bioimprints made from a different cell type. This suggests that the cell-like topography is the physical structure that resulted in Ishikawa cell preferential attachment on (-ve)pST, and this is not due to a non-specific gravitational effect or general surface irregularity.

Although Ishikawa endometrial cancer cells did not show a preference to bind on (+ve)pST compared to flat surface, relative to cells on a flat surface a generally greater cell response was observed on the (+ve)pST than cells on (-ve)pST. Compared to cells on (f)pST, the cells on (+ve)pST showed a greater change in cell spreading, growth and expression of adhesion molecules than the cells on (-ve)pST. Further, the iTRAQ analysis also suggested a larger extent of alteration in protein expression in cells on the (+ve)pST than cells on (-ve)pST relative to cells on (f)pST. A more robust effect observed in Ishikawa cells on (+ve)pST than on (-ve)pST compared to (f)pST may be because the hump-like topography more closely resembles the physiological physical microenviroment. Importantly, the lack of growth response in Ishikawa cells to the (+ve) and (-ve)pST of another cell line (HMEC-1) suggests

that not only the hump-like topography is important but the detailed shape of the nano- or micro-environment is also important in directing cells.

In the extended study using serum-free culture medium for Ishikawa endometrial cancer cell culture on pST substrates, we observed that β1 integrin was not involved in the process of cell adhesion in medium without FBS. This may be because the serum-free culture medium contains no fibronectin that activated β1 integrin. This again implies that the cells respond to both surface physical topography and also chemical factors. Despite this difference in β1 integrin activation, the topography factor, without an effect from FBS, showed enhanced activation of FAK, a reduction effect on cell spreading, and cell growth through cyclin B2 on the (+ve)pST compared to cells on (f) and (-ve)pST. Most importantly, cell culture in medium without FBS supplementation similarly showed greater responses to surface topography on the hump-like topography, in which the cells again showed greater alteration in cell growth and expression of adhesion proteins than cells on pit-like topography (compared to cells on flat substrate). Not surprisingly, the proteomic analysis proposed that cells cultured in medium without FBS have activated stress response molecules. However, the physical topography may have modulated the stress responses that the cells activated. This then regulated the cell responses to clinical drugs, namely cisplatin and paclitaxel, in which cells on (+ve)pST showed less consistent sensitivity to both chemotherapy drugs compared to cells on (f) and (-ve)pST.

In short, the results we present here point out that endometrial cancer cell behaviours are regulated by cell-like physical topography that is working in conjunction with substrate material and culture medium chemical factors.

More work is needed for improving the fabrication of cell-like topography onto polymer, which is mainly related to finding a solution to increase consistency of the Bioimprint topography, and in reducing artefacts on the surface. Also, future studies that incorporate the cell-like topography with substrate stiffness are promising to reveal more about cancer cell responses to mechanical signals. Thus it is possible to make the Bioimprint on PDMS, which is a polymer that can be tailored for different stiffness. Moreover, cell migration on cell-like

topography is worth further study since cell migration has been known to be regulated by surface topography. Also, characterization of protein deposition on these culture substrates may characterize the mechanisms of topographical effect on cell behaviours more. Here we observed a lack of response in Ishikawa cells to a non-native Bioimprint, i.e. the Bioimprint of a different cell type. This is worthy of future study to further characterize the Ishikawa cell behaviours. Also, the contact surface between Ishikawa cells and the Bioimprint can be investigated more deeply to study the details of the response of Ishikawa cells to positive and negative topographies. In addition, this project focused on Ishikawa endometrial cancer cells and the study of influence of cell-like topography on other cancer cell types is worthy of exploration.

This project has revealed promising areas of investigation in the topographical influence on cancer cells, which is poorly explored in cancer research, and we are the first to report topographical influence on endometrial cancer cells. Moreover, the topography we used in this project resembled the real nano- and micro-topography of cells, and the model is promising in providing cells more physiologically relevant physical signals. Also, cell culture on the Bioimprint is relatively less complicated and cheaper compared to 3D culture. Further, it enables a top-down approach to studying mechanical signals influence on cells, with or without incorporation of chemical signals.

It is known that the flat surface is not a natural physical microenvironment that any biological cells would encounter; nonetheless, flat culture substrate has been used widely to investigate cancer cell behaviours and responses to potential drugs. This unnatural environment is now suggested to often induce non-natural cell behaviours, which may explain the low success rate for a potential drug to pass from *in vitro* to *in vivo* testing then to the clinical phase. Therefore this project has potential impact on cancer drug design. Here we showed that endometrial cancer cells were responsive to their microenvironment and we speculate that positively imprinted pST may be a culture surface that provides cells with additional physical microenvironment signals compared to the conventional flat pST. Therefore novel drugs can be designed to target mechanical signal-related biomolecules. Also, new drugs may be designed to directly target the physical characteristics of the tumour microenvironment and thereby reduce cancer development.

Additionally, this thesis demonstrated the ability of a few polymers to direct Ishikawa endometrial cancer cell behaviours in a number of directions. This information can be extracted in other fields such as artificial tissue design and wound healing, which requires high or low cell adhesion in different cases. Here we demonstrated that this can be achieved by the choice of materials (hydrophobic or hydroplilic) and surface physical topography.

In summary, the use of culture utilising fabricated cell-like topography has important influences on cancer cell behaviour and should more commonly be incorporated in laboratory research.

References

Abcouwer, S. F., Marjon, P. L., Loper, R. K., & Vander Jagt, D. L. (2002). Response of VEGF expression to amino acid deprivation and inducers of endoplasmic reticulum stress. *Invest Ophthalmol Vis Sci, 43*(8), 2791-2798.

Akiri, G., Sabo, E., Dafni, H., Vadasz, Z., Kartvelishvily, Y., Gan, N., . . . Neufeld, G. (2003). Lysyl oxidase-related protein-1 promotes tumor fibrosis and tumor progression in vivo. *Cancer Research, 63*(7), 1657-1666.

Albert, P. J., & Schwarz, U. S. (2014). Dynamics of cell shape and forces on micropatterned substrates predicted by a cellular Potts model. *Biophys J, 106*(11), 2340-2352. doi: 10.1016/j.bpj.2014.04.036

Allenspach, E. J., Maillard, I., Aster, J. C., & Pear, W. S. (2002). Notch signaling in cancer. *Cancer Biol Ther, 1*(5), 466-476.

Ambs, S., Merriam, W. G., Ogunfusika, M. O., Bennett, W. P., Ishibe, N., Hussain, S. P., . . . Harris, C. C. (1998). p53 and vascular endothelial growth factor regulate tumor growth of NOS2-expressing human carcinoma cells. *Nat Med, 4*(12), 1371-1376. doi: 10.1038/3957

Androic, I., Kramer, A., Yan, R., Rodel, F., Gatje, R., Kaufmann, M., . . . Yuan, J. (2008). Targeting cyclin B1 inhibits proliferation and sensitizes breast cancer cells to taxol. *BMC Cancer, 8*(1), 391.

Anselme, K., Ploux, L., Ponche, A. (2010). Cell/Material Interfaces: Influence of Surface Chemistry and Surface Topography on Cell Adhesion. *Journal of Adhesion Science and Technology*. 24: 831–852.

Arima, Y., & Iwata, H. (2007). Effect of wettability and surface functional groups on protein adsorption and cell adhesion using well-defined mixed self-assembled monolayers. *Biomaterials, 28*(20), 3074-3082. doi: 10.1016/j.biomaterials.2007.03.013

Baillat, G., Siret, C., Delamarre, E., & Luis, J. (2008). Early adhesion induces interaction of FAK and Fyn in lipid domains and activates raft-dependent Akt signaling in SW480 colon cancer cells. *Biochimica et Biophysica Acta (BBA) - Molecular Cell Research, 1783*(12), 2323-2331. doi: http://dx.doi.org/10.1016/j.bbamcr.2008.08.008

Balaban, N. Q., Schwarz, U. S., Riveline, D., Goichberg, P., Tzur, G., Sabanay, I., . . . Geiger, B. (2001). Force and focal adhesion assembly: a close relationship studied using elastic micropatterned substrates. *Nat Cell Biol, 3*(5), 466-472. doi: 10.1038/35074532

Ballestrem, C., Hinz, B., Imhof, B. A., & Wehrle-Haller, B. (2001). Marching at the front and dragging behind: Differential αVβ3-integrin turnover regulates focal adhesion behavior. *Journal of Cell Biology, 155*(7), 1319-1332.

Bell, E., Ivarsson, B., & Merrill, C. (1979). Production of a tissue-like structure by contraction of collagen lattices by human fibroblasts of different proliferative potential in vitro. *Proceedings of the National Academy of Sciences of the United States of America, 76*(3), 1274-1278.

Bellows, C. G., Melcher, A. H., & Aubin, J. E. (1982). Association between tension and orientation of peridontal ligament fibroblasts and exogenous collagen fibres in collagen gels in vitro. *Journal of Cell Science, Vol. 58*, 125-138.

Besser, A., & Safran, S. A. (2006). Force-induced adsorption and anisotropic growth of focal adhesions. *Biophysical Journal, 90*(10), 3469-3484.

Betz, T., Koch, D., Lu, Y.-B., Franze, K., & K äs, J. A. (2011). Growth cones as soft and weak force generators. *Proceedings of the National Academy of Sciences, 108*(33), 13420-13425. doi: 10.1073/pnas.1106145108

Bissell, M. J., & Hines, W. C. (2011). Why don't we get more cancer? A proposed role of the microenvironment in restraining cancer progression. *Nature Medicine, 17*(3), 320-329.

Bloom, S., Lockard, V. G., & Bloom, M. (1996). Intermediate filament-mediated stretch-induced changes in chromatin: A hypothesis for growth initiation in cardiac myocytes. *Journal of Molecular and Cellular Cardiology, 28*(10), 2123-2127.

Bondza, P.K., Metz, C.N., Akoum, A. (2008). Macrophage migration inhibitory factor up-regulates alpha(v)beta(3) integrin and vascular endothelial growth factor expression in endometrial adenocarcinoma cell line Ishikawa. *J Reprod Immunol*. 77(2):142-51.

Bordeleau, F., Galarneau, L., Gilbert, S., Loranger, A., & Marceau, N. (2010). Keratin 8/18 modulation of protein kinase C-mediated integrin-dependent adhesion and migration of liver epithelial cells. *Mol Biol Cell, 21*(10), 1698-1713. doi: 10.1091/mbc.E09-05-0373

Bordeleau, F., Myrand Lapierre, M. E., Sheng, Y., & Marceau, N. (2012). Keratin 8/18 regulation of cell stiffness-extracellular matrix interplay through modulation of Rho-mediated actin cytoskeleton dynamics. *PLoS One, 7*(6), e38780. doi: 10.1371/journal.pone.0038780

Bouvard, D., Pouwels, J., De Franceschi, N., & Ivaska, J. (2013). Integrin inactivators: balancing cellular functions in vitro and in vivo. *Nat Rev Mol Cell Biol, 14*(7), 430-442. doi: 10.1038/nrm3599

Boyd, N. F., Guo, H., Martin, L. J., Sun, L., Stone, J., Fishell, E., . . . Yaffe, M. J. (2007). Mammographic Density and the Risk and Detection of Breast Cancer. *New England Journal of Medicine, 356*(3), 227-236. doi: doi:10.1056/NEJMoa062790

Carey, S. P., Starchenko, A., McGregor, A. L., & Reinhart-King, C. A. (2013). Leading malignant cells initiate collective epithelial cell invasion in a three-dimensional heterotypic tumor spheroid model. *Clin Exp Metastasis, 30*(5), 615-630. doi: 10.1007/s10585-013-9565-x

Carré, A., & Lacarrière, V. (2010). How substrate properties control cell adhesion. A physical-chemical approach. *Journal of Adhesion Science and Technology, 24*(5), 815-830.

Chang, Y. J., Tsai, C. J., Tseng, F. G., Chen, T. J., & Wang, T. W. (2013). Micropatterned stretching system for the investigation of mechanical tension on neural stem cells behavior. *Nanomedicine, 9*(3), 345-355. doi: 10.1016/j.nano.2012.07.008

Chao, E. Y. S., Inoue, N., Ripamonti, U., & Fenwick, S. (2003). Biophysical stimulation of bone fracture repair, regeneration and remodelling. *European Cells and Materials, 6*, 72-85.

Chen, C. S., Mrksich, M., Huang, S., Whitesides, G. M., & Ingber, D. E. (1997a). Geometric control of cell life and death. *Science, 276*(5317), 1425-1428.

Chitcholtan, K., Asselin, E., Parent, S., Sykes, P. H., & Evans, J. J. (2013). Differences in growth properties of endometrial cancer in three dimensional (3D) culture and 2D cell monolayer. *Experimental Cell Research, 319*(1), 75-87.

Chitcholtan, K., Sykes, P., & Evans, J. (2012a). The resistance of intracellular mediators to doxorubicin and cisplatin are distinct in 3D and 2D endometrial cancer. *Journal of Translational Medicine, 10*(1), 38.

Chou, L., Firth, J. D., Uitto, V. J., & Brunette, D. M. (1998). Effects of titanium substratum and grooved surface topography on metalloproteinase-2 expression in human fibroblasts. *Journal of Biomedical Materials Research, 39*(3), 437-445.

Chrzanowska-Wodnicka, M., & Burridge, K. (1996). Rho-stimulated Contractility Drives the Formation of Stress Fibers and Focal Adhesions. *The Journal of Cell Biology, 133*(6), 1404- 1415.

Chun, T. Y., Bloem, L. J., & Pratt, J. H. (2003). Aldosterone inhibits inducible nitric oxide synthase in neonatal rat cardiomyocytes. *Endocrinology, 144*(5), 1712-1717. doi: 10.1210/en.2002-220956

Cichowski, K., Brugge, J. S., & Brass, L. F. (1996). Thrombin receptor activation and integrin engagement stimulate tyrosine phosphorylation of the proto-oncogene product, p95vav, in platelets. *Journal of Biological Chemistry, 271*(13), 7544-7550.

Ciocca, D. R., & Calderwood, S. K. (2005). Heat shock proteins in cancer: Diagnostic, prognostic, predictive, and treatment implications. *Cell Stress and Chaperones, 10*(2), 86-103. doi: 10.1379/CSC-99r.1

Clarke, M. L., Wang, J., & Chen, Z. (2005). Conformational changes of fibrinogen after adsorption. *J Phys Chem B, 109*(46), 22027-22035. doi: 10.1021/jp054456k

Cross, S. E., Jin, Y.-S., Rao, J., & Gimzewski, J. K. (2007). Nanomechanical analysis of cells from cancer patients. *Nat Nano, 2*(12), 780-783. doi: http://www.nature.com/nnano/journal/v2/n12/suppinfo/nnano.2007.388_S1.html

Crowell, J. A., Steele, V. E., Sigman, C. C., & Fay, J. R. (2003). Is Inducible Nitric Oxide Synthase a Target for Chemoprevention? *Molecular Cancer Therapeutics, 2*(8), 815-823.

Cukierman, E., Pankov, R., Stevens, D. R., & Yamada, K. M. (2001). Taking cell-matrix adhesions to the third dimension. *Science, 294*(5547), 1708-1712. doi: 10.1126/science.1064829

Curtis, A. S. G., Forrester, J. V., McInnes, C., & Lawrie, F. (1983). Adhesion of cells to polystyrene surfaces. *Journal of Cell Biology, 97*(5 I), 1500-1506.

Dai, G., Kaazempur-Mofrad, M. R., Natarajan, S., Zhang, Y., Vaughn, S., Blackman, B. R., . . . Gimbrone Jr, M. A. (2004). Distinct endothelial phenotypes evoked by arterial waveforms derived from atherosclerosis-susceptible and -resistant regions of human vasculature. *Proceedings of the National Academy of Sciences of the United States of America, 101*(41), 14871-14876.

Dalby, M. J., Gadegaard, N., Herzyk, P., Sutherland, D., Agheli, H., Wilkinson, C. D. W., & Curtis, A. S. G. (2007). Nanomechanotransduction and interphase nuclear organization influence on genomic control. *Journal of Cellular Biochemistry, 102*(5), 1234-1244.

Dalby, M. J., Gadegaard, N., Tare, R., Andar, A., Riehle, M. O., Herzyk, P., . . . Oreffo, R. O. C. (2007). The control of human mesenchymal cell differentiation using nanoscale symmetry and disorder. *Nature Materials, 6*(12), 997-1003.

Dann, J. (2011). *Regulation of Vascular Endothelial Growth Factor in Endometrial Cancer Cells by Food Compounds* (Master dissertation). Retrieved from http://ir.canterbury.ac.nz/bitstream/handle/10092/2113/thesis_fulltext.pdf?sequence=1

Decitre, M., Gleyzal, C., Raccurt, M., Peyrol, S., Aubert-Foucher, E., Csiszar, K., & Sommer, P. (1998). Lysyl oxidase-like protein localizes to sites of de novo fibrinogenesis in fibrosis and in the early stromal reaction of ductal breast carcinomas. *Laboratory Investigation, 78*(2), 143-151.

Deng, G., Lu, Y., Zlotnikov, G., Thor, A. D., & Smith, H. S. (1996). Loss of heterozygosity in normal tissue adjacent to breast carcinomas. *Science, 274*(5295), 2057-2059.

Dennerll, T. J., Joshi, H. C., Steel, V. L., Buxbaum, R. E., & Heidemann, S. R. (1988). Tension and compression in the cytoskeleton of PC-12 neurites II: Quantitative measurements. *Journal of Cell Biology, 107*(2), 665-674.

Denti, S., Fernandez-Sanchez, M. E., Rogge, L., & Bianchi, E. (2006). The COP9 signalosome regulates Skp2 levels and proliferation of human cells. *J Biol Chem, 281*(43), 32188-32196. doi: 10.1074/jbc.M604746200

Dewez, J. L., Berger, V., Schneider, Y. J., & Rouxhet, P. G. (1997). Influence of substrate hydrophobicity on the adsorption of collagen in the presence of pluronic F68, albumin, or calf serum. *Journal of Colloid and Interface Science, 191*(1), 1-10.

Dewez, J. L., Lhoest, J. B., Detrait, E., Berger, V., Dupont-Gillain, C. C., Vincent, L. M., . . . Rouxhet, P. G. (1998). Adhesion of mammalian cells to polymer surfaces: from physical chemistry of surfaces to selective adhesion on defined patterns. *Biomaterials, 19*(16), 1441-1445.

Ding, H.F.,Rimsky, S., Batson, S.C., Bustin, M., Hansen, U. (1994). Stimulation of RNA polymerase II elongation by chromosomal protein HMG-14. *Science*, 265(5173), 796-9.

Dobbs, L. G., & Gutierrez, J. A. (2001). Mechanical forces modulate alveolar epithelial phenotypic expression. *Comp Biochem Physiol A Mol Integr Physiol, 129*(1), 261-266.

Dolberg, D. S., & Bissell, M. J. (1984). Inability of Rous sarcoma virus to cause sarcomas in the avian embryo. *Nature, 309*(5968), 552-556.

Dunlop, M. G., Dobbins, S. E., Farrington, S. M., Jones, A. M., Palles, C., Whiffin, N., . . . Houlston, R. S. (2012). Common variation near CDKN1A, POLD3 and SHROOM2 influences colorectal cancer risk. *Nat Genet, 44*(7), 770-776. doi: 10.1038/ng.2293

Dunn, G. A., & Heath, J. P. (1976). A new hypothesis of contact guidance in tissue cells. *Exp Cell Res, 101*(1), 1-14.

Egea, G., Serra-Peinado, C. (2014). Golgi Apparatus: Finally Mechanics Comes to Play in the Secretory Pathway. *Current Biology*. 24 (16): R741–R743.

Ehrlich, H. P., Rockwell, W. B., Cornwell, T. L., & Rajaratnam, J. B. M. (1991). Demonstration of a direct role for myosin light chain kinase in fibroblast-populated collagen lattice contraction. *Journal of Cellular Physiology, 146*(1), 1-7.

Ermakova, S., Choi, B. Y., Choi, H. S., Kang, B. S., Bode, A. M., & Dong, Z. (2005). The intermediate filament protein vimentin is a new target for epigallocatechin gallate. *J Biol Chem, 280*(17), 16882-16890. doi: 10.1074/jbc.M414185200

Evans-Nguyen, K. M., Tolles, L. R., Gorkun, O. V., Lord, S. T., & Schoenfisch, M. H. (2005). Interactions of thrombin with fibrinogen adsorbed on methyl-, hydroxyl-, amine-, and carboxyl-terminated self-assembled monolayers. *Biochemistry, 44*(47), 15561-15568. doi: 10.1021/bi0514358

Fan, F., Gray, M. J., Dallas, N. A., Yang, A. D., Van Buren, G., 2nd, Camp, E. R., & Ellis, L. M. (2008). Effect of chemotherapeutic stress on induction of vascular endothelial growth factor family members and receptors in human colorectal cancer cells. *Mol Cancer Ther, 7*(9), 3064-3070. doi: 10.1158/1535-7163.mct-08-0615

Faure, C., Linossier, M.-T., Malaval, L., Lafage-Proust, M.-H., Peyroche, S., Vico, L., & Guignandon, A. (2008). Mechanical signals modulated vascular endothelial growth factor-A (VEGF-A) alternative splicing in osteoblastic cells through actin polymerisation. *Bone, 42*(6), 1092-1101. doi: http://dx.doi.org/10.1016/j.bone.2008.02.011

Fels, J., Callies, C., Kusche-Vihrog, K., & Oberleithner, H. (2010). Nitric oxide release follows endothelial nanomechanics and not vice versa. *Pflugers Archiv European Journal of Physiology, 460*(5), 915-923.

Fels, J., Jeggle, P., Kusche-Vihrog, K., & Oberleithner, H. (2012). Cortical Actin Nanodynamics Determines Nitric Oxide Release in Vascular Endothelium. *PLoS One, 7*(7), e41520. doi: 10.1371/journal.pone.0041520

Feng, X., Tonnesen, M. G., Peerschke, E. I., & Ghebrehiwet, B. (2002). Cooperation of C1q receptors and integrins in C1q-mediated endothelial cell adhesion and spreading. *J Immunol, 168*(5), 2441-2448.

Fojo, T., & Grady, C. (2009). How much is life worth: cetuximab, non-small cell lung cancer, and the $440 billion question. *J Natl Cancer Inst, 101*(15), 1044-1048. doi: 10.1093/jnci/djp177

Folkman, J., & Moscona, A. (1978). Role of cell shape in growth control. *Nature, 273*(5661), 345-349.

Forscher, P., & Smith, S. J. (1988). Actions of cytochalasins on the organization of actin filaments and microtubules in a neuronal growth cone. *Journal of Cell Biology, 107*(4), 1505-1516.

Fourre, N., Millerot-Serrurot, E., Garnotel, R., Zahm, J. M., Bonnet, N., Millot, J. M., & Jeannesson, P. (2008). Extracellular matrix proteins protect human HT1080 cells against the antimigratory effect of doxorubicin. *Cancer Science, 99*(8), 1699-1705.

Frey, M.T., Tsai, I. Y., Russell, T.P., Hanks, S. K., Wang, Y. L. (2006). Cellular Responses to Substrate Topography: Role of Myosin II and Focal Adhesion Kinase. *Biophysical Journal.* 90(10): 3774-3782.

Fritsch, A., Hockel, M., Kiessling, T., Nnetu, K. D., Wetzel, F., Zink, M., & Kas, J. A. (2010). Are biomechanical changes necessary for tumour progression? *Nat Phys, 6*(10), 730-732.

Galbraith, C. G., Yamada, K. M., & Sheetz, M. P. (2002). The relationship between force and focal complex development. *Journal of Cell Biology, 159*(4), 695-705.

Gehler, S., Ponik, S. M., Riching, K. M., & Keely, P. J. (2013). Bi-directional signaling: extracellular matrix and integrin regulation of breast tumor progression. *Crit Rev Eukaryot Gene Expr, 23*(2), 139-157.

Gilchrist, C. L., Ruch, D. S., Little, D., & Guilak, F. (2014). Micro-scale and meso-scale architectural cues cooperate and compete to direct aligned tissue formation. *Biomaterials, 35*(38), 10015-10024. doi: 10.1016/j.biomaterials.2014.08.047

Gilman, A. (1963). The initial clinical trial of nitrogen mustard. *The American Journal of Surgery, 105*(5), 574-578. doi: http://dx.doi.org/10.1016/0002-9610(63)90232-0

Giovinazzi, S., Lindsay, C. R., Morozov, V. M., Escobar-Cabrera, E., Summers, M. K., Han, H. S., . . . Ishov, A. M. (2012). Regulation of mitosis and taxane response by Daxx and Rassf1. *Oncogene, 31*(1), 13-26. doi: http://www.nature.com/onc/journal/v31/n1/suppinfo/onc2011211s1.html

Gipson, I. K., & Anderson, R. A. (1979). Actin filaments in cells of human trabecular meshwork and Schlemm's canal. *Investigative Ophthalmology and Visual Science, 18*(6), 547-561.

Glushankova, N. A., & Vasil'ev Iu, M. (1986). [Sensitivity of the proliferation of normal and tumor cells to cytochalasin D]. *Tsitologiia, 28*(12), 1294-1298.

Godfrey, V., Martin, A. L., Struthers, A. D., & Lyles, G. A. (2011). Effects of aldosterone and related steroids on LPS-induced increased expression of inducible NOS in rat aortic smooth muscle cells. *Br J Pharmacol, 164*(8), 2003-2014. doi: 10.1111/j.1476-5381.2011.01523.x

Goral, V. N., Hsieh, Y. C., Petzold, O. N., Faris, R. A., & Yuen, P. K. (2011). Hot embossing of plastic microfluidic devices using poly(dimethylsiloxane) molds. *Journal of Micromechanics and Microengineering, 21*(1).

Gormar, F. E., Bernd, A., Bereiter-Hahn, J., & Holzmann, H. (1990). A new model of epidermal differentiation: Induction by mechanical stimulation. *Archives of Dermatological Research, 282*(1), 22-32.

Goto, T., & Brunette, D. M. (1998). Surface topography and serum concentration affect the appearance of tenascin in human gingival fibroblasts in vitro. *Exp Cell Res, 244*(2), 474-480.

Grassian, A.R., Coloff, J.L., Brugge, J.S. (2011). Extracellular matrix regulation of metabolism and implications for tumorigenesis. *Cold Spring Harb Symp Quant Biol*. 76: 313 – 324.

Grinnell, F., & Feld, M. K. (1981). Adsorption characteristics of plasma fibronectin in relationship to biological activity. *Journal of Biomedical Materials Research, 15*(3), 363-381. doi: 10.1002/jbm.820150308

Grinnell, F., & Feld, M. K. (1982). Fibronectin adsorption on hydrophilic and hydrophobic surfaces detected by antibody binding and analyzed during cell adhesion in serum-containing medium. *Journal of Biological Chemistry, 257*(9), 4888-4893.

Grinnell, F., Ho, C.-H., Lin, Y.-C., & Skuta, G. (1998). Differences in the Regulation of Fibroblast Contraction of Floating Versus Stressed Collagen Matrices. *The Journal of Biological Chemistry, 274*(2), 918–923.

Grinnell, F., & Lamke, C. R. (1984). Reorganization of hydrated collagen lattices by human skin fibroblasts. *Journal of Cell Science, VOL. 66*, 51-63.

Gruber, H. E., & Hanley Jr, E. N. (2000). Human disc cells in monolayer vs 3D culture: Cell shape, division and matrix formation. *BMC Musculoskeletal Disorders, 1*, 1-6.

Gu, J. W., Makey, K. L., Tucker, K. B., Chinchar, E., Mao, X., Pei, I., . . . Miele, L. (2013). EGCG, a major green tea catechin suppresses breast tumor angiogenesis and growth via inhibiting the activation of HIF-1alpha and NFkappaB, and VEGF expression. *Vasc Cell, 5*(1), 9. doi: 10.1186/2045-824x-5-9

Haapala, J., Lammi, M. J., Inkinen, R., Parkkinen, J. J., Ågren, U. M., Arokoski, J., . . . Tammi, M. I. (1996). Coordinated regulation of hyaluronan and aggrecan content in the articular cartilage of immobilized and exercised dogs. *Journal of Rheumatology, 23*(9), 1586-1593.

Hamilton, D. W., & Brunette, D. M. (2007). The effect of substratum topography on osteoblast adhesion mediated signal transduction and phosphorylation. *Biomaterials, 28*(10), 1806-1819.

Han, J., Das, B., Wei, W., Van Aelst, L., Mosteller, R. D., Khosravi-Far, R., . . . Broek, D. (1997). Lck regulates Vav activation of members of the Rho family of GTPases. *Molecular and Cellular Biology, 17*(3), 1346-1353.

Hanahan, D. & Weinberg, R.A. (2011). Hallmarks of cancer: the next generation. *Cell*, 144(5), 646-674.

Hanahan, D., Weinberg, R.A. (2000). The Hallmarks of cancer: the next generation. *Cell.* 100(1):57-70.

Harold, F. M. (1962). Depletion and replenishment of the inorganic polyphosphate pool in Neurospora crassa. *J Bacteriol, 83*, 1047-1057.

Harris, A. K., Stopak, D., & Wild, P. (1981). Fibroblast traction as a mechanism for collagen morphogenesis. *Nature, 290*(5803), 249-251.

Harris, A. L. (2002). Hypoxia - A key regulatory factor in tumour growth. *Nature Reviews Cancer, 2*(1), 38-47.

Harrison, R. (1907). Observations on the living developing nerve fiber. *The Anatomical Record.* 1:116-128.

Hayashi, N., & Cunha, G. R. (1991). Mesenchyme-induced Changes in the Neoplastic Characteristics of the Dunning Prostatic Adenocarcinoma. *Cancer Research, 51*(18), 4924-4930.

Hogg, S.J., Evans, J.J., Sykes, P.H., Chitcholtan, K. (2015). A method to investigate the anti-metabolic activity of anti-cancer agents on ovarian cancer cells cultured in a 96-well high throughput format. *Journal of Ovarian Research*. 4;8(1):43.

Hongisto, V., Jernström, S., Fey, V., Mpindi, J.-P., Kleivi Sahlberg, K., Kallioniemi, O., & Perälä, M. (2013). High-Throughput 3D Screening Reveals Differences in Drug

Sensitivities between Culture Models of JIMT1 Breast Cancer Cells. *PLoS One, 8*(10), e77232. doi: 10.1371/journal.pone.0077232

Hooper, S. B., & Wallace, M. J. (2006). Role of the physicochemical environment in lung development. *Clin Exp Pharmacol Physiol, 33*(3), 273-279. doi: 10.1111/j.1440-1681.2006.04358.x

Horbett, T. A., Waldburger, J. J., Ratner, B. D., & Hoffman, A. S. (1988). Cell adhesion to a series of hydrophilic-hydrophobic copolymers studied with a spinning disc apparatus. *Journal of Biomedical Materials Research, 22*(5), 383-404.

Horiuchi, R., Akimoto, T., Hong, Z., & Ushida, T. (2012). Cyclic mechanical strain maintains Nanog expression through PI3K/Akt signaling in mouse embryonic stem cells. *Exp Cell Res, 318*(14), 1726-1732. doi: 10.1016/j.yexcr.2012.05.021

Howlett, A. R., Bailey, N., Damsky, C., Petersen, O. W., & Bissell, M. J. (1995). Cellular growth and survival are mediated by β1 integrins in normal human breast eqithelium but not in breast carcinoma. *Journal of Cell Science, 108*(5), 1945-1957.

Howlett, A. R., Petersen, O. W., Steeg, P. S., & Bissell, M. J. (1994). A novel function for the nm23-H1 gene: Overexpression in human breast carcinoma cells leads to the formation of basement membrane and growth arrest. *Journal of the National Cancer Institute, 86*(24), 1838-1844.

Hu, G., Ryan, S., Zhu, Y., Reed, E., Li, X., Wang, G., & Li, Q. (2003). Vascular endothelial growth factor modulates cisplatin sensitivity in human ovarian carcinoma cells. *Cancer Therapy, 1*, 31-37.

Huang, S., Chen, C. S., & Ingber, D. E. (1998). Control of cyclin D1, p27(Kip1), and cell cycle progression in human capillary endothelial cells by cell shape and cytoskeletal tension. *Mol Biol Cell, 9*(11), 3179-3193.

Ikada, Y. (1994). Surface modification of polymers for medical applications. *Biomaterials*. 15: 725–736.

Ingber, D. E., Prusty, D., Sun, Z., Betensky, H., & Wang, N. (1995). Cell shape, cytoskeletal mechanics, and cell cycle control in angiogenesis. *J Biomech, 28*(12), 1471-1484.

Jamaladdin, S., Kelly, R. D., O'Regan, L., Dovey, O. M., Hodson, G. E., Millard, C. J., . . . Cowley, S. M. (2014). Histone deacetylase (HDAC) 1 and 2 are essential for accurate cell division and the pluripotency of embryonic stem cells. *Proc Natl Acad Sci U S A, 111*(27), 9840-9845. doi: 10.1073/pnas.1321330111

Kajita, M., Itoh, Y., Chiba, T., Mori, H., Okada, A., Kinoh, H., & Seiki, M. (2001). Membrane-type 1 matrix metalloproteinase cleaves CD44 and promotes cell migration. *Journal of Cell Biology, 153*(5), 893-904.

Karuri, N. W., Liliensiek, S., Teixeira, A. I., Abrams, G., Campbell, S., Nealey, P. F., & Murphy, C. J. (2004). Biological length scale topography enhances cell-substratum adhesion of human corneal epithelial cells. *J Cell Sci, 117*(Pt 15), 3153-3164. doi: 10.1242/jcs.01146

Katoh, H., Harada, A., Mori, K., & Negishi, M. (2002). Socius is a novel Rnd GTPase-interacting protein involved in disassembly of actin stress fibers. *Mol Cell Biol, 22*(9), 2952-2964.

Kawahara, H., Soeda, Y., Niwa, K., Takahashi, M., Kawahara, D., & Araki, N. (2004). In vitro study on bone formation and surface topography from the standpoint of biomechanics. *Journal of Materials Science: Materials in Medicine, 15*(12), 1297-1307.

Kelman, Z. (1997). PCNA: structure, functions and interactions. *Oncogene, 14*(6), 629-640. doi: 10.1038/sj.onc.1200886

Keselowsky, B. G., Collard, D. M., & Garcia, A. J. (2004). Surface chemistry modulates focal adhesion composition and signaling through changes in integrin binding. *Biomaterials, 25*(28), 5947-5954. doi: 10.1016/j.biomaterials.2004.01.062

Kidambi, S., Udpa, N., Schroeder, S. A., Findlan, R., Lee, I., & Chan, C. (2007). Cell adhesion on polyelectrolyte multilayer coated polydimethylsiloxane surfaces with varying topographies. *Tissue Engineering, 13*(8), 2105-2117. doi: 10.1089/ten.2006.0151

Kim, W., Seok, K. Y., Soo, K. J., Shin, N.Y., Hanks, S.K., Song, W.K. (2008). The integrin-coupled signaling adaptor p130Cas suppresses Smad3 function in transforming growth factor-beta signaling. *Mol Biol Cell*. 19: 2135 – 2146.

Kirsch, T., Beese, M., Wyss, K., Klinge, U., Haller, H., Haubitz, M., & Fiebeler, A. (2013). Aldosterone modulates endothelial permeability and endothelial nitric oxide synthase activity by rearrangement of the actin cytoskeleton. *Hypertension, 61*(2), 501-508. doi: 10.1161/hypertensionaha.111.196832

Klein, C. E., Dressel, D., Steinmayer, T., Mauch, C., Eckes, B., Krieg, T., . . . Weber, L. (1991). Integrin α2β1 is upregulated in fibroblasts and highly aggressive melanoma cells in three-dimensional collagen lattices and mediates the reorganization of collagen I fibrils. *Journal of Cell Biology, 115*(5), 1427-1436.

Kornberg, L., Earp, H. S., Parsons, J. T., Schaller, M., & Juliano, R. L. (1992). Cell adhesion or integrin clustering increases phosphorylation of a focal adhesion-associated tyrosine kinase. *Journal of Biological Chemistry, 267*(33), 23439-23442.

Kornberg, L. J., Earp, H. S., Turner, C. E., Prockop, C., & Juliano, R. L. (1991). Signal transduction by integrins: Increased protein tyrosine phosphorylation caused by clustering of β1 integrins. *Proceedings of the National Academy of Sciences of the United States of America, 88*(19), 8392-8396.

Kraning-Rush, C. M., Califano, J. P., & Reinhart-King, C. A. (2012). Cellular traction stresses increase with increasing metastatic potential. *PLoS One, 7*(2).

Krtolica, A., Parrinello, S., Lockett, S., Desprez, P. Y., & Campisi, J. (2001). Senescent fibroblasts promote epithelial cell growth and tumorigenesis: A link between cancer and aging. *Proceedings of the National Academy of Sciences of the United States of America, 98*(21), 12072-12077.

Kultz, D. (2005). Molecular and evolutionary basis of the cellular stress response. *Annu Rev Physiol, 67*, 225-257. doi: 10.1146/annurev.physiol.67.040403.103635

Kumar, A., & Boriek, A. M. (2003). Mechanical stress activates the nuclear factor-kappaB pathway in skeletal muscle fibers: a possible role in Duchenne muscular dystrophy. *Faseb j, 17*(3), 386-396. doi: 10.1096/fj.02-0542com.

Kunimura, C., Kikuchi, K., Ahmed, N., Shimizu, A., Yasumoto, S. (1998). Telomerase activity in a specific cell subset co-expressing integrinbeta1/ EGFR but not p75NGFR/bcl2/integrin beta4 in normal human epithelial cells. *Oncogene.* 17: 187 – 197.

Kuroda, H., Takeno, M., Murakami, S., Miyazawa, N., Kaneko, T., & Ishigatsubo, Y. (2010). Inhibition of heme oxygenase-1 with an epidermal growth factor receptor inhibitor and cisplatin decreases proliferation of lung cancer A549 cells. *Lung Cancer, 67*(1), 31-36. doi: 10.1016/j.lungcan.2009.03.015

Kwon, K. W., Choi, J. C., Suh, K. Y., & Doh, J. (2011). Multiscale fabrication of multiple proteins and topographical structures by combining capillary force lithography and microscope projection photolithography. *Langmuir, 27*(7), 3238-3243.

Lamoureux, P., Buxbaum, R. E., & Heidemann, S. R. (1989). Direct evidence that growth cones pull. *Nature, 340*(6229), 159-162. doi: 10.1038/340159a0

Lampin, M., Warocquier-Clérout, R., Legris, C., Degrange, M., & Sigot-Luizard, M. F. (1997). Correlation between substratum roughness and wettability, cell adhesion, and cell migration. *Journal of Biomedical Materials Research, 36*(1), 99-108.

Landriscina, M., Maddalena, F., Laudiero, G., & Esposito, F. (2009). Adaptation to oxidative stress, chemoresistance, and cell survival. *Antioxid Redox Signal, 11*(11), 2701-2716. doi: 10.1089/ars.2009.2692

Le Beyec, J., Xu, R., Lee, S. Y., Nelson, C. M., Rizki, A., Alcaraz, J., & Bissell, M. J. (2007). Cell shape regulates global histone acetylation in human mammary epithelial cells. *Experimental Cell Research, 313*(14), 3066-3075.

Lechner, M., Lirk, P., & Rieder, J. (2005). Inducible nitric oxide synthase (iNOS) in tumor biology: the two sides of the same coin. *Semin Cancer Biol, 15*(4), 277-289. doi: 10.1016/j.semcancer.2005.04.004

Lee, C.Y., Su, M.J., Huang, C.Y., Chen, M.Y., Hsu, H.C., Lin, C.Y., Tang, C.H. (2012). Macrophage migration inhibitory factor increases cell motility and up-regulates αvβ3 integrin in human chondrosarcoma cells. *J Cell Biochem*. 113(5):1590-8.

Lee, D. J., Ho, C.-H., & Grinnell, F. (2003). LPA-stimulated fibroblast contraction of floating collagen matrices does not require Rho kinase activity or retraction of fibroblast extensions. *Experimental Cell Research, 289*, 86-94.

Lee, J., Mhawech-Fauceglia, P., Lee, N., Parsanian, L., Gail Lin, Y., Gayther, S., & Lawrenson, K. (2013). A three-dimensional microenvironment alters protein expression and chemosensitivity of epithelial ovarian cancer cells in vitro. *Lab Invest, 93*(5), 528-542. doi: 10.1038/labinvest.2013.41

Lee, Y., Koay, E. J., Zhang, W., Qin, L., Kirui, D. K., Hussain, F., . . . Ferrari, M. (2014). Human equilibrative nucleoside transporter-1 knockdown tunes cellular mechanics through epithelial-mesenchymal transition in pancreatic cancer cells. *PLoS One, 9*(10).

Lekka, M., Laidler, P., Gil, D., Lekki, J., Stachura, Z., & Hrynkiewicz, A. Z. (1999). Elasticity of normal and cancerous human bladder cells studied by scanning force microscopy. *European Biophysics Journal, 28*(4), 312-316. doi: 10.1007/s002490050213

Lelièvre, S. A., Weaver, V. M., Nickerson, J. A., Larabell, C. A., Bhaumik, A., Petersen, O. W., & Bissell, M. J. (1998). Tissue phenotype depends on reciprocal interactions between the extracellular matrix and the structural organization of the nucleus. *Proceedings of the National Academy of Sciences of the United States of America, 95*(25), 14711-14716.

Levental, K. R., Yu, H., Kass, L., Lakins, J. N., Egeblad, M., Erler, J. T., . . . Weaver, V. M. (2009). Matrix Crosslinking Forces Tumor Progression by Enhancing Integrin Signaling. *Cell, 139*(5), 891-906. doi: http://dx.doi.org/10.1016/j.cell.2009.10.027

Lewis, J.M., Truong, T.N., Schwartz, M.A. (2002). Integrins regulate the apoptotic response to DNA damage through modulation of p53. *Proc Natl Acad Sci USA*. 99: 3627 – 3632.

Leychenko, A., Konorev, E., Jijiwa, M., & Matter, M. L. (2011). Stretch-induced hypertrophy activates NFkB-mediated VEGF secretion in adult cardiomyocytes. *PLoS One, 6*(12), e29055. doi: 10.1371/journal.pone.0029055

Li, L. M., Kilbourn, R. G., Adams, J., & Fidler, I. J. (1991). Role of nitric oxide in lysis of tumor cells by cytokine-activated endothelial cells. *Cancer Res, 51*(10), 2531-2535.

Li, Y., Ahmed, F., Ali, S., Philip, P. A., Kucuk, O., & Sarkar, F. H. (2005). Inactivation of nuclear factor kappaB by soy isoflavone genistein contributes to increased apoptosis induced by chemotherapeutic agents in human cancer cells. *Cancer Res, 65*(15), 6934-6942. doi: 10.1158/0008-5472.can-04-4604

Lien, G.-S., Wu, M.-S., Bien, M.-Y., Chen, C.-H., Lin, C.-H., & Chen, B.-C. (2014). Epidermal Growth Factor Stimulates Nuclear Factor-κB Activation and Heme Oxygenase-1 Expression via c-Src, NADPH Oxidase, PI3K, and Akt in Human Colon Cancer Cells. *PLoS ONE, 9*(8), e104891. doi: 10.1371/journal.pone.0104891

Liliensiek, S. J., Campbell, S., Nealey, P. F., & Murphy, C. J. (2006). The scale of substratum topographic features modulates proliferation of corneal epithelial cells and corneal fibroblasts. *Journal of Biomedical Materials Research - Part A, 79*(1), 185-192.

Lim, J. Y., Hansen, J. C., Siedlecki, C. A., Runt, J., & Donahue, H. J. (2005). Human foetal osteoblastic cell response to polymer-demixed nanotopographic interfaces. *Journal of the Royal Society Interface, 2*(2), 97-108.

Lim, S.T., Chen, X.L., Lim, Y., Hanson, D.A., Vo, T.T., Howerton, K., Larocque, N. et al. (2008). Nuclear FAK promotes cell proliferation and survival through FERM-enhanced p53 degradation. *Mol Cell*. 29: 9 – 22.

Liu, J., Agarwal, S. (2010). Mechanical signals activate vascular endothelial growth factor receptor-2 to upregulate endothelial cell proliferation during inflammation. *J Immunol*. 185: 1215 – 1221.

Liu, N., Zhou, C., Zhao, J., & Chen, Y. (2012). Reversal of paclitaxel resistance in epithelial ovarian carcinoma cells by a MUC1 aptamer-let-7i chimera. *Cancer Invest, 30*(8), 577-582. doi: 10.3109/07357907.2012.707265

Liu, X. H., Kirschenbaum, A., Yao, S., Stearns, M. E., Holland, J. F., Claffey, K., & Levine, A. C. (1999). Upregulation of vascular endothelial growth factor by cobalt chloride-simulated hypoxia is mediated by persistent induction of cyclooxygenase-2 in a metastatic human prostate cancer cell line. *Clin Exp Metastasis, 17*(8), 687-694.

Lizana, L., Bauer, B., & Orwar, O. (2008). Controlling the rates of biochemical reactions and signaling networks by shape and volume changes. *Proceedings of the National Academy of Sciences of the United States of America, 105*(11), 4099-4104.

Lodish, H., Berk, A., Zipursky, S. L., Matsudaira, P., Baltimore, D., & Darnell, J. (2000). Section 18.3, Myosin: The Actin Motor Protein. Molecular Cell Biology (4th edition ed.). New York: W. H. Freeman. Retrieved from Available from: http://www.ncbi.nlm.nih.gov/books/NBK21724/.

Luo, H. Q., Xu, M., Zhong, W. T., Cui, Z. Y., Liu, F. M., Zhou, K. Y., & Li, X. Y. (2014). EGCG decreases the expression of HIF-1alpha and VEGF and cell growth in MCF-7 breast cancer cells. *J buon, 19*(2), 435-439.

MacKenna, D. A., Dolfi, F., Vuori, K., & Ruoslahti, E. (1998). Extracellular signal-regulated kinase and c-Jun NH2-terminal kinase activation by mechanical stretch is integrin-dependent and matrix-specific in rat cardiac fibroblasts. *The Journal of Clinical Investigation, 101*(2), 301-310. doi: 10.1172/JCI1026

Maeda, T., Sakabe, T., Sunaga, A., Sakai, K., Rivera, A. L., Keene, D. R., . . . Sakai, T. (2011). Conversion of mechanical force into TGF-β-mediated biochemical signals. *Current Biology, 21*(11), 933-941.

Maheshwari, G., Brown, G., Lauffenburger, D. A., Wells, A., & Griffith, L. G. (2000). Cell adhesion and motility depend on nanoscale RGD clustering. *J Cell Sci, 113 (Pt 10)*, 1677-1686.

Mammoto, A., Connor, K.M., Mammoto, T., Yung, C.W., Huh, D., Aderman, C.M., Mostoslavsky, G., Smith, L.E., Ingber, D.E. (2009). A mechanosensitive transcriptional mechanism that controls angiogenesis. *Nature*. 457: 1103 – 1108.

Maniotis, A. J., Chen, C. S., & Ingber, D. E. (1997). Demonstration of mechanical connections between integrins, cytoskeletal filaments, and nucleoplasm that stabilize nuclear structure. *Proceedings of the National Academy of Sciences of the United States of America, 94*(3), 849-854.

Mansurova, S. E., Shakhov, Y. A., Belyakova, T. N., & Kulaev, I. S. (1975). Synthesis of inorganic pyrophosphate by animal tissue mitochondria. *FEBS Letters, 55*(1–2), 94-98. doi: http://dx.doi.org/10.1016/0014-5793(75)80967-7

Marchenko, G. N., Ratnikov, B. I., Rozanov, D. V., Godzik, A., Deryugina, E. I., & Strongin, A. Y. (2001). Characterization of matrix metalloproteinase-26, a novel metalloproteinase widely expressed in cancer cells of epithelial origin. *Biochemical Journal, 356*(3), 705-718.

Martin, M., Muller, K., Cadenas, C., Hermes, M., Zink, M., Hengstler, J. G., & Kas, J. A. (2012). ERBB2 overexpression triggers transient high mechanoactivity of breast tumor cells. *Cytoskeleton (Hoboken), 69*(5), 267-277. doi: 10.1002/cm.21023

McGrail, D. J., Kieu, Q. M. N., & Dawson, M. R. (2014). The malignancy of metastatic ovarian cancer cells is increased on soft matrices through a mechanosensitive Rho–ROCK pathway. *Journal of Cell Science, 127*(12), 2621-2626. doi: 10.1242/jcs.144378

Mendez, M. G., Kojima, S.-I., & Goldman, R. D. (2010). Vimentin induces changes in cell shape, motility, and adhesion during the epithelial to mesenchymal transition. *The FASEB Journal, 24*(6), 1838-1851. doi: 10.1096/fj.09-151639

Menhofer, M. H., Kubisch, R., Schreiner, L., Zorn, M., Foerster, F., Mueller, R., . . . Zahler, S. (2014). The actin targeting compound Chondramide inhibits breast cancer metastasis via reduction of cellular contractility. *PLoS One, 9*(11), e112542. doi: 10.1371/journal.pone.0112542

Milkiewicz, M., Mohammadzadeh, F., Ispanovic, E., Gee, E., & Haas, T. L. (2007). Static strain stimulates expression of matrix metalloproteinase-2 and VEGF in microvascular endothelium via JNK- and ERK-dependent pathways. *Journal of Cellular Biochemistry, 100*(3), 750-761.

Millerot-Serrurot, E., Guilbert, M., Fourré, N., Witkowski, W., Said, G., Van Gulick, L., . . . Jeannesson, P. (2010). 3D collagen type I matrix inhibits the antimigratory effect of doxorubicin. *Cancer Cell International, 10*.

Ministry of Health. (2014). *Cancer: New Registrations and Deaths 2011*. Wellington.

Miyata, H., Nishiyama, S., Akashi, K. I., & Kinosita Jr, K. (1999). Protrusive growth from giant liposomes driven by actin polymerization. *Proceedings of the National Academy of Sciences of the United States of America, 96*(5), 2048-2053.

Montesano, R., Orci, L., Vassalli, P. (1983). In vitro rapid organization of endothelial cells into capillary-like networks is promoted by collagen matrices. *J Cell Biol*. 97: 1648 – 1652.

Mordan, L. J., Burnett, T. S., Zhang, L. X., Tom, J., & Cooney, R. V. (1993). Inhibitors of endogenous nitrogen oxide formation block the promotion of neoplastic transformation in C3H 10T1/2 fibroblasts. *Carcinogenesis, 14*(8), 1555-1559.

Mouw, J.K., Yui, Y., Damiano, L., Bainer, R.O., Lakin, J.N., Acerbi, I., Ou, G. et al. (2014). Tissue mechanics modulate microRNA-dependent PTEN expression to regulate malignant progression. *Nat Med*. 20: 360 – 367.

Mrksich, M., Chen, C.S., Xia, Y., Dike, L.E., Ingber, D.E., Whitesides, G.M. (1996). Controlling cell attachment on contoured surfaces with self-assembled monolayers of alkanethiolates on gold. *Cell Biology*. 93: 10775-10778.

Murugan, R., Molnar, P., Rao, K. P., Hickman, J.J. (2009). Biomaterial Surface patterning of self assembled monolayers for controlling neuronal cell behaviour. *International Journal of Biomedical Engineering*. 2(2): 104-134.

Murray, L. (2011). *Endometrial Cancer Cells grown on Bioimprinted Substrate*. The University of Canterbury, Christchurch. New Zealand.

Murray, L. (2012). *Influence of substrate topography and materials on behaviour of biological cells.* (Doctor of Philosophy), University of Canterbury, Christchurch, New Zealand.

Murray, L., Nock, V., Evans, J., & Alkaisi, M. (2014). Bioimprinted polymer platforms for cell culture using soft lithography. *Journal of Nanobiotechnology, 12*(1), 60.

Muta, T., Kang, D., Kitajima, S., Fujiwara, T., & Hamasaki, N. (1997). p32 protein, a splicing factor 2-associated protein, is localized in mitochondrial matrix and is functionally important in maintaining oxidative phosphorylation. *J Biol Chem, 272*(39), 24363-24370.

Mutoh, A., Isshiki, M., & Fujita, T. (2008). Aldosterone enhances ligand-stimulated nitric oxide production in endothelial cells. *Hypertens Res, 31*(9), 1811-1820. doi: 10.1291/hypres.31.1811

Muys, J. J., Alkaisi, M. M., & Evans, J. J. (2006). Cellular replication and atomic force microscope imaging using a UV-Bioimprint technique. *Nanomedicine: Nanotechnology, Biology, and Medicine, 2*(3), 169-176.

Muys, J. J., Alkaisi, M. M., Melville, D. O. S., Nagase, J., Sykes, P., Parguez, G. M., & Evans, J. J. (2006). Cellular transfer and AFM imaging of cancer cells using Bioimprint. *Journal of Nanobiotechnology, 4*.

Nelson, S. A., Li, Z., Newton, I. P., Fraser, D., Milne, R. E., Martin, D. M., . . . Nathke, I. S. (2012). Tumorigenic fragments of APC cause dominant defects in directional cell migration in multiple model systems. *Dis Model Mech, 5*(6), 940-947. doi: 10.1242/dmm.008607

Nishihira, J. (2000). Macrophage Migration Inhibitory Factor (Mif): Its Essential Role In The Immune System And Cell Growth. *Journal Of Interferon And Cytokine Research.* 20:751–762.

Nobes, C. D., & Hall, A. (1995). Rho, Rac, and Cdc42 GTPases regulate the assembly of multimolecular focal complexes associated with actin stress fibers, lamellipodia, and filopodia. *Cell, 81*(1), 53-62.

Nomura, S., Kojima, H., Ohyabu, Y., Kuwabara, K., Mlyauchi, A., & Uemura, T. (2005). Cell culture on nanopillar sheet: Study of HeLa cells on nanopillar sheet. *Japanese Journal of Applied Physics, Part 2: Letters, 44*(37-41), L1184-L1186.

O'Connell, F.C., Martin, F. (2000). Laminin-rich extracellular matrix association with mammary epithelial cells suppresses Brca1 expression. *Cell Death Differ.* 7: 360 – 367.

O'Connor, R.S., Hao, X., Shen, K., Bashour, K., Akimova, T., Hancock, W.W., Kam, L.C., Milone, M.C. (2012). Substrate rigidity regulates human T cell activation and proliferation. *J Immunol.* 189: 1330 – 1339.

Østergaard, L., Simonsen, U., Eskildsen-Helmond, Y., Vorum, H., Uldbjerg, N., Honoré, B., & Mulvany, M. J. (2009). Proteomics reveals lowering oxygen alters cytoskeletal and endoplasmatic stress proteins in human endothelial cells. *Proteomics, 9*(19), 4457-4467.

Ouhtit, A., Gaur, R. L., Abdraboh, M., Ireland, S. K., Rao, P. N., Raj, S. G., . . . Raj, M. H. (2013). Simultaneous Inhibition of Cell-Cycle, Proliferation, Survival, Metastatic Pathways and Induction of Apoptosis in Breast Cancer Cells by a Phytochemical Super-Cocktail: Genes That Underpin Its Mode of Action. *J Cancer, 4*(9), 703-715. doi: 10.7150/jca.7235

Pan, J., Fukuda, K., Saito, M., Matsuzaki, J., Kodama, H., Sano, M., . . . Ogawa, S. (1999). Mechanical stretch activates the JAK/STAT pathway in rat cardiomyocytes. *Circ Res, 84*(10), 1127-1136.

Pan, Y., Zhang, Q., Atsaves, V., Yang, H., & Claret, F. X. (2013). Suppression of Jab1/CSN5 induces radio- and chemo-sensitivity in nasopharyngeal carcinoma through changes to the DNA damage and repair pathways. *Oncogene, 32*(22), 2756-2766. doi: 10.1038/onc.2012.294

Parent, R. A. (1992). *Treatise on Pulmonary Toxicology: Comparative Biology of the Normal Lung*: Taylor & Francis.

Park, H. I., Ni, J., Gerkema, F. E., Liu, D., Belozerov, V. E., & Sang, Q. X. A. (2000). Identification and characterization of human endometase (matrix metalloproteinase-26) from endometrial tumor. *Journal of Biological Chemistry, 275*(27), 20540-20544.

Paszek, M. J., & Weaver, V. M. (2004). The tension mounts: Mechanics meets morphogenesis and malignancy. *Journal of Mammary Gland Biology and Neoplasia, 9*(4), 325-342.

Paszek, M. J., Zahir, N., Johnson, K. R., Lakins, J. N., Rozenberg, G. I., Gefen, A., . . . Weaver, V. M. (2005). Tensional homeostasis and the malignant phenotype. *Cancer Cell, 8*(3), 241-254. doi: http://dx.doi.org/10.1016/j.ccr.2005.08.010.

Pathak, A., Kumar, S. (2012). Independent regulation of tumor cell migration by matrix stiffness and confinement. *Proc Natl Acad Sci USA.* 109: 10334 – 10339.

Paterson, H. F., Self, A. J., Garrett, M. D., Just, I., Aktories, K., & Hall, A. (1990). Microinjection of recombinant p21(rho) induces rapid changes in cell morphology. *Journal of Cell Biology, 111*(3), 1001-1007.

Patch A.M., et al. (2015). Whole-genome characterization of chemoresistant ovarian cancer. *Nature.* 521(7553), 489-94.

Pennisi, C. P., Dolatshahi-Pirouz, A., Foss, M., Chevallier, J., Fink, T., Zachar, V., . . . Yoshida, K. (2011). Nanoscale topography reduces fibroblast growth, focal adhesion size and migration-related gene expression on platinum surfaces. *Colloids Surf B Biointerfaces, 85*(2), 189-197. doi: 10.1016/j.colsurfb.2011.02.028

Perera, P., Wypasek, E., Madhavan, S., Rath-Deschner, B., Liu, J., Nam, J., . . . Agarwal, S. (2010). Mechanical signals control SOX-9, VEGF, and c-Myc expression and cell proliferation during inflammation via integrin-linked kinase, B-Raf, and ERK1/2-dependent signaling in articular chondrocytes. *Arthritis Research & Therapy, 12*(3), R106.

Pickup, M.W., Laklai, H., Acerbi, I., Owens, P., Gorska, A.E., Chytil, A., Aakre, M., Weaver, V.M., Moses, H.L. (2013). Stromally derived lysyl oxidase promotes metastasis of transforming Growth factor-beta deficient mouse mammary carcinoma. *Cancer Res*. 73: 5336 – 5346.

Pickup, M.W., Mouw, J.K. & Weaver, V.M. (2014). The extracellular matrix modulates the hallmarks of cancer. *EMBO Reports.* 15(12), 1243-53.

Plachot, C., & Leli èvre, S. A. (2004). DNA methylation control of tissue polarity and cellular differentiation in the mammary epithelium. *Experimental Cell Research, 298*, 122-132.

Provenzano, P. P., Eliceiri, K. W., Campbell, J. M., Inman, D. R., White, J. G., & Keely, P. J. (2006). Collagen reorganization at the tumor-stromal interface facilitates local invasion. *BMC Medicine, 4*.

Provenzano, P. P., Inman, D. R., Eliceiri, K. W., Trier, S. M., & Keely, P. J. (2008). Contact Guidance Mediated Three-Dimensional Cell Migration is Regulated by Rho/ROCK-Dependent Matrix Reorganization. *Biophysical Journal, 95*(11), 5374-5384. doi: http://dx.doi.org/10.1529/biophysj.108.133116

Provenzano, P.P., Keely, P.J. (2011). Mechanical signaling through the cytoskeleton regulates cell proliferation by coordinated focal adhesion and Rho GTPase signalling. *Journal of Cell Science*. 124: 1195-1205.

Pylayeva, Y., Gillen, K.M., Gerald, W., Beggs, H.E., Reichardt, L.F., Giancotti, F.G. (2009). Ras- and PI3K-dependent breast tumorigenesis in mice and humans requires focal adhesion kinase signaling. *J Clin Invest.* 119: 252 – 266.

Radisky, D.C., Levy, D.D., Littlepage, L.E., Liu, H., Nelson, C.M., Fata, J.E., Leake, D., et al. (2005). Rac1b and reactive oxygen species mediate MMP-3-induced EMT and genomic instability. *Nature*. 436: 123 – 127.

Rathje, L.-S. Z., Nordgren, N., Pettersson, T., Rönnlund, D., Widengren, J., Aspenström, P., & Gad, A. K. B. (2014). Oncogenes induce a vimentin filament collapse mediated by HDAC6 that is linked to cell stiffness. *Proceedings of the National Academy of Sciences, 111*(4), 1515-1520. doi: 10.1073/pnas.1300238111

Redmond, L., & Ghosh, A. (2001). The role of Notch and Rho GTPase signaling in the control of dendritic development. *Curr Opin Neurobiol, 11*(1), 111-117.

Remmerbach, T. W., Wottawah, F., Dietrich, J., Lincoln, B., Wittekind, C., & Guck, J. (2009). Oral Cancer Diagnosis by Mechanical Phenotyping. *Cancer Research, 69*(5), 1728-1732. doi: 10.1158/0008-5472.can-08-4073

Ring, H.Z., Vameghi-Meyers, V., Wang, W., Crabtree, G.R., Franckea, U. (1998). Five SWI/SNF-Related, Matrix-Associated, Actin-Dependent Regulator of Chromatin (SMARC) Genes Are Dispersed in the Human Genome. *Genomics.* 51:140-143.

Rodriguez, S. K., Guo, W., Liu, L., Band, M. A., Paulson, E. K., & Meydani, M. (2006). Green tea catechin, epigallocatechin-3-gallate, inhibits vascular endothelial growth factor angiogenic signaling by disrupting the formation of a receptor complex. *International Journal of Cancer, 118*(7), 1635-1644. doi: 10.1002/ijc.21545

Rovensky, Y. (2011). Topographic Cell Responses. *Adhesive Interactions in Normal and Transformed Cells.* (pp. 153-184): Humana Press.

Rovensky, Y. A., Slavnaja, I. L., & Vasiliev, J. M. (1971). Behaviour of fibroblast-like cells on grooved surfaces. *Exp Cell Res, 65*(1), 193-201.

Rubashkin, M. G., Cassereau, L., Bainer, R., DuFort, C. C., Yui, Y., Ou, G., . . . Weaver, V. M. (2014). Force Engages Vinculin and Promotes Tumor Progression by Enhancing PI3K Activation of Phosphatidylinositol (3,4,5)-Triphosphate. *Cancer Research, 74*(17), 4597-4611. doi: 10.1158/0008-5472.can-13-3698

Rucci, N., Capulli, M., Olstad, O. K., Önnerfjord, P., Tillgren, V., Gautvik, K. M., . . . Teti, A. (2015). The α2β1 binding domain of chondroadherin inhibits breast cancer-induced bone metastases and impairs primary tumour growth: A preclinical study. *Cancer Letters*.

Saltzman, W. M., & Kyriakides, T. R. (2007). Cell interactions with polymers. In R. Lanza, R. Langer & J. Vacanti (Eds.), Principles of tissue engineering (pp. 279-296). San Diego: Academic Press.

Samsuri, F., Alkaisi, M. M., Evans, J. J., Chitcholtan, K., & Mitchell, J. S. (2011). Detection of changes in cell membrane structures using the Bioimprint technique. *Microelectronic Engineering, 88*(8), 1871-1874.

Samsuri, F., Alkaisi, M. M., Mitchell, J. S., & Evans, J. J. (2010). Replication of cancer cells using soft lithography bioimprint technique. *Microelectronic Engineering, 87*(5–8), 699-703. doi: http://dx.doi.org/10.1016/j.mee.2009.12.068

Sanger, J. W. (1975). Changing patterns of actin localization during cell division. *Proceedings of the National Academy of Sciences, 72*(5), 1913-1916.

Sarna, M., Wybieralska, E., Miekus, K., Drukala, J., & Madeja, Z. (2009). Topographical control of prostate cancer cell migration. *Mol Med Rep, 2*(5), 865-871. doi: 10.3892/mmr_00000185

Sartippour, M. R., Shao, Z. M., Heber, D., Beatty, P., Zhang, L., Liu, C., . . . Brooks, M. N. (2002). Green tea inhibits vascular endothelial growth factor (VEGF) induction in human breast cancer cells. *J Nutr, 132*(8), 2307-2311.

Sato, H., Takino, T., Okada, Y., Cao, J., Shinagawa, A., Yamamoto, E., & Seiki, M. (1994). A matrix metalloproteinase expressed on the surface of invasive tumour cells. *Nature, 370*(6484), 61-65.

Schiro, J. A., Chan, B. M. C., Roswit, W. T., Kassner, P. D., Pentland, A. P., Hemler, M. E., . . . Kupper, T. S. (1991). Integrin α2β1 (VLA-2) mediates reorganization and contraction of collagen matrices by human cells. *Cell, 67*(2), 403-410.

Schmidt, C., Pommerenke, H., Durr, F., Nebe, B., & Rychly, J. (1997). Mechanical Stressing of Integrin Receptors Induces Enhanced Tyrosine Phosphorylation of Cytoskeletally Anchored Proteins. *The Journal of Biological Chemistry, 273*(9), 5081- 5085.

Schwartz, M.A., Assoian, R.K. (2001). Integrins and cell proliferation: regulation of cyclin-dependent kinases via cytoplasmic signaling pathways. *J Cell Sci.* 114: 2553 – 2560.

Schwarza, U. S., Erdmanna, T., & Bischofs, I. B. (2006). Focal adhesions as mechanosensors: The two-spring model. *BioSystems, 83*, 225-232.

Sero, J. E., Sailem, H. Z., Ardy, R. C., Almuttaqi, H., Zhang, T., & Bakal, C. (2015). Cell shape and the microenvironment regulate nuclear translocation of NF-κB in breast epithelial and tumor cells. *Molecular Systems Biology, 11*(3), n/a-n/a. doi: 10.15252/msb.20145644

Shanthi, E., Krishna, M. H., Arunesh, G. M., Venkateswara Reddy, K., Sooriya Kumar, J., & Viswanadhan, V. N. (2014). Focal adhesion kinase inhibitors in the treatment of metastatic cancer: A patent review. *Expert Opinion on Therapeutic Patents, 24*(10), 1077-1100.

Shi, Q., & Boettiger, D. (2003). A novel mode for integrin-mediated signaling: Tethering is required for phosphorylation of FAK Y397. *Molecular Biology of the Cell, 14*(10), 4306-4315.

Shraiman, B. I. (2005). Mechanical feedback as a possible regulator of tissue growth. *Proceedings of the National Academy of Sciences of the United States of America, 102*(9), 3318-3323. doi: 10.1073/pnas.0404782102

Stambolic, V., Suzuki, A., de la Pompa, J. L., Brothers, G. M., Mirtsos, C., Sasaki, T., . . . Mak, T. W. (1998). Negative Regulation of PKB/Akt-Dependent Cell Survival by the Tumor Suppressor PTEN. *Cell, 95*(1), 29-39. doi: http://dx.doi.org/10.1016/S0092-8674(00)81780-8

Stamenović, D., & Coughlin, M. F. (1999). The role of prestress and architecture of the cytoskeleton and deformability of cytoskeletal filaments in mechanics of adherent cells: A quantitative analysis. *Journal of Theoretical Biology, 201*(1), 63-74.

Stamenović, D., Fredberg, J. J., Wang, N., Butler, J. P., & Ingber, D. E. (1996). A microstructural approach to cytoskeletal mechanics based on tensegrity. *Journal of Theoretical Biology, 181*(2), 125-136.

Stoker, A. W., Hatier, C., & Bissell, M. J. (1990). The embryonic environment strongly attenuates v-src oncogenesis in mesenchymal and epithelial tissues, but not in endothelia. *Journal of Cell Biology, 111*(1), 217-228.

Storch, K., & Cordes, N. (2012). Focal Adhesion-Chromatin Linkage Controls Tumor Cell Resistance to Radio- and Chemotherapy. *Chemotherapy Research and Practice, 2012*, 10. doi: 10.1155/2012/319287

Storkebaum, E., & Carmeliet, P. (2004). VEGF: a critical player in neurodegeneration. *The Journal of Clinical Investigation, 113*(1), 14-18. doi: 10.1172/JCI20682

Taga, T., Suzuki, A., Gonzalez-Gomez, I., Gilles, F. H., Stins, M., Shimada, H., . . . Laug, W. E. (2002). alpha v-Integrin antagonist EMD 121974 induces apoptosis in brain tumor cells growing on vitronectin and tenascin. *Int J Cancer, 98*(5), 690-697.

Takagi, J., Petre, B. M., Walz, T., & Springer, T. A. (2002). Global Conformational Rearrangements in Integrin Extracellular Domains in Outside-In and Inside-Out Signaling. *Cell, 110*(5), 599-611. doi: http://dx.doi.org/10.1016/S0092-8674(02)00935-2

Tamada, Y. & Ikada, Y. (1994). Fibroblast growth on polymer surfaces and biosynthesis of collagen. *Journal of Biomedical Materials Research*. 28:783–789.

Tamkun, J. W., DeSimone, D. W., Fonda, D., Patel, R. S., Buck, C., Horwitz, A. F., & Hynes, R. O. (1986). Structure of integrin, a glycoprotein involved in the transmembrane linkage between fibronectin and actin. *Cell, 46*(2), 271-282.

Tanaka, K., Babic, I., Nathanson, D., Akhavan, D., Guo, D., Gini, B., . . . Mischel, P. S. (2011). Oncogenic EGFR signaling activates an mTORC2-NF-kappaB pathway that promotes chemotherapy resistance. *Cancer Discov, 1*(6), 524-538. doi: 10.1158/2159-8290.cd-11-0124

Teixeira, A. I., Abrams, G. A., Bertics, P. J., Murphy, C. J., & Nealey, P. F. (2003). Epithelial contact guidance on well-defined micro- and nanostructured substrates. *Journal of Cell Science, 116*(10), 1881-1892.

Terai, Y., Abe, M., Miyamoto, K., Koike, M., Yamasaki, M., Ueda, M., . . . Sato, Y. (2001). Vascular smooth muscle cell growth-promoting factor/F-spondin inhibits angiogenesis via the blockade of integrin alphavbeta3 on vascular endothelial cells. *J Cell Physiol, 188*(3), 394-402. doi: 10.1002/jcp.1122

The New Zealand Gynaecological Cancer Foundation. (n.d.). Gynaecological Cancers. Background Information Sheet. Retrieved 31/01/2015, 2015, from http://rnzcgp.org.nz/assets/documents/News--Events/Gynae-Cancer-Background-information-sheet.pdf

Thevenot, P., Hu, W., & Tang, L. (2008). SURFACE CHEMISTRY INFLUENCE IMPLANT BIOCOMPATIBILITY. *Current topics in medicinal chemistry, 8*(4), 270-280.

Thompson, D. A. W. (1945). *On Growth and Form*: University Press.

Tomoda, K., Yoneda-Kato, N., Fukumoto, A., Yamanaka, S., & Kato, J.-y. (2004). Multiple Functions of Jab1 Are Required for Early Embryonic Development and Growth Potential in Mice. *Journal of Biological Chemistry, 279*(41), 43013-43018. doi: 10.1074/jbc.M406559200

Tong, W. Y., Shen, W., Yeung, C. W. F., Zhao, Y., Cheng, S. H., Chu, P. K., . . . Lam, Y. W. (2012). Functional replication of the tendon tissue microenvironment by a bioimprinted substrate and the support of tenocytic differentiation of mesenchymal stem cells. *Biomaterials, 33*(31), 7686-7698.

Tschumperlin, D. J., Dal, G., Maly, I. V., Kikuchi, T., Lalho, L. H., McVittie, A. K., . . . Drazen, J. M. (2004). Mechanotransduction through growth-factor shedding into the extracellular space. *Nature, 429*(6987), 83-86.

Tsimbouri, P., Gadegaard, N., Burgess, K., White, K., Reynolds, P., Herzyk, P., . . . Dalby, M. J. (2014). Nanotopographical effects on mesenchymal stem cell morphology and phenotype. *Journal of Cellular Biochemistry, 115*(2), 380-390.

Tung, Y. C., Hsiao, A. Y., Allen, S. G., Torisawa, Y. S., Ho, M., & Takayama, S. (2011). High-throughput 3D spheroid culture and drug testing using a 384 hanging drop array. *Analyst, 136*(3), 473-478. doi: 10.1039/c0an00609b

Tzima, E., Del Pozo, M. A., Kiosses, W. B., Mohamed, S. A., Li, S., Chien, S., & Schwartz, M. A. (2002). Activation of Rac1 by shear stress in endothelial cells mediates both

cytoskeletal reorganization and effects on gene expression. *EMBO Journal, 21*(24), 6791-6800.

Tzima, E., Del Pozo, M. A., Shattil, S. J., Chien, S., & Schwartz, M. A. (2001). Activation of integrins in endothelial cells by fluid shear stress mediates Rho-dependent cytoskeletal alignment. *EMBO Journal, 20*(17), 4639-4647.

Tzvetkova-Chevolleau, T., Stephanou, A., Fuard, D., Ohayon, J., Schiavone, P., & Tracqui, P. (2008). The motility of normal and cancer cells in response to the combined influence of the substrate rigidity and anisotropic microstructure. *Biomaterials, 29*(10), 1541-1551. doi: 10.1016/j.biomaterials.2007.12.016

Uria, J. A., & Lopez-Otin, C. (2000). Matrilysin-2, a new matrix metalloproteinase expressed in human tumors and showing the minimal domain organization required for secretion, latency, and activity. *Cancer Research, 60*(17), 4745-4751.

van Wachem, P. B., Hogt, A. H., Beugeling, T., Feijen, J., Bantjes, A., Detmers, J. P., & van Aken, W. G. (1987). Adhesion of cultured human endothelial cells onto methacrylate polymers with varying surface wettability and charge. *Biomaterials, 8*(5), 323-328. doi: 10.1016/0142-9612(87)90001-9

Vargas-Roig, L. M., Gago, F. E., Tello, O., Aznar, J. C., & Ciocca, D. R. (1998). Heat shock protein expression and drug resistance in breast cancer patients treated with induction chemotherapy. *International Journal of Cancer, 79*(5), 468-475. doi: 10.1002/(SICI)1097-0215(19981023)79:5<468::AID-IJC4>3.0.CO;2-Z

Verdanova, M., Broz, A., Kalbac, M., & Kalbacova, M. (2012). Influence of oxygen and hydrogen treated graphene on cell adhesion in the presence or absence of fetal bovine serum. *Physica Status Solidi (B) Basic Research, 249*(12), 2503-2506.

Veselý, P., Rovensky Yu, A., & Slavnaya, I. L. (1981). Cinemicrographic analysis of migration of normal and neoplastic rat cells seeded upon the grooved surface. *Folia Biologica, 27*(2), 81-90.

Vinogradova, O., Velyvis, A., Velyviene, A., Hu, B., Haas, T. A., Plow, E. F., & Qin, J. (2002). A Structural Mechanism of Integrin αIIbβ3 "Inside-Out" Activation as Regulated by Its Cytoplasmic Face. *Cell, 110*(5), 587-597. doi: http://dx.doi.org/10.1016/S0092-8674(02)00906-6

Waddell, N., et al. (2015). Whole genomes redefine the mutational landscape of pancreatic cancer. *Nature*. 518(7540), 495-501.

Wang, F., Weaver, V. M., Petersen, O. W., Larabell, C. A., Dedhar, S., Briand, P., . . . Bissell, M. J. (1998). Reciprocal interactions between β1-integrin and epidermal growth factor receptor in three-dimensional basement membrane breast cultures: A different perspective in epithelial biology. *Proceedings of the National Academy of Sciences of the United States of America, 95*(25), 14821-14826.

Wang, F., Weaver, V. M., Petersen, O. W., Larabell, C. A., Dedhar, S., Briands, P., . . . Bissell, M. J. (1998). Reciprocal interactions between b1-integrin and epidermal growth factor receptor in three-dimensional basement membrane breast cultures: A different perspective in epithelial biology. *Proceedings of the National Academy of Sciences, 95*, 14821–14826.

Wang, H. B., Dembo, M., Hanks, S. K., & Wang, Y. L. (2001). Focal adhesion kinase is involved in mechanosensing during fibroblast migration. *Proceedings of the National Academy of Sciences of the United States of America, 98*(20), 11295-11300.

Wang, H. B., Dembo, M., & Wang, Y. L. (2000). Substrate flexibility regulates growth and apoptosis of normal but not transformed cells. *American Journal of Physiology - Cell Physiology, 279*, C1345- C1350.

Wang, N., Butler, J. P., & Ingber, D. E. (1993). Mechanotransduction across the cell surface and through the cytoskeleton. *Science, 260*(5111), 1124-1127.

Wang, N., Naruse, K., Stamenović, D., Fredberg, J. J., Mijailovich, S. M., Tolić-Nørrelykke, I. M., . . . Ingber, D. E. (2001). Mechanical behavior in living cells consistent with the tensegrity model. *Proceedings of the National Academy of Sciences of the United States of America, 98*(14), 7765-7770.

Wang, P., Chen, S. H., Hung, W. C., Paul, C., Zhu, F., Guan, P. P., . . . Konstantopoulos, K. (2014). Fluid shear promotes chondrosarcoma cell invasion by activating matrix metalloproteinase 12 via IGF-2 and VEGF signaling pathways. *Oncogene*. doi: 10.1038/onc.2014.397

Weaver, V. M., Petersen, O. W., Wang, F., Larabell, C. A., Briand, P., Damsky, C., & Bissell, M. J. (1997). Reversion of the malignant phenotype of human breast cells in three- dimensional culture and in vivo by integrin blocking antibodies. *Journal of Cell Biology, 137*(1), 231-245.

Webb, A., Clark, P., Skepper, J., Compston, A., & Wood, A. (1995). Guidance of oligodendrocytes and their progenitors by substratum topography. *Journal of Cell Science, 108*(8), 2747-2760.

Wei, N., Serino, G., & Deng, X.-W. (2008). The COP9 signalosome: more than a protease. *Trends in Biochemical Sciences, 33*(12), 592-600. doi: http://dx.doi.org/10.1016/j.tibs.2008.09.004

Weiss, P. (1941). Nerve Patterns: The Mechanics of Nerve Growth. *Growth, 5*, 163-203.

Weitkunat, M., Kaya-Çopur, A., Grill, Stephan W., & Schnorrer, F. (2014). Tension and Force-Resistant Attachment Are Essential for Myofibrillogenesis in Drosophila Flight Muscle. *Current Biology, 24*(7), 705-716. doi: 10.1016/j.cub.2014.02.032

Welcsh, P. L., & King, M.-C. (2001). BRCA1 and BRCA2 and the genetics of breast and ovarian cancer. *Human Molecular Genetics, 10*(7), 705-713. doi: 10.1093/hmg/10.7.705

Wilson, B.G., Roberts, C.W. (2011). SWI/SNF nucleosome remodellers and cancer. *Nat Rev Cancer*. 11(7):481-492.

Wolfe, J. N. (1976). Risk for breast cancer development determined by mammographic parenchymal pattern. *Cancer, 37*(5), 2486-2492. doi: 10.1002/1097-0142(197605)37:5<2486::aid-cncr2820370542>3.0.co;2-8

Wong, J. Y., Velasco, A., Rajagopalan, P., & Pham, Q. (2003). Directed movement of vascular smooth muscle cells on gradient-compliant hydrogels. *Langmuir, 19*(5), 1908-1913.

Woo, W.-M., Berry, E., Hudson, M. L., Swale, R. E., Goncharov, A., & Chisholm, A. D. (2008). The C. elegans F-spondin family protein SPON-1 maintains cell adhesion in neural and non-neural tissues. *Development (Cambridge, England), 135*(16), 2747-2756. doi: 10.1242/dev.015289

Wood, A. (1988). Contact guidance on microfabricated substrata: the response of teleost fin mesenchyme cells to repeating topographical patterns. *Journal of Cell Science, 90*, Pt 4/.

Wozniak, M. A., Desai, R., Solski, P. A., Der, C. J., & Keely, P. J. (2003). ROCK-generated contractility regulates breast epithelial cell differentiation in response to the physical properties of a three- dimensional collagen matrix. *The Journal of Cell Biology, 163*(3), 583–595.

Wu, F., Sun, H., Kluz, T., Clancy, H. A., Kiok, K., & Costa, M. (2012). Epigallocatechin-3-gallate (EGCG) protects against chromate-induced toxicity in vitro. *Toxicology and Applied Pharmacology*, 258(2), 166–175.

Xie, K., Huang, S., Dong, Z., Juang, S. H., Gutman, M., Xie, Q. W., . . . Fidler, I. J. (1995). Transfection with the inducible nitric oxide synthase gene suppresses tumorigenicity

and abrogates metastasis by K-1735 murine melanoma cells. *J Exp Med, 181*(4), 1333-1343.

Yang, S. (2012). To revert breast cancer cells, give them the squeeze. 2014, from http://newscenter.berkeley.edu/2012/12/17/malignant-breast-cells-grow-normally-when-compressed/

Yang, Z., Kenny, A. E., Brito, D. A., & Rieder, C. L. (2009). Cells satisfy the mitotic checkpoint in Taxol, and do so faster in concentrations that stabilize syntelic attachments. *The Journal of Cell Biology, 186*(5), 675-684. doi: 10.1083/jcb.200906150

Yeung, T., Georges, P. C., Flanagan, L. A., Marg, B., Ortiz, M., Funaki, M., . . . Janmey, P. A. (2005). Effects of substrate stiffness on cell morphology, cytoskeletal structure, and adhesion. *Cell Motility and the Cytoskeleton, 60*(1), 24-34.

Yildirim, A., & Whish, W. (1997). The role of protein secretion on the adhesion strength of chinese hamster lung (CHL) cells. *Biochem Soc Trans, 25*(3).

Yim, E. K. F., Darling, E. M., Kulangara, K., Guilak, F., & Leong, K. W. (2010). Nanotopography-induced changes in focal adhesions, cytoskeletal organization, and mechanical properties of human mesenchymal stem cells. *Biomaterials, 31*(6), 1299-1306.

Yuan, J., Kramer, A., Matthess, Y., Yan, R., Spankuch, B., Gatje, R., . . . Strebhardt, K. (2005). Stable gene silencing of cyclin B1 in tumor cells increases susceptibility to taxol and leads to growth arrest in vivo. *Oncogene, 25*(12), 1753-1762.

Yu, S.T., Chen, L., Wang, H.J., Tang, X.D., Fang, D.C., Yang, S.M. (2009). hTERT promotes the invasion of telomerase-negative tumor cells in vitro. *Int J Oncol*. 35: 329 – 336.

Zhang, J., Hochwald, S.N. (2014). The role of FAK in tumor metabolism and therapy. *Pharmacol Ther*. 142: 154 – 163.

Zhang, L., Chun, Y. W., & Webster, T. J. (2010a). *Decreased lung carcinoma ceil density on select polymer nanometer surface features for lung replacement therapies.* Paper presented at the Materials Research Society Symposium Proceedings.

Zhang, L., Chun, Y. W., & Webster, T. J. (2010b). Decreased lung carcinoma cell density on select polymer nanometer surface features for lung replacement therapies. *Int J Nanomedicine, 5*, 269-275.

Zhao, G., Cui, J., Qin, Q., Zhang, J., Liu, L., Deng, S., . . . Wang, C. (2010). Mechanical Stiffness of Liver Tissues in Relation to Integrin b1 Expression May Influence the Development of Hepatic Cirrhosis and Hepatocellular Carcinoma. *Journal of Surgical Oncology, 102*, 482- 489.

Zheng, L., Sjölander, A., Eckerdal, J., & Andersson, T. (1996). Antibody-induced engagement of β2 integrins on adherent human neutrophils triggers activation of p21ras through tyrosine phosphorylation of the protooncogene product Vav. *Proceedings of the National Academy of Sciences of the United States of America, 93*(16), 8431-8436.

Zheng, Y., Ritzenthaler, J. D., Roman, J., & Han, S. (2007). Nicotine stimulates human lung cancer cell growth by inducing fibronectin expression. *American Journal of Respiratory Cell and Molecular Biology, 37*(6), 681-690.

Zhong, R., Liu, L., Tian, Y., Wang, Y., Tian, J., Zhu, B.B., … Miao, X.P. (2014). Genetic variant in SWI/SNF complexes influences hepatocellular carcinoma risk: a new clue for the contribution of chromatin remodeling in carcinogenesis. *Scientific Reports*. 21(4):4147.

Zhou, J., Lim, S. H., & Chiu, J. J. (2011). Epigenetic regulation of vascular endothelial biology/pathobiology and response to fluid shear stress. *Cellular and Molecular Bioengineering, 4*(4), 560-578. doi: 10.1007/s12195-011-0199-2.

Zhou, J., Mochizuki, T., Smeets, H., Antignac, C., Laurila, P., de Paepe, A., Tryggvason, K., Reeders, S.T. (1993). Deletion of the paired alpha 5(IV) and alpha 6(IV) collagen genes in inherited smooth muscle tumors. *Science.* 261: 1167 – 1169.

Zhu, B. H., Chen, H. Y., Zhan, W. H., Wang, C. Y., Cai, S. R., Wang, Z., . . . He, Y. L. (2011). (-)-Epigallocatechin-3-gallate inhibits VEGF expression induced by IL-6 via Stat3 in gastric cancer. *World J Gastroenterol, 17*(18), 2315-2325. doi: 10.3748/wjg.v17.i18.2315

Zinger, O., Anselme, K., Denzer, A., Habersetzer, P., Wieland, M., Jeanfils, J., . . . Landolt, D. (2004). Time-dependent morphology and adhesion of osteoblastic cells on titanium model surfaces featuring scale-resolved topography. *Biomaterials, 25*(14), 2695-2711.

Ziółkowska, K., Zukowski, K., Chudy, M., Dybko, A., & Brzózka, Z. (2011). *Enhancing efficiency of double casting prototyping by thermal aging of poly(dimethylsiloxane).* Paper presented at the 15th International Conference on Miniaturized Systems for Chemistry and Life Sciences 2011, MicroTAS 2011.

Zlatanova, J., Caiafa, P., & Van Holde, K. (2000). Linker histone binding and displacement: versatile mechanism for transcriptional regulation. *The FASEB Journal, 14*(12), 1697-1704. doi: 10.1096/fj.99-0869rev